Molecular mechanism for targeting a self-identity protein to the type VI system in *Proteus mirabilis*

A dissertation presented

by

Martha Adriana Zepeda Rivera

to

The Department of Molecular and Cellular Biology

in partial fulfillment of the requirement

for the degree of

Doctor of Philosophy

in the subject of

Biochemistry

Harvard University

Cambridge, Massachusetts

April 2018

Professor Karine A. Gibbs Martha Adriana Zepeda Rivera

Molecular mechanism for targeting a self-identity protein to the type VI system in *Proteus mirabilis*

Abstract

Within a bacterial community, cells can use proteins or small molecules to exchange information that influences the group's behavior. While small molecules, like quorum sensing signals, tend to be freely diffusible, proteins are transported through the cell envelope by a variety of secretion systems. The type VI secretion system (T6S) is widely conserved across Gram-negative bacteria and is used to transport proteins of a variety of sizes and functions. How protein substrates are targeted to the T6S machinery for exchange is poorly understood.

The gut-residing opportunistic pathogen, *Proteus mirabilis*, relies on the secretion of a protein, IdsD, via the T6S, to exchange self-identity information between cells. Interactions between IdsD and its binding partner, IdsE, in a recipient cell regulate self recognition behaviors. Self (clonal) populations merge while non-self populations form a macroscopic boundary in between them. The goal of my thesis research was to understand how IdsD is regulated through the transport process.

Using biochemical, genetic and imaging approaches, I interrogated the hypothesis that IdsD is regulated through interactions with T6S-associated proteins. This research led us to propose a model wherein a proposed-chaperone, IdsC, regulates IdsD prior to secretion. Understanding the pre-transport molecular regulation of IdsD provides us with novel insights into how macromolecular protein complexes can regulate the transcellular

communication of information to influence cellular behavior, such as *P. mirabilis* population dynamics within natural host environments.

Table of Contents

Acknowledgements

"Anything's possible if you've got enough nerve"
-Ginny Weasley in *Harry Potter and the Half-Blood Prince* by J.K. Rowling

Graduate school can sometimes feel like a never-ending series of challenges, and it would have been impossible for me to succeed without the individuals in my life who encouraged me to find the nerve to push through. First and foremost, I would like to thank my dissertation advisor, Dr. Karine A. Gibbs. Thank you for always pushing me to be the best experimentalist, communicator, and overall scientist that you see in me. Thank you for inspiring me to rise to the challenge, and for helping me to develop the tools to succeed. I would also like to thank the members of the Gibbs lab, who throughout the years have not only been a fun group of people to work with, but fellow scientists who have contributed immeasurable feedback to all of my projects and are always willing to help. Dr. Murray Tipping, Dr. Christina Saak, Dr. Kristin Little, Denise Sirias, Achala Chittor, and Jacob Austerman- thank you all for being a source of scientific, technical, and emotional support. I would also like to thank the high school students and undergraduates who have passed through the lab, particularly Emma, Akeem, Amy, Sajal, Edna, and August. Your enthusiasm to engage with science and seeing you develop as scientists on my best days is a source of joy, and on my worst days a source of motivation.

I would also like to thank members of my thesis committee, who have contributed hours of mental engagement, feedback, and experimental suggestions on my projects. Dr. Rachelle Gaudet, who inspires me fall in love with the mystic nature of proteins, Dr. Susan Mango whose voice I hear when trying to design "the best experiment", Dr. Colleen Cavanaugh, whose love for microbes is contagious, Dr. Matthew K. Waldor who

first introduced me to microbiology and in whose lab I fell in love with both bacteria and microscopes, and Dr. Dan Needleman.

There are no words powerful enough to convey my gratitude for the people who support me unconditionally- my family. To my parents, Arnulfo Zepeda Navratil and Adriana Rivera de Zepeda, thank you for always reminding me to face challenges headstrong and with kindness and grace. Thank you for all the late night advice, the care packages that helped me through the long Boston winters and the writing of this dissertation, the Starbucks gift cards to keep me caffeinated, the trips home when I needed to recharge, and for constantly reminding me that I have the nerve and the ability to turn this into a chapter of success in my life. To my brother, Jorge Zepeda Rivera, thank you for always knowing the exact right thing to say, especially on days when I didn't handle things with much fortitude or grace. The three of you together have been my biggest source of consistency, love, and support. Uno para todos y todos para uno. To my grandparents, aunts, uncles, and cousins, who despite multiple time zones, have always found the time to remind me to keep pushing- thank you. Sin Uds. no soy nada.

To my sisters from other misters, Alena Rau and Sasha Mascarenhas, thank you for brightening up my days with funny memes, videos of my feline nephews and nieces, and for letting me decompress during our girls trips. To my crazies, Sneha Joshi and Bo Hartono, thank you for always lending an ear to listen, for the advice you've given me throughout the years, and for always letting me visit when I needed a weekend away. Christina and Denise- our mutual love for Harry Potter, food, and T-Fridays have been an incredible source of energy and joy for me in the past six years, and I am grateful for the Slytherin tendencies that bring us together.

To the friends who reminded me to take a break when needed, and recharge with brunches, impromptu dinner parties, drinks at Felipe's, crafting nights, chocolate tours, weekend trips, and movie nights- thank you. I am eternally grateful to each and every one of you- Beste Mutlu, Stephanie Wang, Maya Sangesland, Thao Truong, Molly Gasperini, Brenda Rodriguez, Lory Henderson, Alyson Ramirez, Alia Qatarneh, Rickey Shah, Linda Honaker, Iman Allewazi, Dina Amouzigh, Alana Van Dervort, Mohammed Mostajo, Alex Bravo, Matt Thoman, and Luis Gamarra.

Lastly, I would like to thank J.K. Rowling for the words of wisdom that I could always count on for understanding and strength. Your words inspire me to be as resourceful as Hermione, as fearless as Ginny, as quirky as Luna, as strong of conviction as Professor McGonagall, as loyal as Molly, and occasionally as reckless as Harry. If he could handle Voldemort, then I can handle graduate school.

List of Figures

Chapter 1

Chapter 2

Chapter 3

Appendix A

List of Tables

*"To all of the little girls [...], never doubt that you are **valuable** and **powerful** and **deserving** of every chance and opportunity in the world to pursue and achieve your own dreams"*
-Hillary Clinton, 2016 Concession Speech

I dedicate this thesis to all girls and women striving to engage in scientific careers. I especially dedicate this to minority women, who can often, subtly and blatantly, be told that they are lucky to be handed opportunities and not earn them. Never doubt the value of your opportunities and your worthiness of receiving them. On days of my own doubt I turn to the words of African-American screenwriter and producer Shonda Rhimes.

*"I am not lucky. I am **smart**, I am **talented**, I take advantage of opportunities that come my way and I work really, really hard. Don't call me lucky. Call me a **badass**."*
-Shonda Rhimes, Year of Yes

Page intentionally left blank

Chapter 1

Chaperone-mediated protein targeting in bacterial secretion systems

Contact-dependent signal exchange modulates behavior

Neighboring cells in direct contact can use the exchange of signals to modulate their interaction. Bacteria have evolved different delivery mechanisms, called secretion systems, to exchange signals encoded within nucleic acids or proteins. In general, these secretion systems are multi-protein, cell-envelope spanning conduits through which signals are sent from the cytoplasm of a bacterial cell into a neighboring cell. This form of communication forms the basis of pathogenic and symbiotic relationships between bacterial species as well as between bacteria and their eukaryotic or plant hosts. To date, at least nine different secretion systems have been described across Gram-positive and Gram-negative bacteria (1-8), each delivering an array of substrates, termed effectors, with differing enzymatic and regulatory functions.

Shigella spp., the causative agent of dysentery, is a Gram-negative primate-restricted intercellular pathogen that utilizes type III secretion (T3S) to modulate host cytoskeletal proteins (9). While subdivided into four species, all *Shigella* cells use intercellular transport to spread within a host. One set of factors required for epithelial cell entry is encoded by the *ipa* operon, which is found next to a T3S gene locus. During early cell entry, the T3S allows insertion of a pore composed of IpaB and IpaC proteins, which allows translocation of IpaA and IpaC into the host cell cytosol (10). IpaC induces actin polymerization and through interactions with the Rho family of GTPases promotes the transition between thin tube-like actin structures, filopodia, into ruffled actin structures, lamellipodia (11). Once *Shigella* entry has begun, IpaA binds to the focal adhesion protein, vinculin, and induces actin depolymerization (12). IpaA deficient mutants are unable to invade host cells (13).

Agrobacterium tumefaciens is a Gram-negative plant pathogen that utilizes type IV secretion (T4S) to exploit its plant host for the production of an exclusive nitrogen source. *A. tumefaciens* carries a plasmid, the tumor-inducing (Ti) plasmid, which encodes multiple genes, including a set of virulence genes and a T4S gene locus (14). Integration of the Ti plasmid into the plant cell genome results in virulence gene expression and crown gall disease or tumor formation in flowering plants. In addition to virulence, the Ti plasmid encodes genes for synthesis and catabolism of specialized amino acids called opines. Transformed plant cells then secrete these opines, which serve as a nitrogen source for *A. tumefaciens* (15).

In these two examples, the secreted effectors are encoded in close genomic proximity to the secretion system that translocates them. Each type of secretion system is a specialized delivery mechanism, and as such, a single type of system exchanges a given substrate. However, an individual bacterial cell can express more than one active secretion system at a time. This presents an interesting question of how a substrate is targeted to its correct delivery system for exchange. While much is known about the structure of secretion systems and the type of cargo they can deliver, relatively little is known about how cargo is targeted. The systems in which this question has been best addressed are the T3S and T4S.

Roles of chaperones in T3S and T4S substrate secretion

T3S are derived from flagellar components and are present in Gram-negative bacteria (16, 17). T3S structural studies have shown it to be a needle-like apparatus that transverses the inner and outer membrane of donor cells and punctures the cellular

membrane of recipient eukaryotic or plant cells (18). T3S substrates are proteins generally identified by an N-terminal signal sequence that is poorly conserved at the sequence level but is an inherently unstructured region enriched in particular amino acids (19-21). T3S effector targeting is mediated by binding of customized chaperones downstream of the signal sequence, generally in non-enzymatic regions (22, 23). This binding interaction prevents substrate degradation by inhibiting substrate aggregation (24-28). While T3S chaperone proteins increase secretion efficiency of T3S substrates, they are not required for substrate export (22, 28-32). T3S chaperones generally do not exhibit sequence similarity, but do share structural similarities across species (33-40).

The T4S machinery is derived from bacterial conjugation components, and therefore can translocate nucleic acids, proteins, or nucleo-protein complexes in both Gram-positive and Gram-negative bacteria through formation of a pilus-like structure (41-44). In T4S, the ATPase VirD4 is believed to dock substrates on to the machinery and as such has been termed the "coupling protein" (45, 46). In certain systems, such as *Legionella*, VirD4 acts in complex with the chaperone-like proteins, IcmS and IcmW (47). While the molecular roles of IcmS and IcmW are poorly understood, they do not appear to unfold effectors like the T3S chaperones, but rather form an extended platform for substrate docking.

While chaperone functions differ between T3S and T4S chaperones, it is enticing to consider that targeting of substrates to their correct delivery system is dependent on system-specific chaperone-substrate interactions and that such chaperones are the key to understanding substrate sorting.

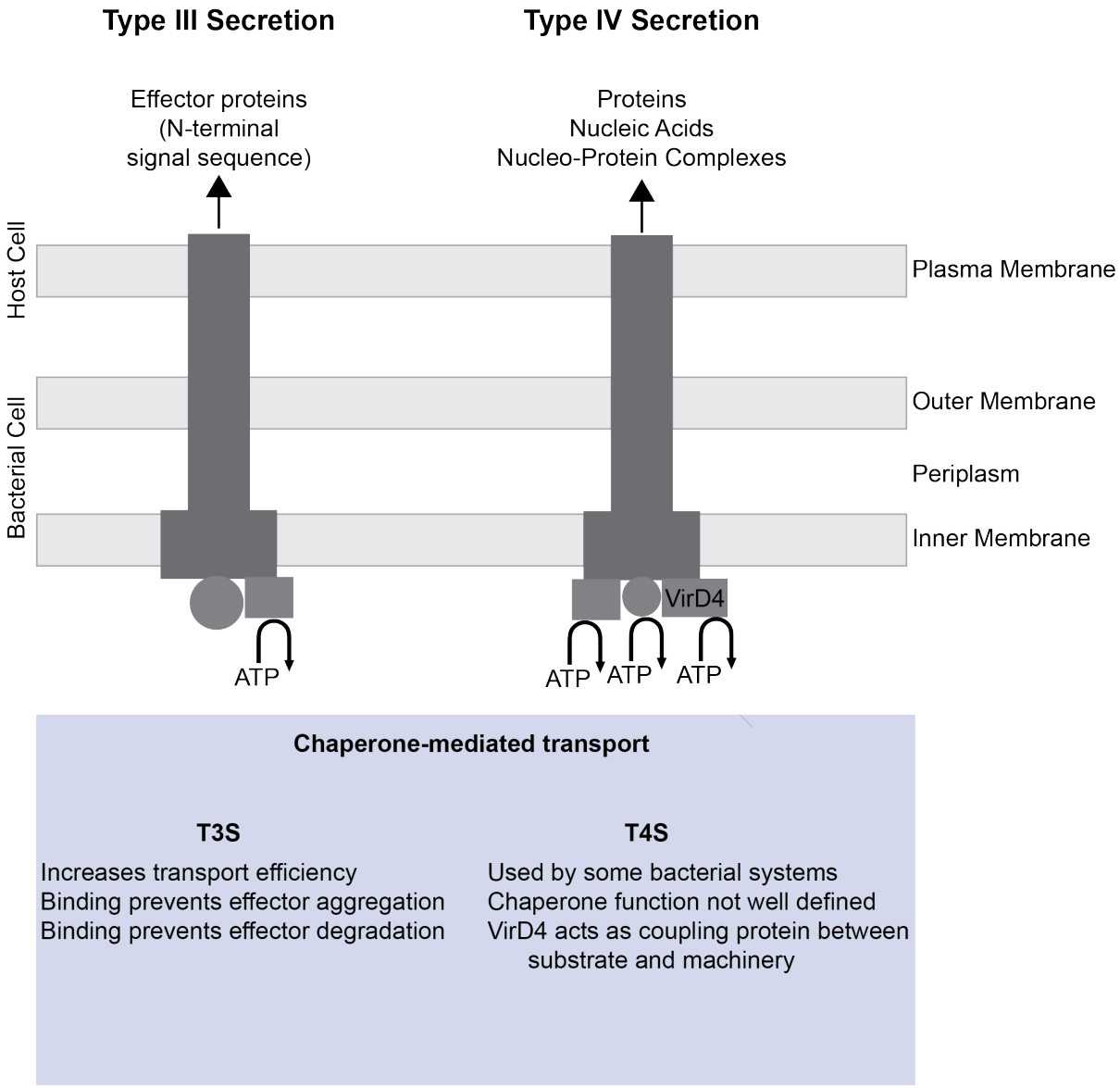

Figure 1.1 Type III and Type IV Secretion in Gram-negative bacteria Some T3S and T4S substrates interact with chaperone-like proteins to aid in their efficient secretion. However, the molecular functions of chaperones within each system are distinct. Oversimplified structures of T3S and T4S machineries are shown with characteristics of described chaperones below.

Recent identification of a chaperone-family in T6S

Recently, a chaperone protein-family has been proposed for type VI secretion (T6S) systems (48, 49). T6S are derived from bacteriophage components, and resemble inverted bacteriophage tails through which substrates are plunged through an inner tube formed of Hcp hexamers. Substrates are generally capped by a tip-forming trimer of VgrG proteins which are themselves often decorated by PAAR-proteins (3, 50-58). About one-third of Gram-negative bacteria encode T6S systems to deliver protein signals into neighboring eukaryotic or prokaryotic cells (59). T6S substrates lack conservation of a signal sequence, and vary in protein size and protein activity. Genetic proximity to genes encoding Hcp, VgrG, or PAAR-protein homologs has classically been used to find putative T6S substrates. Recent bioinformatics described short motif sequences, called MIX motifs, present in known or predicted T6S substrates that may serve as a type of signal sequence (60). Bioinformatics performed by a different research group showed that proteins frequently encoded adjacent to T6S substrates contained a common protein motif- the DUF4123 protein domain. It was proposed that DUF4123-proteins could function as chaperones for T6S substrates (48). While it was demonstrated that DUF4123-proteins bind VgrG proteins *in vitro*, and that they are essential for substrate secretion, it is unclear what molecular functions these chaperone proteins serve and whether targeting to the T6S machinery is one such function (48, 49, 53).

T6S in *Proteus mirabilis* modulates self-recognition behaviors

In the Gram-negative bacterium *Proteus mirabilis*, the T6S is used to deliver proteins that encode information about genetic relatedness. At least two self-recognition

systems, Ids and Idr, use T6S to deliver effectors that encode self-identity information (61, 62). Of these, Ids encodes a DUF4123-protein upstream of the T6S effector (62). Ids is a six-protein system, IdsA through IdsF, encoded within a single operon (**Figure A.1**). IdsA, IdsB, IdsC, and IdsF are well conserved across *P. mirabilis* strains and by protein homology are implicated in aiding in T6S transport; IdsA is an Hcp homolog, IdsB is a VgrG homolog, IdsC is a DUF4123-protein and IdsF is a PAAR-motif protein. However, IdsA is not required for self-recognition to occur (62). IdsD and IdsE encode hypervariable regions (VR) that determine *in vitro* IdsD-IdsE binding. *In vitro* binding correlates to *in vivo* self-recognition behaviors on surfaces (62, 63). Clonal (self) populations will merge upon encountering each other, while non-clonal (non-self) populations will form a macroscopic boundary between them, called the Dienes line (62, 63). Only the binding state of IdsD-IdsE in recipient cells, and not donor cells, contributes to self-recognition behaviors (64). These data led to a model wherein IdsD is secreted from a donor cell in a T6S-dependent manner into a recipient cell. If IdsD is capable of binding IdsE in the recipient cell, this triggers a self recognition phenotype. Conversely, if IdsD is not capable of binding IdsE in the recipient cell, this results in a non-self recognition phenotype.

The regulation of IdsD pre-transport and its targeting to the T6S for delivery remained unresolved questions. Since IdsB and IdsF are required for self-recognition (62), and IdsB is in itself secreted (61), we predicted that they aided in secretion of IdsD and wondered if either IdsB or IdsF played a role in substrate regulation or targeting. The role of IdsC however, remained elusive, until recent literature suggested that DUF4123 proteins function as putative T6S substrate chaperones (48, 49).

In this thesis, I show that IdsD interacts with IdsB, IdsC, and IdsF mostly exclusive of IdsA and IdsE (**Figure 2.1**). This led to a model wherein IdsBCDF form a "secretion" complex in donor cells that was independent of the IdsDE "recognition" complex in recipient cells. I demonstrate that IdsD forms discrete puncta that can be found proximal to the T6S machinery and that these puncta are independent of T6S function as well as IdsE, but do depend on IdsC (Chapter 2). I then show that the IdsC-IdsD interaction is independent of other Ids or T6S proteins and is mediated by the IdsC DUF4123-domain. I show that the IdsC-IdsD interaction is important for localization of IdsD, maintenance of IdsD protein levels, and for secretion of IdsD (Chapter 3). Furthermore, I demonstrate that single amino acid polymorphisms within IdsC uncouple IdsD localization and secretion (**Figure 3.12-Figure 3.14**). This data expanded the molecular model of self-recognition to include IdsC as a protein that clusters IdsD in preparation for delivery in donor cells, and targets it to the T6S machinery. *In vitro*, IdsC and IdsD interact with T6S machinery components, and these interactions are not disrupted by amino acid changes in IdsC. This suggests that IdsC, and perhaps more broadly DUF4123-proteins, couple T6S substrate regulation with substrate secretion and that secretion involves at least three distinct stages: 1) clustering of substrate, 2) targeting to the correct machinery and 3) secretion through machinery.

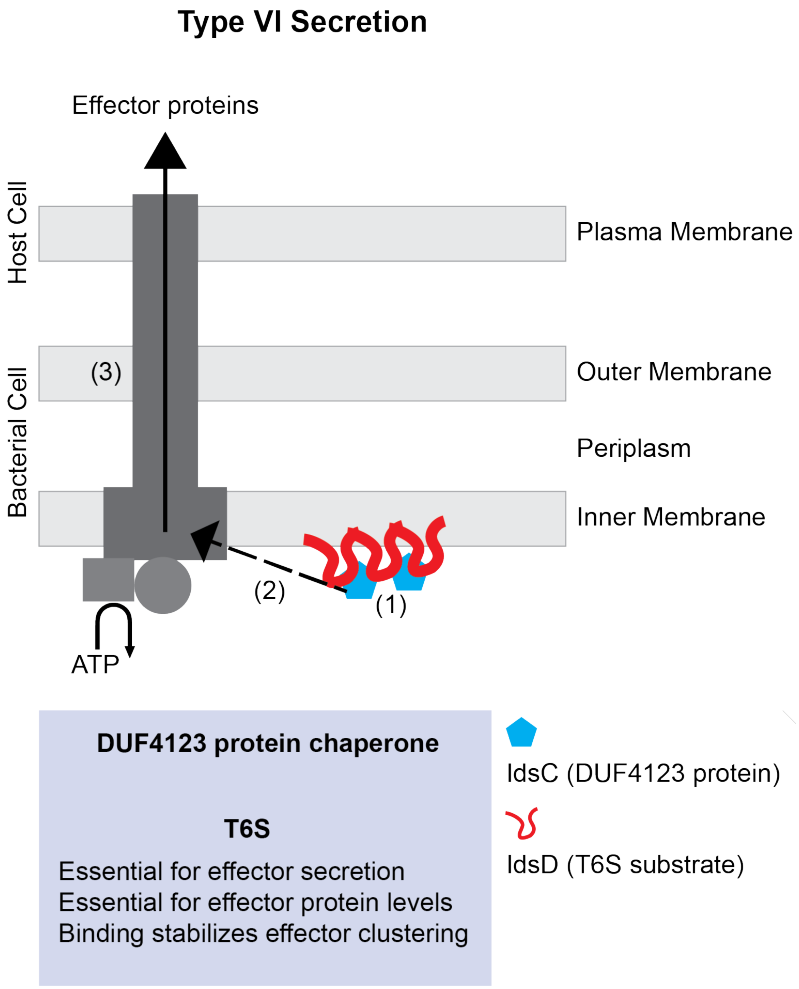

Figure 1.2 Chaperone-dependent regulation of a T6S substrate IdsD is a T6S-dependent effector that encodes self-identity information in *P. mirabilis* (61-63). Based on data presented in this thesis we propose a model wherein (1) IdsC binds IdsD to stabilize IdsD cluster formation in donor cells and couple substrate regulation to (2) substrate targeting. IdsC belong to the recently proposed DUF4123-protein family of T6S chaperones. DUF4123 proteins are commonly found upstream of T6S substrates and have been shown to mediate binding with VgrG proteins, involved in T6S secretion (48, 49, 53). Single amino acid polymorphisms within IdsC uncouple substrate targeting from (3) substrate secretion, indicating that these are distinct steps in the transport of T6S substrates.

Role of *P. mirabilis* self-recognition in nature

While the Gibbs lab has uncovered effects of Ids-mediated self-recognition on *P. mirabilis* population interactions, the role of Ids, and more broadly of self-recognition in natural environments is unclear. *P. mirabilis* is a commensal bacterium in the human gut and an opportunistic pathogen in the human urinary tract, particularly in patients with long-term catheterization. Currently, a mouse host model of *P. mirabilis* exists which has helped provide insights on *P. mirabilis* gene expression (65), cell morphotypes present (66) and factors that influence strain infectivity (65, 67). Using this mouse model, recent work has implicated that Ids is an essential factor for polymicrobial infections of catheter-associated urinary tract infections (68). An open question in the field is whether multiple *P. mirabilis* strains can co-infect a patient and whether social behaviors, like self versus non-self recognition, play a role in colonization of a host. The current mouse model is not sufficient to answer this question due to small sample sizes, cost, and inability to image at a single-bacterial-cell resolution. Therefore, in Chapter 4 I describe work aiming to adapt and expand a *Caenorhabditis elegans* model of *P. mirabilis* infection with the goal of assessing whether laboratory characterization of *P. mirabilis* social behaviors is translatable to *in vivo* conditions in a host.

References

1. **Delepelaire P.** 2004. Type I secretion in gram-negative bacteria. Biochim Biophys Acta **1694:**149-161.

2. **Sato K, Naito M, Yukitake H, Hirakawa H, Shoji M, McBride MJ, Rhodes RG, Nakayama K.** 2010. A protein secretion system linked to bacteroidete gliding motility and pathogenesis. Proc Natl Acad Sci U S A **107:**276-281.

3. **Mougous JD, Cuff ME, Raunser S, Shen A, Zhou M, Gifford CA, Goodman AL, Joachimiak G, Ordonez CL, Lory S, Walz T, Joachimiak A, Mekalanos JJ.** 2006. A virulence locus of *Pseudomonas aeruginosa* encodes a protein secretion apparatus. Science **312:**1526-1530.

4. **Pugsley AP.** 1993. The complete general secretory pathway in gram-negative bacteria. Microbiol Rev **57:**50-108.

5. **Salmond GP, Reeves PJ.** 1993. Membrane traffic wardens and protein secretion in gram-negative bacteria. Trends Biochem Sci **18:**7-12.

6. **Winans SC, Burns DL, Christie PJ.** 1996. Adaptation of a conjugal transfer system for the export of pathogenic macromolecules. Trends Microbiol **4:**64-68.

7. **Brodin P, Rosenkrands I, Andersen P, Cole ST, Brosch R.** 2004. ESAT-6 proteins: protective antigens and virulence factors? Trends Microbiol **12:**500-508.

8. **Provence DL, Curtiss R, 3rd.** 1994. Isolation and characterization of a gene involved in hemagglutination by an avian pathogenic *Escherichia coli* strain. Infect Immun **62:**1369-1380.

9. **Killackey SA, Sorbara MT, Girardin SE.** 2016. Cellular Aspects of *Shigella* Pathogenesis: Focus on the Manipulation of Host Cell Processes. Front Cell Infect Microbiol **6:**38.

10. **Blocker A, Gounon P, Larquet E, Niebuhr K, Cabiaux V, Parsot C, Sansonetti P.** 1999. The tripartite type III secreton of *Shigella flexneri* inserts IpaB and IpaC into host membranes. J Cell Biol **147:**683-693.

11. **Tran Van Nhieu G, Caron E, Hall A, Sansonetti PJ.** 1999. IpaC induces actin polymerization and filopodia formation during *Shigella* entry into epithelial cells. EMBO J **18:**3249-3262.

12. **Bourdet-Sicard R, Rudiger M, Jockusch BM, Gounon P, Sansonetti PJ, Nhieu GT.** 1999. Binding of the *Shigella* protein IpaA to vinculin induces F-actin depolymerization. EMBO J **18:**5853-5862.

13. **Tran Van Nhieu G, Ben-Ze'ev A, Sansonetti PJ.** 1997. Modulation of bacterial entry into epithelial cells by association between vinculin and the *Shigella* IpaA invasin. EMBO J **16:**2717-2729.

14. **Bevan MW, Chilton MD.** 1982. T-DNA of the *Agrobacterium* Ti and Ri plasmids. Annu Rev Genet **16:**357-384.

15. **Schell J, Van Montagu M, De Beuckeleer M, De Block M, Depicker A, De Wilde M, Engler G, Genetello C, Hernalsteens JP, Holsters M, Seurinck J, Silva B, Van Vliet F, Villarroel R.** 1979. Interactions and DNA transfer between *Agrobacterium tumefaciens*, the Ti-plasmid and the plant host. Proc R Soc Lond B Biol Sci **204:**251-266.

16. **Van Gijsegem F, Gough C, Zischek C, Niqueux E, Arlat M, Genin S, Barberis P, German S, Castello P, Boucher C.** 1995. The hrp gene locus of *Pseudomonas solanacearum*, which controls the production of a type III secretion system, encodes eight proteins related to components of the bacterial flagellar biogenesis complex. Mol Microbiol **15:**1095-1114.

17. **Fields KA, Plano GV, Straley SC.** 1994. A low-Ca2+ response (LCR) secretion (ysc) locus lies within the lcrB region of the LCR plasmid in *Yersinia pestis*. J Bacteriol **176:**569-579.

18. **Galan JE, Lara-Tejero M, Marlovits TC, Wagner S.** 2014. Bacterial type III secretion systems: specialized nanomachines for protein delivery into target cells. Annu Rev Microbiol **68:**415-438.

19. **Michiels T, Cornelis GR.** 1991. Secretion of hybrid proteins by the *Yersinia* Yop export system. J Bacteriol **173:**1677-1685.

20. **Ramamurthi KS, Schneewind O.** 2003. Substrate recognition by the *Yersinia* type III protein secretion machinery. Mol Microbiol **50:**1095-1102.

21. **Lloyd SA, Forsberg A, Wolf-Watz H, Francis MS.** 2001. Targeting exported substrates to the *Yersinia* TTSS: different functions for different signals? Trends Microbiol **9:**367-371.

22. **Sory MP, Boland A, Lambermont I, Cornelis GR.** 1995. Identification of the YopE and YopH domains required for secretion and internalization into the cytosol of macrophages, using the *cyaA* gene fusion approach. Proc Natl Acad Sci U S A **92:**11998-12002.

23. **Birtalan SC, Phillips RM, Ghosh P.** 2002. Three-dimensional secretion signals in chaperone-effector complexes of bacterial pathogens. Mol Cell **9:**971-980.

24. **Boyd AP, Lambermont I, Cornelis GR.** 2000. Competition between the Yops of *Yersinia enterocolitica* for delivery into eukaryotic cells: role of the SycE chaperone binding domain of YopE. J Bacteriol **182:**4811-4821.

25. **Feldman MF, Muller S, Wuest E, Cornelis GR.** 2002. SycE allows secretion of YopE-DHFR hybrids by the *Yersinia enterocolitica* type III Ysc system. Mol Microbiol **46:**1183-1197.

26. **Menard R, Sansonetti P, Parsot C, Vasselon T.** 1994. Extracellular association and cytoplasmic partitioning of the IpaB and IpaC invasins of *S. flexneri*. Cell **79:**515-525.

27. **Neyt C, Cornelis GR.** 1999. Role of SycD, the chaperone of the *Yersinia* Yop translocators YopB and YopD. Mol Microbiol **31:**143-156.

28. **Frithz-Lindsten E, Rosqvist R, Johansson L, Forsberg A.** 1995. The chaperone-like protein YerA of *Yersinia pseudotuberculosis* stabilizes YopE in the cytoplasm but is dispensible for targeting to the secretion loci. Mol Microbiol **16:**635-647.

29. **Wattiau P, Bernier B, Deslee P, Michiels T, Cornelis GR.** 1994. Individual chaperones required for Yop secretion by *Yersinia*. Proc Natl Acad Sci U S A **91:**10493-10497.

30. **Wattiau P, Cornelis GR.** 1993. SycE, a chaperone-like protein of *Yersinia enterocolitica* involved in Ohe secretion of YopE. Mol Microbiol **8:**123-131.

31. **Cambronne ED, Cheng LW, Schneewind O.** 2000. LcrQ/YscM1, regulators of the *Yersinia* yop virulon, are injected into host cells by a chaperone-dependent mechanism. Mol Microbiol **37:**263-273.

32. **Cheng LW, Anderson DM, Schneewind O.** 1997. Two independent type III secretion mechanisms for YopE in *Yersinia enterocolitica*. Mol Microbiol **24:**757-765.

33. **Luo Y, Bertero MG, Frey EA, Pfuetzner RA, Wenk MR, Creagh L, Marcus SL, Lim D, Sicheri F, Kay C, Haynes C, Finlay BB, Strynadka NC.** 2001. Structural and biochemical characterization of the type III secretion chaperones CesT and SigE. Nat Struct Biol **8:**1031-1036.

34. **Phan J, Tropea JE, Waugh DS.** 2004. Structure of the *Yersinia pestis* type III secretion chaperone SycH in complex with a stable fragment of YscM2. Acta Crystallogr D Biol Crystallogr **60:**1591-1599.

35. **Singer AU, Desveaux D, Betts L, Chang JH, Nimchuk Z, Grant SR, Dangl JL, Sondek J.** 2004. Crystal structures of the type III effector protein AvrPphF

and its chaperone reveal residues required for plant pathogenesis. Structure **12:**1669-1681.

36. **van Eerde A, Hamiaux C, Perez J, Parsot C, Dijkstra BW.** 2004. Structure of Spa15, a type III secretion chaperone from *Shigella flexneri* with broad specificity. EMBO Rep **5:**477-483.

37. **Birtalan S, Ghosh P.** 2001. Structure of the *Yersinia* type III secretory system chaperone SycE. Nat Struct Biol **8:**974-978.

38. **Evdokimov AG, Tropea JE, Routzahn KM, Waugh DS.** 2002. Three-dimensional structure of the type III secretion chaperone SycE from *Yersinia pestis*. Acta Crystallogr D Biol Crystallogr **58:**398-406.

39. **Stebbins CE, Galan JE.** 2001. Maintenance of an unfolded polypeptide by a cognate chaperone in bacterial type III secretion. Nature **414:**77-81.

40. **Trame CB, McKay DB.** 2003. Structure of the *Yersinia enterocolitica* molecular-chaperone protein SycE. Acta Crystallogr D Biol Crystallogr **59:**389-392.

41. **Bundock P, den Dulk-Ras A, Beijersbergen A, Hooykaas PJ.** 1995. Trans-kingdom T-DNA transfer from *Agrobacterium tumefaciens* to *Saccharomyces cerevisiae*. EMBO J **14:**3206-3214.

42. **Bates S, Cashmore AM, Wilkins BM.** 1998. IncP plasmids are unusually effective in mediating conjugation of *Escherichia coli* and *Saccharomyces cerevisiae*: involvement of the tra2 mating system. J Bacteriol **180:**6538-6543.

43. **Waters VL.** 2001. Conjugation between bacterial and mammalian cells. Nat Genet **29:**375-376.

44. **Grohmann E, Muth G, Espinosa M.** 2003. Conjugative plasmid transfer in gram-positive bacteria. Microbiol Mol Biol Rev **67:**277-301, table of contents.

45. **Gomis-Ruth FX, Sola M, de la Cruz F, Coll M.** 2004. Coupling factors in macromolecular type-IV secretion machineries. Curr Pharm Des **10:**1551-1565.

46. **Atmakuri K, Ding Z, Christie PJ.** 2003. VirE2, a type IV secretion substrate, interacts with the VirD4 transfer protein at cell poles of *Agrobacterium tumefaciens*. Mol Microbiol **49:**1699-1713.

47. **Kwak MJ, Kim JD, Kim H, Kim C, Bowman JW, Kim S, Joo K, Lee J, Jin KS, Kim YG, Lee NK, Jung JU, Oh BH.** 2017. Architecture of the type IV coupling protein complex of *Legionella pneumophila*. Nat Microbiol **2:**17114.

48. **Liang X, Moore R, Wilton M, Wong MJ, Lam L, Dong TG.** 2015. Identification of divergent type VI secretion effectors using a conserved chaperone domain. Proc Natl Acad Sci U S A **112:**9106-9111.

49. **Unterweger D, Kostiuk B, Otjengerdes R, Wilton A, Diaz-Satizabal L, Pukatzki S.** 2015. Chimeric adaptor proteins translocate diverse type VI secretion system effectors in *Vibrio cholerae*. EMBO J **34:**2198-2210.

50. **Pukatzki S, Ma AT, Sturtevant D, Krastins B, Sarracino D, Nelson WC, Heidelberg JF, Mekalanos JJ.** 2006. Identification of a conserved bacterial protein secretion system in *Vibrio cholerae* using the *Dictyostelium* host model system. Proc Natl Acad Sci U S A **103:**1528-1533.

51. **Russell AB, Hood RD, Bui NK, LeRoux M, Vollmer W, Mougous JD.** 2011. Type VI secretion delivers bacteriolytic effectors to target cells. Nature **475:**343-347.

52. **Cianfanelli FR, Alcoforado Diniz J, Guo M, De Cesare V, Trost M, Coulthurst SJ.** 2016. VgrG and PAAR Proteins Define Distinct Versions of a Functional Type VI Secretion System. PLoS Pathog **12:**e1005735.

53. **Bondage DD, Lin JS, Ma LS, Kuo CH, Lai EM.** 2016. VgrG C terminus confers the type VI effector transport specificity and is required for binding with PAAR and adaptor-effector complex. Proc Natl Acad Sci U S A **113:**E3931-3940.

54. **Bonemann G, Pietrosiuk A, Diemand A, Zentgraf H, Mogk A.** 2009. Remodelling of VipA/VipB tubules by ClpV-mediated threading is crucial for type VI protein secretion. EMBO J **28:**315-325.

55. **Hachani A, Allsopp LP, Oduko Y, Filloux A.** 2014. The VgrG proteins are "a la carte" delivery systems for bacterial type VI effectors. J Biol Chem **289:**17872-17884.

56. **Hachani A, Lossi NS, Hamilton A, Jones C, Bleves S, Albesa-Jove D, Filloux A.** 2011. Type VI secretion system in *Pseudomonas aeruginosa*: secretion and multimerization of VgrG proteins. J Biol Chem **286:**12317-12327.

57. **Shneider MM, Buth SA, Ho BT, Basler M, Mekalanos JJ, Leiman PG.** 2013. PAAR-repeat proteins sharpen and diversify the type VI secretion system spike. Nature **500:**350-353.

58. **Whitney JC, Beck CM, Goo YA, Russell AB, Harding BN, De Leon JA, Cunningham DA, Tran BQ, Low DA, Goodlett DR, Hayes CS, Mougous JD.** 2014. Genetically distinct pathways guide effector export through the type VI secretion system. Mol Microbiol **92:**529-542.

59. **Gallique M, Bouteiller M, Merieau A.** 2017. The Type VI Secretion System: A Dynamic System for Bacterial Communication? Front Microbiol **8:**1454.

60. **Salomon D, Kinch LN, Trudgian DC, Guo X, Klimko JA, Grishin NV, Mirzaei H, Orth K.** 2014. Marker for type VI secretion system effectors. Proc Natl Acad Sci U S A **111:**9271-9276.

61. **Wenren LM, Sullivan NL, Cardarelli L, Septer AN, Gibbs KA.** 2013. Two independent pathways for self-recognition in *Proteus mirabilis* are linked by type VI-dependent export. MBio **4**.

62. **Gibbs KA, Urbanowski ML, Greenberg EP.** 2008. Genetic determinants of self identity and social recognition in bacteria. Science **321:**256-259.

63. **Cardarelli L, Saak C, Gibbs KA.** 2015. Two Proteins Form a Heteromeric Bacterial Self-Recognition Complex in Which Variable Subdomains Determine Allele-Restricted Binding. MBio **6:**e00251.

64. **Saak CC, Gibbs KA.** 2016. The Self-Identity Protein IdsD Is Communicated between Cells in Swarming *Proteus mirabilis* Colonies. J Bacteriol **198:**3278-3286.

65. **Pearson MM, Yep A, Smith SN, Mobley HL.** 2011. Transcriptome of *Proteus mirabilis* in the murine urinary tract: virulence and nitrogen assimilation gene expression. Infect Immun **79:**2619-2631.

66. **Jansen AM, Lockatell CV, Johnson DE, Mobley HL.** 2003. Visualization of *Proteus mirabilis* morphotypes in the urinary tract: the elongated swarmer cell is rarely observed in ascending urinary tract infection. Infect Immun **71:**3607-3613.

67. **Sosa V, Schlapp G, Zunino P.** 2006. *Proteus mirabilis* isolates of different origins do not show correlation with virulence attributes and can colonize the urinary tract of mice. Microbiology **152:**2149-2157.

68. **Armbruster CE, Forsyth-DeOrnellas V, Johnson AO, Smith SN, Zhao L, Wu W, Mobley HLT.** 2017. Genome-wide transposon mutagenesis of *Proteus mirabilis*: Essential genes, fitness factors for catheter-associated urinary tract infection, and the impact of polymicrobial infection on fitness requirements. PLoS Pathog **13:**e1006434.

Chapter 2

Localization of a T6S substrate is independent of T6S activity but depends on a DUF4123 proposed chaperone protein

Some of the work presented in this chapter was published as part of Zepeda-Rivera, MA, Saak C.C., Gibbs K.A. A proposed chaperone for the bacterial type VI secretion system functions to constrain a self-identity protein. J Bacteriol. 2018 Mar 19. PMID: 29444703. Full publication can be found in Appendix B.

Abstract

Proteus mirabilis encodes and interprets information about self-identity within two proteins, IdsD and IdsE. Of these, IdsD is exchanged between cells by the type VI secretion (T6S) machinery, which is widely conserved across Gram-negative bacteria. Only after being transported into neighboring cells does IdsD interact with its self-identity protein partner, IdsE. While IdsD secretion is known to be T6S-dependent, IdsD interactions with T6S proteins and its localization relative to the T6S machinery remained unknown. Furthermore, whether these interactions could sequester IdsD in producing cells to inhibit the IdsD-IdsE interaction remained untested. Here I show that IdsD interacts with homologs of known T6S-associated proteins as well as components of the core T6S machinery itself. Additionally, I demonstrate that IdsD localizes into discrete puncta that are often, but not always, found proximal to the T6S machinery. Finally, I show IdsD localization is not dependent on T6S function, but is dependent on IdsC, a protein belonging to a proposed family of T6S-substrate chaperones.

Introduction

Self versus non-self recognition behaviors in the bacterium *Proteus mirabilis* result in the physical separation between clonal (self) populations and foreign (non-self) populations. Self-identity information is encoded within IdsD, a protein that is secreted by the type VI secretion (T6S) machinery into neighboring cells, where it interacts with its self-identity partner protein, IdsE (1-4). Although IdsD is known to be a T6S substrate, its interactions with the T6S machinery and its localization relative to the machinery were unknown. Furthermore, other proteins encoded by the *ids* operon

(**Figure A.1**) share homology with proteins involved in T6S transport in other bacterial systems. Unlike many other bacterial systems, *P. mirabilis* encodes a single T6S locus. It remained unclear whether IdsD interacts with these T6S-associated proteins and whether these interactions would affect IdsD localization or transport in producing cells. Furthermore, previous work demonstrated that IdsD and IdsE do not interact in producing cells (4). One possibility is that interactions between IdsD and the T6S machinery, in preparation for IdsD secretion, prevent IdsD-IdsE interactions in producing cells.

Here I take an unbiased approach to look at IdsD protein partners, and confirm a subset of results through western blot analysis. I assessed that IdsD interacts with both Ids T6S-associated proteins as well as components of the core machinery. I localized IdsD and show that it can be found proximal to the machinery and that its localization is independent of T6S function. Surprisingly, its localization is dependent on one Ids protein, IdsC, which belongs to a proposed family of chaperones for T6S-substrates.

Materials and Methods

Bacterial strains and media

All strains are described in **Table 2.1**. *P. mirabilis* strains were maintained on LSW- agar (5). *P. mirabilis* was grown on CM55 Blood Agar Base agar (Oxoid, Basingstoke, England) for colony growth assays. For broth cultures, all strains were grown in LB broth under aerobic conditions at 37°C. Antibiotics were used at the following concentrations: 15 microgram per milliliter (μg/mL) tetracycline; 35 μg/mL kanamycin; and 50 μg/mL chloramphenicol.

Expression plasmids

All plasmids used are described in **Table 2.2**. Gene fragments (gBlocks) (Integrated DNA Technologies, Coralville, IA) were used for cloning of pIds-derived vectors. Listed gBlocks were sub-cloned into TOPO pCR2.1 vector using the TOPO TA-Cloning Kit (Thermo Fisher Scientific, Waltham, MA). The FLAG epitope is DYKDDDDK and was introduced into genes *idsA*, *idsC*, *idsE*, and *idsF* in pIds using standard Quikchange reaction protocols (Agilent Technologies, Santa Clara, CA). pIds-derived plasmids were constructed via restriction digest using listed restriction enzymes (New England BioLabs, Ipswich, MA) of noted plasmids. Restriction digest was followed by overnight ligation at 16°C and subsequent transformation into OneShot Omnimax2 T1R competent cells (Thermo Fisher Scientific, Waltham, MA). Resultant plasmids were confirmed by sequencing (Genewiz, Inc., South Plainfield, NJ). Vectors were then transformed into S17λpir, which was used to conjugate plasmids into *P. mirabilis* as previously described (1). To test that epitope-tagged proteins remained functional, boundary assays were performed (**Figure A.2**).

Anti-FLAG pull-downs from *P. mirabilis* cell extracts

P. mirabilis strains carrying pIds plasmids were inoculated from overnight cultures onto CM55 swarm agar plates and incubated at 37°C 16-20 hours until the population almost reached the edge of the petri dish. Cells from five plates were re-suspended in 5 mL LB each and harvested by centrifugation. Pellets were re-suspended in 1 mL cell lysis buffer (50mM Tris HCl pH 7.4, 150mM NaCl, 1% triton X-100, 1 mM EDTA) supplemented with 40 µl of either Complete protease inhibitor cocktail (Roche,

Basel, Switzerland) or Biotools protease inhibitor cocktail (Biotools, Houston, TX) and lysed by vortexing with cell disruptor beads (0.1-diameter, Electron Microscopy Sciences, Hatfield, PA). Lysates were cleared by centrifugation and 900 µL was applied to 40 µL pre-equilibrated α-FLAG M2 antibody resin (Sigma-Aldrich, St. Louis, MO; Biotools, Houston, TX). Control lysate (containing pIds with no FLAG-tagged protein) was supplemented with 2 µg of purified FLAG-tagged *E. coli* bacterial alkaline phosphatase (FLAG-BAP) protein (Sigma-Aldrich, St. Louis, MO). Lysates were incubated with resin for two hours at 4°C. Unbound cell extract was removed. Resin was washed five times in wash buffer (50mM Tris HCl pH 7.4, 150mM NaCl, 1% triton X-100), and bound proteins were eluted with 50 µl of elution buffer (50mM Tris HCl pH 7.4, 150mM NaCl, 200 ng/µl 3XFLAG peptide) for 45 minutes at 4°C. The elution was re-centrifuged and the top 40 µl was retained. Samples of load (L), non-binding (-) and binding (+) fractions were separated by SDS-PAGE and analyzed by liquid chromatography tandem mass spectrometry or western blot.

Antibody generation

Antibodies specific to IdsB amino acids 713-723 (CRAKAMKKGTA), IdsD amino acids 4-18 (EVNEKYLTPQERKAR) and IdsE amino acids 298-312 (EQILAKLDQEKEHHA) were raised in rabbits using standard peptide protocols (Covance, Dedham, MA).

SDS-PAGE and western blots

Samples from the above co-immunoprecipitation assays were separated by gel electrophoresis using 12% Tris-Tricine polyacrylamide gels, transferred to nitrocellulose membranes, and probed with: rabbit α-IdsB (1:5000), rabbit α-IdsD (1:2000); rabbit α-IdsE (1:2000); rabbit α-FLAG (1:4000, Sigma-Aldrich, St. Louis, MO); rabbit α-mKate (1:4000, OriGene, Rockville, MD); mouse α-σ^{70} (1:1000, Thermo Fisher Scientific, Waltham, MA) or (1:1000, BioLegend, San Diego, CA) followed by goat α-rabbit or goat α-mouse conjugated to HRP (1:5000, KPL, Inc., Gaithersburg, MD) and developed with Immun-Star HRP Substrate Kit (Bio-Rad Laboratories, Hercules, CA). Blots were visualized using a Chemidoc (Bio-Rad Laboratories, Hercules, CA). Figures were made in Adobe Illustrator (Adobe Systems, San Jose, CA).

Liquid chromatography tandem mass-spectrometry

Binding samples from α-FLAG immunoprecipitations were separated by gel electrophoresis using 12% Tris-Tricine polyacrylamide gels. Bands were cut between 0-37 kDa, 37-75 kDa, and 75-250 kDa and sent to LC-MS/MS analysis (Taplin Mass Spectrometry Core Facility, Harvard Medical School, Boston MA). Technical advice provided by the Taplin Mass Spectrometry Facility led to a three unique peptide cutoff to confirm protein hits. Bioinformatics analysis of Ids and T6S protein hits was done using Pfam 31.0 (6). Full data tables can be found in 'LABSTORAGE' on Gibbs Laboratory Data Computer under 'Martha' 'Mass Spectrometry' 'Data Spreadsheets' subfolder.

Microscopy

Strains were grown overnight shaking in LB supplemented with kanamycin at 37°C. 1.0 mm-thick agar pads of swarming permissive media supplemented with kanamycin were inoculated with 2 μl of overnight cultures and incubated in a humidified chamber at 37° for 4 to 6 hours. Images were acquired either with a Leica DM5500B (Leica Microsystems, Buffalo Grove, IL) with a CoolSnap HQ^2 cooled CCD camera (Photometrics, Tucson, AZ) or an Olympus BX61 (Olympus Corporation, Waltham, MA) with a Hamamatsu C10600-10B CCD camera (Hamamtsu Phototonics K.K., Boston, MA). MetaMorph version 7.8.0.0 (Molecular Devices, Sunnyvale, CA) was used for image acquisition. Figures were made in Fiji (7, 8) and Adobe Illustrator (Adobe Systems, San Jose, CA).

***P. mirabilis* boundary assays**

Self-recognition phenotype of test strains was examined against the parent strain BB2000 and BB2000 lacking the *ids* genes (Δ*ids*), each carrying a plasmid to confer kanamycin resistance. Epitope-tagged and fluorescent-fusion proteins were deemed functional if test strain merged with BB2000 and formed a boundary with Δ*ids* (**Figure A.2**). Strains were grown up in liquid-broth under aerobic conditions at 37°C. Cultures were normalized by optical density at 600 nm (OD_{600}) and spotted on swarming permissive CM55 Blood Agar Base agar (Oxoid, Basingstoke, England) plates supplemented with 2 mg/mL Coomassie blue, 4 mg/mL congo red dyes, and 35 μg/mL kanamycin. Plates were incubated overnight at 37°C.

Table 2.1 Strains used in this study

Strain	Notes	Source	KAG #	MZR #	Plasmid
Δ*ids*	Δ*ids::Tn-Cm(R)*	(1)	006	002	
Δ*ids* + pIds-IdsA-FLAG	Modified protein(s): IdsA-FLAG Δ*ids* carrying a modified pIds plasmid with a C-terminal FLAG-tag encoded in-frame with *idsA*.	(3)	930	029	pLMW06
Δ*ids* + pIds-FLAG-IdsC	Modified protein(s): FLAG-IdsC Δ*ids* carrying a modified pIds plasmid with an N-terminal FLAG-tag encoded in-frame with *idsC*.	This study	644/ 645	039/ 167	pLC-001
Δ*ids* + pIds-FLAG-IdsD	Modified protein(s): FLAG-IdsD Δ*ids* carrying a modified pIds plasmid with an N-terminal FLAG-tag encoded in-frame with *idsD*.	(2)	661	036	pLC-015
Δ*ids* + pIds-FLAG-IdsE	Modified protein(s): FLAG-IdsE Δ*ids* carrying a modified pIds plasmid with an N-terminal FLAG-tag encoded in-frame with *idsE*.	(2)	655	045	pLC-013
Δ*ids* + pIds-IdsF-FLAG	Modified protein(s): IdsF-FLAG Δ*ids* carrying a modified pIds plasmid with a C-terminal FLAG-tag encoded in-frame with *idsF*.	This study	657	042	pLC-014

Table 2.1 Strains used in this study (continued)

Δ*ids:: BB2000_0821-sfGFP*	Modified protein(s): TssB-sfGFP Δ*ids* with chromosomal *BB2000_0821* fused to superfolder GFP.	(9)	2537		
Δ*ids::BB2000_0821-sfGFP* + pIds-FLAG-IdsC-mKate2-IdsD	Modified protein(s): TssB-sfGFP, FLAG-IdsC, mKate2-IdsD Δ*ids::BB2000_0821-sfGFP* carrying a modified pIds plasmid with an N-terminal FLAG-tag encoded in-frame with *idsC* and an N-terminal mKate2 fluorophore fused to *idsD*.	This study	2874	169	pMZ49
Δ*ids:: BB2000_0821*$_{T95G}$ (CCS05)	Modified protein(s): $TssB_{L32R}$ Δ*ids* with chromosomal *BB2000_0821* with a single T → G point mutation at base pair 95. This results in a disrupted T6S sheath.	(4)	2115		
CCS05+pIds-FLAG-IdsC-mKate2-IdsD	Modified protein(s): $TssB_{L32R}$, FLAG-IdsC, mKate2-IdsD CCS05 carrying a modified pIds plasmid with an N-terminal FLAG-tag encoded in-frame with *idsC* and an N-terminal mKate2 fluorophore fused to *idsD*.	This study	3278	302	pMZ49
*BB2000_0808**	Modified protein(s): IcmF* *BB2000_0808::Tn-Cm(R)*. First described as *tssN** in (3).	(3)	633	010	

Table 2.1 Strains used in this study (continued)

*BB2000_0808** +pIds-FLAG-IdsC-mKate2-IdsD	Modified protein(s): IcmF*, FLAG-IdsC, mKate2-IdsD *BB2000_0808** carrying a modified pIds plasmid with an N-terminal FLAG-tag encoded in-frame with *idsC* and an N-terminal mKate2 fluorophore fused to *idsD*.	This study	2870	238	pMZ49
*BB2000_0808** +pIds-FLAG-IdsD	Modified protein(s): IcmF*, FLAG-IdsD *BB2000_0808** carrying a modified pIds plasmid with an N-terminal FLAG-tag encoded in-frame with *idsD*.	(3)	835	037	pLC-015
Δ*ids::BB2000_0814*$_{G1145A}$	Modified protein(s): $TssK_{S382N}$ BB2000 with chromosomal *BB2000_0814* with a G→A point mutation at base pair 1145.	This study	2107		
Δ*ids*::*BB2000_0814*$_{G1145A}$ c. pIds-FLAG-IdsC-mKate2-IdsD	Modified protein(s): $TssK_{S382N}$, FLAG-IdsC, mKate2-IdsD Δ*ids* with chromosomal *BB2000_0814* with a G→A point mutation at base pair 1145 linked to carrying a modified pIds plasmid in which an N-terminal FLAG epitope tag is encoded in-frame with *idsC* and an N-terminal mKate2-fluorophore is encoded in frame with *idsD*.	This study	3282	304	pMZ49

Table 2.1 Strains used in this study (continued)

Δ*ids*::*BB2000_0814*$_{G1145A}$ c. pIds-FLAG-IdsD	Modified protein(s): $TssK_{S382N}$, FLAG-IdsD Δ*ids* with chromosomal *BB2000_0814* with a G→A point mutation at base pair 1145 linked to carrying a modified pIds plasmid in which an N-terminal FLAG epitope tag is encoded in-frame with *idsD*.	This study	3168	266	pLC-015
Δ*ids*::*BB2000_0814*$_{G1329T}$	Modified protein(s): $TssK_{W443C}$ BB2000 with chromosomal *BB2000_0814* with a G→T point mutation at base pair 1329.	This study	2255		
Δ*ids*::*BB2000_0814*$_{G1329T}$ c. pIds-FLAG-IdsC-mKate2-IdsD	Modified protein(s): $TssK_{W443C}$, FLAG-IdsC, mKate2-IdsD Δ*ids* with chromosomal *BB2000_0814* with a G→T point mutation at base pair 1329 carrying a modified pIds plasmid. Plasmid has an N-terminal FLAG epitope tag encoded in-frame with *idsC* and an N-terminal mKate2-fluorophore fused to *idsD*.	This study	3286	306	pMZ49
Δ*ids*::*BB2000_0814*$_{G1329T}$ c. pIds-FLAG-IdsD	Modified protein(s): $TssK_{W443C}$, FLAG-IdsD Δ*ids* with chromosomal *BB2000_0814* with a G→T point mutation at base pair 1329 carrying a modified pIds plasmid. Plasmid has an N-terminal FLAG epitope tag encoded in-frame with *idsD*.	This study	3172	270	pLC-015

Table 2.1 Strains used in this study (continued)

CCS05 c. pIds-723mt-FLAG-IdsC-mKate2-IdsD	Modified protein(s): $TssB_{L32R}$, ΔIdsB, FLAG-IdsC, mKate2-IdsD CCS05 carrying a modified pIds plasmid with a 711-bp disruption of IdsB (1). Plasmid also has an N-terminal FLAG epitope encoded in-frame with *idsC* and an N-terminal mKate2-fluorophore fused to *idsD*.	This study	3180	273	pMZ52
CCS05 c. pIds-FLAG-$IdsC^{\Delta DUF4123}$-mKate2-IdsD	Modified protein(s): $TssB_{L32R}$, FLAG-$IdsC^{\Delta DUF4123}$, mKate2-IdsD CCS05 carrying a modified pIds plasmid with an N-terminal FLAG-tag encoded in-frame with *idsC* with nucleotides 373-762 deleted and an N-terminal mKate2 fluorophore fused to *idsD*.	This study	2730	157	pMZ34
CCS05 c. pIds-FLAG-IdsC-mKate2-IdsD-ΔIdsE	Modified protein(s): $TssB_{L32R}$, FLAG-IdsC, mKate2-IdsD, ΔIdsE Δ*ids* carrying a modified pIds plasmid with an N-terminal FLAG-tag encoded in-frame with *idsC* and an N-terminal mKate2 fluorophore fused to *idsD*. In-frame deletion of *idsE*.	This study	3002	246	pMZ51
Δ*ids* + pIds-FLAG-IdsC-mKate2-IdsD	Modified protein(s): FLAG-IdsC, mKate2-IdsD Δ*ids* carrying a modified pIds plasmid with an N-terminal FLAG-tag encoded in-frame with *idsC* and an N-terminal mKate2 fluorophore fused to *idsD*.	This study	2868	173	pMZ49

Table 2.1 Strains used in this study (continued)

Δ*ids* + pIds-FLAG-IdsC$^{\Delta DUF4123}$-mKate2-IdsD	Modified protein(s): FLAG-IdsC$^{\Delta DUF4123}$, mKate2-IdsD Δ*ids* carrying a modified pIds plasmid with an N-terminal FLAG-tag encoded in-frame with *idsC* with nucleotides 373-762 deleted and an N-terminal mKate2 fluorophore fused to *idsD*.	This study	2720	155	pMZ34
OneShot Omnimax 2 T1R Competent Cells	Cloning strain for pIds-derived plasmids	Thermo Fisher Scientific, Waltham, MA.			
S17λpir	*Escherichia coli* mating strain to introduce plasmids into *P. mirabilis*	(10)	068		

Table 2.2 Primers used in this study

Plasmid	Construction details (primers and gBlocks 5' → 3')
pIds-FLAG-IdsC	FLAG epitope (DYKDDDDK) was introduced 5' of *idsC* in pIds using Quikchange reaction protocols (Agilent Technologies, Santa Clara, CA). F: GCGAAAGCGATGAAAAAAGGAACGGCCTAATGGACTA CAAAGACGATGACGATAAACTCTTGAGTCCAAATCCCC TCTATAAAGCG R: CGCTTTATAGAGGGGATTTGGACTCAAGAGTTTATCGTCAT CGTCTTTGTAGTCCATTAGGCCGTTCCTTTTTTCATCGCTTT CGC
pIds-IdsF-FLAG	FLAG epitope (DYKDDDK) was introduced 3' of *idsF* in pIds using Quikchange reaction protocols (Agilent Technologies, Santa Clara, CA). F: GTTCAGATGGCTGTATACTCGTTGCAACAGATGACTACAAAGACG ATGACGATAAATAAGCGATACCCAATATCATGTATCATAAATAAA AAATGATA R: TATCATTTTTTATTTATGATACATGATATTGGGTATCGCTTATTTAT CGTCATCGTCTTTGTAGTCATCTGTTGCAACGAGTATACAGCCATC TGAAC
pIds-FLAG-IdsC-mKate2-IdsD	Constructed by restriction digest of pIds-mKate2-IdsD and pIds-FLAG-IdsC using BstEII/PacI.
pIds-FLAG-IdsC$^{\Delta DUF4123}$	Deletion of basepairs 373 to 762 in *idsC* in pIds-FLAG-IdsC using gBlock and restriction digest with BstEII/PacI. Geneblock: GGTTACCATTAGCTGAGGATTGCCGTGCGAAAGCGATGAAAAAAG GAACGGCCTAATGGACTACAAAGACGATGACGATAAACTCTTGAG TCCAAATCCCCTCTATAAAGCGTATTGGGTTGCTCAATGCCGTTAT ACTCGCAACGGTGAACAATTCAAGGGGGTGATGACCGTAGCAGGT ACAAGTCAATCACAAGCTATTAAGCAGATGCGCCAGTACTTTACG GCTCACCCAGGTGAATATACCTTTGCGGACTATGACACATTAATCC CTTTAATCACCCATATTGAACAAAGTTCAACCTTAGAATTACCGTT AATACGGCAAGTACGTGAGCAACATAATGCAAAGGTTTCAGCCGT ATTAGTGGATAAATGCAACCTCACACACCCAAGACCGTCAGAAAA AGGCGACATTCATTACCGTGAGGGGCAACCTACGTTTATTGAATAT TCGCATTAA
pIds-FLAG-IdsC$^{\Delta DUF4123}$-mKate2-IdsD	Constructed by restriction digest of pIds-mKate2-IdsD and pIds-FLAG-IdsC$^{\Delta DUF4123}$ using BstEII/PacI.

Table 2.2 Primers used in this study (continued)

pIds-723mt-FLAG-IdsC-mKate2-IdsD	Constructed by restriction digest of pIds-FLAG-IdsC-mKate2-IdsD and pIds-723mt (1) using BstEII/NheI.
pIds-FLAG-IdsC-mKate2-IdsD-ΔIdsE	Deletion of *idsE* in pIds-FLAG-IdsC-mKate2-IdsD using gBlock (4) and restriction digest with EcoNI/KpnI. Geneblock: GCGAACAATTAAAAATGGCAAGTGAAAAAGGTGATTGGAACCCTG AAACAGGTATATTTAAATTTAGTTTGGAAGTACAGTCTCAATTAGT AAATACATATTCTGCTTTTGGTGCACATCCTAATAGCCGTATAGGT ATTGAAGATTTATATTGGTATTATCAAGTCAATCCCGAGGTAACAA CACCGATGCGTTATATCAATTGGGGGGGAGATACCCAAGAAAACA ATCAGCTTTTAGGCTTTATTAACAGGAGAATATCTAAATCAGGAGA AAGAACACCATGCGTAGTTTGGTAAACGGCAGAAAGATTATTTTA GAAAATGATACAACAAATACCGGCGGTACCGTACTTACCGGCTCT

Results

IdsBCDF form a protein interaction network

We predicted that IdsD interacts with T6S-associated Ids proteins in preparation for its delivery. T6S delivery requires contraction of a sheath and plunging of an inner tube comprised of Hcp hexamers (11, 12). T6S substrates typically interact with the Hcp tube as well as VgrG proteins that form the tip of the spike for membrane penetration (13-16). VgrG proteins themselves are often decorated by PAAR-proteins (15, 17). Therefore, IdsD was predicted to interact with IdsA (Hcp homolog), IdsB (VgrG homolog, and IdsF (PAAR-domain protein). To assay for the protein-interactions partners, an established Ids expression system was used in which all *ids* genes are expressed from a plasmid under regulation of the native *ids* promoter (pIds) in a parent strain lacking the *ids* genes (1). IdsD was modified with an N-terminal FLAG-epitope (2), and cell extracts were subjected to anti-FLAG co-immunoprecipitations. To detect direct and indirect interactions partners, the binding fraction was analyzed using liquid chromatography tandem mass spectrometry (LC-MS/MS) (**Table 2.3**). FLAG-IdsD pulled down IdsB, IdsC, IdsD, IdsE, and IdsF. FLAG-IdsD did not pull down IdsA, consistent with previous phenotypic data (1).

To confirm these interactions, I performed anti-FLAG co-immunoprecipitations on cell extracts from *P. mirabilis* separately expressing IdsA-FLAG, FLAG-IdsC, FLAG-IdsE, or IdsF-FLAG. *P. mirabilis* extract with no FLAG-tagged proteins doped with purified FLAG-tagged *Escherichia coli* bacterial alkaline phosphatase (FLAG-BAP) was used as a negative control. The load (L), non-binding (-) and binding (+) fractions were analyzed by western blot using custom polyclonal anti-IdsB, anti-IdsD, anti-IdsE or

commercial anti-FLAG, and anti-sigma70 antibodies. IdsA-FLAG did not pull down any Ids proteins, consistent with previous phenotypic data (1) and was therefore omitted from further analysis (**Figure 2.1**). Due to lack of anti-IdsC and anti-IdsF antibodies, binding fractions were additionally analyzed by LC-MS/MS (**Table 2.4** and **Table 2.5**). IdsB, IdsC, and IdsF pulled down each other and IdsD but not IdsE (**Figure 2.1, Table 2.4** and **Table 2.5**) suggesting these interactions are independent of IdsE. While LC-MS/MS analysis of the FLAG-IdsC binding fraction showed trace amounts of IdsE (**Table 2.4**), this result was not visible by western blot. LC-MS/MS analysis of the IdsF-FLAG binding fraction additionally showed traced amounts of IdsA. Therefore, IdsBCDF appear to interact with each other predominantly without IdsA and IdsE.

Table 2.3 Ids and T6S specific LC-MS/MS hits pulled down by FLAG-IdsD

Protein	No. unique peptides	No. total peptides	% Coverage	Expected Size (kDa)	Gel Fragment (kDa)
IdsB	35	103	42.32	81.5	75-250
IdsC	20	35	35.87	47.1	37-75
IdsD	85	166	57.45	118.2	75-250
IdsF	3	3	25.84	9.1	0-37
BB2000_0820	6	7	13.21	55.8	37-75
BB2000_0818	4	4	7.28	67.9	37-75
BB2000_0814	5	5	10.18	51.2	37-75

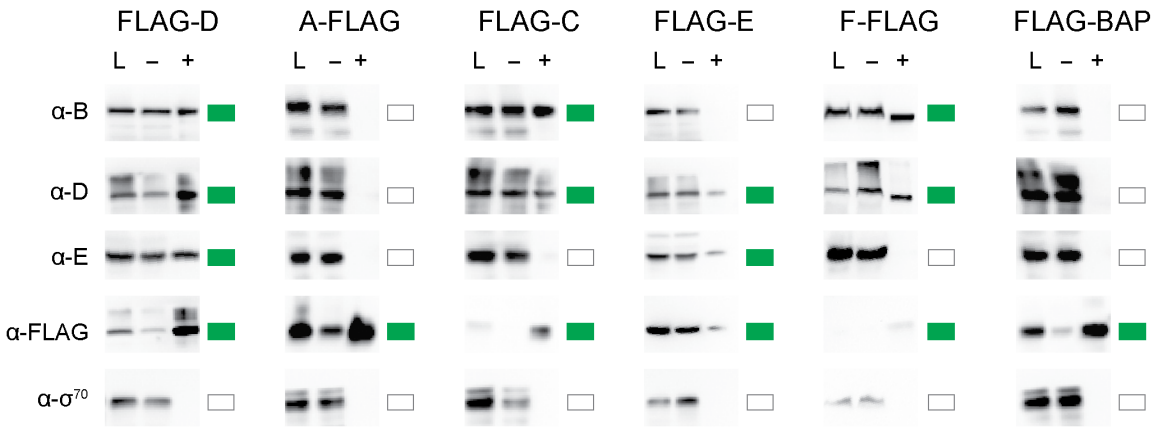

Figure 2.1 IdsBCDF form a protein complex almost exclusive of IdsA and IdsE Anti-FLAG co-immunoprecipitation assays were performed as previously described (2). Soluble (L), non-binding (-) and binding (+) fractions were analyzed via western blot using polyclonal anti-IdsB, polyclonal anti-IdsD, polyclonal anti-IdsE, monoclonal anti-FLAG, and monoclonal anti-sigma70 antibodies. Green boxes indicate a band in the binding fraction; white boxes indicate no band in the binding fraction. Bait samples are labeled above: FLAG-IdsD (2), IdsA-FLAG, FLAG-IdsC, FLAG-IdsE (2), IdsF-FLAG, and FLAG-BAP, which is a purified FLAG-tagged *E. coli* protein mixed with *P. mirabilis* lysate. All Ids proteins were individually modified with a FLAG epitope and expressed in Δ*ids* cells on a modified pIds plasmid (1).

Table 2.4 Ids and T6S specific LC-MS/MS hits pulled down by FLAG-IdsC

Protein	No. unique peptides	No. total peptides	% Coverage	Expected Size (kDa)	Gel Fragment (kDa)
IdsB	42	98	45.37	81.5	75-250
IdsC	21	44	42.01	47.1	37-75
IdsD	80	174	49.52	118.2	75-250
IdsE	3	4	8.33	37	37-75
IdsF	6	10	51.69	9.1	0-37
BB2000_0821	3	5	19.28	18.4	0-37
BB2000_0820	9	10	22.56	55.8	37-75
BB2000_0818	5	7	9.48	67.9	37-75
BB2000_0817	5	6	14.78	39.4	37-75
BB2000_0814	9	15	20.13	51.2	37-75
BB2000_0806	4	5	7.61	67	37-75

Table 2.5 Ids and T6S specific LC-MS/MS hits pulled down by IdsF-FLAG

Protein	No. unique peptides	No. total peptides	% Coverage	Expected Size (kDa)	Gel Fragment (kDa)
IdsA‡	6	12	27.33	18.9	37-75
IdsB	27	66	33.06	81.5	75-250
IdsC	17	23	33.91	47.1	37-75
IdsD	43	90	37.14	118.2	75-250
IdsF	10	26	53.93	9.1	0-37

IdsCDF interact with conserved T6S components

IdsB and IdsF show homology to proteins implicated in T6S-dependent substrate transport in other bacterial systems. IdsC contains a DUF4123 protein motif recently suggested to be present in chaperone proteins encoded upstream of T6S substrates (15, 18, 19). Therefore, LC-MS/MS results were analyzed for T6S components pulled down by FLAG-IdsC, FLAG-IdsD, and IdsF-FLAG (**Table 2.3, Table 2.4,** and **Table 2.5**). Briefly, the T6S subcellular sheath is comprised of TssB and TssC that plunges the interior Hcp tube across the cell envelope through a core membrane complex consisting of several proteins including TssM (11-14, 20-23). The baseplate, composed of TssEFGK proteins, links sheath assembly and the core membrane complex (24, 25). FLAG-IdsC and FLAG-IdsD both pulled down BB2000_0820 (TssC), BB2000_0818 (TssF), and BB2000_0814 (TssK). FLAG-IdsC further pulled down BB2000_0821 (TssB), BB2000_0817 (TssG), and BB2000_0806 (TssF) (**Table 2.3, Table 2.4,** and **Table 2.5**). Therefore, FLAG-IdsC and FLAG-IdsD interact with conserved T6S sheath and baseplate components. IdsF-FLAG surprisingly did not pull down any T6S components.

IdsD forms puncta that localize proximal to T6S sheath

Given that IdsD is a T6S substrate that interacts with conserved T6S sheath components, we predicted that IdsD would be found proximal to the T6S sheath. For all microscopy experiments we used a construct that expressed FLAG-IdsC in conjunction with IdsD fused to an N-terminal mKate2 fluorophore (mKate-IdsD). This construct was expressed in a strain where BB2000_0821 (TssB) is fused to superfolder green fluorescent protein (TssB-sfGFP) (9). mKate-IdsD formed distinct puncta and typically

one to three foci were seen per cell (**Figure 2.2**). To determine what percentage of foci were found proximal to the T6S machinery, only cells that expressed both red (mKate-IdsD) and green (TssB-sfGFP) fluorescence signals were analyzed. Each mKate-IdsD associated puncta was visually determined to either be proximal or not proximal to a TssB-sfGFP associated rod. In 100 cells counted, 26 of them had mKate-IdsD foci that overlapped with the T6S machinery. Of these, 31 out of 113 of the mKate-IdsD foci counted overlapped with TssB-sfGFP fluorescence.

Figure 2.2 mKate-IdsD forms distinct puncta found proximal to the T6S sheath The T6S sheath was labeled using a chromosomal fusion of the sheath component TssB to sfGFP (9). FLAG-IdsC and mKate-IdsD were produced from pIds in this strain background. TssB-sfGFP associated fluorescence formed rod-like structures along cells, while mKate-IdsD associated fluorescence formed discrete foci. For a given cell displaying both mKate-IdsD and TssB-sfGFP signals, mKate-IdsD foci that did (white arrow) or did not (yellow arrow) overlap with the T6S machinery were counted. Of 113 mKate-IdsD puncta counted, 31 of them overlapped with TssB-sfGFP. Left, Phase. Middle left, fluorescence in the RFP channel for mKate2. Middle right, fluorescence in the GFP channel for sfGFP. Right, false-colored overlay in which for contrast, mKate-IdsD fluorescence is in red, and TssB-sfGFP fluorescence is in cyan. Scale bar is 10 μm.

Figure 2.2 mKate-IdsD forms distinct puncta found proximal to the T6S sheath (continued)

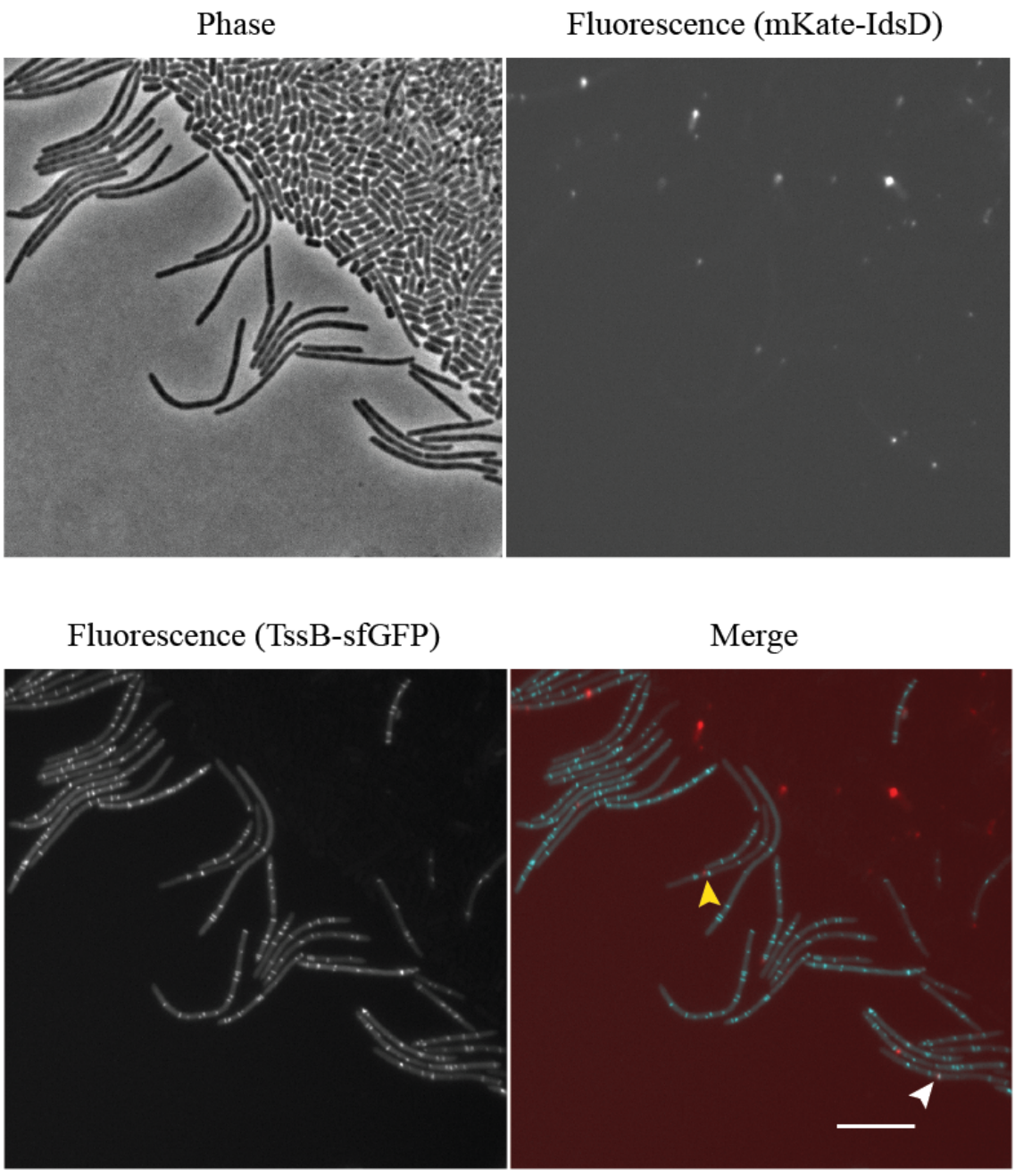

IdsD puncta are independent of T6S machinery

To test whether IdsD puncta formation occurs in preparation for IdsD secretion by the T6S machinery, pIds-FLAG-IdsC-mKate2-IdsD was expressed in four different T6S chromosomal disruptions. Sheath formation was abrogated using a single point mutation in BB2000_0821 (TssB) (4, 9). The core membrane complex was disrupted through a transposon insertion in BB2000_0808 (TssM) (3) . Baseplate formation was disrupted using two independent point mutations in BB2000_0814 (TssK) isolated and characterized by a previous graduate student, Christina C. Saak. The $TssK_{S382N}$ mutation supports sheath formation but results in attenuated secretion while $TssK_{W443C}$ inhibits sheath formation and secretion. In all of these T6S-abrogated strains, mKate-IdsD continued to pattern as foci, suggesting that that IdsD puncta formation is independent of its secretion (**Figure 2.3**).

This suggests that in the absence of T6S function, IdsD continues to interact with proteins that could aid in stabilizing these protein clusters. To test what proteins IdsD interacts with in T6S abrogated strains, co-immunoprecipitation assays were performed on the TssM disruption and both TssK disruption strains expressing FLAG-IdsD. LC-MS/MS data sets from these experiments were compared and only protein hits with at least three unique peptide fragments detected were considered in the analysis (**Figure 2.4** and **Table A.3**). A small subset of hits was shared between all three strains (38 hits), including IdsB, IdsC, IdsD, and IdsF. This suggests that one or more of the other Ids proteins could be important for the formation of IdsD puncta. In both TssK mutant backgrounds, IdsD continued to interact with components of the T6S machinery, including the sheath protein BB2000_0821 (TssB), as well as the baseplate protein

BB2000_0812 (TssJ). While in the $TssK_{S382N}$ background, FLAG-IdsD pulled down BB2000_0814 (TssK), this was not the case in the $TssK_{W443C}$ background. This suggests that sheath formation is important for interactions between IdsD and TssK, or alternatively that the TssK tryptophan at residue 443 is important for that interaction.

Figure 2.3 mKate-IdsD puncta form independently of T6S activity *P. mirabilis* strains with different chromosomal disruptions of T6S activity all expressing pIds-FLAG-IdsC-mKate2-IdsD. (A) Disruption of sheath formation (4), (B-C) disruption of baseplate, and (D) disruption of the core membrane complex (3). Left, Phase. Middle, fluorescence in the RFP channel for mKate2. Right, false-colored overlay in which for contrast, mKate-IdsD fluorescence is in red and phase is in cyan. All scale bars are 10 μm. Illustrations to the right of images depict models for IdsD localization at the membrane. Three main components of the T6S machinery (the baseplate, the membrane-complex and sheath) are shown. Black arrow represents previously tested IdsA (Hcp homolog) secretion, which is a hallmark of T6S activity (3, 4).

Figure 2.3 mKate-IdsD puncta form independently of T6S activity (continued)

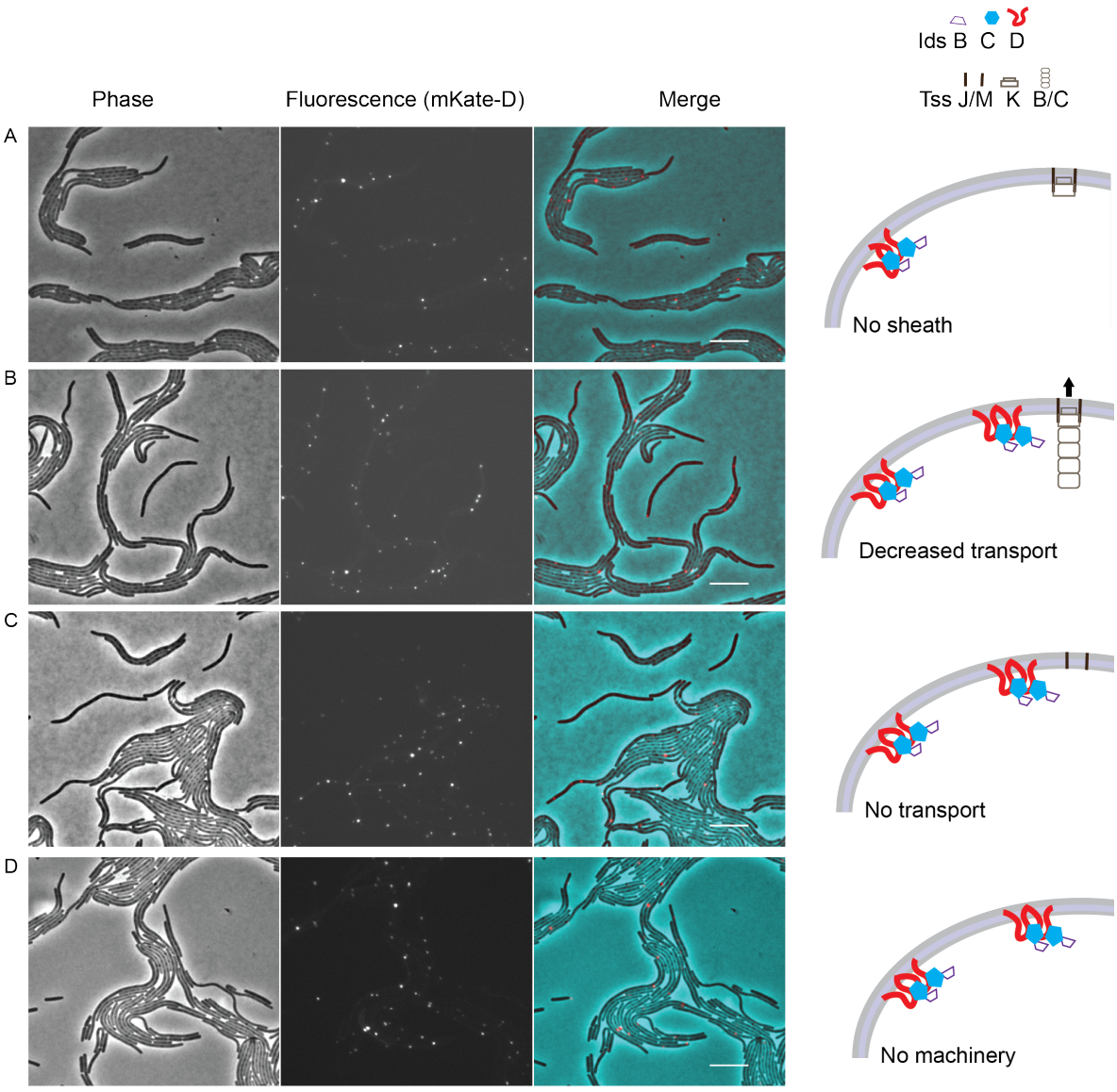

Figure 2.4 Comparison of LC-MS/MS protein hits from FLAG-IdsD co-immunoprecipitations in T6S abrogated strains Protein hits with at least three unique peptides pulled down by FLAG-IdsD in TssM*, $TssK_{S382N}$, or $TssK_{W443C}$ mutant backgrounds were compared using VENNY (26). Full data sets can be found on Gibbs laboratory data storage computer. **Table A.3** lists protein hits by category.

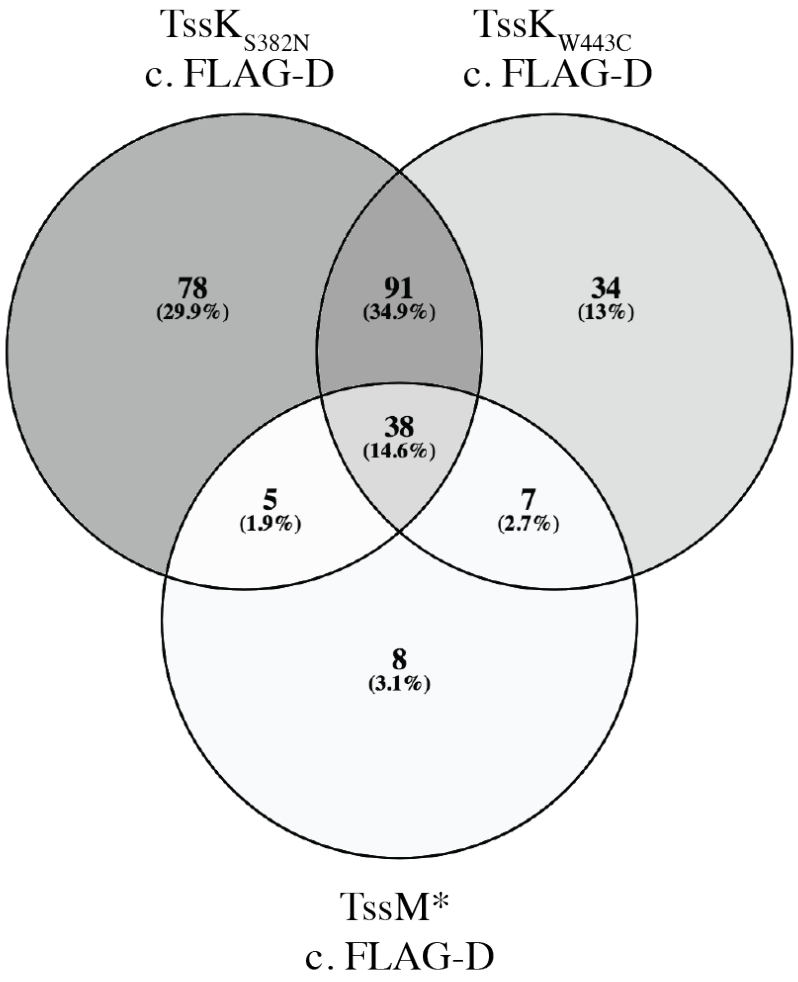

IdsD puncta formation depends on IdsC

Given that none of the four T6S-deficient strains impacted IdsD localization, the TssB chromosomal mutant strain (CCS05) (4, 9) was used as a representative donor-only population. To test the prediction that interactions with other Ids proteins affect IdsD puncta formation in donor cells, pIds-FLAG-IdsC-mKate2-IdsD was modified to disrupt IdsB (VgrG), IdsC (DUF4123) or IdsE (self-identity determinant) and expressed in CCS05. IdsB expression was disrupted as previously described (1), IdsC was disrupted by removing the DUF4123-encoding domain, and *idsE* was removed using a clean deletion (4). Given that IdsD and IdsE do not appear to interact in donor cells (4), we hypothesized that absence of IdsE would not affect IdsD clusters. Indeed, in the absence of IdsE, mKate-IdsD continued to appear as bright puncta. In the absence of IdsB, mKate-IdsD continued to appear as bright puncta. However, in the absence of the DUF4123 domain of IdsC, mKate-IdsD was mostly diffuse along cells (**Figure 2.5**). In some cells, either puncta or a combination of puncta and diffused localization was observed. To test whether diffuse localization was due to fluorophore cleavage, whole cell extracts of Δ*ids* or CCS05 expressing pIds-FLAG-IdsC-mKate2-IdsD or pIds-FLAG-IdsC$^{\Delta DUF4123}$-mKate2-IdsD were subjected to western blot analysis using anti-IdsD, anti-mKate, and anti-sigma70 antibodies. Bands corresponding to the mKate-IdsD fusion were observed, while bands corresponding to unlabeled IdsD or mKate2 alone were minimally found (**Figure 2.6**). These results suggest that while IdsD localization is independent of its transfer, it is dependent on IdsC, which is a protein of a family of recently proposed chaperone proteins for T6S substrates.

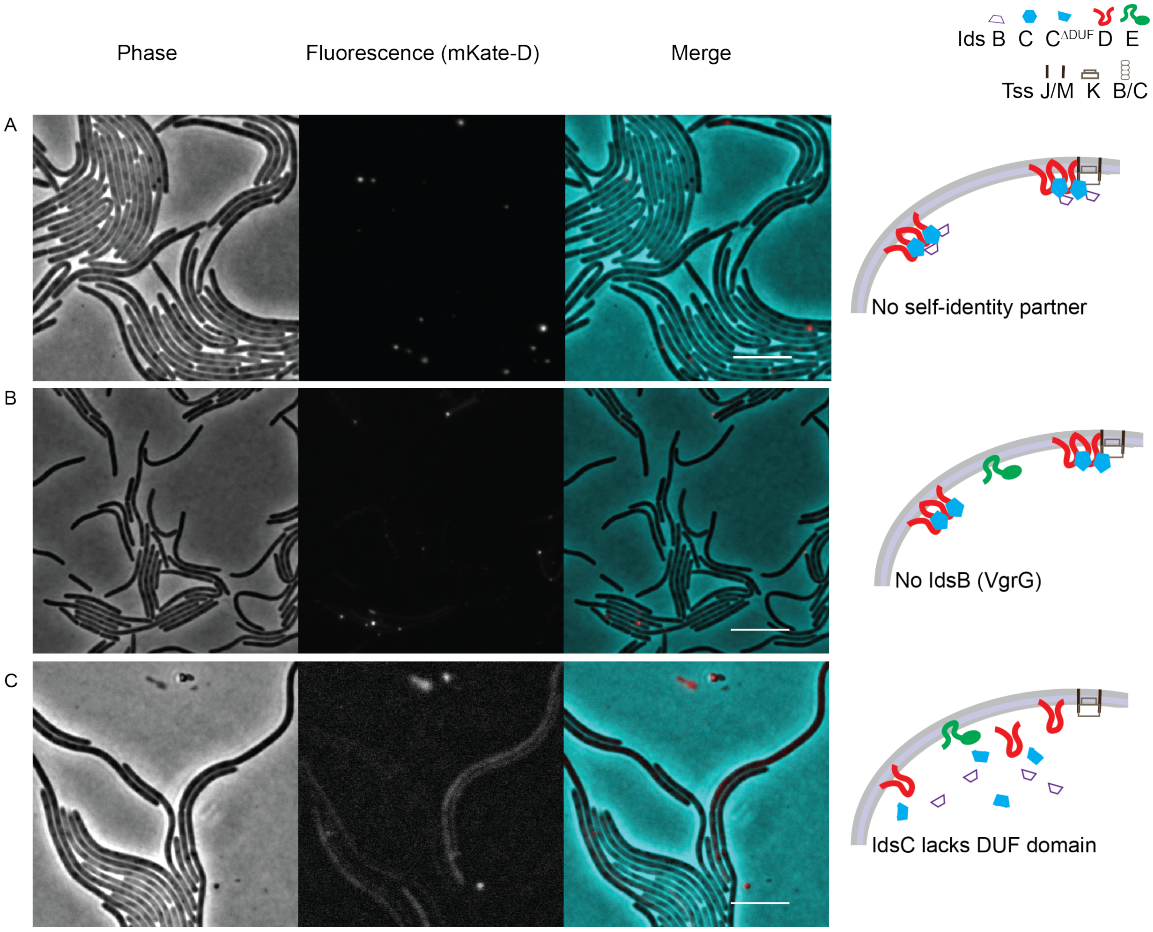

Figure 2.5 mKate-IdsD puncta depend on IdsC, but not IdsE *P. mirabilis* with abrogated sheath formation (4, 9) expressing mKate-IdsD in (A) absence of IdsB, (B) disruption of the DUF4123 domain of IdsC or (C) absence of IdsE. Left, Phase. Middle, fluorescence in the RFP channel for mKate2. Right, false-colored overlay in which for contrast, mKate-IdsD fluorescence is in red and phase is in cyan. All scale bars are 10 μm. Illustrations to the right of images depict models for IdsD localization at the membrane. Three main components of the T6S machinery (the baseplate, the membrane-complex and sheath) are shown.

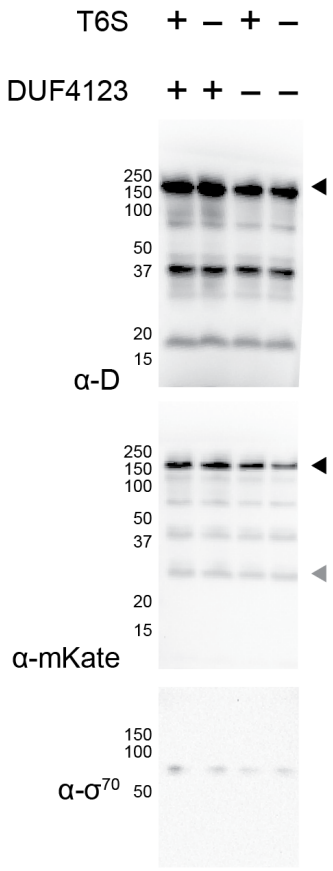

Figure 2.6 mKate-IdsD dispersed signal is not due to fluorophore cleavage Whole cell extracts were collected from *P. mirabilis* strains with functional (T6S +) or disrupted (T6S-) secretion (4) expressing modified pIds vectors producing FLAG-IdsC-mKate2-IdsD (DUF4123+) or FLAG-IdsC$^{\Delta DUF4123}$-mKate2-IdsD (DUF4123-). Extracts were analyzed using polyclonal anti-IdsD, polyclonal anti-mKate, and monoclonal anti-sigma70 antibodies. mKate-IdsD fusion protein (black arrow) versus mKate2 alone (gray arrow) are differentiated by size.

Discussion

In this chapter I have shown that IdsD interacts, either directly or indirectly, with T6S proteins and that as a T6S substrate, it can be found proximal to the T6S machinery. IdsD forms clusters or puncta, even in the absence of a transport-associated protein, IdsB (VgrG) or T6S function. In T6S-deficient strain backgrounds, IdsD continued to pull down IdsB, IdsC, and IdsF. This suggested that perhaps one of these proteins contributed to the formation or the stability of IdsD clusters. Given that IdsD is predicted to have two transmembrane domains, it is impossible that monomers of IdsD interact laterally in the membrane to form these large clusters, and that another protein is important for stabilizing such interactions. I have shown that IdsD clusters do indeed depend on IdsC, a protein in a family proposed to act as T6S-substrate chaperones. When the main protein domain within IdsC (DUF4123) is disrupted, IdsD clusters no longer form and instead IdsD-associated fluorescence is diffuse along cells.

Several open questions remain however, regarding the IdsC-IdsD interaction and its role in the communication of IdsD between neighboring cells. Whether this interaction is direct is unknown, but given that IdsC and IdsD both pulled down components of the T6S machinery, suggests that their interaction occurs pre-IdsD transport. Whether effects on IdsD localization affect IdsD secretion and whether these processes are coupled through IdsC remains to be tested. Additionally, the molecular mechanism by which IdsC acts as a "chaperone" remains elusive. In the following chapter, I probe at these questions.

References

1. **Gibbs KA, Urbanowski ML, Greenberg EP.** 2008. Genetic determinants of self identity and social recognition in bacteria. Science **321:**256-259.

2. **Cardarelli L, Saak C, Gibbs KA.** 2015. Two Proteins Form a Heteromeric Bacterial Self-Recognition Complex in Which Variable Subdomains Determine Allele-Restricted Binding. MBio **6:**e00251.

3. **Wenren LM, Sullivan NL, Cardarelli L, Septer AN, Gibbs KA.** 2013. Two independent pathways for self-recognition in *Proteus mirabilis* are linked by type VI-dependent export. MBio **4**.

4. **Saak CC, Gibbs KA.** 2016. The self-identity protein IdsD is communicated between cells in swarming *Proteus mirabilis* colonies. J Bacteriol **198:**3278-3286.

5. **Belas R, Erskine D, Flaherty D.** 1991. Transposon mutagenesis in *Proteus mirabilis*. J Bacteriol **173:**6289-6293.

6. **Finn RD, Coggill P, Eberhardt RY, Eddy SR, Mistry J, Mitchell AL, Potter SC, Punta M, Qureshi M, Sangrador-Vegas A, Salazar GA, Tate J, Bateman A.** 2016. The Pfam protein families database: towards a more sustainable future. Nucleic Acids Res **44:**D279-285.

7. **Schindelin J, Arganda-Carreras I, Frise E, Kaynig V, Longair M, Pietzsch T, Preibisch S, Rueden C, Saalfeld S, Schmid B, Tinevez JY, White DJ, Hartenstein V, Eliceiri K, Tomancak P, Cardona A.** 2012. Fiji: an open-source platform for biological-image analysis. Nat Methods **9:**676-682.

8. **Schindelin J, Rueden CT, Hiner MC, Eliceiri KW.** 2015. The ImageJ ecosystem: An open platform for biomedical image analysis. Mol Reprod Dev **82:**518-529.

9. **Saak CC, Zepeda-Rivera MA, Gibbs KA.** 2017. A single point mutation in a TssB/VipA homolog disrupts sheath formation in the type VI secretion system of *Proteus mirabilis*. PLoS One **12:**e0184797.

10. **Simon R, Priefer U, Puhler A.** 1983. A broad host range mobilization system for *in vivo* genetic engineering- transposon mutagenesis in gram-negative bacteria. Bio-Technol **1:**784-791.

11. **Basler M, Mekalanos JJ.** 2012. Type 6 secretion dynamics within and between bacterial cells. Science **337:**815.

12. **Basler M, Pilhofer M, Henderson GP, Jensen GJ, Mekalanos JJ.** 2012. Type VI secretion requires a dynamic contractile phage tail-like structure. Nature **483:**182-186.

13. **Hachani A, Lossi NS, Hamilton A, Jones C, Bleves S, Albesa-Jove D, Filloux A.** 2011. Type VI secretion system in *Pseudomonas aeruginosa*: secretion and multimerization of VgrG proteins. J Biol Chem **286:**12317-12327.

14. **Silverman JM, Agnello DM, Zheng H, Andrews BT, Li M, Catalano CE, Gonen T, Mougous JD.** 2013. Haemolysin coregulated protein is an exported receptor and chaperone of type VI secretion substrates. Mol Cell **51:**584-593.

15. **Bondage DD, Lin JS, Ma LS, Kuo CH, Lai EM.** 2016. VgrG C terminus confers the type VI effector transport specificity and is required for binding with PAAR and adaptor-effector complex. Proc Natl Acad Sci U S A **113:**E3931-3940.

16. **Hachani A, Allsopp LP, Oduko Y, Filloux A.** 2014. The VgrG proteins are "a la carte" delivery systems for bacterial type VI effectors. J Biol Chem **289:**17872-17884.

17. **Cianfanelli FR, Alcoforado Diniz J, Guo M, De Cesare V, Trost M, Coulthurst SJ.** 2016. VgrG and PAAR Proteins Define Distinct Versions of a Functional Type VI Secretion System. PLoS Pathog **12:**e1005735.

18. **Unterweger D, Kostiuk B, Otjengerdes R, Wilton A, Diaz-Satizabal L, Pukatzki S.** 2015. Chimeric adaptor proteins translocate diverse type VI secretion system effectors in *Vibrio cholerae*. EMBO J **34:**2198-2210.

19. **Liang X, Moore R, Wilton M, Wong MJ, Lam L, Dong TG.** 2015. Identification of divergent type VI secretion effectors using a conserved chaperone domain. Proc Natl Acad Sci U S A **112:**9106-9111.

20. **Brunet YR, Henin J, Celia H, Cascales E.** 2014. Type VI secretion and bacteriophage tail tubes share a common assembly pathway. EMBO Rep **15:**315-321.

21. **Bonemann G, Pietrosiuk A, Diemand A, Zentgraf H, Mogk A.** 2009. Remodelling of VipA/VipB tubules by ClpV-mediated threading is crucial for type VI protein secretion. EMBO J **28:**315-325.

22. **Douzi B, Spinelli S, Blangy S, Roussel A, Durand E, Brunet YR, Cascales E, Cambillau C.** 2014. Crystal structure and self-interaction of the type VI secretion tail-tube protein from enteroaggregative *Escherichia coli*. PLoS One **9:**e86918.

23. **Brunet YR, Espinosa L, Harchouni S, Mignot T, Cascales E.** 2013. Imaging type VI secretion-mediated bacterial killing. Cell Rep **3:**36-41.

24. **Zoued A, Durand E, Bebeacua C, Brunet YR, Douzi B, Cambillau C, Cascales E, Journet L.** 2013. TssK is a trimeric cytoplasmic protein interacting with components of both phage-like and membrane anchoring complexes of the type VI secretion system. J Biol Chem **288:**27031-27041.

25. **Brunet YR, Zoued A, Boyer F, Douzi B, Cascales E.** 2015. The Type VI Secretion TssEFGK-VgrG Phage-Like Baseplate Is Recruited to the TssJLM Membrane Complex via Multiple Contacts and Serves As Assembly Platform for Tail Tube/Sheath Polymerization. PLoS Genet **11:**e1005545.

26. **Oliveros JC.** 2007-2015. Venny. An interactive tool for comparing lists with Venn's diagrams. http://bioinfogp.cnb.csic.es/tools/venny/index.html.

Chapter 3

Localization and secretion of a T6S substrate can be uncoupled by single residue polymorphisms in its DUF4123 chaperone

Some of the work presented in this chapter was published as part of Zepeda-Rivera, MA, Saak C.C., Gibbs K.A. A proposed chaperone for the bacterial type VI secretion system functions to constrain a self-identity protein. J Bacteriol. 2018 Mar 19. PMID: 29444703. Full publication can be found in Appendix B.

Abstract

IdsD is a self-identity protein exchanged between *Proteus mirabilis* cells by the type VI secretion system (T6S). IdsD can be found proximal to T6S machineries and interacts *in vitro* with T6S-associated proteins as well as core components of the machinery. IdsD localization is impacted if IdsC, a protein belonging to a recently proposed family of chaperones, lacks its main protein domain (DUF4123). Key questions about the IdsC-IdsD interaction remained, specifically whether IdsC couples IdsD localization and secretion, and whether this occurs in producing and/or recipient cells. Here I demonstrate that the IdsC-IdsD interaction is independent of other Ids or T6S proteins and is essential for maintenance of IdsD protein levels. Furthermore I show that IdsD localization and secretion can be uncoupled by single amino acid polymorphisms in IdsC and that this regulatory mechanism occurs only in producing cells, before IdsD exchange.

Introduction

IdsD and IdsE are self-identity determinants in the bacterium *Proteus mirabilis*. IdsD is secreted via the well-conserved type VI secretion (T6S) system from a producing to a recipient cell. The IdsD-IdsE binding state exclusively in recipient cells signals for either self or non-self recognition phenotypes. It remained unclear how IdsD-IdsE interactions are prevented from occurring in producing cells. As a T6S-substrate, IdsD localizes into discrete puncta that can be found proximal to the T6S machinery. However, IdsD localization is independent of T6S assembly or function, and is dependent on another protein-IdsC.

IdsC is a DUF4123-domain protein, a protein family that has recently been proposed to act as chaperones for T6S substrates. DUF4123-proteins are commonly found encoded upstream of known or predicted T6S substrates (1) and in some systems have been shown to be essential for interactions with the VgrG protein and substrate secretion (2, 3). However, the molecular mechanisms by which DUF4123-proteins act as chaperones remained largely unexplored. Given IdsC's role in IdsD localization, it seemed plausible that IdsC couples IdsD localization and secretion. Whether this was the case and whether this could be a general mechanism to prevent IdsD-IdsE interactions in producing cells remained untested.

In this chapter I demonstrate that the IdsC-IdsD interaction is diminished in the absence of the IdsC DUF4123 domain. This in turn affects IdsD localization and maintenance of IdsD protein levels. Furthermore, I show that IdsD localization proximal to the T6S and IdsD secretion can be uncoupled by single amino acid polymorphisms in IdsC. This regulatory mechanism occurs only in producing cells, before IdsD exchange. Therefore, it appears that IdsC acts as chaperone to maintain IdsD protein levels, cluster IdsD, and aid in targeting these clusters to the T6S machinery. However, secretion through the machinery appears to be a distinct additional step. The role of other DUF4123 proteins could be a general yet unexplored mechanism of T6S substrate regulation pre-transport.

Materials and Methods

Bacterial strains and media

All strains are described in **Table 3.1**. *Escherichia coli* strains were maintained on LB agar and *P. mirabilis* strains were maintained on LSW- agar (4). *P. mirabilis* was grown on CM55 Blood Agar Base agar (Oxoid, Basingstoke, England) for colony growth assays. For broth cultures, all strains were grown in LB broth under aerobic conditions at 16°C, 30°C, or 37°C. Antibiotics were used at the following concentrations: 100 microgram per milliliter (μg/mL) carbenicillin; 15 μg/mL tetracycline; 35 μg/mL kanamycin; 50 μg/mL chloramphenicol.

Expression plasmids

All plasmids used are described in **Table 3.2**. Gene fragments (gBlocks) (Integrated DNA Technologies, Coralville, IA) were used for cloning of pIds-derived vectors. Listed gBlocks were sub-cloned into TOPO pCR2.1 vector using the TOPO TA-Cloning Kit (Thermo Fisher Scientific, Waltham, MA). pIds-derived, pAD100-derived, and p_{LTetO} (pTet) plasmids were constructed via restriction digest using listed restriction enzymes (New England BioLabs, Ipswich, MA) of noted plasmids. Restriction digest was followed by overnight ligation at 16°C and subsequent transformation into OneShot Omnimax2 T1R competent cells (Thermo Fisher Scientific, Waltham, MA) or XL10-Gold Ultracompetent cells (Agilent Technologies, Santa Clara, CA). Resultant plasmids were confirmed by sequencing (Genewiz, Inc., South Plainfield, NJ). pIds and pTet vectors were then transformed into S17λpir, which was used to conjugate plasmids into *P. mirabilis* as previously described (5). pAD100 vectors were transformed into *E. coli* strain BL21(DE3) pLysS (Thermo Fisher Scientific, Waltham, MA).

Anti-FLAG co-immunoprecipitations from *P. mirabilis* cell extracts

P. mirabilis strains carrying pIds plasmids were inoculated from overnight cultures onto CM55 swarm agar plates and incubated at 37°C 16-20 hours until the population almost reached the edge of the petri dish. Cells from five plates were re-suspended in 5 mL LB each and harvested by centrifugation. Pellets were re-suspended in 1 mL cell lysis buffer (50mM Tris HCl pH 7.4, 150mM NaCl, 1% triton X-100, 1 mM EDTA) supplemented with 40 µl of either Complete protease inhibitor cocktail (Roche, Basel, Switzerland) or Biotools protease inhibitor cocktail (Biotools, Houston, TX) and lysed by vortexing with cell disruptor beads (0.1-diameter, Electron Microscopy Sciences, Hatfield, PA). Lysates were cleared by centrifugation and 900 µL was applied to 40 µL pre-equilibrated α-FLAG M2 antibody resin (Sigma-Aldrich, St. Louis, MO; Biotools, Houston, TX). Control lysate (containing pIds with no FLAG-tagged protein) was supplemented with 2 µg of purified FLAG-tagged *E. coli* bacterial alkaline phosphatase (FLAG-BAP) protein (Sigma-Aldrich, St. Louis, MO). Lysates were incubated with resin for two hours at 4°C. Unbound cell extract was removed. Resin was washed five times in wash buffer (50mM Tris HCl pH 7.4, 150mM NaCl, 1% triton X-100), and bound proteins were eluted with 50 µl of elution buffer (50mM Tris HCl pH 7.4, 150mM NaCl, 200 ng/µl 3XFLAG peptide) for 45 minutes at 4°C. The elution was re-centrifuged and the top 40 µl was retained. Samples of load (L), non-binding (-) and binding (+) fractions were separated by SDS-PAGE and analyzed by liquid chromatography tandem mass spectrometry or western blot.

Anti-FLAG co-immunoprecipitations from *E. coli* cell extracts

E. coli BL21 (DE3) pLysS cells (Thermo Fisher Scientific, Waltham, MA) were grown in 25 mL of LB supplemented with carbenicillin under shaking conditions at 30°C until optical density at 600 nm (OD_{600}) was between 0.6 and 1. Cultures were cooled on ice, induced with 1 mM isopropyl-β-D-1 thiogalactopyranoside (IPTG), and incubated overnight shaking at 16°C. Cells were harvested by centrifugation. Lysates were mixed to a total volume of 1 ml of which 900 µl was applied to 40 µL pre-equilibrated α-FLAG M2 antibody resin (Sigma-Aldrich, St. Louis, MO; Biotools, Houston, TX). Anti-FLAG co-immunoprecipitation was continued as described above.

Anti-FLAG co-immunoprecipitations from mixed *P. mirabilis* and *E. coli* cell extracts

P. mirabilis and *E. coli* extracts were obtained separately as described above. Lysates were mixed to a total volume of 1 ml of which 900 µl was applied to 40 µL pre-equilibrated α-FLAG M2 antibody resin (Sigma-Aldrich, St. Louis, MO; Biotools, Houston, TX). Anti-FLAG co-immunoprecipitation was continued as described above.

Antibody generation

Antibodies specific to IdsB amino acids 713-723 (CRAKAMKKGTA), IdsD amino acids 4-18 (EVNEKYLTPQERKAR) and IdsE amino acids 298-312 (EQILAKLDQEKEHHA) were raised in rabbits using standard peptide protocols (Covance, Dedham, MA).

SDS-PAGE and western blots

Samples from the above immunoprecipitation assays were separated by gel electrophoresis using 12% Tris-Tricine polyacrylamide gels, transferred to nitrocellulose membranes, and probed with: rabbit α-IdsB (1:5000), rabbit α-IdsD (1:2000); rabbit α-IdsE (1:2000); rabbit α-FLAG (1:4000, Sigma-Aldrich, St. Louis, MO); mouse α-σ^{70} (1:1000, Thermo Fisher Scientific, Waltham, MA) or (1:1000, BioLegend, San Diego, CA) followed by goat α-rabbit or goat α-mouse conjugated to HRP (1:5000, KPL, Inc., Gaithersburg, MD) and developed with Immun-Star HRP Substrate Kit (Bio-Rad Laboratories, Hercules, CA). Blots were visualized using a Chemidoc (Bio-Rad Laboratories, Hercules, CA). Figures were made in Adobe Illustrator (Adobe Systems, San Jose, CA).

Liquid chromatography tandem mass-spectrometry

Binding samples from α-FLAG co-immunoprecipitations were separated by gel electrophoresis using 12% Tris-Tricine polyacrylamide gels. Bands were cut between 0-37 kDa, 37-75 kDa, and 75-250 kDa and sent to LC-MS/MS analysis (Taplin Mass Spectrometry Core Facility, Harvard Medical School, Boston MA). Technical advice provided by the Taplin Mass Spectrometry Facility led to a three unique peptide cutoff to confirm protein hits. Bioinformatics analysis of Ids and T6S protein hits was done using Pfam 31.0 (6). Full data tables can be found in 'LABSTORAGE' on Gibbs Laboratory Data Computer under 'Martha' 'Mass Spectrometry' 'Data Spreadsheets' subfolder.

Colony expansion assay

Colony expansion assays were conducted as previously described (7). Modifications to those protocols are as follows. Swarming-permissive plates supplemented with kanamycin were inoculated with 1 μl of overnight cultures normalized by OD_{600}. Plates were incubated at 37° for 17 hours and swarming radii recorded.

Tricholoroacetic acid (TCA) precipitations

All trichloroacetic acid precipitations were performed as previously described (8). Binding fractions from α-FLAG immunoprecipitations or supernatant fractions from TCA were separated by gel electrophoresis using 12% Tris-Tricine polyacrylamide gels and stained with Coomassie blue as previously described (7, 8). Supernatant fractions from TCA were cut into two bands at 75-150 kDa and 10-25 kDa. LC-MS/MS was performed by the Taplin Mass Spectrometry Facility (Harvard Medical School, Boston, MA). Technical advice provided by the Taplin Mass Spectrometry Facility led to a three unique peptide cutoff to confirm protein hits. Bioinformatics analysis of Ids and T6S protein hits was done using Pfam 31.0 (6). Full data tables can be found in 'LABSTORAGE' on Gibbs Laboratory Data Computer under 'Martha' 'Mass Spectrometry' 'Data Spreadsheets' subfolder.

***P. mirabilis* boundary assays**

Self-recognition phenotype of test strains was examined against the parent strain BB2000 and BB2000 lacking the *ids* genes (Δ*ids*), each carrying a plasmid to confer kanamycin resistance. Strains were grown up in liquid-broth under aerobic conditions at 37°C. Cultures were normalized by OD_{600} and spotted on swarming permissive CM55

Blood Agar Base agar (Oxoid, Basingstoke, England) plates supplemented with 2 mg/mL Coomassie blue, 4 mg/mL congo red dyes, and 35 μg/mL kanamycin. Plates were incubated overnight at 37°C.

Table 3.1 Strains used in this study

Strain	Notes	Source	KAG #	MZR #	Plasmid
BB2000	Wild-type	(4)	001	001	
HI4320	Wild-type		034	008	
CW677	Wild-type	(9)	MLU 4.274		
BB2000::Δ*idsE*	Modified protein(s): ΔIdsE BB2000 with a chromosomal in-frame deletion of *idsE*.	This study	3126		
Δ*ids*	Δ*ids::Tn-Cm(R)*	(5)	006	002	
Δ*ids* c. pIds	Δ*ids* carrying pIds	(5)	036	006	pIds
Δ*ids* c. pIds-ΔIdsABC	Modified protein(s): ΔIdsA, ΔIdsB, ΔIdsC Δ*ids* carrying a modified pIds plasmid with an in-frame deletion of *idsA* through *idsC*. The plasmid was first described as ABC- in (5).	(5)	043		pIds-Δ172-407
Δ*ids* c. pIds-ΔIdsDEF	Modified protein(s): ΔIdsD, ΔIdsE, ΔIdsF Δ*ids* carrying a modified pIds plasmid with an in-frame deletion of *idsD* through *idsF*. The plasmid was first described as DEF- in (5).	(5)	033		pIds-Δ1034-89
Δ*ids* c. pIds-IdsBmt	Modified protein(s): IdsB- Δ*ids* carrying a modified pIds plasmid with a 711-bp disruption of IdsB. The plasmid was first described as B- in (5).	(5)	076		pIds-723mt

Table 3.1 Strains used in this study (continued)

Δ*ids* c. pIds-IdsCmt	Modified protein(s): IdsC- Δ*ids* carrying a modified pIds plasmid with insertion of three stop codons resulting in disruption of IdsC. The plasmid was first described as C- in (5).	(5)	092	131	pIds-407-mt.1
Δ*ids* c. pIds-IdsFmt	Modified protein(s): IdsF- Δ*ids* carrying a modified pIds plasmid with a 1.9 kbp insertion resulting in disruption of IdsF. The plasmid was first described as F- in (5).	(5)	080		pIds-89mt
Δ*ids* c. pIds-FLAG-IdsC	Modified protein(s): FLAG-IdsC Δ*ids* carrying a modified pIds plasmid with an N-terminal FLAG-tag encoded in-frame with *idsC*.	This study	644/ 645	039/ 167	pLC-001
Δ*ids* c. pIds-FLAG-IdsC$^{\Delta DUF4123}$	Modified protein(s): FLAG-IdsC$^{\Delta DUF4123}$ Δ*ids* carrying a modified pIds plasmid with an N-terminal FLAG-tag encoded in-frame with *idsC* with nucleotides 373-762 deleted.	This study	2556	144	pMZ32
Δ*ids* c. pIds-FLAG-IdsC-ΔIdsE	Modified protein(s): FLAG-IdsC, ΔIdsE Δ*ids* carrying a modified pIds plasmid with an N-terminal FLAG-tag encoded in-frame with *idsC*. In-frame deletion of *idsE*.	This study	2749	158	pMZ36

Table 3.1 Strains used in this study (continued)

CCS05	Modified protein(s): $TssB_{L32R}$ Δ*ids* with chromosomal BB2000_0821 with a single T→G point mutation at base pair 95. This results in a disrupted T6S sheath.	(7)	2115		
CCS05 c. pIds-FLAG-IdsC-ΔIdsE	Modified protein(s): $TssB_{L32R}$, FLAG-IdsC, ΔIdsE CCS05 carrying a modified pIds plasmid with an N-terminal FLAG-tag encoded in-frame with *idsC*. In-frame deletion of *idsE*.	This study	2755	159	pMZ36
Δ*ids* c. pIds-FLAG-$IdsC^{\Delta DUF4123}$-ΔIdsE	Modified protein(s): FLAG-$IdsC^{\Delta DUF4123}$, ΔIdsE Δ*ids* carrying a modified pIds plasmid with an N-terminal FLAG-tag encoded in-frame with *idsC* with nucleotides 373-762 deleted. In-frame deletion of *idsE*.	This study	2763	160	pMZ37
CCS05 c. pIds-FLAG-$IdsC^{\Delta DUF4123}$-ΔIdsE	Modified protein(s): $TssB_{L32R}$, FLAG-$IdsC^{\Delta DUF4123}$, ΔIdsE CCS05 carrying a modified pIds plasmid with an N-terminal FLAG-tag encoded in-frame with *idsC* with nucleotides 373-762 deleted. In-frame deletion of *idsE*.	This study	2769	161	pMZ37

Table 3.1 Strains used in this study (continued)

CCS05 c. pIds-FLAG-PelB-IdsC-ΔIdsE	Modified protein(s): $TssB_{L32R}$, FLAG-PelB-IdsC, ΔIdsE CCS05 carrying a modified pIds plasmid with an N-terminal FLAG-tag and a PelB signal sequence encoded in-frame with *idsC*. In-frame deletion of *idsE*.	This study	3925	494	pMZ118
CCS05 c. pIds-FLAG-OmpA-IdsC-ΔIdsE	Modified protein(s): $TssB_{L32R}$, FLAG-OmpA-IdsC, ΔIdsE CCS05 carrying a modified pIds plasmid with an N-terminal FLAG-tag and a OmpA signal sequence encoded in-frame with *idsC*. In-frame deletion of *idsE*.	This study	3887	480	pMZ114
BB2000 c. pTet-FLAG-IdsC	Modified protein(s): FLAG-IdsC BB2000 carrying a modified pTet anhydrotetraclycine inducible plasmid with an N-terminal FLAG-tag encoded in-frame with *idsC*.	This study	3893	483	pMZ116
BB2000::Δ*idsE* c. pTet-FLAG-IdsC	Modified protein(s): FLAG-IdsC, ΔIdsE BB2000:: ΔIdsE carrying a modified pTet anhydrotetraclycine inducible plasmid with an N-terminal FLAG-tag encoded in-frame with *idsC*.	This study	3895	484	pMZ116
Δ*ids:: BB2000_0821-sfGFP*	Modified protein(s): TssB-sfGFP Δ*ids* with chromosomal *BB2000_0821* fused to superfolder GFP.	(10)	2537		

Table 3.1 Strains used in this study (continued)

Δ*ids* c. pIds-FLAG-IdsC^{S38P}	Modified protein(s): FLAG-IdsC^{S38P} Δ*ids* carrying a modified pIds plasmid with an N-terminal FLAG-tag encoded in-frame with *idsC* containing a T→C mutation at nucleotide 112.	This study	3385	183	pMZ69
Δ*ids* c. pIds-FLAG-IdsC^{S38P}-mKate2-IdsD	Modified protein(s): FLAG-IdsC^{S38P}, mKate2-IdsD Δ*ids* carrying a modified pIds plasmid with an N-terminal FLAG-tag encoded in-frame with *idsC* containing a T→C mutation at nucleotide 112 and an N-terminal mKate2-fluorophore fused to *idsD*.	This study	3397	327	pMZ70
Δ*ids:: BB2000_0821-sfGFP* c. pIds-FLAG-IdsC^{S38P}-mKate2-IdsD	Modified protein(s): TssB-sfGFP, FLAG-IdsC^{S38P}, mKate2-IdsD Δ*ids::BB2000_0821-sfGFP* carrying a modified pIds plasmid with an N-terminal FLAG-tag encoded in-frame with *idsC* containing a T→C mutation at nucleotide 112 and an N-terminal mKate2-fluorophore fused to *idsD*.	This study	3403	330	pMZ70
Δ*ids* c. pIds-FLAG-IdsC^{S38P}-ΔIdsE	Modified protein(s): FLAG-IdsC^{S38P}, ΔIdsE Δ*ids* carrying a modified pIds plasmid with an N-terminal FLAG-tag encoded in-frame with *idsC* containing a T→C mutation at nucleotide 112 and an in-frame deletion of *idsE*.	This study	3469	362	pMZ75

Table 3.1 Strains used in this study (continued)

CCS05 c. pIds-FLAG-IdsC^{S38P}-ΔIdsE	Modified protein(s): TssB$_{L32R}$, FLAG-IdsC^{S38P}, ΔIdsE CCS05 carrying a modified pIds plasmid with an N-terminal FLAG-tag encoded in-frame with *idsC* containing a T→C mutation at nucleotide 112 and an in-frame deletion of *idsE*.	This study	3473	364	pMZ75
Δ*ids* c. pIds-FLAG-IdsC^{R186Q}	Modified protein(s): FLAG-IdsC^{R186Q} Δ*ids* carrying a modified pIds plasmid with an N-terminal FLAG-tag encoded in-frame with *idsC* containing a G→A mutation at nucleotide 557.	This study	3413	335	pMZ71
Δ*ids* c. pIds-FLAG-IdsC^{R186Q}-mKate2-IdsD	Modified protein(s): FLAG-IdsC^{R186Q}, mKate2-IdsD Δ*ids* carrying a modified pIds plasmid with an N-terminal FLAG-tag encoded in-frame with *idsC* containing a G→A mutation at nucleotide 557 and an N-terminal mKate2-fluorophore fused to *idsD*.	This study	3425	341	pMZ72
Δ*ids::BB2000_0821-sfGFP* c. pIds-FLAG-IdsC^{R186Q}-mKate2-IdsD	Modified protein(s): TssB-sfGFP, FLAG-IdsC^{R186Q}, mKate2-IdsD Δ*ids::BB2000_0821-sfGFP* carrying a modified pIds plasmid with an N-terminal FLAG-tag encoded in-frame with *idsC* containing a G→A mutation at nucleotide 557 and an N-terminal mKate2-fluorophore fused to *idsD*.	This study	3431	344	pMZ72

Table 3.1 Strains used in this study (continued)

Δ*ids* c. pIds-FLAG-IdsC^{R186Q}-ΔIdsE	Modified protein(s): FLAG-IdsC^{R186Q}, ΔIdsE Δ*ids* carrying a modified pIds plasmid with an N-terminal FLAG-tag encoded in-frame with *idsC* containing a G→A mutation at nucleotide 557 and an in-frame deletion of *idsE*.	This study	3497	376	pMZ77
CCS05 c. pIds-FLAG-IdsC^{R186Q}-ΔIdsE	Modified protein(s): TssB$_{L32R}$, FLAG-IdsC^{R186Q}, ΔIdsE CCS05 carrying a modified pIds plasmid with an N-terminal FLAG-tag encoded in-frame with *idsC* containing a G→A mutation at nucleotide 557 and an in-frame deletion of *idsE*.	This study	3501	378	pMZ77
Δ*ids* c. pIds-FLAG-IdsC$^{S38P/R186Q}$	Modified protein(s): FLAG-IdsC$^{S38P/R186Q}$ Δ*ids* carrying a modified pIds plasmid with an N-terminal FLAG-tag encoded in-frame with *idsC* containing a T→C mutation at nucleotide 112 and a G→A mutation at nucleotide 557.	This study	3441	185	pMZ73

Table 3.1 Strains used in this study (continued)

Δ*ids* c. pIds-FLAG-IdsC$^{S38P/R186Q}$-mKate2-IdsD	Modified protein(s): FLAG-IdsC$^{S38P/R186Q}$, mKate2-IdsD Δ*ids* carrying a modified pIds plasmid with an N-terminal FLAG-tag encoded in-frame with *idsC* containing a T→C mutation at nucleotide 112 and a G→A mutation at nucleotide 557. N-terminal mKate2-fluorophore fused to *idsD*.	This study	3453	354	pMZ74
Δ*ids::BB2000_0821-sfGFP* c. pIds-FLAG-IdsC$^{S38P/R186Q}$-mKate2-IdsD	Modified protein(s): TssB-sfGFP, FLAG-IdsC$^{S38P/R186Q}$, mKate2-IdsD Δ*ids::BB2000_0821-sfGFP* carrying a modified pIds plasmid with an N-terminal FLAG-tag encoded in-frame with *idsC* containing a T→C mutation at nucleotide 112 and a G→A mutation at nucleotide 557. N-terminal mKate2-fluorophore fused to *idsD*.	This study	3459	357	pMZ74
Δ*ids* c. pIds-FLAG-IdsC$^{S38P/R186Q}$-ΔIdsE	Modified protein(s): FLAG-IdsC$^{S38P/R186Q}$, ΔIdsE Δ*ids* carrying a modified pIds plasmid with an N-terminal FLAG-tag encoded in-frame with *idsC* containing a T→C mutation at nucleotide 112 and a G→A mutation at nucleotide 557. In-frame deletion of *idsE*.	This study	3525	390	pMZ79

Table 3.1 Strains used in this study (continued)

CCS05 c. pIds-FLAG-IdsC$^{S38P/R186Q}$-ΔIdsE	Modified protein(s): TssB$_{L32R,}$ FLAG-IdsC$^{S38P/R186Q}$, ΔIdsE CCS05 carrying a modified pIds plasmid with an N-terminal FLAG-tag encoded in-frame with *idsC* containing a T→C mutation at nucleotide 112 and a G→A mutation at nucleotide 557. In-frame deletion of *idsE*.	This study	3529	392	pMZ79
BL21(DE3) pLysS c. pAD-IdsC-FLAG	Modified protein(s): IdsC-FLAG BL21(DE3) pLysS carrying a modified pAD100 plasmid with a C-terminal FLAG-tag encoded in-frame with *idsC*.	This study	2376	113	pMZ14
BL21(DE3) pLysS c. pAD-IdsD$_{BB}$-His$_6$	Modified protein(s): IdsD$_{BB2000}$-His$_6$ BL21(DE3) pLysS carrying a modified pAD100 plasmid with a C-terminal His$_6$-tag encoded in-frame with *idsD* from strain BB2000.	(11)	1101	061	pLC-027
BL21(DE3) pLysS c. pAD-IdsC^{ΔDUF4123}-FLAG	Modified protein(s): IdsC^{ΔDUF4123}-FLAG BL21(DE3) pLysS carrying a modified pAD100 plasmid with a C-terminal FLAG-tag encoded in-frame with *idsC* with nucleotides 382-765 deleted.	This study	2467	168	pMZ28

Table 3.1 Strains used in this study (continued)

BL21(DE3) pLysS c. pAD-IdsD$_{HI}$-His$_6$	Modified protein(s): IdsD$_{HI4320}$-His$_6$ BL21(DE3) pLysS carrying a modified pAD100 plasmid with a C-terminal His$_6$-tag encoded in-frame with *idsD* from strain HI4320.	(11)	1489	116	pLC-050
BL21(DE3) pLysS c. pAD-IdsD$_{CW677}$-His$_6$	Modified protein(s): IdsD$_{CW677}$-His$_6$ BL21(DE3) pLysS carrying a modified pAD100 plasmid with a C-terminal His$_6$-tag encoded in-frame with *idsD* from strain CW677.	This study	3377	182	pMZ68
OneShot Omnimax 2 T1R Competent Cells	Cloning strain for pIds-derived plasmids	Thermo Fisher Scientific, Waltham, MA.			
S17λpir	*E. coli* mating strain to introduce plasmids into *P. mirabilis*	(12)	068		
XL10-Gold Ultracompetent Cells	Cloning strain for pAD100-derived plasmids	Agilent Technologies, Santa Clara, CA.			
OneShot BL21(DE3) pLysS Competent Cells	Strain for protein overexpression from pAD100-derived plasmids.	Thermo Fisher Scientific, Waltham, MA.			

Table 3.2 Primers used in this study

Plasmid	Construction details (primers and gBlocks 5' → 3')
pIds-FLAG-IdsC	FLAG epitope (DYKDDDDK) was introduced 5' of *idsC* in pIds using Quikchange reaction protocols (Agilent Technologies, Santa Clara, CA). F: GCGAAAGCGATGAAAAAAGGAACGGCCTAATGGACTA CAAAGACGATGACGATAAACTCTTGAGTCCAAATCCCC TCTATAAAGCG R: CGCTTTATAGAGGGGATTTGGACTCAAGAGTTTATCGTCAT CGTCTTTGTAGTCCATTAGGCCGTTCCTTTTTTCATCGCTTT CGC
pIds-FLAG-IdsC$^{\Delta DUF4123}$	Deletion of basepairs 373 to 762 in *idsC* in pIds-FLAG-IdsC using gBlock and restriction digest with BstEII/PacI. Geneblock: GGTTACCATTAGCTGAGGATTGCCGTGCGAAAGCGATGAAAAAAG GAACGGCCTAATGGACTACAAAGACGATGACGATAAACTCTTGAG TCCAAATCCCCTCTATAAAGCGTATTGGGTTGCTCAATGCCGTTAT ACTCGCAACGGTGAACAATTCAAGGGGGTGATGACCGTAGCAGGT ACAAGTCAATCACAAGCTATTAAGCAGATGCGCCAGTACTTTACG GCTCACCCAGGTGAATATACCTTTGCGGACTATGACACATTAATCC CTTTAATCACCCATATTGAACAAAGTTCAACCTTAGAATTACCGTT AATACGGCAAGTACGTGAGCAACATAATGCAAAGGTTTCAGCCGT ATTAGTGGATAAATGCAACCTCACACACCCAAGACCGTCAGAAAA AGGCGACATTCATTACCGTGAGGGGCAACCTACGTTTATTGAATAT TCGCATTAA
pIds-FLAG-IdsC-ΔIdsE	Deletion of *idsE* in pIds-FLAG-IdsC using gBlock (7) and restriction digest with EcoNI/KpnI. Geneblock: GCGAACAATTAAAAATGGCAAGTGAAAAAGGTGATTGGAACCCTG AAACAGGTATATTTAAATTTAGTTTGGAAGTACAGTCTCAATTAGT AAATACATATTCTGCTTTTGGTGCACATCCTAATAGCCGTATAGGT ATTGAAGATTTATATTGGTATTATCAAGTCAATCCCGAGGTAACAA CACCGATGCGTTATATCAATTGGGGGGGAGATACCCAAGAAAACA ATCAGCTTTTAGGCTTTATTAACAGTGAGAATATCTAAATCAGGAG AAAGAACACCATGCGTAGTTTGGTAAACGGCAGAAAGATTATTTT AGAAAATGATACAACAAATACCGGCGGTACCGTACTTACCGGCTC TTCTATTGCTAAACAAACACAAGGGG

Table 3.2 Primers used in this study (continued)

pIds-FLAG-IdsC$^{\Delta DUF4123}$-ΔIdsE	Deletion of *idsE* in pIds-FLAG-IdsC$^{\Delta DUF4123}$ using gBlock (7) and restriction digest with EcoNI/KpnI. Geneblock (oCS80): GCGAACAATTAAAAATGGCAAGTGAAAAAGGTGATTGGAACCCTG AAACAGGTATATTTAAATTTAGTTTGGAAGTACAGTCTCAATTAGT AAATACATATTCTGCTTTTGGTGCACATCCTAATAGCCGTATAGGT ATTGAAGATTTATATTGGTATTATCAAGTCAATCCCGAGGTAACAA CACCGATGCGTTATATCAATTGGGGGGGAGATACCCAAGAAAACA ATCAGCTTTTAGGCTTTATTAACAGTGAGAATATCTAAATCAGGAG AAAGAACACCATGCGTAGTTTGGTAAACGGCAGAAAGATTATTTT AGAAAATGATACAACAAATACCGGCGGTACCGTACTTACCGGCTC TTCTATTGCTAAACAAACACAAGGGG
pIds-FLAG-IdsC-mKate2-IdsD	Constructed by restriction digest of pIds-mKate2-IdsD and pIds-FLAG-IdsC using BstEII/PacI.
pIds-FLAG-IdsC-mKate2-IdsD-ΔIdsE	Deletion of *idsE* in pIds-FLAG-IdsC-mKate2-IdsD using gBlock (7) and restriction digest with EcoNI/KpnI. Geneblock: GCGAACAATTAAAAATGGCAAGTGAAAAAGGTGATTGGAACCCTG AAACAGGTATATTTAAATTTAGTTTGGAAGTACAGTCTCAATTAGT AAATACATATTCTGCTTTTGGTGCACATCCTAATAGCCGTATAGGT ATTGAAGATTTATATTGGTATTATCAAGTCAATCCCGAGGTAACAA CACCGATGCGTTATATCAATTGGGGGGGAGATACCCAAGAAAACA ATCAGCTTTTAGGCTTTATTAACAGTGAGAATATCTAAATCAGGAG AAAGAACACCATGCGTAGTTTGGTAAACGGCAGAAAGATTATTTT AGAAAATGATACAACAAATACCGGCGGTACCGTACTTACCGGCTC TTCTATTGCTAAACAAACACAAGGGG
pIds-FLAG-IdsC $^{\Delta DUF4123}$-mKate2-IdsD	Constructed by restriction digest of pIds-mKate2-IdsD and pIds-FLAG-IdsC $^{\Delta DUF4123}$ using BstEII/PacI.
pIds-FLAG-IdsC $^{\Delta DUF4123}$-mKate2-IdsD-ΔIdsE	Deletion of *idsE* in pIds-FLAG-IdsC $^{\Delta DUF4123}$-mKate2-IdsD using gBlock (7) and restriction digest with EcoNI/KpnI. Geneblock: GCGAACAATTAAAAATGGCAAGTGAAAAAGGTGATTGGAACCCTG AAACAGGTATATTTAAATTTAGTTTGGAAGTACAGTCTCAATTAGT AAATACATATTCTGCTTTTGGTGCACATCCTAATAGCCGTATAGGT ATTGAAGATTTATATTGGTATTATCAAGTCAATCCCGAGGTAACAA CACCGATGCGTTATATCAATTGGGGGGGAGATACCCAAGAAAACA ATCAGCTTTTAGGCTTTATTAACAGGAGAATATCTAAATCAGGAGA AAGAACACCATGCGTAGTTTGGTAAACGGCAGAAAGATTATTTTA GAAAATGATACAACAAATACCGGCGGTACCGTACTTACCGGCTCT

Table 3.2 Primers used in this study (continued)

pIds-OmpA-FLAG-IdsC	Constructed by restriction digest of pIds and gBlock using BstEII/PacI; Geneblock: AATGAAGGGTTACCATTAGCTGAGGATTGCCGTGCGAAAGCGATG AAAAAAGGAACGGCCTAATGAAAAAGACAGCTATCGCATTAGCA GTGGCAGTGGCAGCTTTCGCAACTGCAGCGCAAGCAATGGACTAC AAAGACGATGACGATAAACTCTTGAGTCCAAATCCCCTCTATAAA GCGTATTGGGTTGCTCAATGCCGTTATACTCGCAACGGTGAACAAT TCAAGGGGGTGATGACCGTAGCAGGTACAAGTCAATCACAAGCTA TTAAGCAGATGCGCCAGTACTTTACGGCTCACCCAGGTGAATATAC CTTTGCGGACTATGACACATTAATCCCTTTAATCACCCATATTGAA CAAAGTTCAACCTTAGAATTACCGTTAATACGGCAAGTACGTGAG CAACATAATGCAAAGGTTTCAGCCGTATTAGTGGATAAATGCAAC CTCACACACCCAAGGCCTTCAGAAAAAGGCGACATTCATTACCGT GAGGGGCAACCTACGTTTATTGAATATTCGCATCTCTATGTCGTCA TTGACAGTGGGGAATACCACCGCCAAACCGGGCAACATCTTGTAC CGAAACTGCATGGCTCACAACTGCCATGGAAATCACTCTATCAAG GAGAAACCCAAGACAGCCTTGAAGATAAAGCCCCTTATTTGGTAC ACATTGCCGCCAATCAAGCCGGTCAGCGGTTTCTGGCTCATTACTT GAATTTACCACATAAAGCGAGTCTCGGATTATTTATCAATAGCCTC AAACCCTTTACCGATATTCACCGGCAAATGCGAAAACTCACCTATT TATATAATCAAAAACTGGAGAGTTGGAATTTCTTTCGTTTTTATGA TGTTAAGCACTTTATCCCATTTATTGAGTCTTTGACTCACGGACAG TTAATTAATGTGGCCAATG
pIds-OmpA-FLAG-IdsC-ΔIdsE	Deletion of *idsE* in pIds-OmpA-FLAG-IdsC using gBlock (7) and restriction digest with EcoNI/KnpI. Geneblock: GCGAACAATTAAAAATGGCAAGTGAAAAAGGTGATTGGAACCCTG AAACAGGTATATTTAAATTTAGTTTGGAAGTACAGTCTCAATTAGT AAATACATATTCTGCTTTTGGTGCACATCCTAATAGCCGTATAGGT ATTGAAGATTTATATTGGTATTATCAAGTCAATCCCGAGGTAACAA CACCGATGCGTTATATCAATTGGGGGGGAGATACCCAAGAAAACA ATCAGCTTTTAGGCTTTATTAACAGGAGAATATCTAAATCAGGAGA AAGAACACCATGCGTAGTTTGGTAAACGGCAGAAAGATTATTTTA GAAAATGATACAACAAATACCGGCGGTACCGTACTTACCGGCTCT

Table 3.2 Primers used in this study (continued)

pIds-PelB-FLAG-IdsC-ΔIdsE	Constructed by restriction digest of pIds-OmpA-FLAG-IdsC-ΔIdsE and gBlock using BstEII/StuI. Geneblock: AATGAAGGGTTACCATTAGCTGAGGATTGCCGTGCGAAAGCGATG AAAAAAGGAACGGCCTAATGAAATACCTATTGCCTACGGCAGCCG CTGGATTGTTATTACTCGCTGCCCAACCAGCGATGGCCATGGACTA CAAAGACGATGACGATAAACTCTTGAGTCCAAATCCCCTCTATAA AGCGTATTGGGTTGCTCAATGCCGTTATACTCGCAACGGTGAACAA TTCAAGGGGGTGATGACCGTAGCAGGTACAAGTCAATCACAAGCT ATTAAGCAGATGCGCCAGTACTTTACGGCTCACCCAGGTGAATAT ACCTTTGCGGACTATGACACATTAATCCCTTTAATCACCCATATTG AACAAAGTTCAACCTTAGAATTACCGTTAATACGGCAAGTACGTG AGCAACATAATGCAAAGGTTTCAGCCGTATTAGTGGATAAATGCA ACCTCACACACCCAAGGCCTTCAGAAAAAG
pTet-FLAG-IdsC	Constructed by amplification of FLAG-IdsC from pIds-FLAG-IdsC followed by restriction digest of PCR fragment and modified p_{LTetO} using SacI/AgeI.
pIds-FLAG-IdsC^{S38P}	Nucleotide change was introduced in pIds-FLAG-IdsC using Quikchange reaction protocols (Agilent Technologies, Santa Clara, CA). F: GTACAAGTCAACCACAAGCTATTAAGC R: GCTTAATAGCTTGTGGTTGACTTGTAC
pIds-FLAG-IdsC^{S38P}-mKate2-IdsD	Nucleotide change was introduced in pIds-FLAG-IdsC-mKate2-IdsD using Quikchange reaction protocols (Agilent Technologies, Santa Clara, CA). F: GTACAAGTCAACCACAAGCTATTAAGC R: GCTTAATAGCTTGTGGTTGACTTGTAC
pIds-FLAG-IdsC^{S38P}-ΔIdsE	Deletion of *idsE* in pIds-FLAG-IdsC^{S38P} using gBlock (7) and restriction digest with EcoNI/KnpI. Geneblock: GCGAACAATTAAAAATGGCAAGTGAAAAAGGTGATTGGAACCCTG AAACAGGTATATTTAAATTTAGTTTGGAAGTACAGTCTCAATTAGT AAATACATATTCTGCTTTTGGTGCACATCCTAATAGCCGTATAGGT ATTGAAGATTTATATTGGTATTATCAAGTCAATCCCGAGGTAACAA CACCGATGCGTTATATCAATTGGGGGGGAGATACCCAAGAAAACA ATCAGCTTTTAGGCTTTATTAACAGGAGAATATCTAAATCAGGAGA AAGAACACCATGCGTAGTTTGGTAAACGGCAGAAAGATTATTTTA GAAAATGATACAACAAATACCGGCGGTACCGTACTTACCGGCTCT

Table 3.2 Primers used in this study (continued)

pIds-FLAG-IdsC^{R186Q}	Nucleotide change was introduced in pIds-FLAG-IdsC using Quikchange reaction protocols (Agilent Technologies, Santa Clara, CA). F: CAAGCCGGTCAGCAGTTTCTGGCTCATTAC R: GTAATGAGCCAGAAACTGCTGACCGGCTTG
pIds-FLAG-IdsC^{R186Q}-mKate2-IdsD	Nucleotide change was introduced in pIds-FLAG-IdsC-mKate2-IdsD using Quikchange reaction protocols (Agilent Technologies, Santa Clara, CA). F: CAAGCCGGTCAGCAGTTTCTGGCTCATTAC R: GTAATGAGCCAGAAACTGCTGACCGGCTTG
pIds-FLAG-IdsC^{R186Q}-ΔIdsE	Deletion of *idsE* in pIds-FLAG-IdsC^{R186Q} using gBlock (7) and restriction digest with EcoNI/KnpI. Geneblock: GCGAACAATTAAAAATGGCAAGTGAAAAAGGTGATTGGAACCCTG AAACAGGTATATTTAAATTTAGTTTGGAAGTACAGTCTCAATTAGT AAATACATATTCTGCTTTTGGTGCACATCCTAATAGCCGTATAGGT ATTGAAGATTTATATTGGTATTATCAAGTCAATCCCGAGGTAACAA CACCGATGCGTTATATCAATTGGGGGGGAGATACCCAAGAAAACA ATCAGCTTTTAGGCTTTATTAACAGGAGAATATCTAAATCAGGAGA AAGAACACCATGCGTAGTTTGGTAAACGGCAGAAAGATTATTTTA GAAAATGATACAACAAATACCGGCGGTACCGTACTTACCGGCTCT
pIds-FLAG-IdsC$^{S38P/R186Q}$	Nucleotide change was introduced in pIds-FLAG-IdsC^{R186Q} using Quikchange reaction protocols (Agilent Technologies, Santa Clara, CA). F: GTACAAGTCAACCACAAGCTATTAAGC R: GCTTAATAGCTTGTGGTTGACTTGTAC
pIds-FLAG-IdsC$^{S38P/R186Q}$-mKate2-IdsD	Nucleotide change was introduced in pIds-FLAG-IdsC^{R186Q}-mKate2-IdsD using Quikchange reaction protocols (Agilent Technologies, Santa Clara, CA). F: GTACAAGTCAACCACAAGCTATTAAGC R: GCTTAATAGCTTGTGGTTGACTTGTAC

Table 3.2 Primers used in this study (continued)

pIds-FLAG-IdsC$^{S38P/R186Q}$-ΔIdsE	Deletion of *idsE* in pIds-FLAG-IdsC$^{S38P/R186Q}$ using gBlock (7) and restriction digest with EcoNI/KnpI. Geneblock: GCGAACAATTAAAAATGGCAAGTGAAAAAGGTGATTGGAACCCTG AAACAGGTATATTTAAATTTAGTTTGGAAGTACAGTCTCAATTAGT AAATACATATTCTGCTTTTGGTGCACATCCTAATAGCCGTATAGGT ATTGAAGATTTATATTGGTATTATCAAGTCAATCCCGAGGTAACAA CACCGATGCGTTATATCAATTGGGGGGGAGATACCCAAGAAAACA ATCAGCTTTTAGGCTTTATTAACAGGAGAATATCTAAATCAGGAGA AAGAACACCATGCGTAGTTTGGTAAACGGCAGAAAGATTATTTTA GAAAATGATACAACAAATACCGGCGGTACCGTACTTACCGGCTCT
pAD-IdsC-FLAG-His	Constructed by restriction digest of pAD100 and gBlock using BspHI/XbaI. Geneblock: TCATGATTCTCTTGAGTCCAAATCCCCTCTATAAAGCGTATTGGGT TGCTCAATGCCGTTATACTCGCAACGGTGAACAATTCAAGGGGGT GATGACCGTAGCAGGTACAAGTCAATCACAAGCTATTAAGCAGAT GCGCCAGTACTTTACGGCTCACCCAGGTGAATATACCTTTGCGGAC TATGACACATTAATCCCTTTAATCACCCATATTGAACAAAGTTCAA CCTTAGAATTACCGTTAATACGGCAAGTACGTGAGCAACATAATG CAAAGGTTTCAGCCGTATTAGTGGATAAATGCAACCTCACACACC CAAGACCGTCAGAAAAAGGCGACATTCATTACCGTGAGGGGCAAC CTACGTTTATTGAATATTCGCATCTCTATGTCGTCATTGACAGTGG GGAATACCACCGCCAAACCGGGCAACATCTTGTACCGAAACTGCA TGGCTCACAACTGCCATGGAAATCACTCTATCAAGGAGAAACCCA AGACAGCCTTGAAGATAAAGCCCCTTATTTGGTACACATTGCCGCC AATCAAGCCGGTCAGCGGTTTCTGGCTCATTACTTGAATTTACCAC ATAAAGCGAGTCTCGGATTATTTATCAATAGCCTCAAACCCTTTAC CGATATTCACCGGCAAATGCGAAAACTCACCTATTTATATAATCAA AAACTGGAGAGTTGGAATTTCTTTCGTTTTTATGATGTTAAGCACT TTATCCCATTTATTGAGTCTTTGACTCACGGACAGTTAATTAATGT GGCCAATGGGGTAAATGCGTTCTACGGCTATAGTGCACAATACCC CGATGGGGTTGAAATCACCTTTCACCCAGATTATCTGTATGACGGC AGTAAGCGAGAGCCGTTATTTATTAATACCTATTTATACAATCACT ACGCGAATATCACACAGATGCAAACTGTGGCTAAAGCTAAGGCAC TGATTGAACAATTTTCTCAGGTAGAAGGGGATGAGTTAGAGGGTG ACGCATTAATGGGCTACTGTATACACGCAGCAAATTGCAGTTTTTT AGACGATATTCATCAATCAAAAGCGTTATTGTACGATTTGCAAGCT CGCTATTTGTGCCGTCATCAACCGAGAACATGGCAGATCGCCAAT GAAAAAGCTGCACCTTATAAATACAACCAAGTTTTATTGAGTTACC ACCGTTATATCGCCTGCTTAAATACCCAAGGAGAAATGAAAGGTC TAGACTAC

Table 3.2 Primers used in this study (continued)

pAD-IdsC-FLAG	Constructed by restriction digest of pAD100 and gBlock using PacI/BglII. Geneblock: CGCGCGTTAATTAATGTGGCCAATGGGGTAAATGCGTTCTACGGCT ATAGTGCACAATACCCCGATGGGGTTGAAATCACCTTTCACCCAG ATTATCTGTATGACGGCAGTAAGCGAGAGCCGTTATTTATTAATAC CTATTTATACAATCACTACGCGAATATCACACAGATGCAAACTGTG GCTAAAGCTAAGGCACTGATTGAACAATTTTCTCAGGTAGAAGGG GATGAGTTAGAGGGTGACGCATTAATGGGCTACTGTATACACGCA GCAAATTGCAGTTTTTTAGACGATATTCATCAATCAAAAGCGTTAT TGTACGATTTGCAAGCTCGCTATTTGTGCCGTCATCAACCGAGAAC ATGGCAGATCGCCAATGAAAAAGCTGCACCTTATAAATACAACCA AGTTTTATTGAGTTACCACCGTTATATCGCCTGCTTAAATACCCAA GGAGAAATGAAAGGTCTAGACTACAAGGACGACGATGACAAGAG ATCTCGCGCG
pAD-$IdsD_{CW677}$-His_6	Constructed by amplification of 5' portion of IdsD from genomic DNA of CW677. F: CGGATAACAATTTCACACAGGAAACAGACCATGGGGACTGGAGAA GTGAATGAGAGATATTTAAC R: CTTTTGAGTGGCTGCTTAATCCCT SliCE cloning was used to piece together PCR product, pAD100 digested with NcoI/BglII restriction enzymes, and gBlock. Geneblock: ACTGGAAGGGATTAAGCAGCCACTCAAAAGTTTCTCAAAGAATAT GAAGAAGATGTTTGATTGGGATACTCGATTTAAATCAGCGGGTCT AAAACAGATTATCACAACCGCTAAATTTAAATTAATGGAAGGCTA CAGTGCTATGTATTTACCTACAGATAAGAAATCCTTAAACGCTCAC ATGAAATTAGCACTAGATATTTATACACTGCTCACAAGTATCATTG AATTTAGTACAGTTTCACATACGAAAGAGTTTGATAAACAAGACC CATTAAATGCCGCTGCCGTGAATATATTTCGTGTTCAAATGGTGGC ACATATTTTAAATACCGCAGAAGCAGTAGTTGAAATACGCCAAGC AGCTCGAGGTTATGCGACATCAGTGACTTTTCCACCGCTTCAGCGG TTATTGACTAAAATTCAGTTGCCTGAAATCCAAACCAAGTTAGGGA AAGTGGGCTTAAAAGGGCTTGGATATACCGTGGCAATTTTAGGGG TCGCATTACCCCTCGCGGAGGCATCAACAGAGTTTTATAACCATGA TTACATTACAGGCTCAGCAAAAATTGCGGAAGCGGTAGGGACATT GGCTTTTTCAGTGGGGCTAGCAGCATGGGGTGCCACTGAGGGTGT AGTTGCAACTACCATTGCGGCATTTGCGTGGGAGTTAATAGTTATC GGTGCGATCGTCTATGGCGTCGGTGCGGCAATTTACACGTATTTTA

Table 3.2 Primers used in this study (continued)

	AAACAGATTCGTTTGAAAAGTTATTGAAGCAGTGTTTTTGGGGTAA TGGGGATAAGTATTTTGCGGGGGGATATAAATTAAAGGAAGGGCA AAAAATCAAAAGACCTGATACTACAGATGCTCAATTGGAGATTTA TATTCGATATATTGAAGAATATAAATCTTACTTTCAAATGGAGTTA CAAGAATTTGCCAATCTTTTCTTTACCTCTCAGCTACAAGTCAAAG CAATACTAAAACCCGATTTTCAACCAAGCTATGGTACAGCACGCT ACTCTATTCAATATCAATTTAAATTGTCCAATTTTCAATATGGTATT TCAGATATTGAATATCAGTTGGTAGAAAAGAAAATGCCACATATT TATCCATCAGAGACTCCGATTAAGTATATATCTAAACAAGGTAATA CCGTGGTTAAATATAAAGGTGCTGAATATTTAGCTTCACAACAAAC AAAATTTAATACCGCATTTGAAATGGCTTTACAACACACCATTGAA GCAGCTTTACAAAAGGACACAATGCTAGGTAATGGGCTGCTTACT CTAAATTTTGAGATAGAAGCAGGTATATTTACGGGGGATCCGATA GGAAAATCCATCCCTTCTATTTACTGGTATTACATTGTAGATCGCA TTAAAGGCGAAATTGCACCATTACGTTACCGAAACGGCAACCCCG ACGATAAAATATATGGCTGTATTGATGAGGAGGGCACGGAACACC ATCATCACCATCACTGAGTGACTGAGATCTAACTAGCATAACCCCT TGGGGCCTCTAAAC

Results

IdsC binds IdsD directly via the DUF4123 domain

To test whether the IdsC-IdsD interaction depended on other Ids or T6S proteins, IdsC-FLAG and IdsD-His_6 were separately produced from pAD100-derived plasmids (13) in *Escherichia coli* strain BL21(DE3) pLysS, which lacks Ids or T6S (14). pAD100 is an IPTG-inducible plasmid optimized for protein expression. Anti-FLAG co-immunoprecipitation assays were performed on a mixture of cell lysates. Lysate expressing IdsD-His_6 was doped with purified FLAG-tagged *E. coli* bacterial alkaline phosphatase (FLAG-BAP) as a negative control. The load (L), non-binding (-) and binding (+) fractions were analyzed by western blot using a custom polyclonal anti-IdsD antibody, commercial anti-FLAG and anti-sigma70 antibodies. IdsC-FLAG pulled down IdsD-His_6 (**Figure 3.1**), showing that this interaction is independent of T6S or other Ids proteins.

The main protein domain within IdsC is a DUF4123 domain. To test whether this domain is required for the IdsC-IdsD interaction, IdsC lacking the DUF4123 domain ($IdsC^{\Delta DUF4123}$-FLAG) was produced and mixed with IdsD-His_6 and subjected to anti-FLAG co-immunoprecipitation assays. Considerably less IdsD-His_6 was pulled down (**Figure 3.1**), indicating that lack of the DUF4123 domain decreases the interaction between IdsC and IdsD. These results suggest that IdsC binds IdsD directly and that the DUF4123 domain helps mediate this interaction.

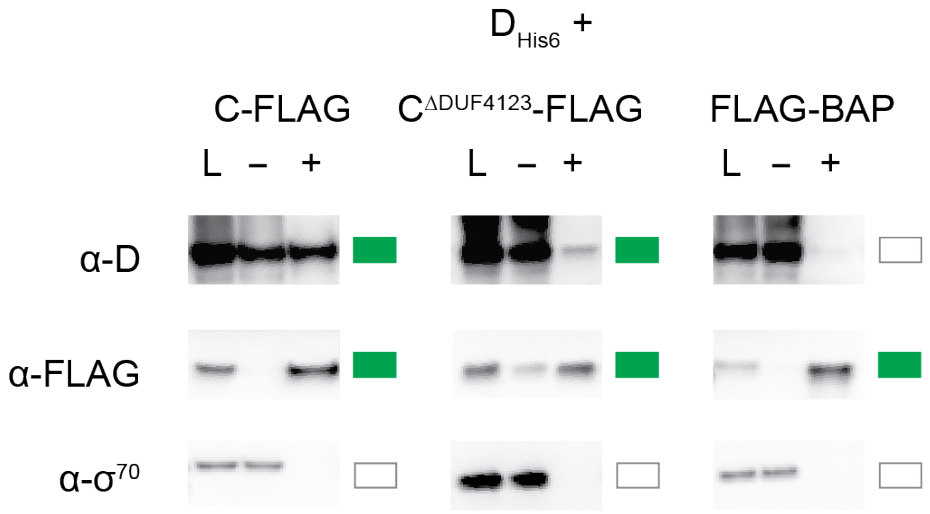

Figure 3.1 DUF4123 domain of IdsC is necessary for IdsC-IdsD interaction Anti-FLAG co-immunoprecipitation assays were performed as previously described on lysates of *E. coli* BL21(DE3) pLysS expressing Ids proteins from modified pAD100 vectors (11, 13). Soluble (L), non-binding (-) and binding (+) fractions were analyzed via western blot using a custom polyclonal anti-IdsD, and commercial monoclonal anti-FLAG and anti-sigma70 antibodies. Green boxes indicate a band in the binding fraction; white boxes indicate no bind in the binding fraction. Lysate mixtures are labeled above: IdsD-His_6 mixed with IdsC-FLAG, IdsD-His_6 mixed with $IdsC^{\Delta DUF4123}$-FLAG, and IdsD-His_6 mixed with FLAG-BAP, a purified FLAG-tagged *E. coli* protein, as a negative control.

IdsC-IdsD interaction is essential for maintenance of IdsD protein levels

To confirm these results in *P. mirabilis*, an established Ids expression system was used in which all *ids* genes are expressed on a plasmid under regulation of the native *ids* promoter (pIds) in a parent strain lacking the *ids* genes (Δ*ids*). Anti-FLAG co-immunoprecipitations were attempted on a strain expressing FLAG-IdsC lacking the DUF4123 domain (FLAG-IdsC$^{\Delta DUF4123}$). FLAG-IdsC$^{\Delta DUF4123}$ and IdsD protein levels overall appeared to be diminished in this strain. Therefore, protein was supplemented by adding *E. coli* lysate expressing IdsC$^{\Delta DUF4123}$-FLAG. As a control, *P. mirabilis* lysate expressing FLAG-IdsC was supplemented with *E. coli* lysate expressing IdsC-FLAG. While FLAG-IdsC pulled down IdsB and IdsD, FLAG-IdsC$^{\Delta DUF4123}$ did not pull down IdsB or IdsD (**Figure 3.2**).

To further test if lower IdsD protein levels were due to changes in IdsC, relative levels of IdsD in cell extracts from *P. mirabilis* strains lacking expression of one or more of the Ids proteins were examined. IdsD appeared to be lower or absent in strains completely lacking IdsC or IdsD (**Figure 3.3**). This observation correlated to the lower levels of mKate-IdsD observed in previous experiments (**Figure 2.5**). However, the mKate-IdsD fusion appears to stabilize IdsD in the absence of full-length IdsC (**Figure 2.6**). It is possible that the N-terminal mKate2 flourophore occludes a degradation signal or allows IdsD to adopt a more stable tertiary structure, but these possibilities remain to be tested.

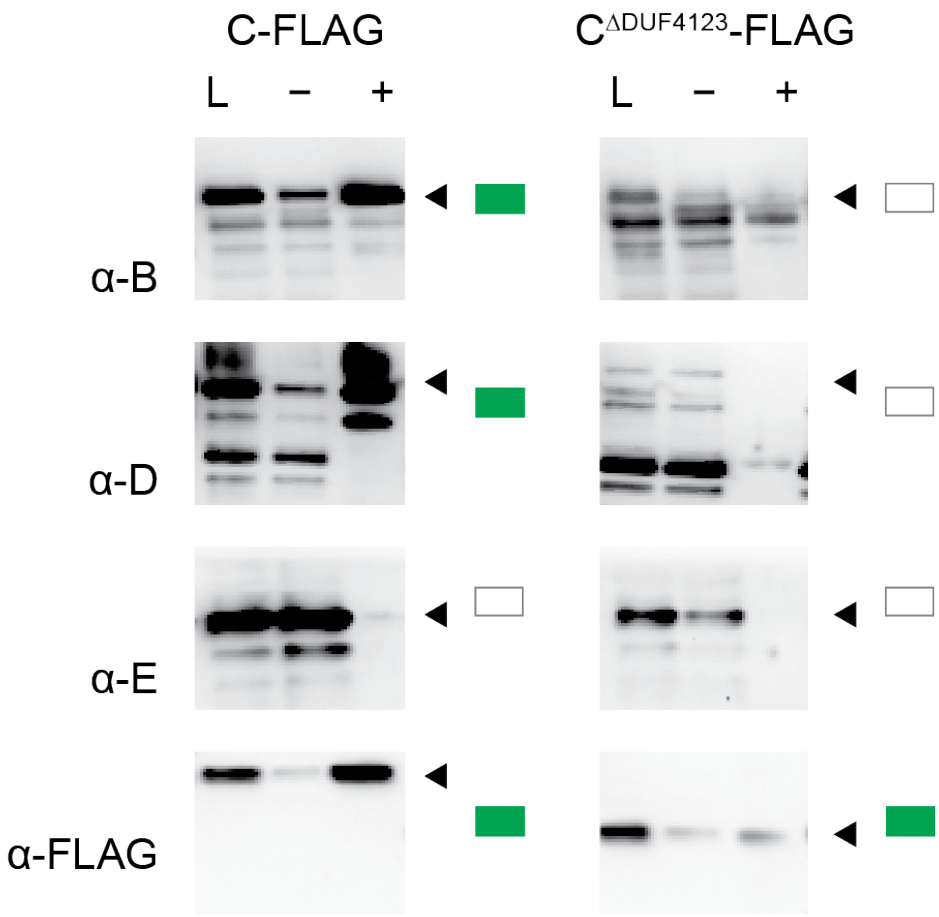

Figure 3.2 DUF4123 domain of IdsC is necessary for IdsBCD complex formation

Anti-FLAG co-immunoprecipitation assays were performed as previously described on *P. mirabilis* lysate doped with *E. coli* lysate expressing IdsC-FLAG or IdsC $^{\Delta DUF4123}$-FLAG. Soluble (L), non-binding (-) and binding (+) fractions were analyzed via western blot using a custom polyclonal anti-IdsB, anti-IdsD, anti-IdsE, and commercial monoclonal anti-FLAG antibodies. Black arrows indicate expected sizes of IdsB, IdsD, IdsE, IdsC, and IdsC$^{\Delta DUF4123}$.

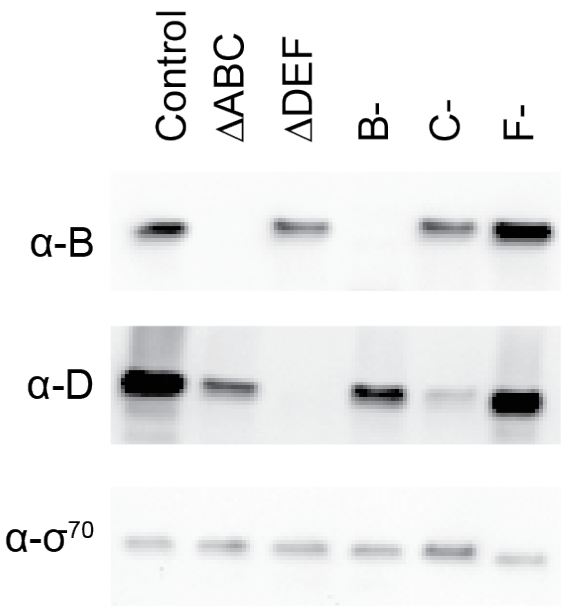

Figure 3.3 IdsD protein levels are diminished in absence of IdsC Whole cell extracts of *P. mirabilis* strains expressing pIds (control) or modified pIds vectors that result in absence of IdsA-IdsC, IdsD-IdsF or IdsB, IdsC, IdsF individually were analyzed via western blot using custom polyclonal anti-IdsB, anti-IdsD, and monoclonal anti-sigma70 antibodies.

IdsC-IdsD interaction is necessary for IdsD secretion

Given that lack of the DUF4123 domain in IdsC disrupts the IdsBCD interaction and results in overall lower IdsD protein levels, we predicted that a FLAG-IdsC$^{\Delta DUF4123}$ strain would be unable to secrete IdsD. An *in vivo* IdsD transfer assay was used where secretion of IdsD into neighboring cells that lack the self-identity binding partner, IdsE, results in a restricted colony migration radius. Disruption of T6S activity, through a chromosomal point mutation in the sheath protein TssB, alleviates this restriction (7). *P. mirabilis* expressing FLAG-IdsC and lacking IdsE displayed a restricted colony radius that was alleviated upon T6S disruption (**Figure 3.4**). *P. mirabilis* expressing FLAG-IdsC$^{\Delta DUF4123}$ and lacking IdsE showed a large colony radius which showed no synergistic effects upon T6S disruption (**Figure 3.4**). Given that the mKate-IdsD fusion appears to maintain IdsD protein levels to a detectable extent, we repeated this assay in cells lacking IdsE but expressing FLAG-IdsC or FLAG-IdsC$^{\Delta DUF4123}$ and mKate-IdsD. Similar results were obtained (**Figure A.3**). This *in vivo* assay was complemented by *in vitro* tricholoroacetic acid precipitations. The supernatants of liquid-grown cells of T6S-positive strains expressing FLAG-IdsC or FLAG-IdsC$^{\Delta DUF4123}$ and either unlabeled IdsD or mKate-IdsD were concentrated using tricholoroacetic acid and sent to liquid chromatography tandem mass spectrometry (LC-MS/MS) for analysis. While IdsD peptides could be detected in the supernatants of FLAG-IdsC strains, they were not detected in FLAG-IdsC$^{\Delta DUF4123}$ strains (**Table 3.3** and **Table A.4**).

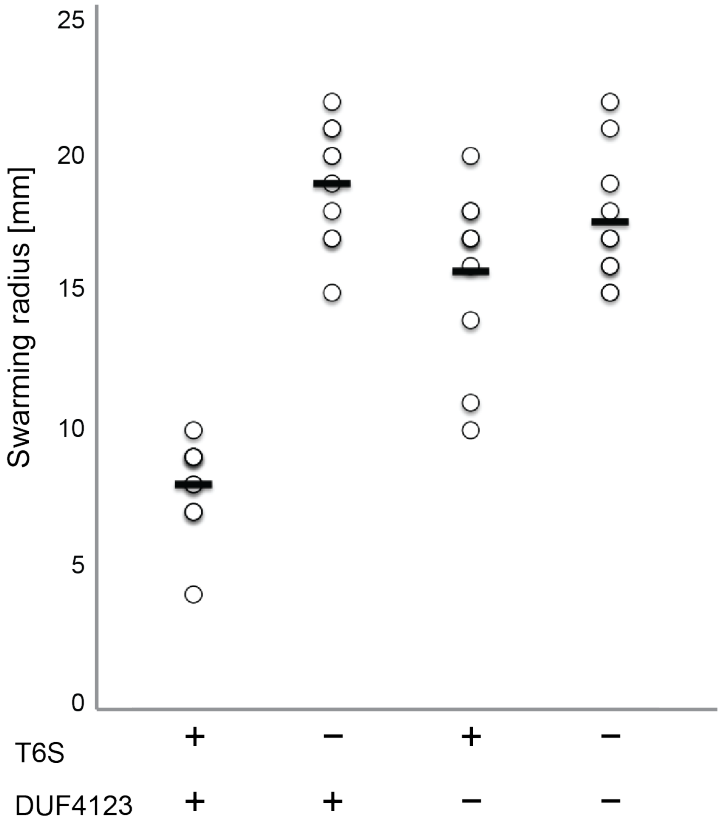

Figure 3.4 IdsC-IdsD interaction is essential for IdsD secretion *In vivo* assay for IdsD cell-to-cell transfer in which IdsD secretion results in reduced colony, while lack of transport alleviates this restriction (7). *P. mirabilis* strains expressing modified pIds vectors producing FLAG-IdsC (+) or FLAG-IdsC$^{\Delta DUF4123}$ (-). T6S+ is a *P. mirabilis* strain producing a fully functional T6S system; T6S- is the TssB chromosomal mutant (7). Open circles indicate migration radii per replicate and bars indicate average migration radius. N=10.

Table 3.3 Ids specific LC-MS/MS hits secreted by FLAG-IdsC and FLAG-IdsC$^{\Delta DUF4123}$ strains

TCA	Protein	No. unique peptides	No. total peptides	% Coverage
FLAG-C	IdsB	4	4	8.85
	IdsD	3	3	3.09
	σ^{70}	0	0	0
FLAG-C$^{\Delta DUF4123}$	IdsB	0	0	0
	IdsD	0	0	0
	σ^{70}	0	0	0

IdsC appears to be an IdsD-specific chaperone

DUF4123 proteins in other bacterial systems have been shown to be specific for the T6S substrate encoded immediately downstream (1-3). To test whether IdsC is specifically involved in IdsD secretion or whether IdsC acts as a more general secretion chaperone, LC-MS/MS data sets from the tricholoroacetic acid precipitation experiments were compared. Only protein hits with at least three unique peptide fragments detected were considered in the analysis. The majority of detected secreted proteins were found in the concentrated supernatants of both FLAG-IdsC and FLAG-IdsC$^{\Delta DUF4123}$ (242 hits) (**Figure 3.5** and **Table A.5**), suggesting that disruption of the DUF4123 domain in IdsC does not broadly alter the T6S-dependent secretome. Proteins that were found to be secreted exclusively in FLAG-IdsC (45 hits) or FLAG- IdsC$^{\Delta DUF4123}$ (55 hits) were further run through SecReT6 (15), a database that allows comparison of protein sequences to known T6S substrates. None of these proteins were found to be homologous to known T6S substrates. If IdsC acts on another unique T6S substrate not in the SecReT6 (15) database, the prediction would be that FLAG-IdsC would pull down this substrate and secrete it, and that secretion of that substrate would be abrogated in FLAG-IdsC$^{\Delta DUF4123}$. To test this, the LC-MS/MS data set for proteins pulled down by FLAG-IdsC was analyzed for those proteins that were exclusively secreted by FLAG-IdsC (45 hits). This comparison generated a list of 8 proteins (**Figure 3.6** and **Table A.6**), including IdsB and IdsD. Of these, the only known T6S-dependent substrate is IdrD (8), a protein that is predicted to function in an effector/immunity pair to also signal self-identity. However, given that the Idr system is known to function independently of the

Ids system (8), it is unlikely that IdsC is required for IdrD secretion. This suggests that IdsC is most likely an IdsD-specific chaperone.

Figure 3.5 Comparison of LC-MS/MS proteins secreted by FLAG-IdsC and FLAG-IdsC$^{\Delta DUF4123}$ Protein hits with at least three unique peptides detected in concentrated supernatants of liquid-grown FLAG-IdsC or FLAG-IdsC$^{\Delta DUF4123}$ cells were compared using VENNY (16). Full data sets can be found on Gibbs laboratory data storage computer. **Table A.5** lists protein hits by category.

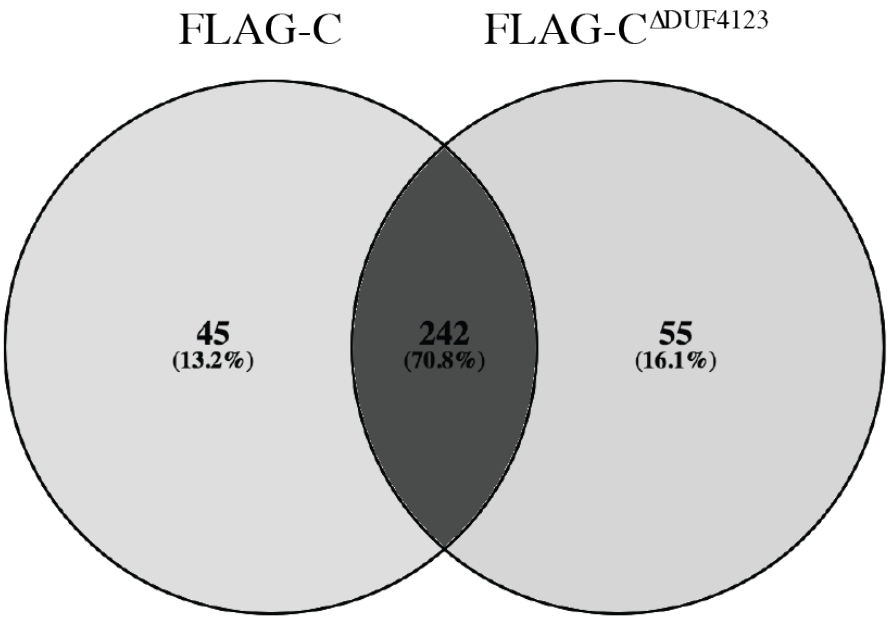

Figure 3.6 Comparison of LC-MS/MS proteins secreted exclusively by and pulled down with FLAG-IdsC Protein hits with at least three unique peptides detected in concentrated supernatant of liquid-grown FLAG-IdsC but not FLAG-IdsC$^{\Delta DUF4123}$ cells was compared to proteins pulled down by FLAG-IdsC using VENNY (16). Full data sets can be found on Gibbs laboratory data storage computer. **Table A.6** lists protein hits.

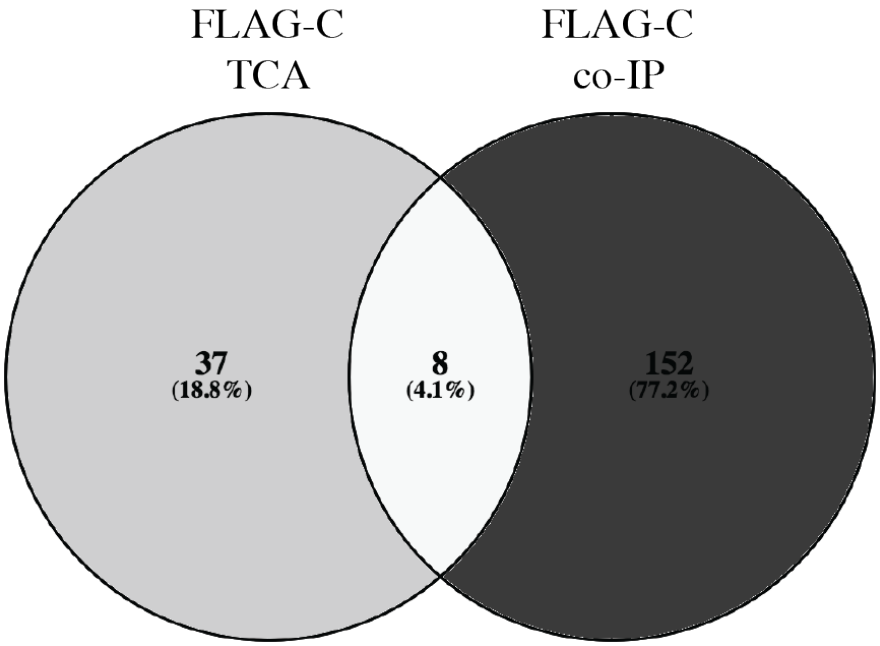

IdsC acts on IdsD only in producing cells

These results led to a model wherein the DUF4123 domain of IdsC mediates binding of IdsD in producing cells, independent of interactions with other Ids proteins or the T6S machinery, to form a transport-ready complex with IdsB and IdsF. The subcellular location of IdsD after transport is not known, as T6S substrates can be delivered to the cytoplasm or the periplasm of neighboring cells (17-22). To test whether IdsC could bind and regulate IdsD transferred from a neighboring cell, we expressed FLAG-IdsC in the periplasm or excess FLAG-IdsC in the cytoplasm. To test periplasmic expression, FLAG-IdsC was targeted to the periplasm with either a PelB (23) or an OmpA (23) signal sequence. IdsE was deleted in each construct and the resultant pIds plasmids expressed in the TssB chromosomal mutant strain that lacks T6S activity. Each strain was tested for self-recognition phenotypes against the parent strain BB2000, or a strain lacking the *ids* locus. If periplasmic FLAG-IdsC is sufficient to bind and neutralize transferred IdsD, then these strains should recognize BB2000 as self. However, strains expressing periplasmic FLAG-IdsC recognized BB2000 as non-self (**Figure 3.7**). To test cytoplasmic expression, FLAG-IdsC was induced in an anhydrotetracyline inducible plasmid (24) in either BB2000 or BB2000 with a chromosomal *idsE* deletion (BB2000::Δ*idsE*). BB2000::Δ*idsE* shows restricted colony migration as compared to BB2000 in the absence of FLAG-IdsC induction (**Figure 3.8**). If cytoplasmic IdsC is able to bind and neutralize transferred IdsD, then induction of FLAG-IdsC in BB2000::Δ*idsE* should display an equivalent colony radius to BB2000. Induction of FLAG-IdsC in BB2000::Δ*idsE* did not restore colony migration (**Figure 3.8**). Together, these results indicate that IdsC exclusively binds IdsD produced within the same cell.

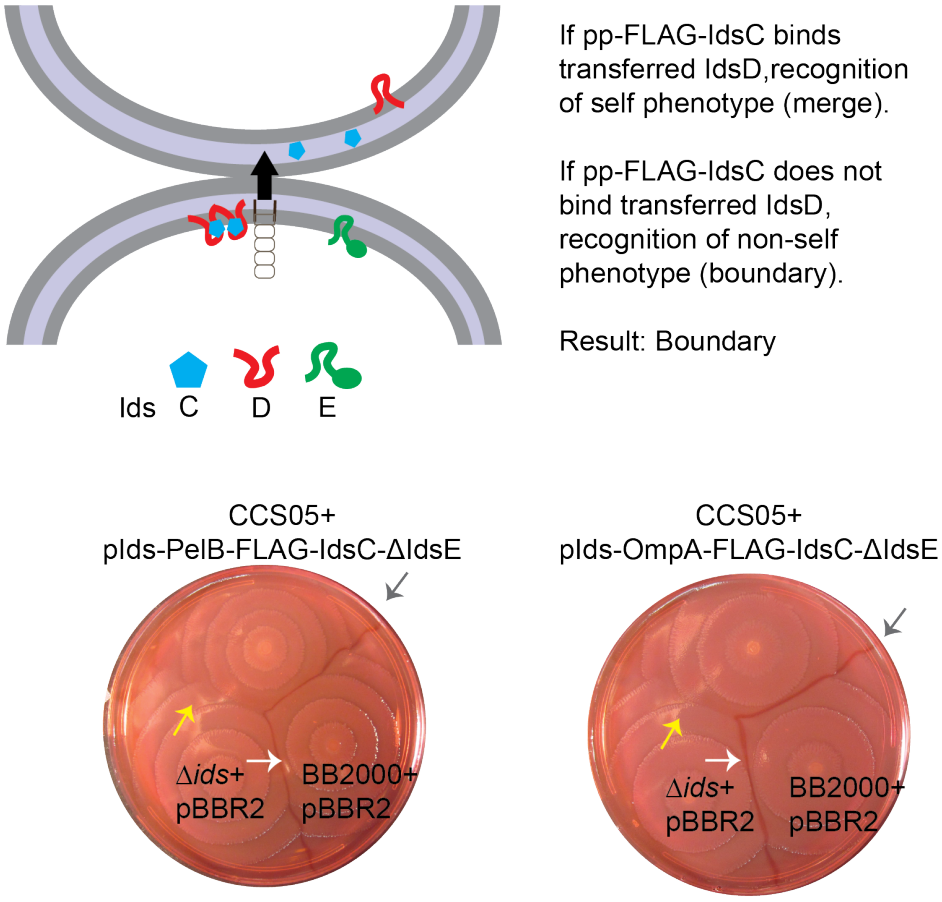

Figure 3.7 Periplasmic FLAG-IdsC does not neutralize transferred IdsD pIds-FLAG-IdsC-ΔIdsE was modified to target FLAG-IdsC to the periplasm with either a PelB (23) or an OmpA (25) signal sequence in the TssB chromosomal mutant strain. If IdsD is secreted into the periplasm, and periplasmic FLAG-IdsC (pp-FLAG-IdsC) is sufficient to bind and neutralize incoming IdsD, then the prediction is that this strain would recognize a parent strain (BB2000) as self. Self-recognition was tested via boundary formation, and strains expressing periplasmic FLAG-IdsC formed a boundary with BB2000 (grey arrow) indicating a non-self phenotype.

Figure 3.8 Excess cytoplasmic FLAG-IdsC does not neutralize transferred IdsD

BB2000 or BB2000 with a chromosomal IdsE deletion (BB2000::Δ*idsE*) carried an anhydrotetracycline-inducible plasmid expressing FLAG-IdsC. If IdsD is secreted into the cytoplasm, and excess cytoplasmic FLAG-IdsC (cyto-FLAG-IdsC) can bind and neutralize incoming IdsD, then the prediction is that BB2000::Δ*idsE* will no longer display inhibited swarm colony expansion upon inducing expressing of FLAG-IdsC with micromolar (μM) anhydrotetracyline [aTc]. Open circles indicate migration radii per replicate and bars indicate average migration radius. N=3.

Figure 3.8 Excess cytoplasmic FLAG-IdsC does not neutralize transferred IdsD (continued)

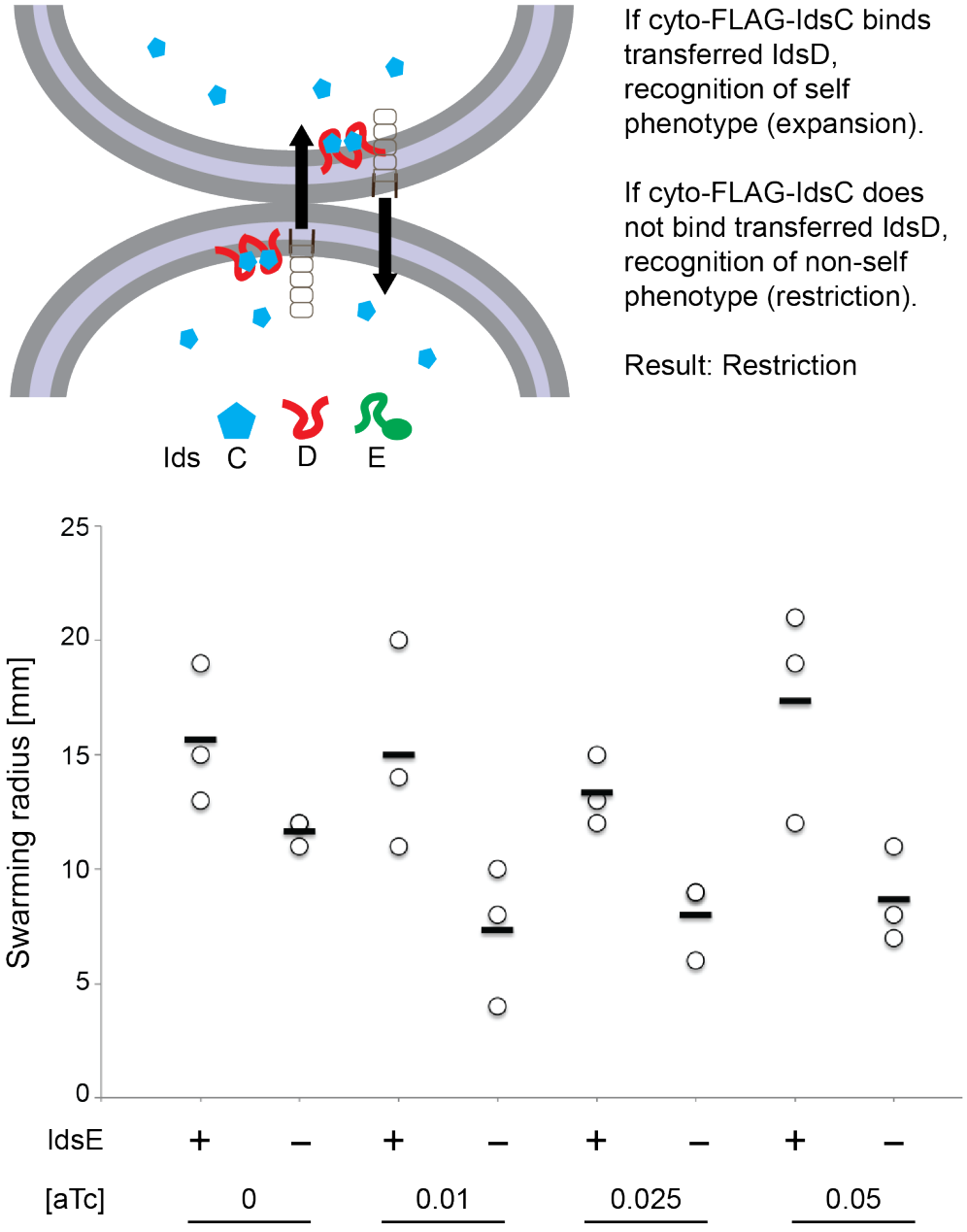

IdsC is highly conserved and can bind IdsD originating from various strains

To test whether IdsC regulation of IdsD was exclusive to strain BB2000 or if it is a more general mechanism used, I compared protein sequences of IdsC and IdsD across several *P. mirabilis* strains. IdsC was of equivalent length and showed high sequence conservation across strains (**Figure 3.9**). IdsD proteins are either 1033(4) or 1072 amino acids in length and while they show high sequence conservation in the first 57 amino acids, the protein sequences then diverge based on protein length (**Figure 3.10**) (5, 11). The high sequence conservation of IdsC suggests this is a general mechanism, and the prediction would be that IdsC proteins are interchangeable between strains. If so, then IdsC from strain BB2000 would be able to bind IdsD proteins from different strains. I tested whether IdsC-FLAG from strain BB2000 binds IdsD from strains HI4320 ($IdsD_{HI}$-His_6) and strain CW677 ($IdsD_{CW677}$-His_6). Each was expressed separately in *E. coli* strain BL21(DE3) pLysS and lysates were mixed and subjected to anti-FLAG co-immunoprecipitations. IdsC-FLAG from strain BB2000 pulled down IdsD proteins from BB2000 (**Figure 3.1**), strain HI4320 and strain CW677 (**Figure 3.11**).

Figure 3.9 IdsC is highly conserved across *P. mirabilis* strains Alignment of IdsC protein sequences from *P. mirabilis* strains BB2000, HI4320, CW677, S4/3, CW977, I5/5, G151, and WGLW6. The DUF4123 domain (amino acids 127-254) is highlighted above alignment with a black line. The color scheme is based on ClustalX (26). Sequences were accessed by NCBI using a BLASTp PSI-BLAST search of the sequence database. Alignments were constructed using ClustalW2 (26-28) and then displayed using JalView (29). The polymorphic amino acid residues are highlighted with an asterisk above alignment.

Figure 3.9 IdsC is highly conserved across *P. mirabilis* strains (continued)

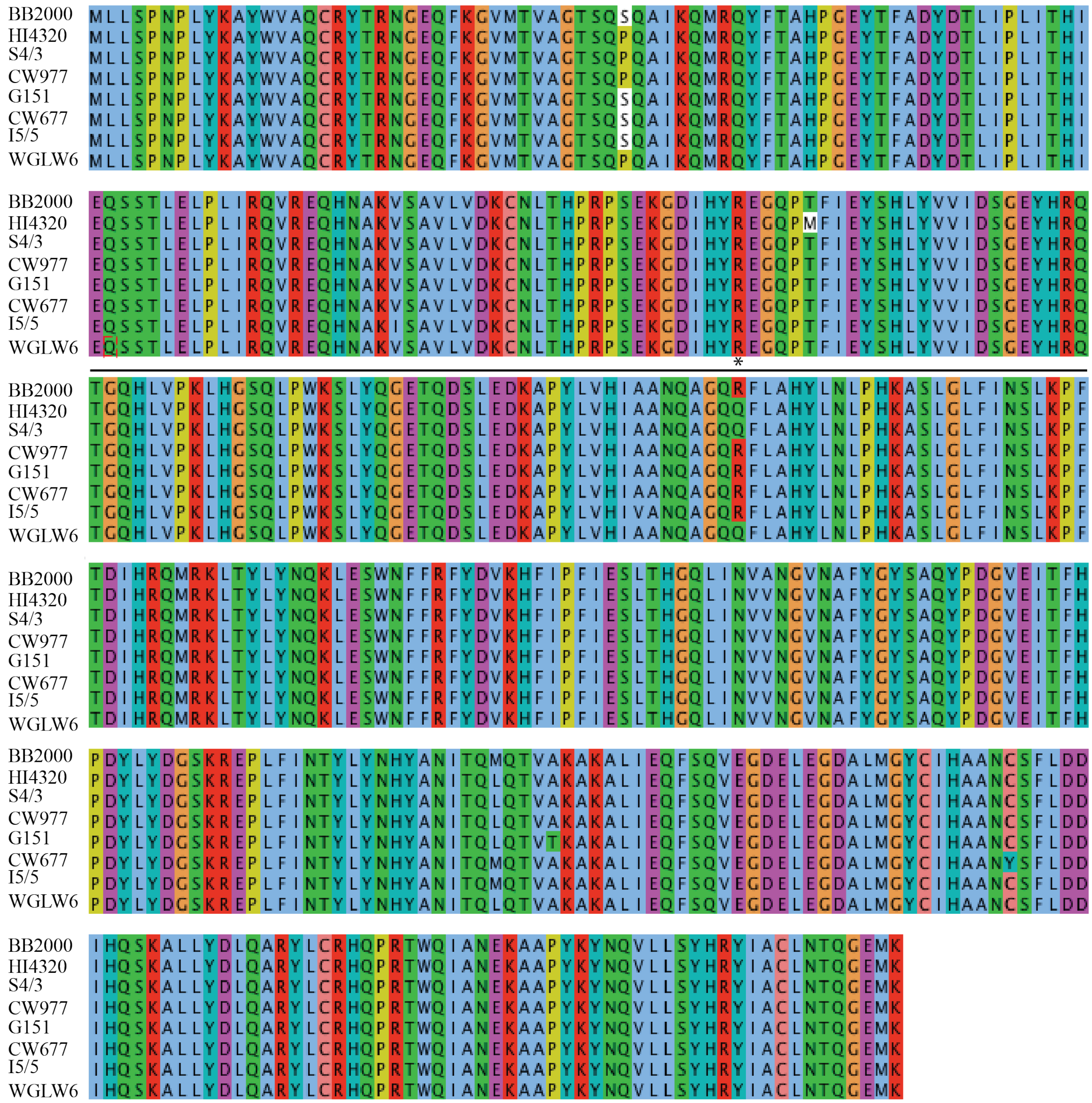

Figure 3.10 The first 57 amino acids of IdsD are highly conserved across *P. mirabilis* strains Alignment of IdsD protein sequences highlighting the first 70 amino acids from *P. mirabilis P. mirabilis* strains BB2000, HI4320, CW677, S4/3, CW977, I5/5, G151, and WGLW6. The color scheme is based on ClustalX (26). Sequences were accessed by NCBI using a BLASTp PSI-BLAST search of the sequence database. Alignments were constructed using ClustalW2 (26-28) and then displayed using JalView (29). Full sequence alignment of IdsD can be found in Cardarelli et al (11).

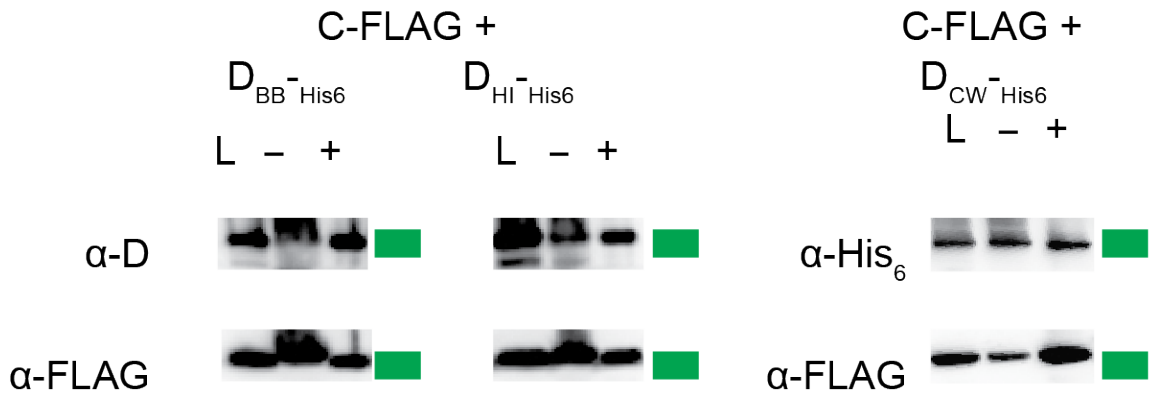

Figure 3.11 IdsC binds IdsD from various *P. mirabilis* strains Anti-FLAG co-immunoprecipitation assays were performed on lysate mixtures of *E. coli* BL21(DE3) pLysS expressing Ids proteins from modified pAD100 vectors (11, 13). Soluble (L), non-binding (-) and binding (+) fractions were analyzed via western blot using a custom polyclonal anti-IdsD, and commercial monoclonal anti-FLAG and anti-sigma70 antibodies. Green boxes indicate a band in the binding fraction; white boxes indicate no bind in the binding fraction. Lysate mixtures are labeled above: IdsC-FLAG with $IdsD_{BB}$-His_6, IdsC-FLAG with Ids_{HI}-His_6, and IdsC-FLAG with $IdsD_{CW677}$-His_6.

Functions of IdsC can be uncoupled by single amino acid changes

Although IdsC is highly conserved there are a few single amino acid polymorphisms across strains. Of these, we noted that three appeared to be present in about half of the protein sequences we analyzed. In reference to the IdsC sequence from BB2000 these amino acids are a serine to proline change at position 38 (S38P), an arginine to glutamine change at position 186 (R186Q), and a methionine to leucine change at position 309 (M309L). Based on the dramatic differences in amino acid properties, we focused on S38P and R186Q. We generated modified pIds-FLAG-IdsC constructs with each of these single changes (FLAG-IdsC^{S38P} and FLAG-IdsC^{R186Q}) as well as the double mutant (FLAG-IdsC$^{S38P/R186Q}$) and expressed these in *P. mirabilis*. Lysates were subjected to anti-FLAG co-immunoprecipitations and resulting fractions analyzed via western blot using custom polyclonal anti-IdsB, anti-IdsD, and anti-IdsE antibodies. FLAG-IdsC, FLAG-IdsC^{S38P}, FLAG-IdsC^{R186Q}, and FLAG-IdsC$^{S38P/R186Q}$ all pull down IdsB and IdsD (**Figure 2.1** and **Figure 3.12**). Trace amounts of IdsE were pulled down by FLAG-IdsC^{S38P} (**Figure 3.12**). These are perhaps indirect interactions between IdsC and IdsE mediated by IdsD due to *in vitro* reassortment. To test whether these amino acid changes alter IdsC interactions with Ids or T6S machinery components (**Table 2.4**), the binding fractions of these co-immunoprecipitations were analyzed by LC-MS/MS. FLAG-IdsC^{S38P} (**Table 3.4**), FLAG-IdsC^{R186Q} (**Table 3.5**), and FLAG-IdsC$^{S38P/R186Q}$ (**Table 3.6**) all pulled down IdsB, IdsD, and IdsF. They all additionally pulled down BB2000_0820 (TssC) and BB2000_0814 (TssK), sheath and baseplate components of the machinery respectively.

To test whether these amino acid changes in FLAG-IdsC supported mKate-IdsD puncta formation proximal to the T6S machinery (**Figure 2.2**), these constructs were expressed in a strain where BB2000_0821 (TssB) is fused to superfolder green fluorescent protein (TssB-sfGFP) (10). Epifluorescence microscopy showed that mKate-IdsD localized into puncta that could be found proximal to the T6S machinery in all of these strains (**Figure 3.13, Figure A.4**-**Figure A.6**).

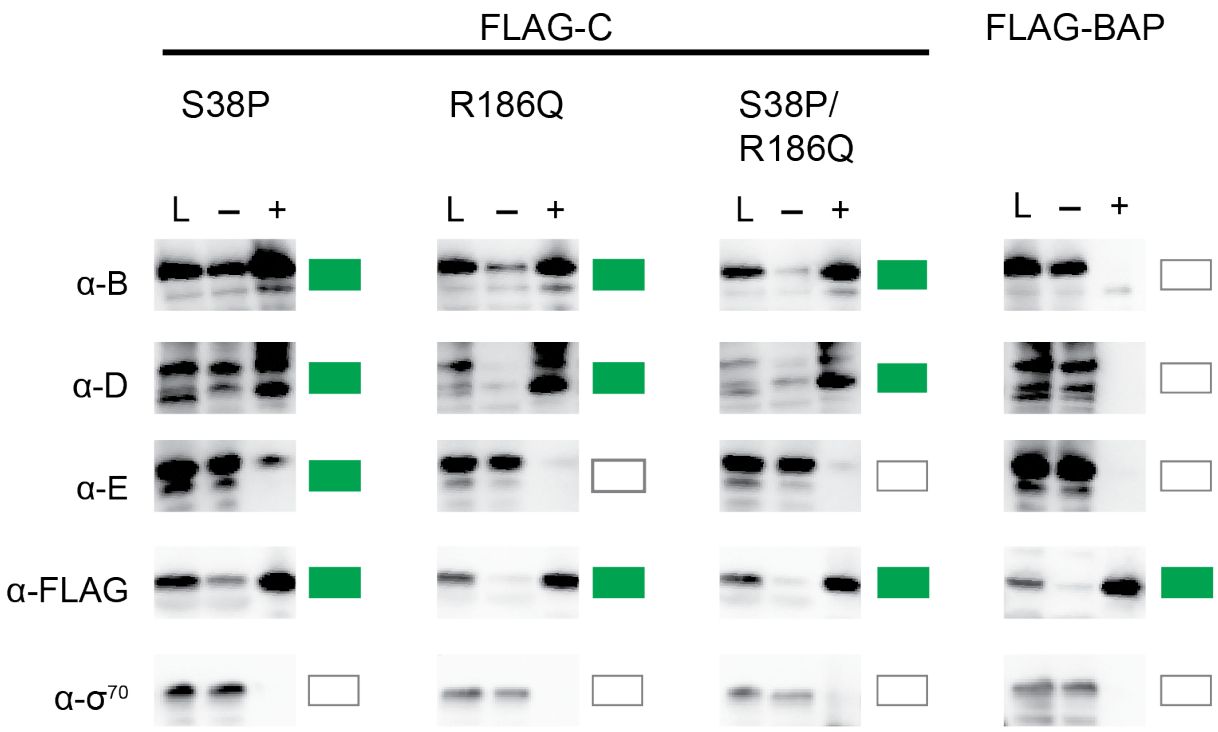

Figure 3.12 FLAG-IdsC single residue polymorphisms do not alter binding to IdsB or IdsD Anti-FLAG co-immunoprecipitation assays were performed on *P. mirabilis* extracts expressing FLAG-IdsC, FLAG-IdsC^{S38P}, FLAG-IdsC^{R186Q}, or FLAG-IdsC$^{S38P/R186Q}$. *P. mirabilis* lysate doped with FLAG-BAP was used as a negative control. Soluble (L), non-binding (-) and binding (+) fractions were analyzed via western blot using polyclonal anti-IdsB, polyclonal anti-IdsD, polyclonal anti-IdsE, monoclonal anti-FLAG, and monoclonal anti-sigma70 antibodies. Green boxes indicate a band in the binding fraction; white boxes indicate no band in the binding fraction.

Table 3.4 Ids and T6S specific LC-MS/MS hits pulled down by FLAG-IdsC^{S38P}

Protein	No. unique peptides	No. total peptides	% Coverage	Expected Size (kDa)	Gel Fragment (kDa)
IdsB	13	18	23.24	81.5	37-75
IdsC	14	24	30.71	47.1	37-75
IdsD	42	64	33.08	118.2	75-250
IdsF	4	4	50.56	9.1	0-37
BB2000_0820	4	4	8.54	55.8	37-75
BB2000_0814	6	7	13.86	51.2	37-75

Table 3.5 Ids and T6S specific LC-MS/MS hits pulled down by FLAG-IdsC^{R186Q}

Protein	No. unique peptides	No. total peptides	% Coverage	Expected Size (kDa)	Gel Fragment (kDa)
IdsB	16	21	25.45	81.5	37-75
IdsC	18	43	33.42	47.1	37-75
IdsD	43	85	35.69	118.2	75-250
IdsF	4	6	39.33	9.1	0-37
BB2000_0820	10	11	22.76	55.8	37-75
BB2000_0814	7	9	17.70	51.2	37-75

Table 3.6 Ids and T6S specific LC-MS/MS hits pulled down by FLAG-IdsC$^{S38P/R186Q}$

Protein	No. unique peptides	No. total peptides	% Coverage	Expected Size (kDa)	Gel Fragment (kDa)
IdsB	14	19	23.65	81.5	37-75
IdsC	15	37	29.98	47.1	37-75
IdsD	43	85	35.69	118.2	75-250
IdsF	5	8	50.56	9.1	0-37
BB2000_0820	13	15	27.03	55.8	37-75
BB2000_0814	9	10	18.58	51.2	37-75

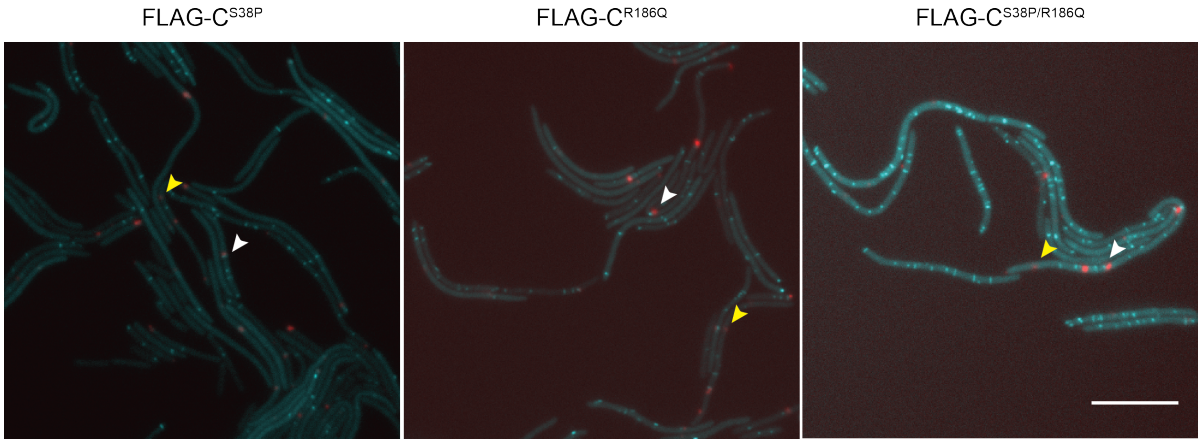

Figure 3.13 FLAG-IdsC polymorphisms support mKate-IdsD puncta formation The T6S sheath was labeled using a chromosomal fusion of the sheath component TssB to sfGFP (10). pIds-FLAG-IdsC-mKate2-IdsD was modified to express FLAG-IdsC^{S38P}, FLAG-IdsC^{R186Q}, or FLAG-IdsC$^{S38P/R186Q}$. All three FLAG-IdsC variants supported mKate-IdsD puncta formation. Foci that did (white arrow) or did not (yellow arrow) overlap with the T6S machinery were observed. False-colored overlay in which for contrast, mKate-IdsD fluorescence is in red, and TssB-sfGFP fluorescence is in cyan. Scale bar is 10 μm. Full figures can be found in Appendix A (**Figure A.4-Figure A.6**).

Given that the mutant variants of FLAG-IdsC bind IdsD, as well as T6S baseplate and sheath proteins, and support the presence of subcellular clusters that could be found proximal to the T6S machinery, we hypothesized they would likewise secrete IdsD. To test secretion, both the *in vivo* IdsD transfer assay and *in vitro* trichloroacetic acid precipitations were used. Populations of cells expressing FLAG-IdsC^{S38P}or FLAG-IdsC^{R186Q} and lacking IdsE showed restricted colony expansion that was alleviated upon T6S disruption, similar to the pattern observed in cells expressing FLAG-IdsC (**Figure 3.14**). However, cells expressing FLAG-IdsC$^{S38P/R186Q}$ and lacking IdsE showed increased colony expansion, with and without T6S activity, indicating lack of IdsD exchange (**Figure 3.14**). The prediction from these *in vivo* results was that IdsD would be detected in the supernatant of cells expressing FLAG-IdsC, FLAG-IdsC^{S38P} or FLAG-IdsC^{R186Q} but would not be detected in the supernatant of cells expressing FLAG-IdsC$^{S38P/R186Q}$. IdsB was detected in supernatants of liquid-grown cells expressing FLAG-IdsC^{S38P}, FLAG-IdsC^{R186Q}, and FLAG-IdsC$^{S38P/R186Q}$ (**Table 3.7**). However, IdsD was only detected above the limit of three unique peptides in the supernatant of cells expressing FLAG-IdsC^{R186Q} (**Table 3.7**). These results show that IdsC binding of IdsD can be uncoupled from IdsD secretion. While T6S secretion of IdsB was not disrupted, secretion of IdsD was specifically abrogated with the S38P point mutation, individually and in conjunction with the R186Q change. These results support a model (**Figure 3.15**) where IdsC functions to bind IdsD in producing cells, which allows IdsD cluster formation, targeting of IdsD to the T6S machinery and separately IdsD secretion through the T6S machinery.

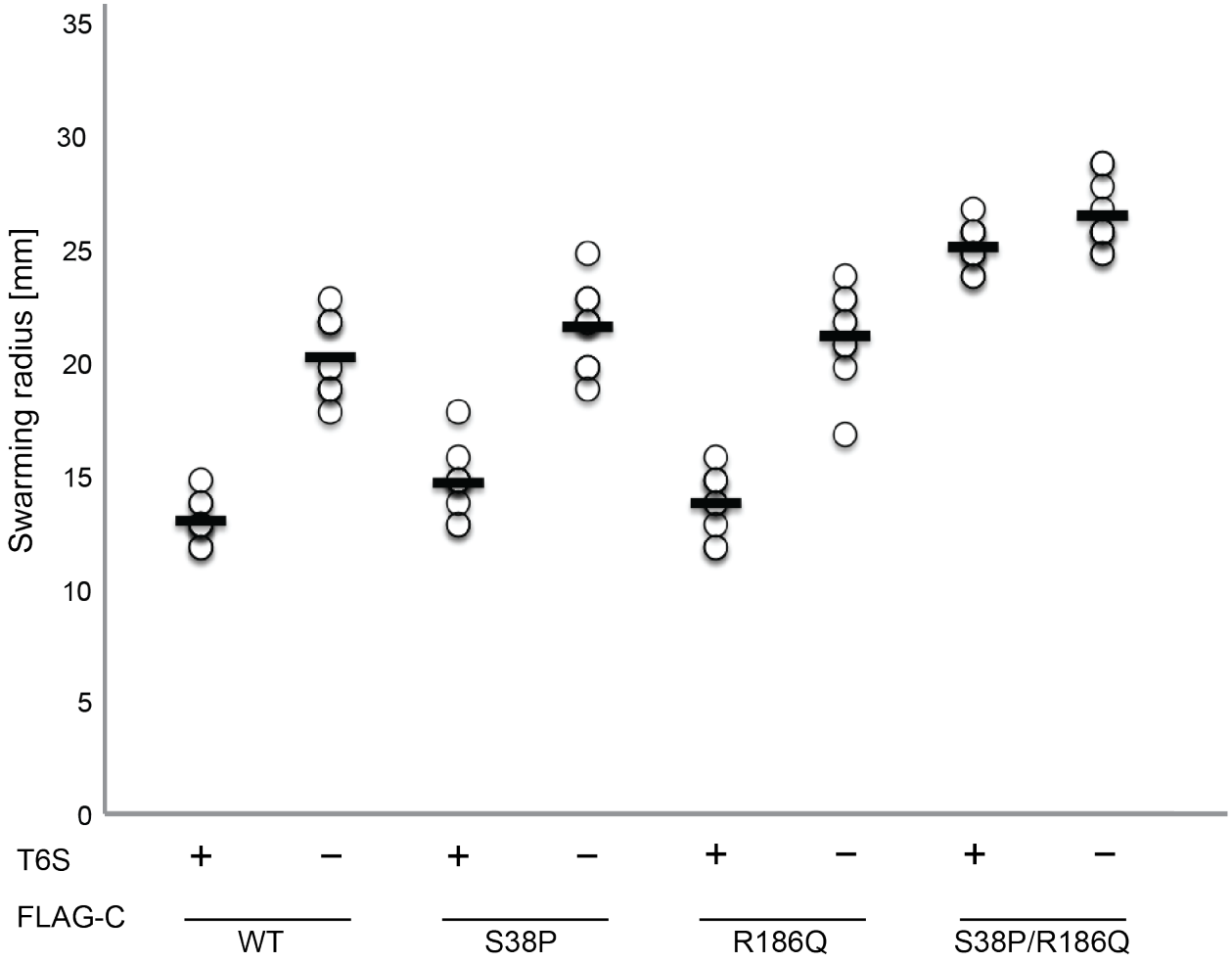

Figure 3.14 FLAG-IdsC polymorphisms impact IdsD secretion *In vivo* assay for IdsD cell-to-cell transfer in which IdsD secretion results in reduced colony, while lack of transport alleviates this restriction (7). *P. mirabilis* strains expressing modified pIds vectors producing FLAG-IdsC (WT), FLAG-IdsC^{S38P}, FLAG-IdsC^{R186Q}, FLAG-IdsC$^{S38P/R186Q}$. T6S+ is a *P. mirabilis* strain producing a fully functional T6S system; T6S- is the TssB chromosomal mutant (7). Open circles indicate migration radii per replicate and bars indicate average migration radius. N=10.

Table 3.7 Ids specific LC-MS/MS hits secreted by FLAG-IdsC variants

TCA	Protein	No. unique peptides	No. total peptides	% Coverage
FLAG-C	IdsB	10	12	18.67
	IdsD	6	6	5.90
	σ^{70}	2	2	4.21
FLAG-C^{S38P}	IdsB	8	8	16.18
	IdsD	1	1	1.35
	σ^{70}	0	0	0
FLAG-C^{R186Q}	IdsB	10	11	12.72
	IdsD	7	7	6.58
	σ^{70}	0	0	0
FLAG-C$^{S38P/R186Q}$	IdsB	7	8	12.72
	IdsD	2	2	2.03
	σ^{70}	0	0	12.30

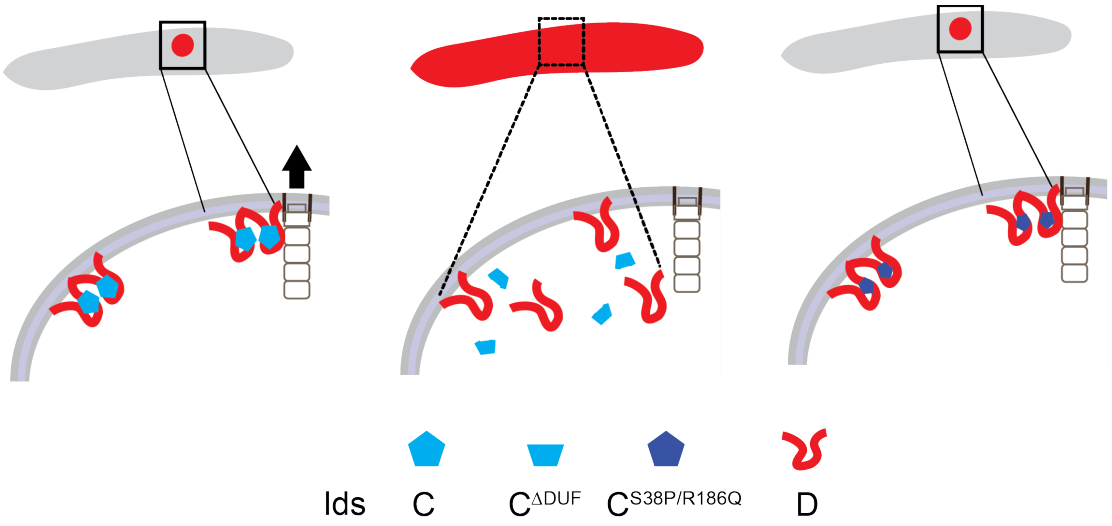

Figure 3.15 Model for IdsD targeting to T6S machinery We propose a model where IdsC, a DUF4123-protein, targets IdsD to the T6S machinery. Transport of IdsD occurs at distinct steps: 1) clustering of IdsD, 2) targeting to the machinery, particularly to the sheath and baseplate components, and 3) secretion through the machinery (black arrow). The DUF4123 domain of IdsC is essential for all of these steps. Single amino acid changes in IdsC can uncouple substrate targeting and secretion.

IdsC variants appear to only affect IdsD secretion

Each of the FLAG-IdsC variants showed slight differences in IdsD secretion phenotypes. FLAG-IdsC^{S38P} *in vivo* results suggested IdsD transfer but *in vitro* showed no IdsD secretion. FLAG-IdsC^{R186Q} phenotypically indicated IdsD transfer and *in vitro* IdsD secretion was detected. FLAG-IdsC$^{S38P/R186Q}$ showed no *in vivo* IdsD transfer and *in vitro* IdsD secretion was not detected. To assess whether these differences could be attributed to differential protein interactions and whether secretion of any other T6S effector was impacted, LC-MS/MS datasets from FLAG-IdsC and each FLAG-IdsC variant strain were compared. Only protein hits with at least three unique peptide fragments detected were considered in the analysis. From the LC-MS/MS analysis of resultant binding fractions from co-immunoprecipitation experiments (**Figure 3.16** and **Table A.7**), a majority of hits were shared amongst all four strains (60 hits), including IdsB, IdsC, IdsD, and IdsF, or were unique to FLAG-IdsC (70 hits). There were few unique hits to FLAG-IdsC^{S38P} (3 hits), FLAG-IdsC^{R186Q} (10 hits) or FLAG-IdsC$^{S38P/R186Q}$ (7 hits). All three mutant variants however had four unique hits, including a molecular chaperone, HtpG (BB2000_2317). BB2000_2317 is homologous to the heat-shock protein chaperone, Hsp90, and by PSI-BLAST has protein homologs found in closely related bacteria, including *Xenorhabdus* spp, *Photorabdhus* spp, *Yersinia* spp, and *Morganella* spp. To compare results relative to *in vitro* IdsD secretion, hits shared between FLAG-IdsC and FLAG-IdsC^{R186Q} were compared to hits shared between FLAG-IdsC^{S38P} and FLAG-IdsC$^{S38P/R186Q}$. FLAG-IdsC/FLAG-IdsC^{R186Q} unique hits included BB2000_1317, a yet uncharacterized hypothetical protein with a DUF945 domain. FLAG-IdsC^{S38P}/FLAG-IdsC$^{S38P/R186Q}$ shared two unique hits, including BB2000_2575, a

Yjj family DUF3029 protein. This suggests that differences in IdsD secretion are not due to differential protein interactions between IdsC variants but perhaps differences in affinity of key interactions, such as those with IdsB, IdsD, IdsF or the T6S machinery components.

To test whether the effects on substrate secretion were specifically for IdsD or whether other substrates were also affected, TCA LC-MS/MS data sets were compared and only hits with at least three unique peptide fragments were included in the analysis (**Figure 3.17** and **Table A.8**). The majority of secreted proteins were shared amongst all four strains (103 hits), suggesting that effects of these point mutations on IdsD secretion do not broadly affect the T6S secretome. To test whether effects on IdsD secretion affect any other particular T6S substrate, secretomes of strains in which IdsD secretion could be detected, FLAG-IdsC/FLAG-IdsC^{R186Q} (7 hits), were compared to secretomes of strains in which IdsD secretion could not be detected, FLAG-IdsC^{S38P}/FLAG-IdsC$^{S38P/R186Q}$ (4 hits). Unique protein hits for either category lacked any known or predicted T6S effector. To test whether any of the variants affected secretion of other T6S substrates, hits specific to FLAG-IdsC were analyzed (23 hits). Of these, only IdsF is a known or predicted T6S substrate that is uniquely secreted. This suggests that any effects of IdsC on secretion are specific to IdsD.

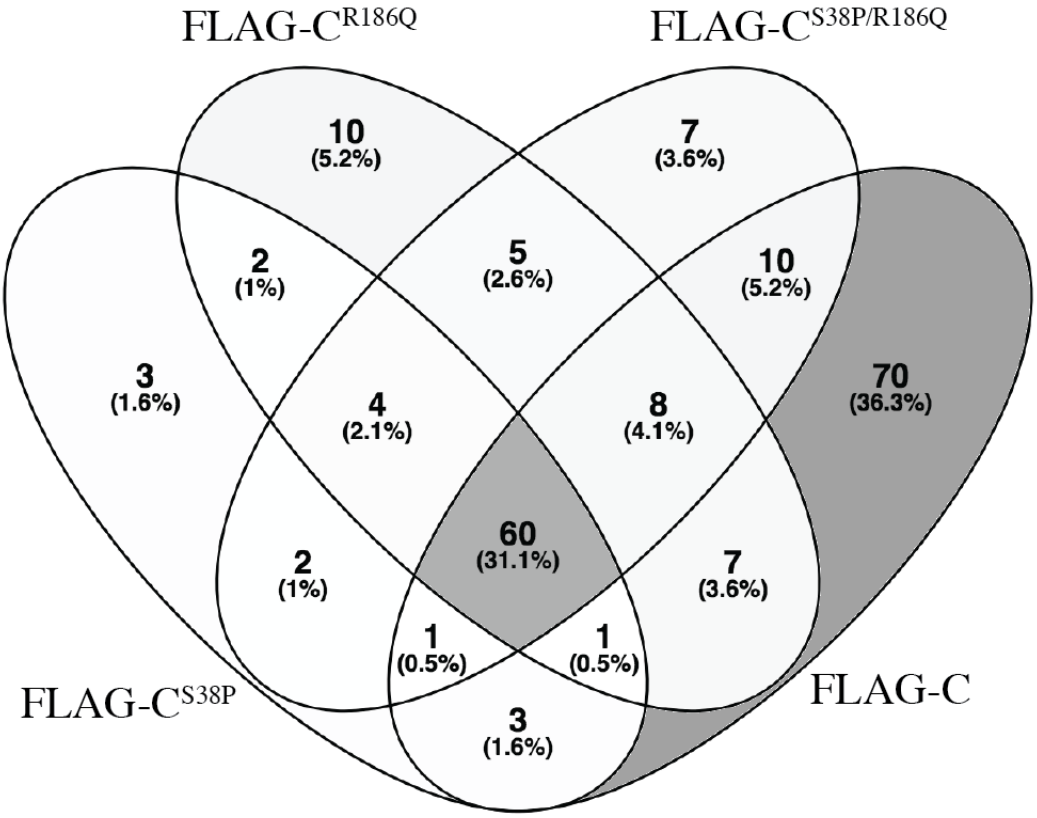

Figure 3.16 Comparison of LC-MS/MS protein hits from FLAG-IdsC variant co-immunoprecipitations Protein hits with at least three unique peptides pulled down by FLAG-IdsC, FLAG-IdsC^{S38P}, FLAG-IdsC^{R186Q}, or FLAG-IdsC$^{S38P/R186Q}$ were compared using VENNY (16). Full data sets can be found on Gibbs laboratory data storage computer. **Table A.7** lists protein hits by category.

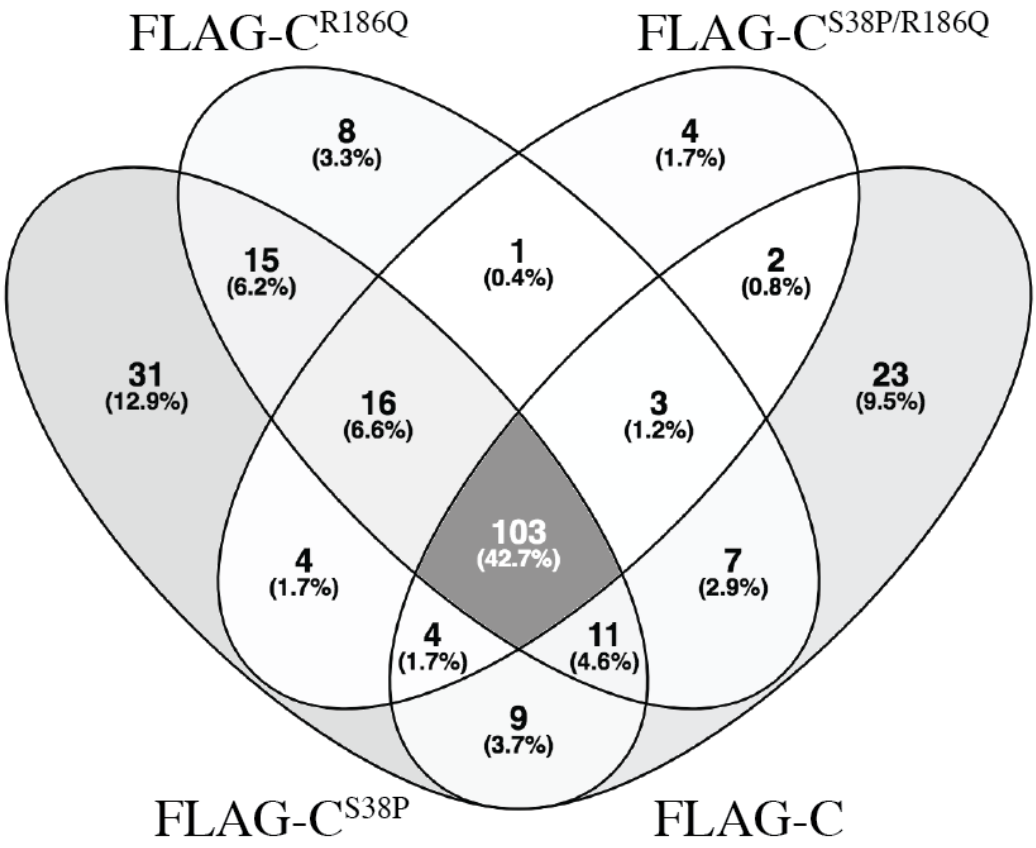

Figure 3.17 Comparison of LC-MS/MS protein hits from FLAG-IdsC variant trichloroacetic acid precipitations Protein hits with at least three unique peptides secreted by FLAG-IdsC, FLAG-IdsC^{S38P}, FLAG-IdsC^{R186Q}, or FLAG-IdsC$^{S38P/R186Q}$ were compared using VENNY (16). Full data sets can be found on Gibbs laboratory data storage computer. **Table A.8** lists protein hits by category.

Discussion

In this chapter I have shown that the IdsC-IdsD interaction is independent of other Ids or T6S proteins and is likely mediated by the DUF4123 domain of IdsC. Further studies, such as using a combination of size exclusion chromatography and light scattering experiments, are required to investigate the stoichiometric ratio of the IdsC-IdsD interaction. I demonstrate that this interaction is essential for maintenance of IdsD protein levels, and that IdsD localization proximal to the T6S machinery and secretion can be uncoupled by single amino acid changes in IdsC. While these amino acid changes do not appear to impact *in vitro* interactions with T6S sheath and baseplate components, it is possible they alter binding affinities between IdsC-IdsD or IdsC and the machinery, impacting IdsD secretion. Intriguingly for each single amino acid change, the *in vivo* assay results suggested that IdsD was still being secreted, but to a lesser extent than in the control strain. However, *in vitro*, IdsD secretion could only be detected in the FLAG-IdsC^{R186Q} mutant and not the FLAG-IdsC^{S38P} mutant, despite comparable levels of IdsB secretion. This suggests that a certain threshold of IdsD secretion may be required to induce *in vivo* phenotypic responses and that this must be taken into account when comparing *in vivo* and *in vitro* secretion assay results. It also suggests that the serine to proline amino acid change impacts IdsD secretion to a greater extent than the arginine to glutamine change.

I furthermore showed in this chapter that IdsC exclusively acts on IdsD produced in the same cell, and not IdsD transferred from neighboring cells. Taken together, this data suggests that IdsC prevents IdsD-IdsE interactions in producing cells and provides an alternative mechanism by which T6S substrates are regulated pre-transport. The

prevailing model in the field is that cognate immunity proteins bind T6S substrates both pre- and post- transport (19, 22, 30, 31). However, the Ids system offers an example where a chaperone protein (IdsC) binds the T6S substrate (IdsD) exclusively pre-transport and a cognate immunity protein (IdsE) binds the substrate exclusively post-transport.

DUF4123-proteins have been shown to be specific to the immediately adjacent T6S substrate (1-3). Comparisons of proteins secreted by FLAG-IdsC and FLAG-IdsC$^{\Delta DUF4123}$ showed that the majority of protein hits were shared. This suggests that disruption of the DUF4123 domain of IdsC does not widely impact the T6S secretome. To test whether IdsC acts as a chaperone on any other T6S substrate, proteins secreted in cells expressing FLAG-IdsC but not FLAG-IdsC$^{\Delta DUF4123}$ were compared to proteins pulled down by FLAG-IdsC. These proteins included IdsB and IdsD, as well as another known T6S substrate, IdrD. However, given that Idr proteins are known to act independently of Ids proteins (8), it is unlikely that IdsC regulates IdrD, although this remains to be functionally tested. No other predicted T6S substrate was found through this comparison, indicating that IdsC likely acts exclusively on IdsD and does not act as a broad T6S chaperone.

However if the DUF4123 domain is well conserved and helps mediate the IdsC-IdsD interaction it is unclear how substrate-specificity is therefore obtained. It is possible that as these proteins are co-produced their interaction is immediately formed and their binding affinity is sufficient to prevent chaperone-substrate re-assortment. The stabilization of the N-terminal fluorophore tag on IdsD in cells expressing FLAG-IdsC$^{\Delta DUF4123}$ could indicate that stabilization at the N-terminal end of IdsD occurs. It is

also possible that structural differences between T6S substrates impact these interactions. Further experiments testing whether co-production of these proteins is required for their interaction as well as experiments testing the binding affinity between IdsC-IdsD and IdsC variants and IdsD, perhaps through isothermal titration calorimetry, could help elucidate the formation of their interaction. Testing chaperone-substrate binding using substrate truncation constructions will help define substrate regions recognized by DUF4123 proteins. In the case of IdsC-IdsD, given that IdsC can bind different IdsD variants that are most highly conserved at the N-terminus, the first 53 amino acids of IdsD are likely involved in this interaction. Understanding this interface between other DUF4123-proteins and their substrates in conjunction with refined protein structures of a wider variety of T6S substrates could aid in comparison of structural differences in these regions to begin understanding chaperone-substrate specificity.

In this chapter I also describe IdsC point mutations where localization and maintenance of IdsD protein levels is uncoupled from its secretion. A comparison of proteins pulled down and secreted by FLAG-IdsC, FLAG-IdsC^{S38P}, FLAG-IdsC^{R186Q}, FLAG-IdsC$^{S38P/R186Q}$ showed that the majority of protein hits were shared amongst all four or were exclusive to FLAG-IdsC. Additionally, no other known or predicted T6S substrate was exclusively secreted in FLAG-IdsC/FLAG-IdsC^{R186Q} as compared to FLAG-IdsC^{S38P}/FLAG-IdsC$^{S38P/R186Q}$. This data further supports that IdsC acts exclusively on IdsD. These point mutations could serve as valuable tools for understanding how large substrates are shuttled through the machinery. Using protein structure studies, such as electron microscopy, the structure of the T6S machinery with FLAG-IdsC^{S38P} or FLAG-IdsC$^{S38P/R186Q}$ and IdsD at the machinery could be obtained.

Other structural studies have been able to observe the entire T6S structure, or structures of smaller substrates within the sheath of the machinery. However, no structure of a large substrate at the machinery has yet been obtained.

While we now understand more of the molecular details of self-recognition in *P. mirabilis*, the biological impact of self-recognition on *P. mirabilis* populations, particularly within host systems, remains elusive. In the following chapter, I probe at this by attempting to set up a host system that allows manipulation of *P. mirabilis* populations and imaging of their dynamics over time.

References

1. **Liang X, Moore R, Wilton M, Wong MJ, Lam L, Dong TG.** 2015. Identification of divergent type VI secretion effectors using a conserved chaperone domain. Proc Natl Acad Sci U S A **112:**9106-9111.

2. **Bondage DD, Lin JS, Ma LS, Kuo CH, Lai EM.** 2016. VgrG C terminus confers the type VI effector transport specificity and is required for binding with PAAR and adaptor-effector complex. Proc Natl Acad Sci U S A **113:**E3931-3940.

3. **Unterweger D, Kostiuk B, Otjengerdes R, Wilton A, Diaz-Satizabal L, Pukatzki S.** 2015. Chimeric adaptor proteins translocate diverse type VI secretion system effectors in *Vibrio cholerae*. EMBO J **34:**2198-2210.

4. **Belas R, Erskine D, Flaherty D.** 1991. Transposon mutagenesis in Proteus mirabilis. J Bacteriol **173:**6289-6293.

5. **Gibbs KA, Urbanowski ML, Greenberg EP.** 2008. Genetic determinants of self identity and social recognition in bacteria. Science **321:**256-259.

6. **Finn RD, Coggill P, Eberhardt RY, Eddy SR, Mistry J, Mitchell AL, Potter SC, Punta M, Qureshi M, Sangrador-Vegas A, Salazar GA, Tate J, Bateman A.** 2016. The Pfam protein families database: towards a more sustainable future. Nucleic Acids Res **44:**D279-285.

7. **Saak CC, Gibbs KA.** 2016. The self-identity protein IdsD is communicated between cells in swarming *Proteus mirabilis* colonies. J Bacteriol **198:**3278-3286.

8. **Wenren LM, Sullivan NL, Cardarelli L, Septer AN, Gibbs KA.** 2013. Two independent pathways for self-recognition in *Proteus mirabilis* are linked by type VI-dependent export. MBio **4**.

9. **Senior BW.** 1977. The Dienes phenomenon: identification of the determinants of compatibility. J Gen Microbiol **102:**235-244.

10. **Saak CC, Zepeda-Rivera MA, Gibbs KA.** 2017. A single point mutation in a TssB/VipA homolog disrupts sheath formation in the type VI secretion system of *Proteus mirabilis*. PLoS One **12:**e0184797.

11. **Cardarelli L, Saak C, Gibbs KA.** 2015. Two Proteins Form a Heteromeric Bacterial Self-Recognition Complex in Which Variable Subdomains Determine Allele-Restricted Binding. MBio **6:**e00251.

12. **Simon R, Priefer U, Puhler A.** 1983. A broad host range mobilization system for *in vivo* genetic engineering- transposon mutagenesis in gram-negative bacteria. Bio-Technol **1:**784-791.

13. **Davidson AR, Sauer RT.** 1994. Folded proteins occur frequently in libraries of random amino acid sequences. Proc Natl Acad Sci U S A **91:**2146-2150.

14. **Jeong H, Barbe V, Lee CH, Vallenet D, Yu DS, Choi SH, Couloux A, Lee SW, Yoon SH, Cattolico L, Hur CG, Park HS, Segurens B, Kim SC, Oh TK, Lenski RE, Studier FW, Daegelen P, Kim JF.** 2009. Genome sequences of *Escherichia coli* B strains REL606 and BL21(DE3). J Mol Biol **394:**644-652.

15. **Li J, Yao Y, Xu HH, Hao L, Deng Z, Rajakumar K, Ou HY.** 2015. SecReT6: a web-based resource for type VI secretion systems found in bacteria. Environ Microbiol **17:**2196-2202.

16. **Oliveros JC.** 2007-2015. Venny. An interactive tool for comparing lists with Venn's diagrams. http://bioinfogp.cnb.csic.es/tools/venny/index.html.

17. **Basler M, Ho BT, Mekalanos JJ.** 2013. Tit-for-tat: type VI secretion system counterattack during bacterial cell-cell interactions. Cell **152:**884-894.

18. **Basler M, Mekalanos JJ.** 2012. Type 6 secretion dynamics within and between bacterial cells. Science **337:**815.

19. **Hood RD, Singh P, Hsu F, Guvener T, Carl MA, Trinidad RR, Silverman JM, Ohlson BB, Hicks KG, Plemel RL, Li M, Schwarz S, Wang WY, Merz AJ, Goodlett DR, Mougous JD.** 2010. A type VI secretion system of *Pseudomonas aeruginosa* targets a toxin to bacteria. Cell Host Microbe **7:**25-37.

20. **Mougous JD, Cuff ME, Raunser S, Shen A, Zhou M, Gifford CA, Goodman AL, Joachimiak G, Ordonez CL, Lory S, Walz T, Joachimiak A, Mekalanos JJ.** 2006. A virulence locus of *Pseudomonas aeruginosa* encodes a protein secretion apparatus. Science **312:**1526-1530.

21. **Pukatzki S, Ma AT, Sturtevant D, Krastins B, Sarracino D, Nelson WC, Heidelberg JF, Mekalanos JJ.** 2006. Identification of a conserved bacterial protein secretion system in *Vibrio cholerae* using the *Dictyostelium* host model system. Proc Natl Acad Sci U S A **103:**1528-1533.

22. **Russell AB, Hood RD, Bui NK, LeRoux M, Vollmer W, Mougous JD.** 2011. Type VI secretion delivers bacteriolytic effectors to target cells. Nature **475:**343-347.

23. **Lei SP, Lin HC, Wang SS, Callaway J, Wilcox G.** 1987. Characterization of the *Erwinia carotovora* pelB gene and its product pectate lyase. J Bacteriol **169:**4379-4383.

24. **Lutz R, Bujard H.** 1997. Independent and tight regulation of transcriptional units in *Escherichia coli* via the LacR/O, the TetR/O and AraC/I1-I2 regulatory elements. Nucleic Acids Res **25:**1203-1210.

25. **Movva NR, Nakamura K, Inouye M.** 1980. Amino acid sequence of the signal peptide of ompA protein, a major outer membrane protein of *Escherichia coli*. J Biol Chem **255:**27-29.

26. **Larkin MA, Blackshields G, Brown NP, Chenna R, McGettigan PA, McWilliam H, Valentin F, Wallace IM, Wilm A, Lopez R, Thompson JD, Gibson TJ, Higgins DG.** 2007. Clustal W and Clustal X version 2.0. Bioinformatics **23:**2947-2948.

27. **Goujon M, McWilliam H, Li W, Valentin F, Squizzato S, Paern J, Lopez R.** 2010. A new bioinformatics analysis tools framework at EMBL-EBI. Nucleic Acids Res **38:**W695-699.

28. **McWilliam H, Li W, Uludag M, Squizzato S, Park YM, Buso N, Cowley AP, Lopez R.** 2013. Analysis Tool Web Services from the EMBL-EBI. Nucleic Acids Res **41:**W597-600.

29. **Waterhouse AM, Procter JB, Martin DM, Clamp M, Barton GJ.** 2009. Jalview Version 2--a multiple sequence alignment editor and analysis workbench. Bioinformatics **25:**1189-1191.

30. **Hachani A, Allsopp LP, Oduko Y, Filloux A.** 2014. The VgrG proteins are "a la carte" delivery systems for bacterial type VI effectors. J Biol Chem **289:**17872-17884.

31. **Whitney JC, Chou S, Russell AB, Biboy J, Gardiner TE, Ferrin MA, Brittnacher M, Vollmer W, Mougous JD.** 2013. Identification, structure, and function of a novel type VI secretion peptidoglycan glycoside hydrolase effector-immunity pair. J Biol Chem **288:**26616-26624.

Chapter 4

Establishing an *in vivo* host model to study *Proteus mirabilis* interstrain interactions

This work was accomplished with help and materials from the labs of Dr. Erel Levine and Dr. Susan Mango. Special thanks go to Dr. Andrzej Nowojewski and Beste Mutlu.

Abstract

The bacterium *Proteus mirabilis* is found in a wide array of environments, including soil, seawater, and as a commensal bacterium in the human gastrointestinal tract. Multiple studies have concluded that a population of *P. mirabilis* descends from the gastrointestinal tract to the urinary tract during infection in patients with long-term catheterization. However, none of the methods used can discriminately assay whether this *P. mirabilis* population is comprised of a single strain or multiple strains and whether self-recognition systems impact host colonization. I attempted to analyze *P. mirabilis* interstrain interactions within a host by using the nematode model *Caenorhabditis elegans*. Consistent with other published work, I show that *C. elegans* requires an intact innate immune system to survive the presence of *P. mirabilis*. In N2 wild-type worms, *P. mirabilis* strains persist in the nematode gut, and in some cases appear to be concentrated in the nematode pharynx. When feeding on a mix of two *P. mirabilis* strains, only a single strain persists in the *C. elegans* gut. However, sequential feeding experiments showed that a second strain displaces the first. Overall, these experiments suggest that a single strain of *P. mirabilis* is predominantly present within a host at any given time. This work set up a system that could potentially be used to stringently test and visualize *P. mirabilis* in an animal host, particularly to test whether self-recognition behaviors impact interstrain and interspecies interactions.

Introduction

P. mirabilis is a commensal bacterium in the human gut and an opportunistic pathogen in the human urinary tract, particularly in patients with long-term catheterization. Multiple factors influence *P. mirabilis* strain infectivity (1), but of these,

urease secretion leads to the formation of ammonia and leads to an increase in pH of urine (2, 3). Precipitation of calcium and magnesium phosphates under these conditions leads to the formation of a crystalline biofilm that blocks urine flow. This typically results in an encrustation around the catheter resulting in its surgical removal (4-7).

There have been multiple methods to assess variability of *P. mirabilis* isolates present in samples from human patients. It has been found that multiple methods, including the Dienes line test, ribotyping post restriction digest with EcoRI and pulsed-field gel electrophoresis (PFGE) post restriction digest with SfiI all have comparable indices of discrimination- suggesting that they are all equally valid methods for discriminating *P. mirabilis* isolates (8). However, there are isolates that are undistinguishable by the Dienes line test that are distinguishable by PFGE (9). These tests have shown that the *P. mirabilis* population present in a patients urine is genotypically identical to that found in the crystalline biofilm catheter encrustation (9). This suggests that *P. mirabilis* descends from the gastrointestinal tract to the urinary tract during infection, as opposed to coming from outside contamination during catheter exchange. However, none of these approaches clarify whether a single *P. mirabilis* strain is present in patients or if the population is comprised of multiple strains. The Dienes line test assays for the boundary phenotype of the population at the edge of a *P. mirabilis* colony and work from our lab has shown that in a mixed strain population, one will reproducibly sequester the other to the center of the colony (10). Both ribotyping and PFGE do not have the sensitivity to distinguish if different strains are present within one sample. Therefore, an open question in the field is whether multiple *P. mirabilis* strains can co-

infect a patient and whether social behaviors, like self versus non-self recognition, play a role in colonization of a host.

Currently, a mouse host model of *P. mirabilis* exists which has helped provide insights on *P. mirabilis* gene expression (1), cell morphotypes present (11) and factors that influence strain infectivity (1, 12). However, resolution of inter-strain *P. mirabilis* dynamics is limited by small sample sizes, cost, and inability to image at a single-bacterial-cell resolution. To overcome these challenges, we aimed to establish a *Caenorhabditis elegans* model of *P. mirabilis* infection. Established infection assays, *in vivo* microscopy protocols, and genetic and biochemical tools make *C. elegans* a robust host model for host interactions (13-18). Such models have been established with both Gram-positive and Gram-negative bacterial species including *Pseudomonas aeruginosa*, *Burkholderia* species, and *Serratia marcescens* (14, 19-22). A previous study showed that *C. elegans* with compromised innate immune systems are susceptible to both *P. mirabilis* and *P. vulgaris* (23). This suggests that an uncompromised immune system is required for worm viability in the presence of *Proteus* species. Wild-type worms showed comparable lifespan to worms fed the standard lab food source, *Escherichia coli* OP50 (23). Given this, in addition to rapid generation time, low cost, natural tissue transparency and use of bacteria as a food source, we proposed that *C. elegans* would allow us to capture *P. mirabilis* dynamics *in vivo* over the two-week life-span of an individual host.

My goal was to assess whether the *P. mirabilis* developmental cycle and social behaviors characterized under laboratory conditions would be translatable to *in vivo* conditions in *C. elegans*. Here I show that four strains of *P. mirabilis* do not impact viability of wild-type worms. I then used two of these strains and show that *C. elegans*

requires an intact innate immune system to survive *P. mirabilis*. I further show through concurrent and sequential feeding experiments that a single strain is predominantly present in the *C. elegans* gut, and that a strain fed secondly will displace the first.

Materials and Methods

Developing L4-stage *C. elegans*

For all *C. elegans* strains used (**Table 4.1**), adults were maintained by transferring to fresh nematode growth media (NGM) plates with *E. coli* OP50 (16). M9 buffer (0.2 molar (M) monopotassium phosphate, 0.4M disodium phosphate, 0.9M sodium chloride, 0.001M magnesium sulfate) (16) was poured on the plate to transfer worms into a 15 milliliter (mL) Falcon tube that was spun down at 2000 revolutions per minute (rpm) for 1 minute. Buffer was poured out such that 1.5 mL remained in the tube. 1.5 mL of a 1:1 bleach:1M sodium hydroxide solution was added to lyse open worms. Lysing was left for no longer than four minutes and was quenched with an excess of M9 buffer. Tube was spun down at 2000 rpm for 1 minute, supernanant was removed and the tube filled again with M9 buffer. Tube was inverted and vortexed. This was step was repeated three times. Tube was filled with M9 buffer and left on a nutator at room temperature for 16 to 48 hours. Worms were plated on NGM media with lawns of *E. coli* OP50 and left to develop for 36 hours to reach L4-stage.

C. elegans viability assay

L4-stage worms of N2, *pmk-1*, *dbl-1*, *fshr-1 C. elegans* strains were transferred on to a *P. mirabilis* strain BB2000 or strain HI4320 swarm colony on swarming permissive

CM55 Blood Agar Base agar (Oxoid, Basingstoke, England). Poking each individual worm with a worm poker and looking for movement assessed viability. If alive, worm was transferred to a fresh *P. mirabilis* swarm colony. Viability was assessed at every 24-hour interval.

P. mirabilis **colonization of** ***C. elegans*** **gut**

P. mirabilis strains were grown up in liquid LB broth culture under aerobic conditions at 37°C. All strains used are listed in **Table 4.2**. Cultures were normalized by optical density at a wavelength of 600 nanometers (OD_{600}). Swarming permissive CM55 Blood Agar Base agar (Oxoid, Basingstoke, England) plates were inoculated with individual strains. N2 L4-stage *C. elegans* were transferred on this plate and allowed to feed. At 24-hour intervals the majority of worms were transferred to fresh *P. mirabilis* swarm colonies. About 10 worms each day was transferred to an NGM plate seeded with *E. coli* OP50. After 24 hours of feeding on *E. coli* OP50, worms were anesthetized, washed, and lysed as described below and intestinal contents were plated for bacterial colony-forming units as described below.

Imaging of a ***P. mirabilis*** **fluorescent strain in** ***C. elegans***

NGM buffer was used to dissolve a 10% agarose solution (18). Microscopy pads were prepared and worms that had fed on a fluorescently-marked derivative of *P. mirabilis* strain BB2000 transferred directly on to pad. Images were acquired with a Leica DM5500B (Leica Microsystems, Buffalo Grove, IL) with a CoolSnap HQ2 cooled CCD camera (Photometrics, Tucson, AZ). MetaMorph version 7.8.0.0 (Molecular Devices,

Sunnyvale, CA) was used for image acquisition. Figures were made in Fiji (24, 25) and Adobe Illustrator (Adobe Systems, San Jose, CA).

P. mirabilis mixed strain feeding assay

P. mirabilis strains were grown up in liquid LB broth culture under aerobic conditions at 37°C. All strains used are listed in **Table 4.2**. Cultures were normalized by OD_{600}. Swarming permissive CM55 Blood Agar Base agar (Oxoid, Basingstoke, England) plates were inoculated with a 1:1 mix of strains. N2 L4-stage *C. elegans* were transferred on this plate and allowed to feed. At 24-hour intervals the majority of worms were transferred to fresh *P. mirabilis* swarm colonies. About 10 worms each day were anesthetized, washed, and lysed as described below and intestinal contents were plated for bacterial colony-forming units as described below.

P. mirabilis sequential strain feeding assay

P. mirabilis strains were grown up in liquid LB broth culture under aerobic conditions at 37°C. All strains used are listed in **Table 4.2**. Cultures were normalized by OD_{600}. Swarming permissive CM55 Blood Agar Base agar (Oxoid, Basingstoke, England) plates were inoculated with individual strains. N2 L4-stage *C. elegans* were transferred on this plate and allowed to feed on strain BB2000 for 48 hours and then transferred to feeding on either strain HI4320 or strain CW677 for an additional 48 hours. At 24-hour intervals the majority of worms were transferred to fresh *P. mirabilis* swarm colonies. About 10 worms each day were anesthetized, washed, and lysed as described below and intestinal contents were plated for bacterial colony-forming units as described below.

Colony-forming units assay

Worms were prepared as follows. About 10 worms were placed on a droplet of 50 microliters (μL) of 25mM levamisole and 0.1% Triton-X (levamisole+Triton-X). Droplet was then transferred to 1 mL of levamisole+Triton-X and spun down in a 1.5 mL eppendorf tube at 50g for 30 seconds. Tube was vortexed for 10-20 seconds and centrifuged again at 50g for 30 seconds. Contents were left to settle for 5 minutes at which point the supernant was aspirated. This wash procedure was repeated three additional times. Worms were then incubated in 1 mL of 25mM levamisole with 100 microgram per milliliter (μg/mL) gentamicin and 1 milligram per milliliter (mg/mL) ampicillin for 1 hour. Wash procedure was repeated three times using 25mM levamisole. At end of last wash, 350 μL of levamisole+Triton-X was added. An equal volume of silicone-carbide 1.0mm sharp particles (BioSpec Products, Bartlesville, OK) was added and a mortar and pestle was used to lyse the worms. Serial dilutions of these contents were prepared and plated on non-swarming permissive (LSW-) agar (26) with appropriate antibiotics for strain-specific selection.

***P. mirabilis* mixed population strain dominance assay**

P. mirabilis strains were grown up in liquid LB broth culture under aerobic conditions at 37°C. All strains used are listed in **Table 4.2**. Cultures were normalized by OD_{600} and individual strains and a 1:1 mix of the two strains were each spotted on swarming permissive CM55 Blood Agar Base agar (Oxoid, Basingstoke, England) plates supplemented with 2 mg/mL Coomassie blue and 4 mg/mL congo red dyes and incubated at 37°C overnight.

Table 4.1 *Caenorhabditis elegans* strains used in this study

Strain	**Notes**
N2	Wild-type
N2 *pmk-1*	N2 lacking *pmk-1* gene
N2 *dbl-1*	N2 lacking *dbl-1* gene
N2 *fshr-1*	N2 lacking *fhsr-1* gene

Table 4.2 Bacterial strains used in this study

Strain	**Notes**	**Source**	**KAG#**	**MZR#**
BB2000	Wild-type	(26)	001	001
BB2000Δ*ids*	Δ*ids::Tn-Cm(R)*	(27)	006	002
HI4320	Wild-type	(28)	034	008
ATCC29906	Wild-type	Stephen Saum	611	
BB2000::*gfp*	BB2000 produces constitutive chromosomal *gfp*	(27)	1400	022
BB2000:*rfp*	BB2000 produces constitutive chromosomal *rfp*	(27)	107	
BB2000Δ*ids*::*gfp*	Δ*ids::Tn-Cm(R)*produces constitutive chromosomal *gfp.* Made using pKG2012-1 (27).	This study	966	026
CW677	Wild-type	(29)	MLU4.274	

Results

P. mirabilis does not impact wild-type C. elegans viability

Worm embryos were allowed to develop on standard NGM media plates with lawns of *E. coli* OP50 as a food source (16). Worms in the last larval stage (L4) were transferred on to a *P. mirabilis* swarm colonies of strains ATCC29906, HI4320, BB2000 and a BB2000 derivate, BB2000Δ*ids*. Of these, HI4320 and BB2000 were used to test viability of immunocompromised worms. These two were chosen on the basis that *P. mirabilis* social behaviors have best been characterized in the BB2000 strain (10, 27, 30, 31) while mice model studies of infectivity have predominantly used strain HI4320 (1, 32-34). At 24-hour intervals, worms were transferred to fresh *P. mirabilis* swarming colonies and viability assessed. While N2 worms showed expected lifespan (**Figure 4.1A**), immunocompromised worms showed susceptibility to both *P. mirabilis* strains (**Figure 4.1B-D**). Immunocompromised mutants in three separate immunity pathways were used (**Figure 4.1B-D**) and impact on viability varied, however, worms fed *P. mirabilis* HI4320 were consistently less viable than those fed BB2000. These results are consistent with a previous study (23), and from this we concluded that our strains of *P. mirabilis* are poor pathogens for *C. elegans*, and while an intact immune system is required, viability in wild-type worms is sufficiently long enough to assess *in vivo P. mirabilis* dynamics within the host.

P. mirabilis colonizes C. elegans gut

We reasoned that *P. mirabilis* long-term dynamics would likely depend on colonization of the worm intestine, as opposed to transient passing through the intestinal

tract. To establish whether *P. mirabilis* colonizes the host, *C. elegans* embryos were developed on *P. mirabilis* swarm colonies of either strain BB2000 with a chromosomal green fluorescent protein (GFP) marker (BB2000::*gfp*) or strain HI4320. At 24-hour intervals a subset of worms was transferred to fresh *P. mirabilis* swarm colonies while the rest were transferred to *E. coli* OP50. For the latter, after 24 hours worms were washed and lysed (17) and serial dilutions of intestinal contents were plated on selective non-swarming permissive (LSW-) media. Preliminary data suggests that a significant amount of *P. mirabilis* remains after 24 hours on *E. coli*, suggesting that *P. mirabilis* is colonizing the gut as opposed to being solely a bacterial food source transiently occupying the intestinal tract (**Figure 4.2**).

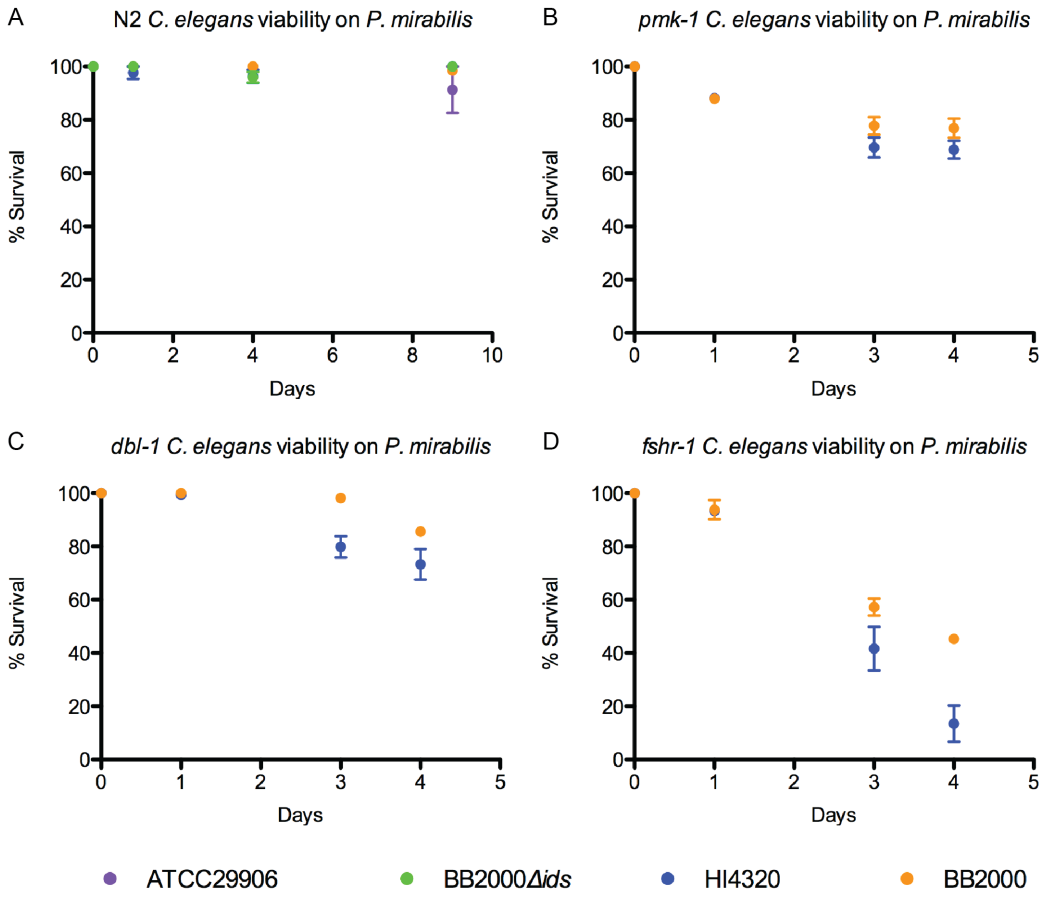

Figure 4.1 *P. mirabilis* affects viability of immunocompromised *C. elegans* (A) Wild-type N2 or (B-D) immunocompromised worms were developed on standard NGM media and fed *E. coli* OP50. L4 stage worms were transferred to swarms of a single *P. mirabilis* strain (ATCC29906, BB2000Δ*ids*, HI4320, or BB2000) as indicated. At 24-hour intervals, worm viability was assessed using a poker (17) and viable worms were transferred to fresh *P. mirabilis* swarms. (B-D) Disruption of p38 MAP-K signaling (*pmk-1*), TGF-β signaling (*dbl-1*), and a glycopeptide hormone receptor implicated in bacterial pathogen response (*fshr-1*) (35) were tested.

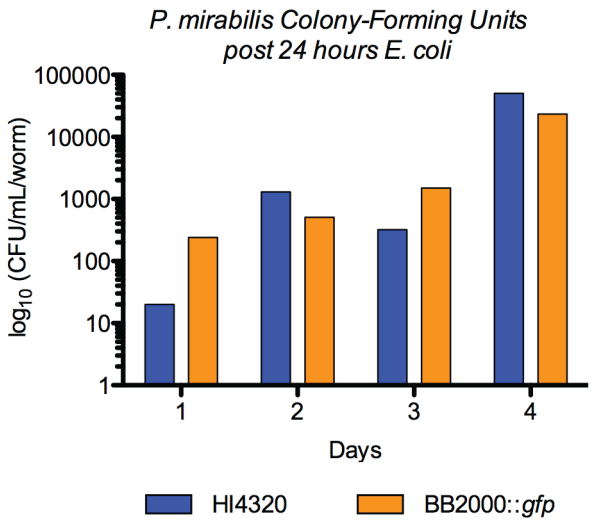

Figure 4.2 *P. mirabilis* appears to colonize *C. elegans* gut Wild-type N2 worms were developed on *P. mirabilis* swarms of strain HI4320 or strain BB2000 carrying a chromosomal GFP marker (BB2000::*gfp)*. At 24-hour intervals worms were transferred to fresh swarms, while a subset of worms were transferred to lawns of *E. coli* OP50 on standard NGM media. For this subset, worms were fed *E. coli* for 24 hours, and then anesthetized, vigorously washed in the presence of detergent, and lysed. Intestinal contents were plated on tetracycline selective plates, as *P. mirabilis* is naturally tetracycline resistant while *E. coli* is not. Serial dilutions were plated on LSW- agar with tetracyline and colony-forming units calculated per mL per worm and plotted on a $\log_{10}$ scale.

P. mirabilis colonization appears to be uniform with some concentration in C. elegans pharynx

To establish if colonization occurred uniformly along the gut, worms were developed as above and fed strain BB2000 carrying a chromosomal red-fluorescent protein marker (BB2000::*rfp*). We avoided using BB2000::*gfp* as fat granules have previously been reported to auto-fluoresce in the GFP emission range (36). Worms were immobilized on agarose (18) and imaged using an upright epi-fluorescence microscope. RFP fluorescence could be found along the gut (**Figure 4.3**), however in some worms, high intensity signal was found in the pharynx, consistent with previous reports (23) (**Figure 4.3**). However, this led us to conclude that *P. mirabilis* did not colonize a particular intestinal niche, giving us a larger tissue area in which to visualize *in vivo* dynamics.

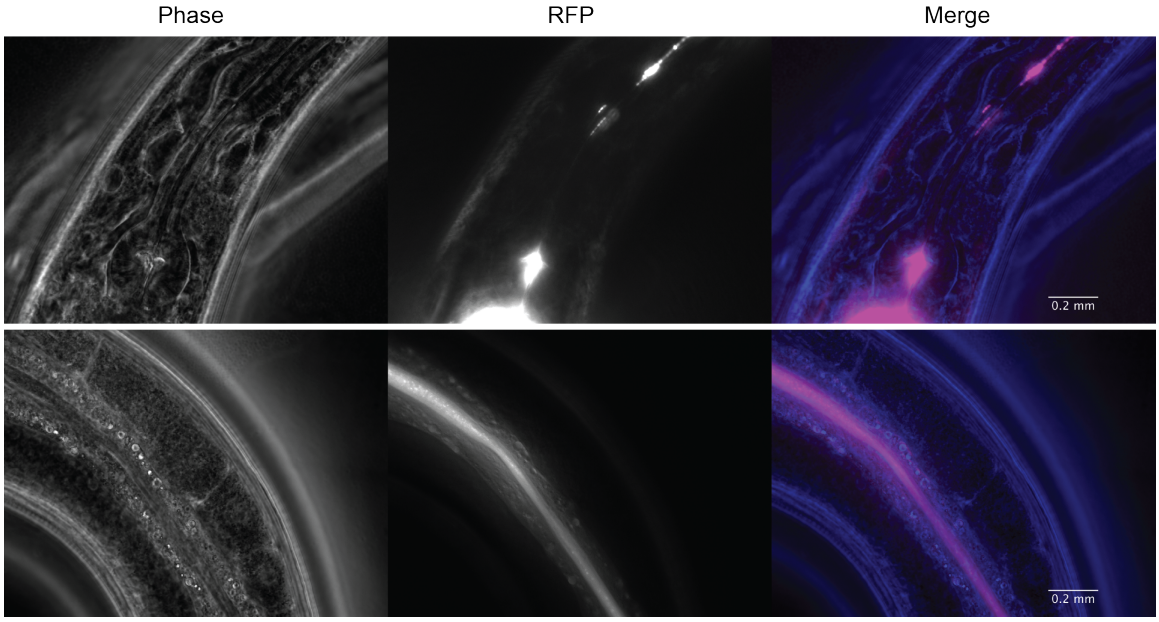

Figure 4.3 Fluorescence corresponding to *P. mirabilis* is found along *C. elegans* gut

Wild-type N2 worms were developed on a swarm of *P. mirabilis* BB2000 with a chromosomal RFP marker for 48 hours (BB2000::*rfp*). Worms were immobilized on 10% agarose dissolved in NGM buffer and imaged using standard epifluorescent microscope. Left, Phase. Middle, fluorescence in RFP channel. Right, false-colored overlay in which RFP channel is in magenta and phase is in blue. Scale bar is 0.2mm.

P. mirabilis social behaviors and interstrain dynamics within C. elegans gut

P. mirabilis social behaviors include strain restriction to the center of a mixed colony and macroscopic boundary formation between populations (10, 29). At least three genetic loci are known to be involved in these behaviors, *ids, idr,* and the secretion system both utilize, the type VI secretion system (T6S) (10, 27). Under laboratory conditions, strain dominance is assayed by normalizing strains by OD_{600} and mixing two strains at a 1:1 ratio. This mixed population is then spotted against each individual monoclonal strain population and whichever strain merges with the mixed population is deemed "dominant".

To assess whether *P. mirabilis* social behaviors are likely to occur within the *C. elegans* gut, strains BB2000::*gfp* and HI4320 (**Figure 4.4A**) were mixed at a 1:1 ratio. This mix was compared to BB2000 lacking the *ids* locus with a chromosomal GFP marker (BB2000Δ*ids*::*gfp*) mixed with HI4320 (**Figure 4.4B**). Under laboratory conditions HI4320 is dominant over both BB2000::*gfp* and BB2000Δ*ids*::*gfp* (**Figure A.7**). N2 worms were developed on a mixed colony and strain-selective colony-forming unit assays were performed. Preliminary data suggests there is a relative abundance of HI4320 compared to BB2000::*gfp* or BB2000Δ*ids*::*gfp* (**Figure 4.4**).

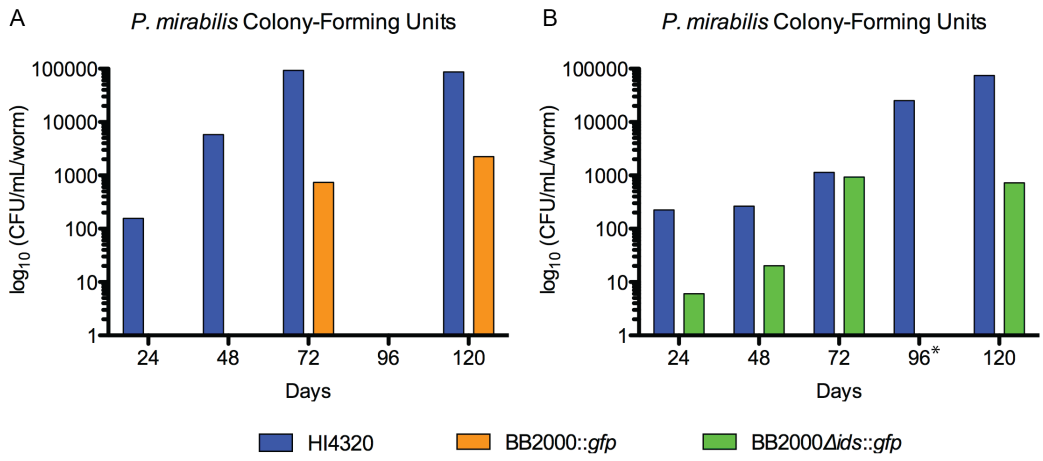

Figure 4.4 *P. mirabilis* strain HI4320 outcompetes strain BB2000 in *C. elegans* gut A) Wild-type N2 worms were developed on a *P. mirabilis* mix of strains HI4320 and strain BB2000::*gfp*. Plates at 96 hours could not be included in analysis due to plate contamination. (B) To test effect of a self-recognition loci worms were developed on a mix of HI4320 and BB2000 lacking the *ids* system with a chromosomal GFP marker (BB2000Δ*ids*::*gfp*). At 24-hour intervals worms were transferred to a fresh lawn of each mix and a subset of worms were taken for analysis. These were anesthetized, vigorously washed in the presence of detergent, and lysed. Intestinal contents were plated on strain-selective media using a carbenicillin resistance marker in BB2000::*gfp* and BB2000Δ*ids*::*gfp*. Serial dilutions were plated on LSW- agar with tetracycline, with and without carbenicillin, and colony-forming units calculated per mL per worm and plotted on a $\log_{10}$ scale.

This abundance could result from *ids*-mediated strain competition, but it could also be impacted by *C. elegans* feeding preference or physical distribution of each strain within the mixed colony. To test this possibility, N2 adult worms were fed strain BB2000 for 48 hours and then switched to strain HI4320 or strain CW677 for 48 hours. At 24-hour intervals worms were washed and strain-specific colony-forming units were assayed. Under laboratory conditions HI4320 is dominant over BB2000 but CW677 is not (**Figure A.7**). Therefore, if strain competition were occurring, one would expect that HI4320 would displace BB2000 but CW677 would not. However, both HI4320 and CW677 displaced BB2000 (**Figure 4.5**). One explanation is that in the host there is a lack of strain-dependent colonization or alternatively that there are inherent differences in dominance between laboratory conditions and within a host.

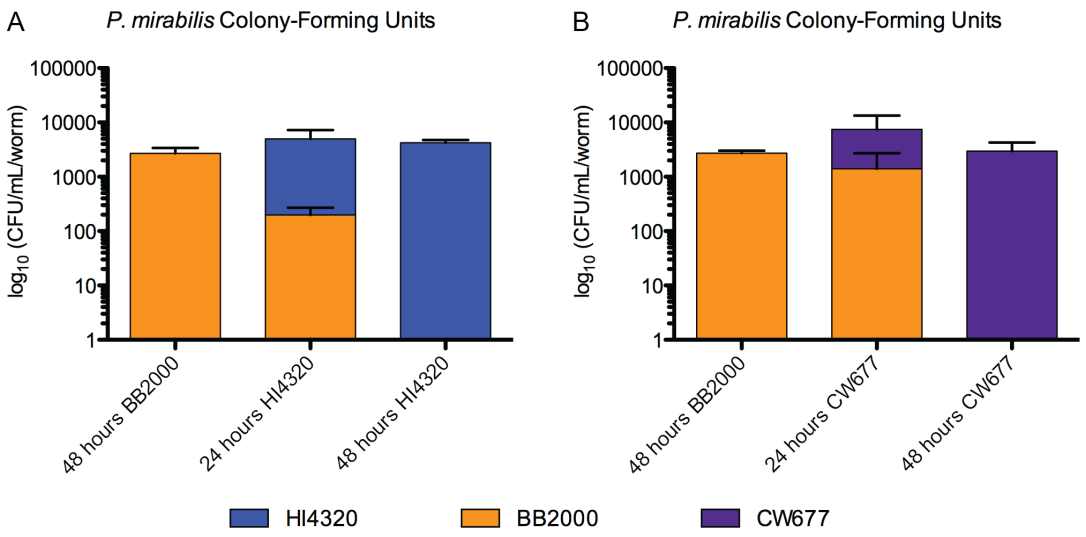

Figure 4.5 During serial feeding second *P. mirabilis* strain displaces the first Wild-type N2 worms were developed on *E. coli* OP50. L4-stage worms were transferred to a *P. mirabilis* swarm of strain BB2000. Worms were fed BB2000 for 48 hours before transfer to (A) strain HI4320 or (B) strain CW677 for an additional 48 hours. At 24-hour intervals, 10 worms were anesthetized, vigorously washed in the presence of detergent, and lysed. Intestinal contents were plated on LSW- agar with strain selective antibiotics as all three strains are naturally tetracycline resistant but only strain BB2000 is rifampicin resistant. Total colony-forming units were calculated per mL per worm from tetracycline plates and BB2000 colony-forming units were calculated per mL per worm from rifampicin plates. The difference of these two numbers was calculated as colony-forming units per mL per worm for HI4320 or CW677. Calculations plotted on a $\log_{10}$ scale.

Discussion

In this chapter I have adapted and extended a *C. elegans* model for *P. mirabilis* host colonization of the gut for the lab. I show that different clinical isolates of *P. mirabilis* do not affect wild-type *C. elegans* viability. Preliminarily, the data suggests that a single strain of *P. mirabilis* predominantly resides in the *C. elegans* gut at a time and that an incoming strain will displace an established strain. However, the data is inconclusive as to the role of the *ids* self-recognition system in influencing strain dynamics.

With these established protocols, this system could be used in the future to more stringently test interstrain interactions in the gut. This would include re-testing the influence of the Ids system using the BB2000Δ*ids* strain, as well as using strains deficient in Ids signaling, such as Δ*ids* + pIds-FLAG-IdsC$^{\Delta DUF4123}$ (**Chapter 3**) or Δ*ids* + pIds-*ΔidsE* (30). To test the impact of the Idr self-recognition system, *idr* mutants already present in the lab can be used in similar assays. Since the acquisition of this data we have further evidence in the lab that Ids is a non-lethal system while Idr is a classic toxin-antitoxin system (30). Given this, I predict that an *idr* mutant would be more susceptible during competitions in the *C. elegans* gut. The T6S is used for export of Ids, Idr, and other proteins. It is possible that T6S activity, and delivery of the combination of these proteins, is important for these dynamics. *P. mirabilis* T6S deficient mutants established in the lab (10, 30, 37, 38) as well as an Ids/Idr deficient mutant could be used to test this.

It is also possible that the presence of other bacterial species impacts *P. mirabilis* interstrain dynamics. If the interactions between different *P. mirabilis* strains are well established, this host system could be used to test how other bacterial species affect these.

To do so, bacterial communities comprised of *P. mirabilis* and other members, found either in the human gastrointestinal tract or during catheter-associated urinary tract infections, could be fed to the worms and similar assays as described here conducted.

References

1. **Pearson MM, Yep A, Smith SN, Mobley HL.** 2011. Transcriptome of *Proteus mirabilis* in the murine urinary tract: virulence and nitrogen assimilation gene expression. Infect Immun **79:**2619-2631.

2. **Griffith DP, Musher DM, Itin C.** 1976. Urease. The primary cause of infection-induced urinary stones. Invest Urol **13:**346-350.

3. **Jones BD, Mobley HL.** 1987. Genetic and biochemical diversity of ureases of *Proteus*, *Providencia*, and *Morganella* species isolated from urinary tract infection. Infect Immun **55:**2198-2203.

4. **Macleod SM, Stickler DJ.** 2007. Species interactions in mixed-community crystalline biofilms on urinary catheters. J Med Microbiol **56:**1549-1557.

5. **Stickler D, Ganderton L, King J, Nettleton J, Winters C.** 1993. *Proteus mirabilis* biofilms and the encrustation of urethral catheters. Urol Res **21:**407-411.

6. **Stickler D, Morris N, Moreno MC, Sabbuba N.** 1998. Studies on the formation of crystalline bacterial biofilms on urethral catheters. Eur J Clin Microbiol Infect Dis **17:**649-652.

7. **Stickler DJ, Morgan SD.** 2008. Observations on the development of the crystalline bacterial biofilms that encrust and block Foley catheters. J Hosp Infect **69:**350-360.

8. **Pfaller MA, Mujeeb I, Hollis RJ, Jones RN, Doern GV.** 2000. Evaluation of the discriminatory powers of the Dienes test and ribotyping as typing methods for *Proteus mirabilis*. J Clin Microbiol **38:**1077-1080.

9. **Sabbuba NA, Mahenthiralingam E, Stickler DJ.** 2003. Molecular epidemiology of *Proteus mirabilis* infections of the catheterized urinary tract. J Clin Microbiol **41:**4961-4965.

10. **Wenren LM, Sullivan NL, Cardarelli L, Septer AN, Gibbs KA.** 2013. Two independent pathways for self-recognition in *Proteus mirabilis* are linked by type VI-dependent export. MBio **4**.

11. **Jansen AM, Lockatell CV, Johnson DE, Mobley HL.** 2003. Visualization of *Proteus mirabilis* morphotypes in the urinary tract: the elongated swarmer cell is rarely observed in ascending urinary tract infection. Infect Immun **71:**3607-3613.

12. **Sosa V, Schlapp G, Zunino P.** 2006. *Proteus mirabilis* isolates of different origins do not show correlation with virulence attributes and can colonize the urinary tract of mice. Microbiology **152:**2149-2157.

13. **Brenner S.** 1974. The genetics of *Caenorhabditis elegans*. Genetics **77:**71-94.

14. **Tan MW, Ausubel FM.** 2000. *Caenorhabditis elegans*: a model genetic host to study *Pseudomonas aeruginosa* pathogenesis. Curr Opin Microbiol **3:**29-34.

15. **Sifri CD, Begun J, Ausubel FM.** 2005. The worm has turned--microbial virulence modeled in *Caenorhabditis elegans*. Trends Microbiol **13:**119-127.

16. **Stiernagle T.** 2006. Maintenance of *C. elegans*. WormBook doi:10.1895/wormbook.1.101.1**:**1-11.

17. **Shapira M, Tan MW.** 2008. Genetic analysis of *Caenorhabditis elegans* innate immunity. Methods Mol Biol **415:**429-442.

18. **Kim E, Sun L, Gabel CV, Fang-Yen C.** 2013. Long-term imaging of *Caenorhabditis elegans* using nanoparticle-mediated immobilization. PLoS One **8:**e53419.

19. **Kurz CL, Chauvet S, Andres E, Aurouze M, Vallet I, Michel GP, Uh M, Celli J, Filloux A, De Bentzmann S, Steinmetz I, Hoffmann JA, Finlay BB, Gorvel JP, Ferrandon D, Ewbank JJ.** 2003. Virulence factors of the human opportunistic pathogen *Serratia marcescens* identified by in vivo screening. EMBO J **22:**1451-1460.

20. **O'Quinn AL, Wiegand EM, Jeddeloh JA.** 2001. *Burkholderia pseudomallei* kills the nematode *Caenorhabditis elegans* using an endotoxin-mediated paralysis. Cell Microbiol **3:**381-393.

21. **Gan YH, Chua KL, Chua HH, Liu B, Hii CS, Chong HL, Tan P.** 2002. Characterization of *Burkholderia pseudomallei* infection and identification of novel virulence factors using a *Caenorhabditis elegans* host system. Mol Microbiol **44:**1185-1197.

22. **Couillault C, Ewbank JJ.** 2002. Diverse bacteria are pathogens of *Caenorhabditis elegans*. Infect Immun **70:**4705-4707.

23. **JebaMercy G, Vigneshwari L, Balamurugan K.** 2013. A MAP Kinase pathway in *Caenorhabditis elegans* is required for defense against infection by opportunistic *Proteus* species. Microbes Infect **15:**550-568.

24. **Schindelin J, Arganda-Carreras I, Frise E, Kaynig V, Longair M, Pietzsch T, Preibisch S, Rueden C, Saalfeld S, Schmid B, Tinevez JY, White DJ, Hartenstein V, Eliceiri K, Tomancak P, Cardona A.** 2012. Fiji: an open-source platform for biological-image analysis. Nat Methods **9:**676-682.

25. **Schindelin J, Rueden CT, Hiner MC, Eliceiri KW.** 2015. The ImageJ ecosystem: An open platform for biomedical image analysis. Mol Reprod Dev **82:**518-529.

26. **Belas R, Erskine D, Flaherty D.** 1991. Transposon mutagenesis in *Proteus mirabilis*. J Bacteriol **173:**6289-6293.

27. **Gibbs KA, Urbanowski ML, Greenberg EP.** 2008. Genetic determinants of self identity and social recognition in bacteria. Science **321:**256-259.

28. **Pearson MM, Sebaihia M, Churcher C, Quail MA, Seshasayee AS, Luscombe NM, Abdellah Z, Arrosmith C, Atkin B, Chillingworth T, Hauser H, Jagels K, Moule S, Mungall K, Norbertczak H, Rabbinowitsch E, Walker D, Whithead S, Thomson NR, Rather PN, Parkhill J, Mobley HL.** 2008. Complete genome sequence of uropathogenic *Proteus mirabilis*, a master of both adherence and motility. J Bacteriol **190:**4027-4037.

29. **Senior BW.** 1977. The Dienes phenomenon: identification of the determinants of compatibility. J Gen Microbiol **102:**235-244.

30. **Saak CC, Gibbs KA.** 2016. The Self-Identity Protein IdsD Is Communicated between Cells in Swarming *Proteus mirabilis* Colonies. J Bacteriol **198:**3278-3286.

31. **Cardarelli L, Saak C, Gibbs KA.** 2015. Two Proteins Form a Heteromeric Bacterial Self-Recognition Complex in Which Variable Subdomains Determine Allele-Restricted Binding. MBio **6:**e00251.

32. **Pearson MM, Mobley HL.** 2007. The type III secretion system of *Proteus mirabilis* HI4320 does not contribute to virulence in the mouse model of ascending urinary tract infection. J Med Microbiol **56:**1277-1283.

33. **Alamuri P, Lower M, Hiss JA, Himpsl SD, Schneider G, Mobley HL.** 2010. Adhesion, invasion, and agglutination mediated by two trimeric autotransporters in the human uropathogen *Proteus mirabilis*. Infect Immun **78:**4882-4894.

34. **Armbruster CE, Forsyth-DeOrnellas V, Johnson AO, Smith SN, Zhao L, Wu W, Mobley HLT.** 2017. Genome-wide transposon mutagenesis of *Proteus mirabilis*: Essential genes, fitness factors for catheter-associated urinary tract infection, and the impact of polymicrobial infection on fitness requirements. PLoS Pathog **13:**e1006434.

35. **Powell JR, Kim DH, Ausubel FM.** 2009. The G protein-coupled receptor FSHR-1 is required for the *Caenorhabditis elegans* innate immune response. Proc Natl Acad Sci U S A **106:**2782-2787.

36. **Hsiao JY, Chen CY, Yang MJ, Ho HC.** 2013. Live and dead GFP-tagged bacteria showed indistinguishable fluorescence in *Caenorhabditis elegans* gut. J Microbiol **51:**367-372.

37. **Saak CC, Zepeda-Rivera MA, Gibbs KA.** 2017. A single point mutation in a TssB/VipA homolog disrupts sheath formation in the type VI secretion system of *Proteus mirabilis*. PLoS One **12:**e0184797.

38. **Zepeda-Rivera MA, Saak CC, Gibbs KA.** A proposed chaperone of the bacterial type VI secretion system functions to constrain a self-identity protein. J Bacteriol doi:10.1128/JB.00688-17.

Chapter 5

Discussion

Bacteria use specialized machineries, called secretion systems, to secrete signals into neighboring cells in order to modulate intercellular interactions. The structures of various secretion systems have been well studied, as well as the class of signals that they secrete. These classes of signals could for example be proteins, nucleic acids, or nucleo-protein complexes. However, how a substrate is targeted to its specific secretion system for delivery is not well understood for any secretion system. This becomes a particularly intriguing problem for bacterial cells that express more than one type of secretion system at a time and must target signals to the correct system for exchange. In this work, the Ids system of the Gram-negative bacterium *Proteus mirabilis* was used as a model to study how a type VI secretion (T6S) system substrate is targeted for delivery.

T6S systems are multi-protein channels that span the inner and outer membranes of a producing Gram-negative bacterial cell to delivery protein effectors into neighboring eukaryotic or prokaryotic cells. In a recipient eukaryotic cell, the machinery penetrates the plasma membrane to deliver effectors into the cytosol. In a recipient prokaryotic cell, the machinery can penetrate the outer membrane to deliver effectors into the periplasmic space, or can additionally penetrate the inner membrane to deliver them into the cytoplasm. T6S systems are derived from bacteriophage components, and resemble an inverted bacteriophage tail that plunges proteins through an inner tube capped with a spike-like protein trimer of VgrG proteins for infiltration of cellular membranes (1-10). T6S substrates range in function and size, from <20 kDa to over 100 kDa. For some secretion systems, such as the type III secretion (T3S) system, signal sequences are used to identify substrates. However, no conserved signal sequence has been found for T6S substrates. Bioinformatics has uncovered short protein motifs, called MIX motifs, present

in known or predicted T6S substrates (11). However, not all known substrates contain MIX motifs. Further bioinformatics uncovered that proteins encoded immediately upstream of known or predicted T6S substrates contain a particular protein motif, called the DUF4123 domain (12, 13). In two bacterial systems, a DUF4123 protein was shown to be required for interactions with the VgrG cap protein and substrate secretion and it was therefore proposed that DUF4123 proteins act as chaperones for T6S substrate secretion systems (12, 13). However, the molecular functions of such chaperones were not detailed in these studies.

The best-described T6S substrates show toxic activity post-transfer into recipient cells. This activity is thought to be inhibited in producing cells by binding of a cognate immunity protein cell (3, 7, 14, 15). If the recipient cell contains the cognate immunity protein, toxic effector activity is inhibited. If the recipient cell lacks the cognate immunity protein they are susceptible to the effectors toxicity. The toxic nature of these proteins makes it difficult to study their targeting to the T6S machinery independent of their interactions with the cognate immunity protein. However, one well-described T6S substrate that shows population-modulatory but not cell killing activity is the *P. mirabilis* IdsD protein (16, 17).

The *P. mirabilis* Ids system functions to establish and communicate self-identity (18, 19). The Gibbs lab has uncovered many details of the molecular mechanism behind this communication, but the role of self-recognition in natural environments still requires further study (Chapter 4). What is known is that IdsD is secreted in a T6S-dependent manner for exchange of self-identity information (16-19). The binding status of IdsD with its strain-specific binding partner IdsE in recipient cells contributes to population

self-recognition behaviors (16). Clonal (self) populations will merge upon their encounter while non-clonal (non-self) populations will form a macroscopic boundary between them (19). IdsD-IdsE mismatch strains, however, show equivalent cell viability and growth to strains in which IdsD-IdsE match (16). The Ids system contains four additional proteins (IdsA, IdsB, IdsC, and IdsF). All except IdsA are implicated in aiding the transport of IdsD through self-recognition assays and protein homology comparisons (**Figure A.1**) (19). IdsC, encoded immediately upstream of IdsD, contains a DUF4123 domain and its function had previously remained unexplored.

IdsD forms distinct clusters that can be found proximal to the T6S machinery. The presence of these clusters is independent of T6S function and the strain-specific binding partner IdsE, but does depend on IdsC (Chapter 2). IdsC binds IdsD independently of other Ids or T6S proteins, and the DUF4123 domain helps mediate this interaction. While IdsC is highly conserved across *P. mirabilis* strains, single amino acid polymorphisms uncouple IdsD targeting from IdsD secretion (Chapter 3). This has led to a deeper understanding of T6S substrate delivery. This work indicates that a DUF4123-chaperone has at least two distinct functions, to maintain substrate levels pre-transport and target it to the machinery. However, delivery through the machinery constitutes an additional third step. We hypothesize that IdsC might actually directly hand IdsD over to IdsB (VgrG) and/or the T6S proteins, particularly sheath and baseplate components, when the IdsC-IdsD complex is localized at the T6S machinery. Given that the amino acid changes we introduced into IdsC did not show changes in protein interaction partners, it is possible that these changes alter binding affinities, either between IdsC and the T6S machinery or between IdsC and IdsD. Such changes would diminish the efficiency of

handing off IdsD to the machinery. It is also possible that a third yet unidentified protein factor mediates the IdsC-IdsD interaction and that the IdsC amino acid variants alter this interaction. Since IdsC and IdsD produced from *Escherichia coli* bind *in vitro*, this third unidentified protein would have to be present in both *E. coli* and *P. mirabilis*.

Regardless, the amino acid polymorphisms uncovered here could serve as future tools for structural studies of T6S substrates at the machinery pre-delivery. Multiple conserved T6S components have been crystallized, and electron microscopy studies of the entire assembled machinery can take advantage of these crystal structures to elucidate the entire assembled machine. One could imagine using the IdsC amino acid variants in such structural studies to lock IdsD at the machinery and observe how a large substrate is docked. This would be particularly exciting for larger T6S substrates, like IdsD, whose mechanism of transport is less understood. Such variants in other DUF4123 proteins have not been described, but further research in this area is required. A comparison of how a variety of substrates are docked on to the machinery could help expand in the understanding of the commonalities in secretion of substrates that can be so divergent in size and function.

The proposed mechanism presented here for IdsC function is reminiscent of chaperone activities in other bacterial transport systems, like the T3S chaperones. However several questions remain. Clusters of IdsD are present regardless of the transport machinery, however, whether these clusters self-assemble or require an additional nucleating proteins remains to be tested. A comparison of IdsD protein binding partners from three T6S abrogated strain backgrounds showed thirty-eight shared binding partners, including IdsB, IdsC, and IdsF. Since IdsB is not essential for the formation of

these clusters, this raises the possibility that IdsC itself might gather IdsD into clusters when IdsD is not actively transported. Since few IdsD clusters are seen per cell, it seems as if these clusters are formed in preparation for delivery into a recipient cell. It also suggests that perhaps response to IdsD activity is dose-dependent, as these clusters are formed of multiple IdsD monomers. Further studies, such as through size exclusion chromatography and light scattering experiments, are required to assess the number of IdsD monomers per puncta. Dose dependency of an *in vivo* response to IdsD transfer is also suggested by the differences observed between the *in vivo* and *in vitro* IdsD secretion assays in the FLAG-IdsC amino acid variant strains.

In other bacterial systems, a DUF4123 protein shows specificity for secretion of the immediately adjacent substrate, suggesting that chaperones are not interchangeable (5, 13). A comparison of proteins secreted by FLAG-IdsC but not by FLAG-IdsC$^{\Delta DUF4123}$ did not indicate that IdsC impacts secretion of any other known T6S effector, except for IdrD. However, since Idr proteins are known to function independently of Ids (17), it is unlikely that IdsC regulates IdrD. This data therefore suggests that like in other systems, IdsC is specific for the substrate encoded immediately downstream. How chaperone-substrate specificity is acquired however, is unclear. Given that IdsC from one *P. mirabilis* strain can bind IdsD proteins from various strains and that the first 57 amino acids of IdsD are the mostly highly conserved between them suggests the N-terminus of IdsD is involved in the IdsC-IdsD interaction. This is intriguing since two MIX motifs lie within this region (11). It has remained untested whether DUF4123 domains rely on MIX motif presence or combinations for identifying T6S substrates. Further experiments mutating or deleting the MIX motifs of IdsD could be used to test this. It is also possible

that as these genes are co-transcribed and co-translated chaperone-substrate complexes are immediately formed. Perhaps the binding affinity between them is strong enough and/or the rate of targeting to active machineries fast enough to prevent chaperone-substrate reassortment. While likely due to the high sensitivity of LC-MS/MS, it was noted that both FLAG-IdsD and FLAG-IdsC pull down multiple components of both the large and small ribosomal subunits, which could support this hypothesis. Further experiments, perhaps ectopic expression of either IdsC or IdsD could serve to test this. It is also possible that structural differences between T6S substrates contribute to chaperone-specificity. Intriguingly however, not all T6S substrates show a DUF4123 protein encoded upstream (12). It is possible that, like the substrates of the T3S system, that there are subclasses of T6S substrates whose mechanism of targeting differs.

Tackling the question of substrate targeting using the Ids system added an additional probing question. In the T6S field, it is known that effectors are bound and inhibited by cognate immunity proteins. The prevalent model is that this binding interaction occurs in both donor and kin recipient cells (3, 7, 14, 15). However, the Ids system provided a unique context in which the binding interaction between the effector (IdsD) and the cognate immunity protein (IdsE) appears to only occur in recipient cells (16). Given that the IdsC-IdsD interaction appear to be restricted to donor cells suggests an alternative model where a T6S substrate is bound and inhibited by a well-conserved chaperone protein pre-transport to prevent effector-immunity pair interactions in donor cells. Given the prevalence of DUF4123 proteins it is tantalizing to consider that this could be a more widespread mechanism used to ensure that communication via exchange of protein signals is restricted to occurring intercellularly.

References

1. **Mougous JD, Cuff ME, Raunser S, Shen A, Zhou M, Gifford CA, Goodman AL, Joachimiak G, Ordonez CL, Lory S, Walz T, Joachimiak A, Mekalanos JJ.** 2006. A virulence locus of *Pseudomonas aeruginosa* encodes a protein secretion apparatus. Science **312:**1526-1530.

2. **Pukatzki S, Ma AT, Sturtevant D, Krastins B, Sarracino D, Nelson WC, Heidelberg JF, Mekalanos JJ.** 2006. Identification of a conserved bacterial protein secretion system in *Vibrio cholerae* using the *Dictyostelium* host model system. Proc Natl Acad Sci U S A **103:**1528-1533.

3. **Russell AB, Hood RD, Bui NK, LeRoux M, Vollmer W, Mougous JD.** 2011. Type VI secretion delivers bacteriolytic effectors to target cells. Nature **475:**343-347.

4. **Cianfanelli FR, Alcoforado Diniz J, Guo M, De Cesare V, Trost M, Coulthurst SJ.** 2016. VgrG and PAAR Proteins Define Distinct Versions of a Functional Type VI Secretion System. PLoS Pathog **12:**e1005735.

5. **Bondage DD, Lin JS, Ma LS, Kuo CH, Lai EM.** 2016. VgrG C terminus confers the type VI effector transport specificity and is required for binding with PAAR and adaptor-effector complex. Proc Natl Acad Sci U S A **113:**E3931-3940.

6. **Bonemann G, Pietrosiuk A, Diemand A, Zentgraf H, Mogk A.** 2009. Remodelling of VipA/VipB tubules by ClpV-mediated threading is crucial for type VI protein secretion. EMBO J **28:**315-325.

7. **Hachani A, Allsopp LP, Oduko Y, Filloux A.** 2014. The VgrG proteins are "a la carte" delivery systems for bacterial type VI effectors. J Biol Chem **289:**17872-17884.

8. **Hachani A, Lossi NS, Hamilton A, Jones C, Bleves S, Albesa-Jove D, Filloux A.** 2011. Type VI secretion system in *Pseudomonas aeruginosa*: secretion and multimerization of VgrG proteins. J Biol Chem **286:**12317-12327.

9. **Shneider MM, Buth SA, Ho BT, Basler M, Mekalanos JJ, Leiman PG.** 2013. PAAR-repeat proteins sharpen and diversify the type VI secretion system spike. Nature **500:**350-353.

10. **Whitney JC, Beck CM, Goo YA, Russell AB, Harding BN, De Leon JA, Cunningham DA, Tran BQ, Low DA, Goodlett DR, Hayes CS, Mougous JD.** 2014. Genetically distinct pathways guide effector export through the type VI secretion system. Mol Microbiol **92:**529-542.

11. **Salomon D, Kinch LN, Trudgian DC, Guo X, Klimko JA, Grishin NV, Mirzaei H, Orth K.** 2014. Marker for type VI secretion system effectors. Proc Natl Acad Sci U S A **111:**9271-9276.

12. **Liang X, Moore R, Wilton M, Wong MJ, Lam L, Dong TG.** 2015. Identification of divergent type VI secretion effectors using a conserved chaperone domain. Proc Natl Acad Sci U S A **112:**9106-9111.

13. **Unterweger D, Kostiuk B, Otjengerdes R, Wilton A, Diaz-Satizabal L, Pukatzki S.** 2015. Chimeric adaptor proteins translocate diverse type VI secretion system effectors in *Vibrio cholerae*. EMBO J **34:**2198-2210.

14. **Hood RD, Singh P, Hsu F, Guvener T, Carl MA, Trinidad RR, Silverman JM, Ohlson BB, Hicks KG, Plemel RL, Li M, Schwarz S, Wang WY, Merz AJ, Goodlett DR, Mougous JD.** 2010. A type VI secretion system of *Pseudomonas aeruginosa* targets a toxin to bacteria. Cell Host Microbe **7:**25-37.

15. **Whitney JC, Chou S, Russell AB, Biboy J, Gardiner TE, Ferrin MA, Brittnacher M, Vollmer W, Mougous JD.** 2013. Identification, structure, and function of a novel type VI secretion peptidoglycan glycoside hydrolase effector-immunity pair. J Biol Chem **288:**26616-26624.

16. **Saak CC, Gibbs KA.** 2016. The Self-Identity Protein IdsD Is Communicated between Cells in Swarming *Proteus mirabilis* Colonies. J Bacteriol **198:**3278-3286.

17. **Wenren LM, Sullivan NL, Cardarelli L, Septer AN, Gibbs KA.** 2013. Two independent pathways for self-recognition in *Proteus mirabilis* are linked by type VI-dependent export. MBio **4**.

18. **Cardarelli L, Saak C, Gibbs KA.** 2015. Two Proteins Form a Heteromeric Bacterial Self-Recognition Complex in Which Variable Subdomains Determine Allele-Restricted Binding. MBio **6:**e00251.

19. **Gibbs KA, Urbanowski ML, Greenberg EP.** 2008. Genetic determinants of self identity and social recognition in bacteria. Science **321:**256-259.

Appendix A

Supplementary Figures and Tables

Figure A.1 *Proteus mirabilis* BB2000 identity for self (*ids*) operon The six-gene *ids* operon is involved in encoding and communicating self-identity information between populations of *P. mirabilis*. Four of these genes, *idsA, idsB, idsC,* and *idsF,* encode homologs to proteins involved in type VI secretion (T6S) transport in other bacterial systems. Two of these, *idsD* and *idsE*, encode the strain-determinant proteins IdsD and IdsE. Binding interactions between IdsD and IdsE in recipient cells determines population self-recognition behaviors. Depicted below is the *ids* operon from strain BB2000 with known protein homologs and predicted protein sizes listed.

Figure A.2 Tagged Ids proteins are functional A Δ*ids* strain complemented with pIds, a plasmid encoding *idsA-idsF* driven by the native ids promoter, will merge with BB2000 (1). To test functionality of Ids proteins tagged with a FLAG-epitope or IdsD fused to an N-terminal mKate-2 fluorophore, Δ*ids* c. modified pIds plasmids are tested on kanamycin against BB2000 and Δ*ids* each carrying an empty plasmid that confers kanamycin resistance. Functionality is confirmed if this population merges with BB2000 (white arrows) and forms a boundary against Δ*ids* (black arrows).

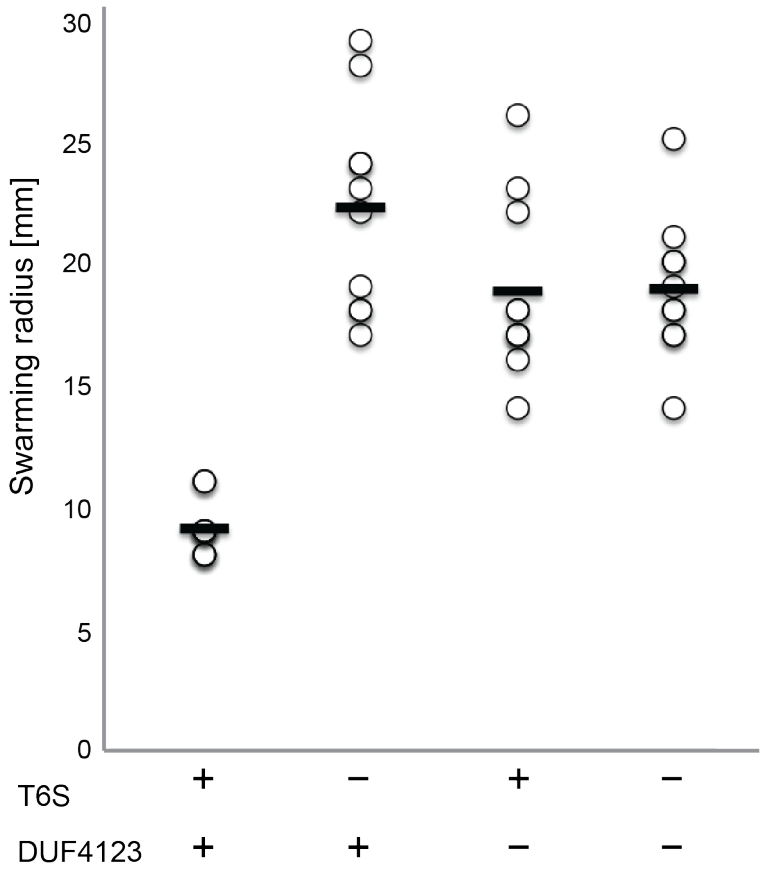

Figure A.3 IdsC-IdsD interaction is essential for mKate-IdsD secretion *In vivo* assay for IdsD cell-to-cell transfer in which IdsD secretion results in reduced colony, while lack of transport alleviates this restriction (2). *P. mirabilis* strains expressing modified pIds vectors producing FLAG-IdsC (+DUF4123) or FLAG-IdsC$^{\Delta DUF4123}$ (DUF4123-) with mKate2-IdsD. T6S+ is a *P. mirabilis* strain producing a fully functional T6S system; T6S- is the TssB chromosomal mutant (2). Open circles indicate migration radii per replicate and bars indicate average migration radius. N=10

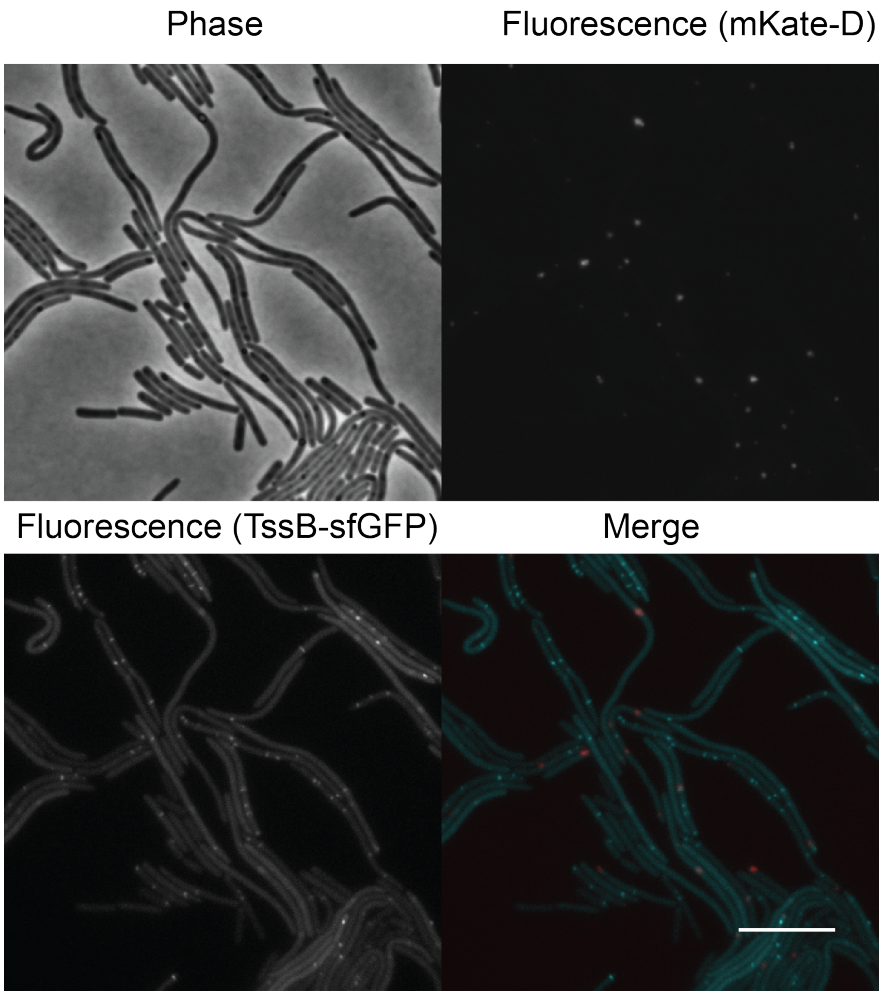

Figure A.4 FLAG-IdsC^{S38P} supports mKate-IdsD puncta formation The T6S sheath was labeled using a chromosomal fusion of the sheath component TssB to sfGFP (3). FLAG-IdsC^{S38P} and mKate-IdsD were produced from pIds in this strain background. TssB-sfGFP associated fluorescence formed rod-like structures along cells, while mKate-IdsD associated fluorescence formed discrete foci. Top left, Phase. Top right, fluorescence in the RFP channel for mKate2. Bottom left, fluorescence in the GFP channel for sfGFP. Bottom right, false-colored overlay in which for contrast, mKate-IdsD fluorescence is in red, and TssB-sfGFP fluorescence is in cyan. Scale bar is 10 μm.

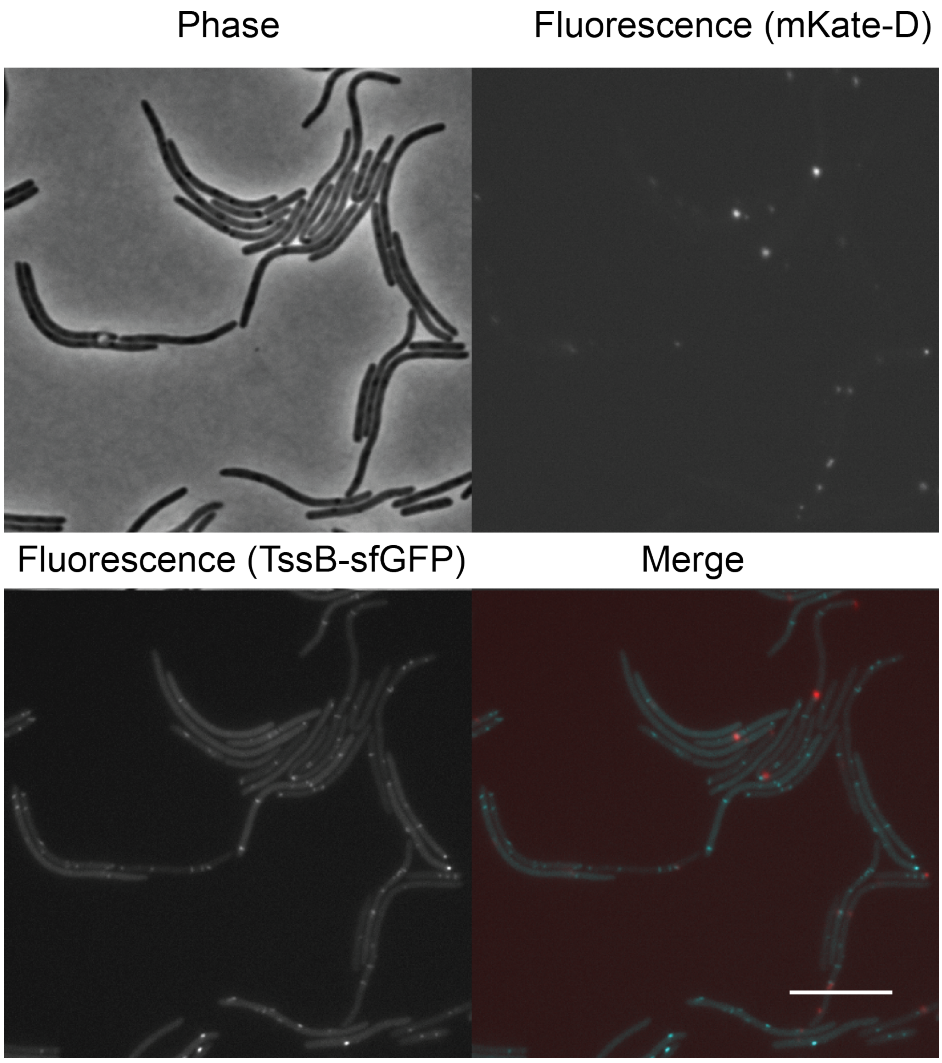

Figure A.5 FLAG-IdsC^{R186Q} supports mKate-IdsD puncta formation The T6S sheath was labeled using a chromosomal fusion of the sheath component TssB to sfGFP (3). FLAG-IdsC^{R186Q} and mKate-IdsD were produced from pIds in this strain background. TssB-sfGFP associated fluorescence formed rod-like structures along cells, while mKate-IdsD associated fluorescence formed discrete foci. Top left, Phase. Top right, fluorescence in the RFP channel for mKate2. Bottom left, fluorescence in the GFP channel for sfGFP. Bottom right, false-colored overlay in which for contrast, mKate-IdsD fluorescence is in red, and TssB-sfGFP fluorescence is in cyan. Scale bar is 10 μm.

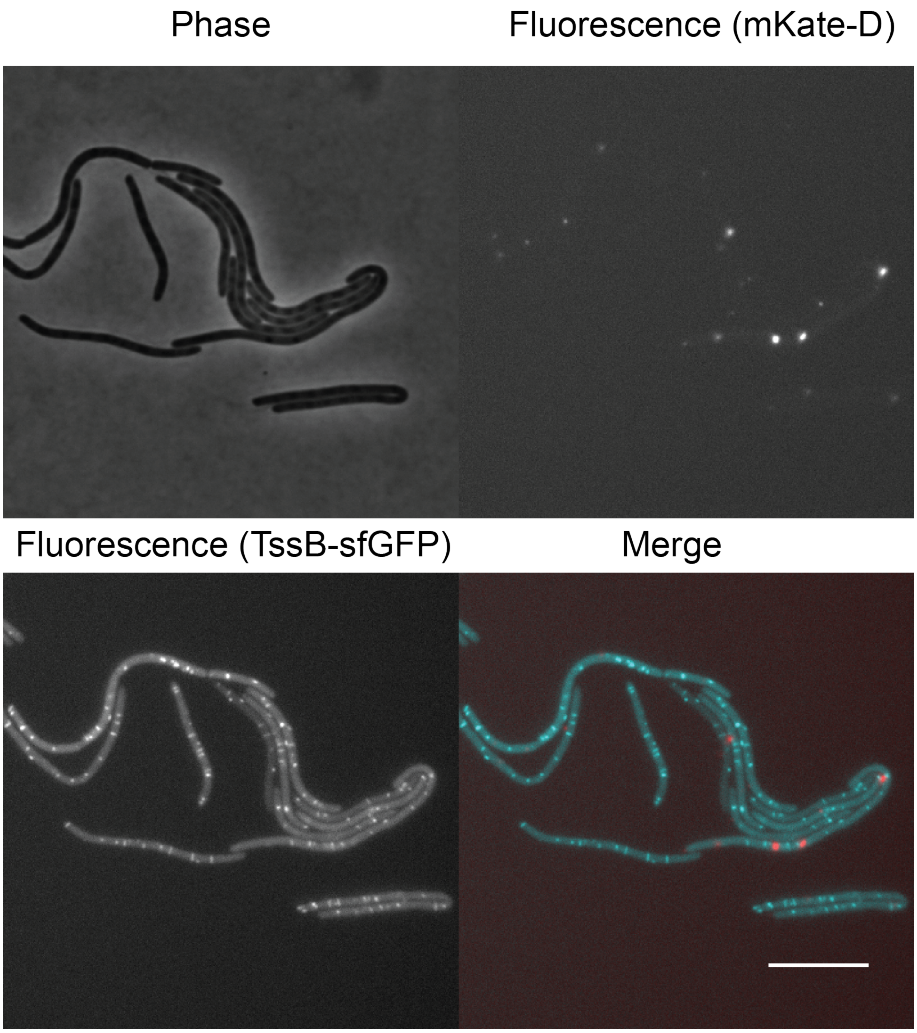

Figure A.6 FLAG-IdsC$^{S38P/R186Q}$ supports mKate-IdsD puncta formation The T6S sheath was labeled using a chromosomal fusion of the sheath component TssB to sfGFP (3). FLAG-IdsC$^{S38P/R186Q}$ and mKate-IdsD were produced from pIds in this strain background. TssB-sfGFP associated fluorescence formed rod-like structures along cells, while mKate-IdsD associated fluorescence formed discrete foci. Top left, Phase. Top right, fluorescence in the RFP channel for mKate2. Bottom left, fluorescence in the GFP channel for sfGFP. Bottom right, false-colored overlay in which for contrast, mKate-IdsD fluorescence is in red, and TssB-sfGFP fluorescence is in cyan. Scale bar is 10 μm.

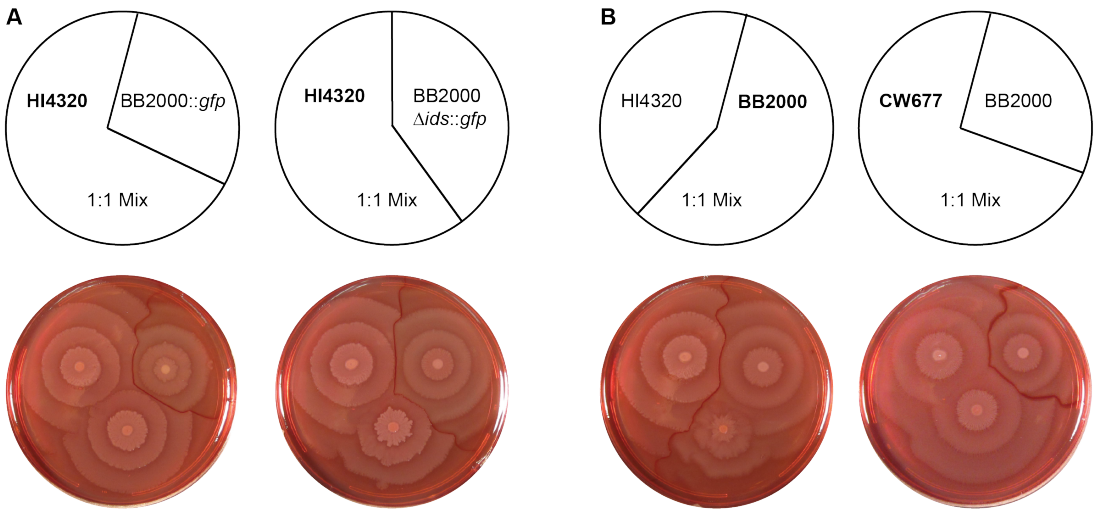

Figure A.7 *P. mirabilis* mixed populations show strain dominance by Dienes line test

P. mirabilis cultures were normalized to OD_{600} of 0.1 and 1 ul of each strain or a 1:1 mix of two strains were inoculated on swarming-permissive media. The 1:1 mix will boundary with one of the two individual strains and merge with the other. The strain with which it merges is determined to be the dominant strain in the mix. (A) Strains HI43230, BB2000::*gfp*, and BB2000Δ*ids*::*gfp* were used to test *in vitro* dominance to predict *in vivo* dominance for assay in **Figure 4.4**. The presence of GFP alters the interaction between BB2000 and HI4320. (B) Strains HI4320, BB2000, and CW677 were used to test *in vitro* dominance to predict *in vivo* dominance for assay in **Figure 4.5**.

Table A.1 Strains used in this study

Strain	Notes	Source	KAG #	MZR #	Plasmid
BB2000	Wild-type	(4)	001	001	
HI4320	Wild-type		034	008	
CW677	Wild-type	(5)	MLU 4.274		
BB2000 c. pKG101	BB2000 carrying a plasmid expressing promoterless green fluorescent protein.	(6)	066	019	pKG101
BB2000::GFP	BB2000 constitutively expressing chromosomally encoded green fluorescent protein.	(1)	1400	022	
Δ*ids*	Δ*ids::Tn-Cm(R)*	(1)	006	002	
Δ*ids* c. pKG101	Δ*ids* carrying a plasmid expressing promoterless green fluorescent protein.	(6)	067	020	pKG101
Δ*ids*::GFP	Δ*ids* constitutively expressing chromosomally encoded green fluorescent protein. Made using pKG2012-1 (1).	This study	966	026	
Δ*ids* + pIds-IdsA-FLAG	Modified protein(s): IdsA-FLAG Δ*ids* carrying a modified pIds plasmid with a C-terminal FLAG-tag encoded in-frame with *idsA*.	(7)	930	029	pLMW06
Δ*ids* c. pIds-FLAG-IdsC	Modified protein(s): FLAG-IdsC Δ*ids* carrying a modified pIds plasmid with an N-terminal FLAG-tag encoded in-frame with *idsC*.	This study	644/ 645	039/ 167	pLC-001

Table A.1 Strains used in this study (continued)

Δ*ids* + pIds-FLAG-IdsD	Modified protein(s): FLAG-IdsD Δ*ids* carrying a modified pIds plasmid with an N-terminal FLAG-tag encoded in-frame with *idsD*.	(8)	661	036	pLC-015
Δ*ids* + pIds-FLAG-IdsE	Modified protein(s): FLAG-IdsE Δ*ids* carrying a modified pIds plasmid with an N-terminal FLAG-tag encoded in-frame with *idsE*.	(8)	655	045	pLC-013
Δ*ids* + pIds-IdsF-FLAG	Modified protein(s): IdsF-FLAG Δ*ids* carrying a modified pIds plasmid with a C-terminal FLAG-tag encoded in-frame with *idsF*.	This study	657	042	pLC-014
Δ*ids* +pIds-FLAG-IdsC-mKate2-IdsD	Modified protein(s): FLAG-IdsC, mKate2-IdsD Δ*ids* carrying a modified pIds plasmid with an N-terminal FLAG-tag encoded in-frame with *idsC* and an N-terminal mKate2 fluorophore fused to *idsD*.	This study			pMZ49
Δ*ids* c. pIds-FLAG-IdsC-mKate-IdsD-ΔIdsE	Modified protein(s): FLAG-IdsC, mKate2-IdsD, ΔidsE Δ*ids* carrying a modified pIds plasmid with an N-terminal FLAG-tag encoded in-frame with *idsC* and an N-terminal mKate2 fluorophore fused to *idsD*. In-frame deletion of *idsE*.	This study			

Table A.1 Strains used in this study (continued)

Δ*ids* c. pIds-FLAG-IdsC $^{\Delta DUF4123}$-mKate-IdsD	Modified protein(s): FLAG-IdsC$^{\Delta DUF4123}$, mKate2-IdsD Δ*ids* carrying a modified pIds plasmid with an N-terminal FLAG-tag encoded in-frame with *idsC* with nucleotides 373-762 deleted and an N-terminal mKate2 fluorophore fused to *idsD*.				
Δ*ids* c. pIds-FLAG-IdsC $^{\Delta DUF4123}$-mKate-IdsD-ΔIdsE	Modified protein(s): FLAG-IdsC$^{\Delta DUF4123}$, mKate2-IdsD, ΔIdsE Δ*ids* carrying a modified pIds plasmid with an N-terminal FLAG-tag encoded in-frame with *idsC* with nucleotides 373-762 deleted and an N-terminal mKate2 fluorophore fused to *idsD*. In-frame deletion of *idsE*.	This study			
CCS05	Modified protein(s): $TssB_{L32R}$ Δ*ids* with chromosomal BB2000_0821 with a single T→G point mutation at base pair 95. This results in a disrupted T6S sheath.	(2)	2115		
CCS05 c. pIds-FLAG-IdsC-mKate2-IdsD-ΔIdsE	Modified protein(s): $TssB_{L32R}$, FLAG-IdsC, mKate2-IdsD, ΔIdsE CCS05 carrying a modified pIds plasmid with an N-terminal FLAG-tag encoded in-frame with *idsC* and an N-terminal mKate2 fluorophore fused to *idsD*. In-frame deletion of *idsE*.	This study			

Table A.1 Strains used in this study (continued)

CCS05 c. pIds-FLAG-IdsC $^{\Delta DUF4123}$-mKate2-IdsD-ΔIdsE	Modified protein(s): $TssB_{L32R}$, FLAG-$IdsC^{\Delta DUF4123}$, mKate2-IdsD, ΔIdsE CCS05 carrying a modified pIds plasmid with an N-terminal FLAG-tag encoded in-frame with *idsC* with nucleotides 373-762 deleted and an N-terminal mKate2 fluorophore fused to *idsD*. In-frame deletion of *idsE*.	This study			
Δ*ids::BB2000_0821-sfGFP* c. pIds-FLAG-$IdsC^{S38P}$-mKate2-IdsD	Modified protein(s): TssB-sfGFP, FLAG-$IdsC^{S38P}$, mKate2-IdsD Δ*ids::BB2000_0821-sfGFP* carrying a modified pIds plasmid with an N-terminal FLAG-tag encoded in-frame with *idsC* containing a T→C mutation at nucleotide 112 and an N-terminal mKate2-fluorophore fused to *idsD*.	This study	3403	330	pMZ70
Δ*ids::BB2000_0821-sfGFP* c. pIds-FLAG-$IdsC^{R186Q}$-mKate2-IdsD	Modified protein(s): TssB-sfGFP, FLAG-$IdsC^{S38P/R186Q}$, mKate2-IdsD Δ*ids::BB2000_0821-sfGFP* carrying a modified pIds plasmid with an N-terminal FLAG-tag encoded in-frame with *idsC* containing a G→A mutation at nucleotide 557 and an N-terminal mKate2-fluorophore fused to *idsD*.	This study	3431	344	pMZ72

Table A.1 Strains used in this study (continued)

Δ*ids::BB2000_0821-sfGFP* c. pIds-FLAG-IdsC$^{S38P/R186Q}$-mKate2-IdsD	Modified protein(s): TssB-sfGFP, FLAG-IdsC$^{S38P/R186Q}$, mKate2-IdsD Δ*ids::BB2000_0821-sfGFP* carrying a modified pIds plasmid with an N-terminal FLAG-tag encoded in-frame with *idsC* containing a T→C mutation at nucleotide 112 and a G→A mutation at nucleotide 557. N-terminal mKate2-fluorophore fused to *idsD*.	This study	3459	357	pMZ74
OneShot Omnimax 2 T1R Competent Cells	Cloning strain for pIds-derived plasmids	Thermo Fisher Scientific, Waltham, MA.			
S17λpir	*E. coli* mating strain to introduce plasmids into *P. mirabilis*	(9)	068		

Table A.2 Primers used in this study

Plasmid	Construction details (primers and gBlocks 5' → 3')
pIds-FLAG-IdsC	FLAG epitope (DYKDDDDK) was introduced 5' of *idsC* in pIds using Quikchange reaction protocols (Agilent Technologies, Santa Clara, CA). F: GCGAAAGCGATGAAAAAAGGAACGGCCTAATGGACTA CAAAGACGATGACGATAAACTCTTGAGTCCAAATCCCC TCTATAAAGCG R: CGCTTTATAGAGGGGATTTGGACTCAAGAGTTTATCGTCAT CGTCTTTGTAGTCCATTAGGCCGTTCCTTTTTTCATCGCTTT CGC
pIds-IdsF-FLAG	FLAG epitope (DYKDDDK) was introduced 3' of *idsF* in pIds using Quikchange reaction protocols (Agilent Technologies, Santa Clara, CA). F: GTTCAGATGGCTGTATACTCGTTGCAACAGATGACTACAAAGACG ATGACGATAAATAAGCGATACCCAATATCATGTATCATAAATAAA AAATGATA R: TATCATTTTTTATTTATGATACATGATATTGGGTATCGCTTATTTAT CGTCATCGTCTTTGTAGTCATCTGTTGCAACGAGTATACAGCCATC TGAAC
pIds-FLAG-IdsC-mKate2-IdsD	Constructed by restriction digest of pIds-mKate2-IdsD and pIds-FLAG-IdsC using BstEII/PacI.
pIds-FLAG-IdsC-mKate2-IdsD-ΔIdsE	Deletion of *idsE* in pIds-FLAG-IdsC-mKate2-IdsD using gBlock (2) and restriction digest with EcoNI/KpnI. Geneblock: GCGAACAATTAAAAATGGCAAGTGAAAAAGGTGATTGGAACCCTG AAACAGGTATATTTAAATTTAGTTTGGAAGTACAGTCTCAATTAGT AAATACATATTCTGCTTTTGGTGCACATCCTAATAGCCGTATAGGT ATTGAAGATTTATATTGGTATTATCAAGTCAATCCCGAGGTAACAA CACCGATGCGTTATATCAATTGGGGGGGAGATACCCAAGAAAACA ATCAGCTTTTAGGCTTTATTAACAGGAGAATATCTAAATCAGGAGA AAGAACACCATGCGTAGTTTGGTAAACGGCAGAAAGATTATTTTA GAAAATGATACAACAAATACCGGCGGTACCGTACTTACCGGCTCT

Table A.2 Primers used in this study (continued)

pIds-FLAG-IdsC$^{\Delta DUF4123}$	Deletion of basepairs 373 to 762 in *idsC* in pIds-FLAG-IdsC using gBlock and restriction digest with BstEII/PacI. Geneblock: GGTTACCATTAGCTGAGGATTGCCGTGCGAAAGCGATGAAAAAAG GAACGGCCTAATGGACTACAAAGACGATGACGATAAACTCTTGAG TCCAAATCCCCTCTATAAAGCGTATTGGGTTGCTCAATGCCGTTAT ACTCGCAACGGTGAACAATTCAAGGGGGTGATGACCGTAGCAGGT ACAAGTCAATCACAAGCTATTAAGCAGATGCGCCAGTACTTTACG GCTCACCCAGGTGAATATACCTTTGCGGACTATGACACATTAATCC CTTTAATCACCCATATTGAACAAAGTTCAACCTTAGAATTACCGTT AATACGGCAAGTACGTGAGCAACATAATGCAAAGGTTTCAGCCGT ATTAGTGGATAAATGCAACCTCACACACCCAAGACCGTCAGAAAA AGGCGACATTCATTACCGTGAGGGGCAACCTACGTTTATTGAATAT TCGCATTAA
pIds-FLAG-IdsC$^{\Delta DUF4123}$-mKate2-IdsD	Constructed by restriction digest of pIds-mKate2-IdsD and pIds-FLAG-IdsC$^{\Delta DUF4123}$ using BstEII/PacI.
pIds-FLAG-IdsC$^{\Delta DUF4123}$-mKate2-IdsD-ΔIdsE	Deletion of *idsE* in pIds-FLAG-IdsC$^{\Delta DUF4123}$-mKate2-IdsD using gBlock (2) and restriction digest with EcoNI/KpnI. Geneblock: GCGAACAATTAAAAATGGCAAGTGAAAAAGGTGATTGGAACCCTG AAACAGGTATATTTAAATTTAGTTTGGAAGTACAGTCTCAATTAGT AAATACATATTCTGCTTTTGGTGCACATCCTAATAGCCGTATAGGT ATTGAAGATTTATATTGGTATTATCAAGTCAATCCCGAGGTAACAA CACCGATGCGTTATATCAATTGGGGGGGAGATACCCAAGAAAACA ATCAGCTTTTAGGCTTTATTAACAGGAGAATATCTAAATCAGGAGA AAGAACACCATGCGTAGTTTGGTAAACGGCAGAAAGATTATTTTA GAAAATGATACAACAAATACCGGCGGTACCGTACTTACCGGCTCT

Table A.3 Comparison of LC-MS/MS protein hits pulled down by FLAG-IdsD in T6S abrogated strains

TssM*, $TssK_{S382N}$, $TssK_{W443C}$	
AccC	Acetyl-CoA carboxylase, biotin carboxylase subunit
AceE	Pyruvate dehydrogenase E1 component
AceF	Pyruvate dehydrogenase E2 component
AtpA	ATP synthase subunit alpha
AtpD	ATP synthase subunit beta
BB2000_2388	Sulfide:quinone oxidoreductase
DeoD	Purine-nucleoside phosphorylase
DnaK	Molecular chaperone
Eno	Enolase
FbaB	Fructose-bisphosphate aldolase
FliC1	Flagellin
FumC	Fumarate hydratase
FusA	Elongation factor G
GapA	Glyceraldehyde 3-phosphate dehydrogenase
GlpK	Glycerol kinase
GlpT	Glycerol-3-phosphate transporter
GroL	Chaperonin
Icd	Isocitrate dehydrogenase
IdsB	Type VI secretion system secreted protein VgrG
IdsC	DUF4123 protein
IdsD	Self-recognition protein (Ids locus)
IdsF	PAAR-protein
LpdA	Dihydrolipoamide dehydrogenase
MdeA	Methionine-gamma-lyase
OmpF	Outer membrane pore protein
PykF	Pyruvate kinase
RplA	Large subunit ribosomal protein L1
RplI	Large subunit ribosomal protein L9
RplJ	Large subunit ribosomal protein L10
RpoB	DNA-directed RNA polymerase subunit beta
RpoC	DNA-directed RNA polymerase subunit beta
RpsD	Small subunit ribosomal protein S4
SucA	2-oxoglutarate dehydrogenase E1 component
SucC	Succinate dehydrogenase / fumarate reductase
Tsf	Elongation factor Ts
TufB	Elongation factor Tu
Udp	Uridine phosphorylase
ZapA	Metalloprotease

Table A.3 Comparison of LC-MS/MS protein hits pulled down by FLAG-IdsD in T6S abrogated strains (continued)

TssM*, TssK$_{S382N}$	
Aas	Acyl-[acyl-carrier-protein]-phospholipid O-acyltransferase / long-chain-fatty-acid--[acyl-carrier-protein] ligase
BB2000_0144	Hypothetical protein
GlpD	Glycerol-3-phosphate dehydrogenase
GltI	Glutamate/aspartate transport system substrate-binding protein
TalB	Transaldolase
TssM*, TssK$_{W443C}$	
AspC	Aspartate aminotransferase
BB2000_1317	Hypothetical protein (DUF945 family)
BB2000_2575	Hypothetical protein (DUF3029 family)
MaeB	Malate dehydrogenase
OmpA	Outer membrane protein A
Pgk	Phosphoglycerate kinase
TktA	Transketolase
TssK$_{S382N}$, TssK$_{W443C}$	
AcnB	Aconitate hydratase 2 / 2-methylisocitrate dehydratase
AcrB	Multidrug efflux pump
AdhE	Bifunctional acetaldehyde-CoA
AhpC	Peroxiredoxin
AlaS	Alanine-tRNA ligase
AspA	Aspartate ammonia-lyase
AtpF	F-type H+-transporting ATPase subunit beta
AtpG	F-type H+-transporting ATPase subunit gamma
BB2000_0213	5'-nucleotidase
BB2000_0373	Uncharacterized protein (GenBank: Alpha-keto acid decarboxylase)
BB2000_0808	Type VI secretion protein IcmF
BB2000_0809	Type VI secretion protein VasJ
BB2000_0812	Type VI secretion protein VasG
BB2000_0820	Type VI secretion protein ImpC
BB2000_0885	Chromosome partitioning protein
BB2000_1592	Uncharacterized protein (GenBank: Surface polysaccharide modification acyltransferase)
BB2000_1824	Uncharacterized protein (GenBank: Phage protein)
BB2000_1967	Uncharacterized protein (GenBank: alpha-2-macroglobulin-like lipoprotein)
BB2000_2094	2-octaprenylphenol hydroxylase
BB2000_2967	Iron complex transport system substrate-binding protein
BB2000_3128	Uncharacterized protein (GenBanK: Glycosyltransferase)
BB2000_3210	Hypothetical protein
BudB	Acetolactate synthase I/II/III large subunit
Crp	CRP/FNR family transcriptional regulator

Table A.3 Comparison of LC-MS/MS protein hits pulled down by FLAG-IdsD in T6S abrogated strains (continued)

DegQ	Serine protease
DeoB	Phosphopentomutase
Eco	Ecotin
EmrR	MarR family transcriptional regulator, negative regulator of the multidrug operon emrRAB
Ffh	Signal recognition particle protein
GadB	Glutamate decarboxylase
GcvP	Glycine dehydrogenase
GlnA	Glutamine synthetase
GuaB	IMP dehydrogenase
IdrA	Type VI secretion system secreted protein Hcp
IdsE	Self-recognition protein (Ids locus)
IleS	Isoleucyl-tRNA synthetase
LeuS	Leucyl-tRNA synthetase
Mdh	Malate dehydrogenase
MetK	S-adenosylmethionine synthetase
MreB	Rod shape-determining protein
MukB	Chromosome partition protein
Ndk	Nucleoside-diphosphate kinase
OppA	Oligopeptide transport system substrate-binding protein
PckA	Phosphoenolpyruvate carboxykinase
PepB	PepB aminopeptidase
PepD	Dipeptidase D
PfkA	6-phosphofructokinase
PrsA	Ribose-phosphate pyrophosphokinase
Pta	Phosphate acetyltransferase
PurA	Adenylosuccinate synthase
RecA	Recombination protein RecA
RfaD	ADP-L-glycero-D-manno-heptose 6-epimerase
Rho	Transcription termination factor
RplB	Large subunit ribosomal protein L2
RplC	Large subunit ribosomal protein L3
RplD	Large subunit ribosomal protein L4
RplE	Large subunit ribosomal protein L5
RplF	Large subunit ribosomal protein L6
RplK	Large subunit ribosomal protein L11
RplM	Large subunit ribosomal protein L13
RplN	Large subunit ribosomal protein L14
RplO	Large subunit ribosomal protein L15
RplP	Large subunit ribosomal protein L16
RplQ	Large subunit ribosomal protein L17
RplT	Large subunit ribosomal protein L20

Table A.3 Comparison of LC-MS/MS protein hits pulled down by FLAG-IdsD in T6S abrogated strains (continued)

RplV	Large subunit ribosomal protein L22
RpoA	DNA-directed RNA polymerase subunit alpha
RpsA	Small subunit ribosomal protein S1
RpsB	Small subunit ribosomal protein S2
RpsC	Small subunit ribosomal protein S3
RpsE	Small subunit ribosomal protein S5
RpsG	Small subunit ribosomal protein S7
RpsI	Small subunit ribosomal protein S9
RpsJ	Small subunit ribosomal protein S10
RpsK	Small subunit ribosomal protein S11
RpsM	Small subunit ribosomal protein S13
RpsO	Small subunit ribosomal protein S15
RpsR	Small subunit ribosomal protein S18
RpsT	Small subunit ribosomal protein S20
SdhB	Succinate dehydrogenase / fumarate reductase
SecA	Preprotein translocase subunit SecA
SecD	Preprotein translocase subunit SecD
SerC	Phosphoserine aminotransferase
SfcA	Malate dehydrogenase
SucB	2-oxoglutarate dehydrogenase E2 component
SucD	Succinyl-CoA synthetase alpha subunit
Tig	Trigger factor
Upp	Uracil phosphoribosyltranferase
ZapB	Type I secretion ATP-binding protein
ZapC	Type I secretion protein
TssM*	
DadA	D-amino-acid dehydrogenase
Dld	D-lactate dehydrogenase
Gcd	Quinoprotein glucose dehydrogenase
Hns	DNA-binding protein H-NS
HupA	DNA-binding protein HU-alpha
RplL	Large subunit ribosomal protein L7/L12
SppA	Protease IV
TrxB	Thioredoxin reductase
$TssK_{S382N}$	
AccA	Acetyl-coenzyme A carboxylase carboxyl tranferase subunit alpha
AsnA	Aspartate-ammonia ligase
AsnC	Asparagine-tRNA ligase
BB2000_0157	Uncharacterized protein (GenBank: Putative ABC transporter ATP-binding protein)
BB2000_0401	Uncharacterized protein (GenBank: Lipoprotein)
BB2000_0806	Type VI secretion system protein ImpG

Table A.3 Comparison of LC-MS/MS protein hits pulled down by FLAG-IdsD in T6S abrogated strains (continued)

BB2000_0807	Type VI secretion system protein VasL
BB2000_0814	Type VI secretion system protein TssK (ImpJ)
BB2000_0924	Uncharacterized protein (GenBank: Phage protein)
BB2000_1222	Hypothetical protein
BB2000_1584	Uncharacterized protein (GenBank: Transcriptional regulator)
BB2000_1678	Putative protease
BB2000_1761	Methyl-accepting chemotaxis protein IV
BB2000_1812	Uncharacterized protein (GenBank: Phage protein)
BB2000_1823	Uncharacterized protein (GenBank: Phage protein)
BB2000_2033	Hypothetical protein
BB2000_2222	Uncharacterized protein (GenBank: Exported amino acid deaminase)
BB2000_2435	Pyrimidine/purine-5'-nucleotide nucleosidase
BB2000_2820	Uncharacterized protein (GenBank: Methyl-accepting chemotaxis protein)
BB2000_2947	Hypothetical protein
Bcp	Peroxiredoxin Q/BCP
BudC	Meso-butanediol dehydrogenase
CarB	Carbamoyl-phosphate synthase
CheB	Two-component system, chemotaxis family, protein-glutamate methylesterase/glutaminase
ClpX	ATP-dependent Clp protease ATP-binding subunit
CysK	Cysteine synthase A
DeoA	Thymidine phosphorylase
FabG	3-oxoacyl-[acyl-carrier protein] reductase
FliD	Flagellar hook-associated protein 2
FtsZ	Cell division protein
GldA	Glycerol dehydrogenase
GlmU	Bifunctional UDP-N-acetylglucosamine pyrophosphorylase
GlyA	Glycine hydroxymethyltransferase
Gnd	6-phosphogluconate dehydrogenase
GuaA	GMP synthase
GyrA	DNA gyrase subunit
HemX	Uroporphyrin-III C-methyltransferase
HflC	Membrane protease subunit HflC
HflK	Membrane protease subunit HflK
HisC	Histidinol-phosphate aminotransferase
HpmA	Hemolysin
HslU	ATP-dependent HslUV protease ATP-binding subunit
InfB	Translation initiation factor IF-2
Lrp	Lrp/AsnC family transcriptional regulator
MetQ	D-methionine transport system substrate-binding protein
MinD	Septum site-determining protein

Table A.3 Comparison of LC-MS/MS protein hits pulled down by FLAG-IdsD in T6S abrogated strains (continued)

NadE	NAD+ synthase
NqrA	Na+-transporting NADH:ubiquinone oxidoreductase subunit A
OppA	Oligopeptide transport system substrate-binding protein
PepQ	Xaa-Pro dipeptidase
PotD	Spermidine/putrescine transport system substrate-binding protein
PurB	Adenylosuccinate lyase
PutA	Bifunctional PutA protein
PykA	Pyruvate kinase
PyrD	Dihydroorotate dehydrogenase
RfaE	D-beta-D-heptose 7-phosphate kinase / D-beta-D-heptose 1-phosphate adenosyltransferase
RhlB	ATP-dependent RNA helicase
Rne	Ribonuclease
RplS	Large subunit ribosomal protein L19
RplX	Large subunit ribosomal protein L24
RpsF	Small subunit ribosomal protein S6
RpsH	Small subunit ribosomal protein S8
RpsN	Small subunit ribosomal protein S14
RpsP	Small subunit ribosomal protein S16
SdaC	Serine transporter
SecB	Preprotein translocase subunit
SerS	Seryl-tRNA synthetase
SodA	Superoxide dismutase, Fe-Mn family
SthA	NAD(P) transhydrogenase
SufB	Fe-S cluster assembly protein
SufC	Fe-S cluster assembly ATP-binding protein
SufD	Fe-S cluster assembly protein
TpiA	Triosephosphate isomerase
UspG	Universal stress protein G
UvrA	Excinuclease ABC subunit A
Zwf	Glucose-6-phosphate 1-dehydrogenase
$TssK_{W443C}$	
ArnA	UDP-4-amino-4-deoxy-L-arabinose formyltransferase / UDP-glucuronic acid dehydrogenase
ArnB	UDP-4-amino-4-deoxy-L-arabinose-oxoglutarate aminotransferase
AtpC	F-type H+-transporting ATPase subunit epsilon
AtpH	F-type H+-transporting ATPase subunit delta
BB2000_0960	Outer membrane receptor for ferrienterochelin and colicins
BB2000_2426	Hypothetical protein
BB2000_2497	SH3 domain protein
BB2000_2819	Uncharacterized protein (GenBank: Methyl-accepting chemotaxis protein)

Table A.3 Comparison of LC-MS/MS protein hits pulled down by FLAG-IdsD in T6S abrogated strains (continued)

CpdB	2',3'-cyclic-nucleotide 2'-phosphodiesterase / 3'-nucleotidase
CydA	Cytochrome bd ubiquinol oxidase subunit
DeaD	ATP-dependent RNA helicase
DnaJ	Molecular chaperone
FabI	Enoyl-[acyl-carrier protein] reductase
FadE	Acyl-CoA dehydrogenase
FbaA	Fructose-bisphosphate aldolase
FlgE	Flagellar hook protein
FtsH	Cell division protease
GltA	Citrate synthase
IdsA	Type VI secretion system secreted protein Hcp
LipA	Lipoyl synthase
Lon	Protease
MotB	Chemotaxis protein
Ndh	NADH dehydrogenase
PflB	Formate C-acetyltransferase
Pnp	Polyribonucleotide nucleotidyltransferase
PpsA	Pyruvate, water dikinase
PrlC	Oligopeptidase A
ProS	Proline-tRNA ligase
RffH	Glucose-1-phosphate thymidylyltransferase
RpsU	Small subunit ribosomal protein S21
SdhA	Succinate dehydrogenase / fumarate reductase, flavoprotein subunit
SpeA	Arginine decarboxylase
TerD	Tellurium resistance protein
YaeT	Outer membrane protein insertion porin family

Table A.4 Ids specific-LC-MS/MS protein hits secreted by FLAG-IdsC$^{\Delta DUF4123}$-mKate2-IdsD

TCA	Protein	No. unique peptides	No. total peptides	% Coverage
FLAG-C-mKate-IdsD	IdsB	10	10	21.02
	IdsD	5	6	4.84
	σ^{70}	3	3	4.85
FLAG-C$^{\Delta DUF4123}$-mKate-IdsD	IdsB	6	6	11.34
	IdsD	0	0	0
	σ^{70}	7	9	12.30

Table A.5 Comparison of LC-MS/MS protein hits secreted by FLAG-IdsC or FLAG-IdsC$^{\Delta DUF4123}$

FLAG-IdsC	
Aas	Acyl-[acyl-carrier-protein]-phospholipid O-acyltransferase / long-chain-fatty-acid--[acyl carrier-protein] ligase
AcrB	Multidrug efflux pump
AtfA	Major type 1 subunit fimbrin
BamD	Outer membrane protein assembly factor
BB2000_0153	Uncharacterized protein (GenBank: TonB-dependent receptor)
BB2000_0438	Uncharacterized protein (GenBank: Glycosyl hydrolase)
BB2000_0468	PLP dependent protein
BB2000_0495	Iron complex outermembrane recepter protein
BB2000_0808	Type VI secretion system protein IcmF
BB2000_0915	Hypothetical protein
BB2000_0951	Elongation factor P
BB2000_1825	Uncharacterized protein (GenBank: Phage protein)
BB2000_1910	Starvation-inducible DNA-binding protein
BB2000_1962	Cytoskeleton protein RodZ
BB2000_2606	Uncharacterized protein (GenBank: Fimbrial subunit)
BB2000_2670	Uncharacterized protein (GenBank: Lipoprotein)
BB2000_3109	N-acetylglucosamine kinase
BB2000_3136	Hypothetical protein
BB2000_3250	Uncharacterized protein (GenBank: Amidohydrolase/metallopeptidase)
BB2000_3426	Hypothetical protein
Bfr	Bacterioferritin
CoaD	Pantetheine-phosphate adenylyltransferase
DeoB	Phosphopentomutase
FadL	Long-chain fatty acid transport protein
FbaA	Fructose-bisphosphate aldolase
FdoG	Formate dehydrogenase major subunit
FldA	Flavodoxin I
FolB	7,8-dihydroneopterin aldolase/epimerase/oxygenase
Ggt	Gamma-glutamyltranspeptidase / glutathione hydrolase
GlmM	Phosphoglucosamine mutase
GroS	Chaperonin
HemB	Porphobilinogen synthase
HisF	Cyclase
IdrD	Self-recognition protein (Idr locus)
IdsB	Type VI secretion system secreted protein VgrG
IdsD	Self-recognition protein (Ids locus)
IhfA	Integration host factor subunit alpha
MaeB	Malate dehydrogenase
NagE	PTS system, N-acetylglucosamine-specific IIA component
NhaR	LysR family transcriptional regulator

Table A.5 Comparison of LC-MS/MS protein hits secreted by FLAG-IdsC or FLAG-IdsC$^{\Delta DUF4123}$ (continued)

RecC	Exodeoxyribonuclease V gamma subunit
Slt	Soluble lytic murein transglycosylase
SodC	Superoxide dismutase, Cu-Zn family
SpeF	Ornithine decarboxylase
UvrA	Excinuclease ABC subunit A
FLAG-IdsC$^{\Delta DUF4123}$	
AccC	Acetyl-CoA carboxylase, biotin carboxylase subunit
AnsB	L-asparaginase
ArnB	UDP-4-amino-4-deoxy-L-arabinose-oxoglutarate aminotransferase
BB2000_0117	Aminobenzoyl-glutamate utilization protein A
BB2000_0213	5'-nucleotidase
BB2000_0653	Hypothetical protein
BB2000_0707	Uncharacterized protein (GenBank: Amidohydrolase)
BB2000_0779	Ribosomal protein S12 methylthiotransferase accessory factor
BB2000_0986	TatD DNase family protein
BB2000_1098	Uncharacterized protein (GenBank: Fimbrial protein)
BB2000_1102	Uncharacterized protein (GenBank: Fimbrial protein)
BB2000_1317	Hypothetical protein (DUF945 family)
BB2000_1496	Uncharacterized protein (GenBank: Fimbrial outer membrame usher protein)
BB2000_1690	N-acetylmuramoyl-L-alanine amidase
BB2000_2040	Hypothetical protein
BB2000_2110	Small conductance mechanosensitive channel
BB2000_3430	Translocation and assembly module TamA
CutF	Copper homeostasis protein
CysP	Sulfate transport system substrate-binding protein
Def	Peptide deformylase
DeoC	Deoxyribose-phosphate aldolase
DkgA	2,5-diketo-D-gluconate reductase A
FdhF	Formate dehydrogenase
FliD	Flagellar hook-associated protein 2
GlnA	Glutamine synthetase
GltA	Citrate synthase
Gnd	6-phosphogluconate dehydrogenase
GntR	Uncharacterized protein (GenBank: GntR-family transcriptional regulator)
Gor	Glutathione reductase
GyrA	DNA gyrase subunit
HpmB	Hemolysin activation/secretion protein
IdsA	Type VI secretion system secreted protein Hcp
IspG	(E)-4-hydroxy-3-methylbut-2-enyl-diphosphate synthase
KduI	4-deoxy-L-threo-5-hexosulose-uronate ketol-isomerase

Table A.5 Comparison of LC-MS/MS protein hits secreted by FLAG-IdsC or FLAG-IdsC$^{\Delta DUF4123}$ (continued)

MetG	Methionyl-tRNA synthetase
MetQ	D-methionine transport system substrate-binding protein
MraZ	Cell division protein
NagB	Glucosamine-6-phosphate deaminase
NusA	N utilization substance protein A
OppA	Oligopeptide transport system substrate-binding protein
PepA	Leucyl aminopeptidase
Pgi	Glucose-6-phosphate isomerase
Pgm	Beta-phosphoglucomutase
PmfD	Uncharacterized protein (GenBank: Fimbrial chaperone protein)
PmfE	Uncharacterized protein (GenBank: Minor fimbrial subunit)
ProC	Pyrooline-5-carboxylate reductase
PurE	5-(carboxyamino)imidazole ribonucleotide mutase
RbsB	Ribose transport system substrate-binding protein
RplQ	Large subunit ribosomal protein L17
RpsG	Small subunit ribosomal protein S7
SitA	Manganese/iron transport system substrate-binding protein
SufI	Suppressor of FtsI
Uca	Major fimbrial subunit

Table A.6 Comparison of LC-MS/MS protein hits secreted exclusively by and pulled down with FLAG-IdsC

FLAG-IdsC	
Aas	Acyl-[acyl-carrier-protein]-phospholipid O-acyltransferase / long-chain-fatty-acid--[acyl-carrier-protein] ligase
AcrB	Multidrug efflux pump
BB2000_0808	Type VI secretion system protein IcmF
BB2000_1910	Starvation-inducible DNA-binding protein
IdrD	Self-recognition protein (Ids locus)
IdsB	Type VI secretion system secreted protein VgrG
IdsD	Self-recognition protein (Idr locus)
IhfA	Integration host factor subunit alpha

Table A.7 Comparison of LC-MS/MS protein hits from pulled down by FLAG-IdsC variants

FLAG-IdsC, FLAG-IdsC^{S38P}, FLAG-IdsC^{R186Q}, FLAG-IdsC$^{S38P/R186Q}$	
Aas	Acyl-[acyl-carrier-protein]-phospholipid O-acyltransferase / long-chain-fatty-acid--[acyl-carrier-protein] ligase
AceE	Pyruvate dehydrogenase E1 component
AceF	Pyruvate dehydrogenase E2 component
AdhE	Bifunctional acetaldehyde-CoA
AspA	Aspartate ammonia-lyase
AspC	Aspartate aminotransferase
AtpA	ATP synthase subunit alpha
AtpD	ATP synthase subunit beta
AtpF	F-type H+-transporting ATPase subunit b
BB2000_0401	Uncharacterized protein (GenBank: Lipoprotein)
BB2000_0814	Type VI secretion system protein TssK (ImpJ)
BB2000_0820	Type VI secretion system protein ImpC
BB2000_1824	Uncharacterized protein (GenBank: Phage protein)
BB2000_2967	Iron complex transport system substrate-binding protein
DeoD	Purine-nucleoside phosphorylase
DnaJ	Molecular chaperone
DnaK	Molecular chaperone
EmrR	MarR family transcriptional regulator, negative regulator of the multidrug operon emrRAB
Eno	Enolase
FliC1	Flagellin
FumC	Fumarate hydratase
FusA	Elongation factor G
GapA	Glyceraldehyde 3-phosphate dehydrogenase
GcvP	Glycine dehydrogenase
GlnA	Glutamine synthetase
GlpK	Glycerol kinase
GlpT	Glycerol-3-phosphate transporter
GroL	Chaperonin
Icd	Isocitrate dehydrogenase
IdsB	Type VI secretion system secreted protein VgrG
IdsC	DUF4123 protein
IdsD	Self-recognition protein (Ids locus)
IdsF	PAAR-protein
LpdA	Dihydrolipoamide dehydrogenase
Mdh	Malate dehydrogenase
MetQ	D-methionine transport system substrate-binding protein
OmpA	Outer membrane protein A
OmpF	Outer membrane pore protein
Pgk	Phosphoglycerate kinase

Table A.7 Comparison of LC-MS/MS protein hits from pulled down by FLAG-IdsC variants (continued)

PmfA	Uncharacterized protein (GenBank: Major Fimbrial subunit)
PykF	Pyruvate kinase
RfaD	ADP-L-glycero-D-manno-heptose 6-epimerase
RplA	Large subunit ribosomal protein L1
RplB	Large subunit ribosomal protein L2
RplD	Large subunit ribosomal protein L4
RplJ	Large subunit ribosomal protein L10
RplL	Large subunit ribosomal protein L7/L12
RplM	Large subunit ribosomal protein L13
RplQ	Large subunit ribosomal protein L17
RpoB	DNA-directed RNA polymerase subunit beta
RpoC	DNA-directed RNA polymerase subunit beta
RpsA	Small subunit ribosomal protein S1
RpsC	Small subunit ribosomal protein S3
RpsD	Small subunit ribosomal protein S4
SucA	2-oxoglutarate dehydrogenase E1 component
SucB	2-oxoglutarate dehydrogenase E2 component
SucC	Succinate dehydrogenase / fumarate reductase
Tig	Trigger factor
TufB	Elongation factor Tu
ZapA	Metalloprotease
FLAG-IdsC, FLAG-IdsC^{S38P}, FLAG-IdsC^{R186Q}	
BB2000_2820	Uncharacterized protein (GenBank: Methyl-accepting chemotaxis protein)
FLAG-IdsC, FLAG-IdsC^{S38P}, FLAG-IdsC$^{S38P/R186Q}$	
RplC	Large subunit ribosomal protein L3
FLAG-IdsC, FLAG-IdsC^{R186Q}, FLAG-IdsC$^{S38P/R186Q}$	
AccC	Acetyl-CoA carboxylase, biotin carboxylase subunit
AtpG	F-type H+-transporting ATPase subunit gamma
CpdB	2',3'-cyclic-nucleotide 2'-phosphodiesterase / 3'-nucleotidase
HflK	Membrane protease subunit HflK
MdeA	Methionine-gamma-lyase
RplI	Large subunit ribosomal protein L9
RpoA	DNA-directed RNA polymerase subunit alpha
SdhA	Succinate dehydrogenase / fumarate reductase, flavoprotein subunit
FLAG-IdsC^{S38P}, FLAG-IdsC^{R186Q}, FLAG-IdsC$^{S38P/R186Q}$	
BB2000_0213	5'-nucleotidase
BB2000_1015	Uncharacterized protein (GenBank: Lipase)
FbaB	Fructose-bisphosphate aldolase
HtpG	Molecular chaperone
FLAG-IdsC, FLAG-IdsC^{S38P}	
RpsR	Small subunit ribosomal protein S18

Table A.7 Comparison of LC-MS/MS protein hits from pulled down by FLAG-IdsC variants (continued)

Tsf	Elongation factor Ts
Udp	Uridine phosphorylase
FLAG-IdsC, FLAG-IdsC^{R186Q}	
BB2000_1317	Hypothetical protein (DUF945 family)
GltL	Glutamate/aspartate transport system ATP-binding protein
Lpp	ATP-dependent Clp protease, protease subunit
RecA	Recombination protein RecA
RplN	Large subunit ribosomal protein L14
SecD	Preprotein translocase subunit SecD
SucD	Succinyl-CoA synthetase alpha subunit
FLAG-IdsC, FLAG-IdsC$^{S38P/R186Q}$	
AcnB	Aconitate hydratase 2 / 2-methylisocitrate dehydratase
AhpC	Peroxiredoxin
BB2000_0806	Type VI secretion system protein ImpG
BudB	Acetolactate synthase I/II/III large subunit
HupA	DNA-binding protein HU-alpha
IdsE	Self-recognition protein (Ids locus)
RplV	Large subunit ribosomal protein L22
RpsE	Small subunit ribosomal protein S5
SpeA	Arginine decarboxylase
TktA	Transketolase
FLAG-IdsC^{S38P}, FLAG-IdsC^{R186Q}	
HflC	Membrane protease subunit HflC
Rne	Ribonuclease
FLAG-IdsC^{S38P}, FLAG-IdsC$^{S38P/R186Q}$	
BB2000_2575	Hypothetical protein (DUF3029 family)
MaeB	Malate dehydrogenase
FLAG-IdsC^{R186Q}, FLAG-IdsC$^{S38P/R186Q}$	
BB2000_2533	Hypothetical protein
GlpD	Glycerol-3-phosphate dehydrogenase
OppA	Oligopeptide transport system substrate-binding protein
PepB	PepB aminopeptidase
UshA	Cys-tRNA(Pro)/Cys-tRNA(Cys) deacylase
FLAG-IdsC	
AcrB	Multidrug efflux pump
Adk	Adenylate kinase
BB2000_0144	Hypothetical protein
BB2000_0463	Iron complex transport system substrate-binding protein
BB2000_0808	Type VI secretion system protein IcmF
BB2000_0809	Type VI secretion system protein VasJ
BB2000_0812	Type VI secretion system protein VasG
BB2000_0817	Type VI secretion system protein ImpH

Table A.7 Comparison of LC-MS/MS protein hits from pulled down by FLAG-IdsC variants (continued)

BB2000_0818	Type VI secretion system protein ImpG
BB2000_0821	Type VI secretion system protein TssB (ImpB)
BB2000_0885	Chromosome partitioning protein
BB2000_1369	Uncharacterized protein (GenBank: Lipoprotein)
BB2000_1483	Hypothetical protein
BB2000_1762	Methyl-accepting chemotaxis protein I, serine sensor receptor
BB2000_1910	Starvation-inducible DNA-binding protein
BB2000_2094	2-octaprenylphenol hydroxylase
BB2000_2819	Uncharacterized protein (GenBank: Methyl-accepting chemotaxis protein)
BB2000_2947	Hypothetical protein
BB2000_3107	Hypothetical protein
Bcp	Peroxiredoxin Q/BCP
Crp	CRP/FNR family transcriptional regulator
DeoC	Deoxyribose-phosphate aldolase
Dps	Starvation-inducible DNA-binding protein
FabG	3-oxoacyl-[acyl-carrier protein] reductase
FabI	Enoyl-[acyl-carrier protein] reductase
FkpA	FKBP-type peptidyl-prolyl cis-trans isomerase
Frr	Ribosome recycling factor
FtsH	Cell division protease
GpmA	2,3-bisphosphoglycerate-dependent phosphoglycerate mutase
Hfq	Host factor-I protein
HupB	DNA-binding protein HU-beta
IdrD	Self-recognition protein (Idr locus)
IhfA	Integration host factor subunit alpha
Lon	Protease
MotB	Chemotaxis protein
Ndh	NADH dehydrogenase
Ndk	Nucleoside-diphosphate kinase
OmpH	Outer membrane protein
Pal	Peptidoglycan-associated outer membrane lipoprotein
PrsA	Ribose-phosphate pyrophosphokinase
PurA	Adenylosuccinate synthase
RbsB	Ribose transport system substrate-binding protein
RplA	large subunit ribosomal protein L1
RplE	Large subunit ribosomal protein L5
RplF	Large subunit ribosomal protein L6
RplK	Large subunit ribosomal protein L11
RplO	Large subunit ribosomal protein L15
RplR	Large subunit ribosomal protein L18
RplS	Large subunit ribosomal protein L19

Table A.7 Comparison of LC-MS/MS protein hits from pulled down by FLAG-IdsC variants (continued)

RplX	Large subunit ribosomal protein L24
RpmC	Large subunit ribosomal protein L29
RpmD	Large subunit ribosomal protein L30
RpsB	Small subunit ribosomal protein S2
RpsF	Small subunit ribosomal protein S6
RpsG	Small subunit ribosomal protein S7
RpsH	Small subunit ribosomal protein S8
RpsI	Small subunit ribosomal protein S9
RpsJ	Small subunit ribosomal protein S10
RpsK	Small subunit ribosomal protein S11
RpsM	Small subunit ribosomal protein S13
RpsO	Small subunit ribosomal protein S15
RpsP	Small subunit ribosomal protein S16
RpsU	Small subunit ribosomal protein S21
SecF	Preprotein translocase subunit
SodA	Superoxide dismutase, Fe-Mn family
SspA	Stringent starvation protein A
TalB	Transaldolase
Tpx	Uncharacterized protein (GenBank: Heat shock protein HtpX)
TrxA	Thioredoxin 1
FLAG-IdsC^{S38P}	
FadE	Acyl-CoA dehydrogenase
RplT	Large subunit ribosomal protein L20
SerS	Seryl-tRNA synthetase
FLAG-IdsC^{R186Q}	
ClpB	ATP-dependent Clp protease ATP-binding subunit
FlgE	Flagellar hook protein
FliF	Flagellar M-ring protein
GlpQ	Glycerophosphoryl diester phosphodiesterase
GltA	Citrate synthase
Gnd	6-phosphogluconate dehydrogenase
HpmA	Hemolysin
KatA	Catalase
LexA	Repressor
PtsI	Phosphotransferase system, enzyme I
FLAG-IdsC$^{S38P/R186Q}$	
AtpH	F-type H+-transporting ATPase subunit delta
BB2000_1812	Uncharacterized protein (GenBank: Phage protein)
GlyA	Glycine hydroxymethyltransferase
IdrB	Type VI secretion system secreted protein VgrG
Ppx	Exopolyphosphatase / guanosine-5'-triphosphate,3'-diphosphate pyrophosphatase

Table A.7 Comparison of LC-MS/MS protein hits from pulled down by FLAG-IdsC variants (continued)

RplW	Large subunit ribosomal protein L23
SerC	phosphoserine aminotransferase

Table A.8 Comparison of LC-MS/MS protein hits secreted by FLAG-IdsC variants

FLAG-IdsC, FLAG-CS38P, FLAG-CR186Q, FLAG-IdsCS38P/R186Q	
AceE	Pyruvate dehydrogenase E1 component
AcnA	Aconitate hydratas
AcnB	Aconitate hydratase 2 / 2-methylisocitrate dehydratase
AdhE	Bifunctional acetaldehyde-CoA
AhpC	Peroxiredoxin
AlaS	Alanine-tRNA ligase
AphA	Acid phosphatase
ArtI	Fused signal recognition particle recepto
BB2000_0101	Phospholipid transport system substrate-binding protein
BB2000_0134	Hypothetical protein
BB2000_0401	Uncharacterized protein (GenBank: Lipoprotein)
BB2000_1044	Copper resistance protein C
BB2000_1179	Hypothetical protein
BB2000_1494	Uncharacterized protein (GenBank: Fimbrial subunit)
BB2000_1499	Major type 1 subunit fimbrin
BB2000_1812	Uncharacterized protein (GenBank: Phage protein)
BB2000_1846	Hypothetical protein
BB2000_1967	Uncharacterized protein (GenBank: Alpha-2-macroglobulin-like lipoprotein)
BB2000_2191	Hypothetical protein
BB2000_2350	Minor pilin subunit PapF
BB2000_2351	Minor pilin subunit PapK
BB2000_2653	Chitin-binding protein
BB2000_2827	Putative redox protein
BB2000_2847	Uncharacterized protein (GenBank: Endoribonuclease)
BB2000_2890	Glucose-1-phosphatase
BB2000_2898	Uncharacterized protein (GenBank: Lipoprotein)
BB2000_3016	Mat/Ecp fimbriae major subunit
BB2000_3426	Hypothetical protein
Bcp	Peroxiredoxin Q/BCP
ClpB	ATP-dependent Clp protease ATP-binding subunit
Crr	TetR/AcrR family transcriptional regulator
DeoD	Purine-nucleoside phosphorylase
DnaK	Molecular chaperone
Dps	Starvation-inducible DNA-binding protein
DsbA	Thiol:disulfide interchange protein
Eco	Fused signal recognition particle receptor
EmrR	MarR family transcriptional regulator, negative regulator of the multidrug operon emrRAB
Eno	Enolase
FabA	3-hydroxyacyl-[acyl-carrier protein] dehydratase / trans-2-decenoyl-[acyl-carrier protein] isomerase

Table A.8 Comparison of LC-MS/MS protein hits secreted by FLAG-IdsC variants (continued)

FabG	3-oxoacyl-[acyl-carrier protein] reductase
FabI	Enoyl-[acyl-carrier protein] reductase
FkpA	FKBP-type peptidyl-prolyl cis-trans isomerase
FliC1	Flagellin
FliD	Flagellar hook-associated protein 2
Frr	Ribosome recycling factor
FusA	Elongation factor G
GapA	Glyceraldehyde 3-phosphate dehydrogenase
GcvP	Glycine dehydrogenase
GmhA	D-sedoheptulose 7-phosphate isomerase
GroL	Chaperonin
GroS	Chaperonin
HpmA	Hemolysin
IdrA	Type VI secretion system secreted protein Hcp
IdrB	Type VI secretion system secreted protein VgrG
IdsB	Type VI secretion system secreted protein VgrG
IleS	Isoleucyl-tRNA synthetase
IreA	Outer membrane receptor for ferrienterochelin and colicins
LeuS	Leucyl-tRNA synthetase
MrcB	Penicillin-binding protein 1B
MrpA	Uncharacterized protein (GenBank: Major mannose-resistant fimbrial protein)
MrpE	Uncharacterized protein (GenBank: Fimbrial subunit)
OmpA	Outer membrane protein A
OmpF	Outer membrane pore protein
OmpH	Outer membrane protein H
OmpW	Outer membrane protein W
Pal	Peptidoglycan-associated outer membrane lipoprotein
PepN	Aminopeptidase N
PheT	Phenylalanyl-tRNA synthetase beta chain
PmfA	Uncharacterized protein (GenBank: Major fimbrial subunit)
PmfF	Uncharacterized protein (GenBank: Minor fimbrial subunit)
PmpA	Major pilin subunit
Pnp	Polyribonucleotide nucleotidyltransferase
PotD	Spermidine/putrescine transport system substrate-binding protein
Ppa	Undecaprenyl phosphate-alpha-L-ara4N flippase subunit
PpiA	Peptidyl-prolyl cis-trans isomerase A
PtrA	Protease III
PtrB	Oligopeptidase B
RpiA	Ribose 5-phosphate isomerase A
RplL	Large subunit ribosomal protein L7/L12
RplT	Large subunit ribosomal protein L20

Table A.8 Comparison of LC-MS/MS protein hits secreted by FLAG-IdsC variants (continued)

RpoB	DNA-directed RNA polymerase subunit beta
RpoC	DNA-directed RNA polymerase subunit beta
RpsG	Small subunit ribosomal protein S7
RpsM	Small subunit ribosomal protein S13
SlyB	Outer membrane lipoprotein
SodB	Superoxide dismutase, Fe-Mn family
SodC	Superoxide dismutase, Cu-Zn family
SspA	Stringent starvation protein A
SucA	2-oxoglutarate dehydrogenase E1 component
TerD	Tellurium resistance protein
TerE	Tellurium resistance protein
ThrS	Threonyl-tRNA synthetase
TktA	Transketolase
TopA	DNA topoisomerase I
Tpx	Uncharacterized protein (GenBank: Heat shock protein HtpX)
Tsf	Elongation factor Ts
UvrA	Excinuclease ABC subunit A
ValS	Valyl-tRNA synthetase
YaeT	Outer membrane protein insertion porin family
ZapA	Metalloprotease
FLAG-IdsC, FLAG-IdsC^{S38P}, FLAG-IdsC^{R186Q}	
BB2000_1717	Hypothetical protein
BB2000_1824	Uncharacterized protein (GenBank: Phage protein)
BB2000_3107	Hypothetical protein
CpdB	2',3'-cyclic-nucleotide 2'-phosphodiesterase / 3'-nucleotidase
Ggt	Gamma-glutamyltranspeptidase / glutathione hydrolase
GuaB	IMP dehydrogenase
LpdA	Dihydrolipoamide dehydrogenase
Mdh	Malate dehydrogenase
MrpC	Uncharacterized protein (GenBank: Fimbrial outer membrane usher protein)
PutA	Bifunctional PutA protein
Tex	Transcription accessory protein
FLAG-IdsC, FLAG-IdsC^{S38P}, FLAG-IdsC$^{S38P/R186Q}$	
BB2000_0271	Hypothetical protein
IdrD	Self-recognition protein (Idr locus)
RpsD	Small subunit ribosomal protein S4
RspK	Small subunit ribosomal protein S11
FLAG-IdsC, FLAG-IdsC^{R186Q}, FLAG-IdsC$^{S38P/R186Q}$	
IdsA	Type VI secretion system secreted protein Hcp
Prc	Carboxyl-terminal processing protease
RplJ	Large subunit ribosomal protein L10

Table A.8 Comparison of LC-MS/MS protein hits secreted by FLAG-IdsC variants (continued)

FLAG-IdsC^{S38P}, FLAG-IdsC^{R186Q}, FLAG-IdsC$^{S38P/R186Q}$	
AceF	Pyruvate dehydrogenase E2 component
Adk	Adenylate kinase
AspC	Aspartate aminotransferase
BB2000_0216	Hypothetical protein
BB2000_0261	Cyclic-di-GMP-binding protein
BB2000_1483	Hypothetical protein
BB2000_1693	Hypothetical protein
BB2000_2336	Uncharacterized protein (GenBank: Isochorismatase)
Bfr	Bacterioferritin
ElbB	Uncharacterized protein (GenBank: Isoprenoid biosynthesis protein with amidotransferase-like domain)
FlgK	Flagellar hook-associated protein 1
HupA	DNA-binding protein HU-alpha
MogA	Molybdopterin adenylyltransferase
Ndk	Nucleoside-diphosphate kinase
RpsA	Small subunit ribosomal protein S1
SodA	Superoxide dismutase, Fe-Mn family
FLAG-IdsC, FLAG-IdsC^{S38P}	
BB2000_1102	Uncharacterized protein (GenBank: Fimbrial protein)
BB2000_1369	Uncharacterized protein (GenBank: Lipoprotein)
OppA	Oligopeptide transport system substrate-binding protein
RplD	Large subunit ribosomal protein L4
RplI	Large subunit ribosomal protein L9
RplN	Large subunit ribosomal protein L14
RpsC	Small subunit ribosomal protein S3
RpsE	Small subunit ribosomal protein S5
RpsI	Small subunit ribosomal protein S9
FLAG-IdsC, FLAG-IdsC^{R186Q}	
Crp	CRP/FNR family transcriptional regulator
IdsD	Self-recognition protein
PflB	Formate C-acetyltransferase
PrlC	Oligopeptidase A
Pta	Phosphate acetyltransferase
PykF	Pyruvate kinase
UshA	Cys-tRNA(Pro)/Cys-tRNA(Cys) deacylase
FLAG-IdsC, FLAG-IdsC$^{S38P/R186Q}$	
FrdA	Fumarate reductase flavoprotein subunit
Lpp	ATP-dependent Clp protease, protease subunit
FLAG-IdsC^{S38P}, FLAG-IdsC^{R186Q}	
AtfA	Major type 1 subunit fimbrin
BB2000_0137	Uncharacterized protein (GenBank: Lipoprotein)

Table A.8 Comparison of LC-MS/MS protein hits secreted by FLAG-IdsC variants (continued)

BB2000_0804	Uncharacterized protein (GenBank: Metallo-beta-lactamase superfamily protein)
BB2000_1808	Hypothetical protein
BB2000_1875	Hypothetical protein
GrpE	Molecular chaperone
Gst	Glutathione S-transferase
GuaA	GMP synthase
HslV	ATP-dependent HslUV protease, peptidase subunit
NuoG	NADH-quinone oxidoreductase subunit
PmfD	Uncharacterized protein (GenBank: Fimbrial chaperone protein)
PurA	Adenylosuccinate synthase
PyrH	Uridylate kinase
Uca	2-oxoglutarate dehydrogenase E1 component
Udk	Uridine kinase
FLAG-IdsC^{S38P}, FLAG-IdsC$^{S38P/R186Q}$	
BB2000_1383	Hypothetical protein
BB2000_2108	Hypothetical protein
Def	Peptide deformylase
Lon	Protease
FLAG-IdsC^{R186Q}, FLAG-IdsC$^{S38P/R186Q}$	
BB2000_0438	Uncharacterized protein (GenBank: Glycosyl hydrolase)
FLAG-IdsC	
Acs	Acetyl-CoA synthetase
ArnA	UDP-4-amino-4-deoxy-L-arabinose formyltransferase / UDP-glucuronic acid dehydrogenase
AtpA	ATP synthase subunit alpha
AtpD	ATP synthase subunit beta
BB2000_0960	Outer membrane receptor for ferrienterochelin and colicins
BB2000_1015	Uncharacterized protein (GenBank: Lipase)
BB2000_2479	Subtilase-type serine protease
CarB	Carbamoyl-phosphate synthase
EngA	GTPase
FtsZ	Cell division protein
GyrA	DNA gyrase subunit
IdsF	PAAR-protein
MaeB	Malate dehydrogenase
MreB	Rod shape-determining protein
PpsA	Pyruvate, water dikinase
RecA	Recombination protein RecA
RplB	Large subunit ribosomal protein L2
RplE	Large subunit ribosomal protein L5
RplM	Large subunit ribosomal protein L13

Table A.8 Comparison of LC-MS/MS protein hits secreted by FLAG-IdsC variants (continued)

RplQ	Large subunit ribosomal protein L17
SecA	Preprotein translocase subunit SecA
SpeA	Arginine decarboxylase
TolB	Translocation protein
FLAG-IdsC^{S38P}	
AsnC	Asparagine-tRNA ligase
AspA	Bifunctional aspartokinase / homoserine dehydrogenase 1
BamD	Outer membrane protein assembly factor
BB2000_0093	Lipopolysaccharide export system protein LptA
BB2000_0160	Uncharacterized protein (GenBank: NTPase)
BB2000_0821	Type VI secretion system protein TssB (ImpB)
BB2000_1058	Soluble lytic murein transglycosylase
BB2000_1204	Hypothetical protein
BB2000_1497	Fimbrial chaperone protein
BB2000_1572	Hypothetical protein
BB2000_1628	Hypothetical protein
BB2000_1825	Uncharacterized protein (GenBank: Phage protein)
BB2000_2606	Uncharacterized protein (GenBank: Fimbrial subunit)
BB2000_3100	Uncharacterized protein (GenBank: Fimbrial chaperone)
Can	Monofunctional glycosyltransferase
ChrR	Chromate reductase, NAD(P)H dehydrogenase
CysS	Cysteinyl-tRNA synthetase
FolE	GTP cyclohydrolase
GreA	Transcription elongation factor
GrxA	Glutaredoxin 1
HtpG	Molecular chaperone
Icd	Isocitrate dehydrogenase
LplA	Lipoate---protein ligase
MgsA	Methylglyoxal synthase
MipA	MipA family protein
MrpD	Uncharacterized protein (GenBank: Fimbrial chaperone protein)
RlpA	Large subunit ribosomal protein L1
RlpB	Large subunit ribosomal protein L2
RpsJ	Small subunit ribosomal protein S10
TalB	Transaldolase
FLAG-IdsC^{R186Q}	
BB2000_0554	Hemoglobin/transferrin/lactoferrin receptor protein
BB2000_0586	Uncharacterized protein (GenBank: Metal resistance protein)
ClpP	ATP-dependent Clp protease, protease subunit
FumC	Fumarate hydratase
GidB	16S rRNA (guanine527-N7)-methyltransferase
PmfE	Uncharacterized protein (GenBank: Minor fimbrial subunit)

Table A.8 Comparison of LC-MS/MS protein hits secreted by FLAG-IdsC variants (continued)

PurL	Phosphoribosylformylglycinamidine synthase
SucB	2-oxoglutarate dehydrogenase E2 component
FLAG-IdsC$^{S38P/R186Q}$	
MrpB	Uncharacterized protein (GenBank: Fimbrial subunit)
RibA	GTP cyclohydrolase II
Rnr	Ribonuclease R
TrxA	Thioredoxin 1

References

1. **Gibbs KA, Urbanowski ML, Greenberg EP.** 2008. Genetic determinants of self identity and social recognition in bacteria. Science **321:**256-259.

2. **Saak CC, Gibbs KA.** 2016. The self-identity protein IdsD is communicated between cells in swarming *Proteus mirabilis* colonies. J Bacteriol **198:**3278-3286.

3. **Saak CC, Zepeda-Rivera MA, Gibbs KA.** 2017. A single point mutation in a TssB/VipA homolog disrupts sheath formation in the type VI secretion system of *Proteus mirabilis*. PLoS One **12:**e0184797.

4. **Belas R, Erskine D, Flaherty D.** 1991. Transposon mutagenesis in Proteus mirabilis. J Bacteriol **173:**6289-6293.

5. **Senior BW.** 1977. The Dienes phenomenon: identification of the determinants of compatibility. J Gen Microbiol **102:**235-244.

6. **Gibbs KA, Wenren LM, Greenberg EP.** 2011. Identity gene expression in *Proteus mirabilis*. J Bacteriol **193:**3286-3292.

7. **Wenren LM, Sullivan NL, Cardarelli L, Septer AN, Gibbs KA.** 2013. Two independent pathways for self-recognition in *Proteus mirabilis* are linked by type VI-dependent export. MBio **4**.

8. **Cardarelli L, Saak C, Gibbs KA.** 2015. Two Proteins Form a Heteromeric Bacterial Self-Recognition Complex in Which Variable Subdomains Determine Allele-Restricted Binding. MBio **6:**e00251.

9. **Simon R, Priefer U, Puhler A.** 1983. A broad host range mobilization system for *in vivo* genetic engineering- transposon mutagenesis in gram-negative bacteria. Bio-Technol **1:**784-791.

Appendix B

JB Accepted Manuscript Posted Online 19 March 2018
J. Bacteriol. doi:10.1128/JB.00688-17

A proposed chaperone of the bacterial type VI secretion system functions to constrain a self-identity protein

Martha A. Zepeda-Rivera, Christina C. Saak, and Karine A. Gibbs*

Department of Molecular and Cellular Biology, Harvard University, 16 Divinity Ave, Cambridge MA, 02138, USA

*Corresponding author:
Karine A. Gibbs, Ph.D.
Department of Molecular and Cellular Biology
Harvard University
16 Divinity Avenue
Cambridge, MA 02138
Ph: 617-496-1637 (ET)
Em: *kagibbs@mcb.harvard.edu*

Keywords: chaperone, type VI secretion (T6S), effector regulation, Ids, self-identity, self recognition, *Proteus mirabilis*, DUF4123

Abstract

The bacterium *Proteus mirabilis* can communicate identity through the secretion of the self-identity protein, IdsD, via the type VI secretion (T6S) system. IdsD secretion is essential for self versus non-self recognition behaviors in these populations. Here we provide an answer to the unresolved question of how the activity of a T6S substrate, such as IdsD, is regulated before secretion. We demonstrate that IdsD is found in clusters that form independently of the T6S machinery and activity. We show that the protein IdsC, which is a member of the proposed DUF4123 chaperone family, is essential for the maintenance of these clusters as well as the IdsD protein itself. We provide evidence that amino acid disruptions in IdsC are sufficient to disrupt IdsD secretion but not IdsD localization into subcellular clusters, strongly supporting that IdsC functions in at least two different ways: maintaining IdsD levels and secreting IdsD. We propose that IdsC, and likely other DUF4123-containing proteins, function to regulate T6S substrates in the donor cell by both maintaining protein levels and mediating secretion at the T6S machinery.

Significance Statement

Understanding the subcellular dynamics of self-identity proteins is crucial for developing models of self versus non-self recognition. We directly addressed how a bacterium restricts self-identity information before cell-cell exchange. We resolved two conflicting models for type VI secretion (T6S) substrate regulation by focusing on the self-identity protein IdsD. One model is that a cognate immunity protein binds the substrate, inhibiting pre-transport activity. Another model proposes that DUF4123-proteins act as chaperones in the donor cell, but no detailed molecular mechanism was previously known. We resolve this discrepancy and propose a model wherein a chaperone couples IdsD sequestration with its localization. Such a molecular

mechanism restricts the communication of identity, and possibly other T6S substrates, in producing cells.

Introduction

Self versus non-self recognition is a broadly observed behavior. For single-celled organisms, recognition can allow organisms of close genetic relatedness to cooperate and access benefits that individual cells could otherwise not achieve. There are many described mechanisms for these recognition behaviors, such as the exchanges of lethal proteins (1-8), of freely diffusible molecules (9-14), and of non-lethal identity proteins (15, 16). For several non-lethal mechanisms, such as in the amoeba *Dictyostelium discoideum* during spore formation (17-19) and in the bacterium *Myxococcus xanthus* during outer membrane exchange (20-23), communicating identity among sibling cells depends on cell-to-cell contact wherein binding interactions between surface-exposed proteins on neighboring cells signal the presence or absence of kin. Similarly, self recognition in the bacterium *Proteus mirabilis* depends on cell-to-cell contact while migrating on a surface, a behavior termed "swarming" (15). In contrast to *D. discoideum* and *M. xanthus*, identity in *P. mirabilis* is conveyed by the transfer of a self-identity protein, IdsD, into a neighboring cell where it interacts with its identity partner protein, IdsE (16, 24). Strain-specific variable regions, comprised of several amino acids, within IdsD and IdsE confer binding specificity. Cognate IdsD and IdsE variants bind, while non-cognate IdsD and IdsE variants do not bind (24). Intriguingly, IdsD and IdsE are co-regulated and predicted to localize to the inner membrane of *P. mirabilis* cells (24, 25), yet only the binding status of IdsD and IdsE in the recipient cell contributes to self recognition (16, 24). IdsD that is bound by IdsE allows proficient population swarming, while IdsD that is not bound results in restricted population swarming (16). Abolishing the exchange of IdsD between cells alleviates this restriction (16), indicating that IdsD and IdsE likely do not interact in the producing (donor) cell

before IdsD secretion. These findings provoked the question of how IdsD activity is regulated in the donor cell to prevent self-restriction.

IdsD secretion depends on a type VI secretion (T6S) system (26). T6S systems are multi-protein, cell-envelope spanning transport machineries found broadly among gram-negative bacteria. These T6S systems generally act as conduits through which substrates are sent from the interior of a donor cell into the interior of a recipient cell (26-32). For secretion out of the donor cell, T6S substrates often interact with components of the T6S transport machinery and associated proteins, including the proposed DUF4123-containing protein chaperones as well as VgrG- and PAAR-containing proteins (33-40). Once in the recipient cell, many of the T6S substrates, termed “effectors”, have binding partners ("immunity proteins") that neutralize the effector's activity if the donor and recipient cells are related (29, 32, 41, 42). For many of these cognate two-partner proteins, the immunity protein is predicted to also prevent effector activity in donor cells. IdsD’s interaction partners for secretion out of a donor cell are yet unknown. Given this, and that IdsD does not interact with IdsE before transport, a pressing question has been how IdsD activity is regulated in donor cells before secretion.

Here we have combined biochemical, genetic, and imaging techniques to address whether protein-protein interactions regulate IdsD before secretion. We demonstrate that a third protein, IdsC, which contains a predicted DUF4123 domain, is essential for the stabilization of IdsD into subcellular clusters in the donor cell independently of transport via T6S. Formation and localization of IdsD-containing clusters were unaffected by the absence of IdsE. We further show that strain-specific single amino acid variations across IdsC do not impact the IdsC-IdsD binding interaction or the formation of IdsD clusters but do disrupt IdsD secretion. Taken together, these data support that there are minimally two chaperone functions for IdsC: maintaining IdsD levels

and aiding in the secretion of IdsD. This predicted chaperone activity provides one explanation for why IdsD and IdsE do not bind in a single cell.

Results

IdsD subcellular localization is independent of secretion

The subcellular location of IdsD, as well as other T6S substrates in *P. mirabilis*, was previously unknown. We predicted that IdsD would localize with the T6S machinery, minimally in preparation for secretion. Therefore, we used a well-established expression system: a low-copy plasmid is used as the sole allele for *in trans* expression of all six *ids* genes (Figure SF1A) from the native *ids* promoter ($pIds_{BB}$) in *P. mirabilis* strain BB2000 lacking the chromosomal *ids* genes (Δ*ids*) (15, 16, 24, 26). We engineered a variant of this plasmid to produce an N-terminal mKate2 protein fusion to IdsD (mKate-IdsD) and an N-terminal FLAG epitope-tagged IdsC (FLAG-IdsC). This plasmid was expressed in Δ*ids*, and we confirmed that the mKate-IdsD and FLAG-IdsC fusion proteins were functional using a self recognition assay (Figure SF1B). We then inoculated this strain on swarm-permissive agar, allowed the population to grow at 37°C for four to six hours, and then imaged actively swarming cells using epifluorescence microscopy. We observed that fluorescence associated with mKate-IdsD was found as discrete foci, often near the poles, in a subset of cells (Figure 1A).

We next examined whether these IdsD-associated foci were found proximal to the T6S machinery. We used a Δ*ids*-derived strain in which the chromosomal sheath-encoding gene, *tssB*, retains a C-terminal fusion to superfolder Green Fluorescent Protein (sfGFP) (43). Briefly, T6S function occurs as follows: the contraction of a subcellular sheath comprised of TssB and TssC

proteins plunges an interior tube of Hcp protein hexamers across the cell envelope, through a core membrane complex consisting of several proteins including TssM (28, 35, 36, 44-48). The baseplate protein, TssK, links sheath assembly and the core membrane complex (49, 50). We found that in cells producing mKate-IdsD and TssB-sfGFP, 27% of the mKate-IdsD associated foci were found proximal to the fluorescence associated with TssB-sfGFP. However, the remaining 74% of IdsD-associated foci were not found proximal to any of the multiple T6S machineries within a given cell (Figure SF2). We hypothesized that the IdsD-containing foci might form independently of the T6S machinery or of active secretion.

To interrogate this hypothesis, we examined the localization of mKate-IdsD in cells in which T6S function was disrupted via distinct mechanisms. Sheath formation was abrogated using a single point mutation in the gene *tssB*; this strain (CCS05) was previously described (16, 43). The core membrane complex was impaired by disrupting the gene encoding the TssM homolog as previously described (26). Baseplate formation was disrupted using two novel independent point mutations independently introduced into the gene encoding the TssK homolog. One mutation, $TssK_{null}$, prevented sheath formation (Figure SF3) and secretion (Figure SF4). The other mutation, $TssK_{partial}$, resulted in reduced sheath formation (Figure SF3) and secretion of Hcp homologs but not of IdsD (Figure SF4). The four mutant strains impaired sheath formation and IdsD secretion to different extents (Figures SF3, SF4) (16, 26, 43). In all of these populations, mKate-IdsD-associated fluorescence was patterned as foci along the cell periphery (Figure 1B, SF5). Therefore, neither the T6S machinery nor active secretion is necessary for the subcellular localization of IdsD.

IdsD subcellular localization depends on IdsC (DUF4123) but not IdsE

One hypothesis for regulation was that IdsE is necessary for IdsD subcellular localization in donor cells. Therefore, we examined IdsD localization in cells lacking IdsE. We used the CCS05 strain background to limit observations of IdsD localization to only regulation without secretion (16, 43). We then modified the Ids expression plasmid to produce mKate-IdsD and to contain a deletion of *idsE*. We performed epifluorescence microscopy on a swarming population and observed that IdsD-associated fluorescence was in discrete foci in these cells (Figures 1C). Thus, IdsE is not necessary for the subcellular localization of IdsD.

An alternative hypothesis is that a DUF4123-containing protein regulates IdsD in donor cells. DUF4123-containing proteins have recently been shown to bind VgrG proteins and T6S substrates and are proposed chaperones of T6S systems in other bacterial species (34, 40). The gene *idsC* encodes a DUF4123-containing protein and is required for IdsD activity (15, 25, 26). Therefore, we hypothesized that the IdsC protein might be essential for the subcellular localization of IdsD. We disrupted FLAG-IdsC by deleting the DUF4123 domain on the plasmid-encoded *idsC* gene, resulting in FLAG-*idsC*$^{\Delta DUF}$. In cells producing the protein FLAG-IdsC$^{\Delta DUF}$, we observed that the mKate-IdsD-associated fluorescence was diffuse across the cell interior with few to no foci visible (Figure 1D). To control for the possibility that dispersed fluorescence was due to cleavage of mKate2 from IdsD, we performed western blot analysis on whole cell extracts from the strains producing either FLAG-IdsC$^{\Delta DUF}$ or FLAG-IdsC strains. A band corresponding to the mKate-IdsD fusion was readily apparent; bands corresponding to mKate2 or IdsD alone were minimal (Figure 2A). We concluded that cleavage of mKate-IdsD did not explain the dispersed fluorescence, and as such, IdsC is necessary for the presence of the mKate-IdsD foci.

163 In the course of our studies, we observed that the mKate-IdsD-associated fluorescence
164 appeared dimmer in the strain producing FLAG-IdsC$^{\Delta DUF}$. As the N-terminal fusion of mKate2
165 was readily observed, we deduced that it might mask potential effects of the FLAG-IdsC$^{\Delta DUF}$
166 mutation by stabilizing IdsD, perhaps by occluding a degradation signal. Therefore, we
167 examined the relative levels of unlabeled IdsD in the presence and absence of IdsC. We
168 performed western blots on cell extracts of Δids strains carrying previously characterized
169 mutations of the pIds$_{BB}$ plasmid (15). We marked the cell extracts based on which proteins are
170 missing. We found that unlabeled IdsD was lower or absent in strains completely lacking IdsC or
171 IdsD and was readily apparent in strains lacking only IdsB (VgrG homolog) or IdsF (PAAR
172 motif) (Figure 2B). While some IdsD was present in a strain lacking IdsA, IdsB, and IdsC, this
173 was likely due to a higher production of IdsD, IdsE, and IdsF; in this construct, the *idsD, idsE,*
174 and *IdsF* genes are in closer proximity to the *ids* promoter than normal. We concluded that IdsD
175 protein levels are reduced in the absence of IdsC. Therefore, IdsC contributes to the subcellular
176 localization and protein levels of IdsD.
177
178 *The IdsC-IdsD interaction is essential for IdsD secretion*
179 Give these results, we hypothesized that IdsC (Figure 3A) and IdsD likely interact with
180 each other. IdsC and IdsD interactions were examined in *E. coli* strain BL21(DE3) pLysS where
181 no Ids or T6S proteins are otherwise found (51). IdsD was fused to a His$_6$ epitope tag (IdsD-His$_6$)
182 (24), and IdsC was fused to a FLAG epitope tag (IdsC-FLAG). Each epitope-tagged protein was
183 separately produced from an overexpression plasmid (52) in the *E. coli* strain. Cell extracts were
184 isolated, mixed, and subjected to anti-FLAG co-immunoprecipitation assays followed by western
185 blot analysis. IdsC-FLAG pulled down IdsD-His$_6$ (Figure 3B). The negative control, FLAG-

BAP, which is *E. coli* bacterial alkaline phosphatase fused to an N-terminal FLAG epitope, did not pull down IdsD-His_6 (Figure 3B). These results indicated that IdsC and IdsD bind each other independently of other Ids and T6S proteins.

As the molecular function of the major domain within IdsC remains unknown, we considered whether the DUF4123 domain (Figure 3A) is essential for IdsC-IdsD interactions. A derivative of IdsC-FLAG without the DUF4123 domain ($IdsC^{\Delta DUF}$-FLAG) was constructed, produced in *E. coli*, and then subjected to co-immunoprecipitation assays as above. Considerably less IdsD-His_6 was detected in the pull-down with $IdsC^{\Delta DUF}$-FLAG than with IdsC-FLAG (Figure 3B). Therefore, the DUF4123 domain is essential for the binding interaction between IdsC and IdsD.

We reasoned that as IdsC was essential for the subcellular localization of IdsD (Figure 1D) and for IdsD recognition activity (15), then an interaction with IdsC was likely required for IdsD transport itself. This hypothesis was strengthened by evidence that DUF4123-containing proteins are essential for binding of VgrG proteins and for secretion of T6S substrates in other bacteria (34, 39, 40). To quantify the contribution of IdsC-IdsD binding for secretion, we assessed Δ*ids* strains producing either full-length FLAG-IdsC or FLAG-$IdsC^{\Delta DUF}$. The resultant strains were subjected to an established *in vivo* recognition assay. In this assay, secretion of IdsD into neighboring cells that lack IdsE results in a small colony radius. This restriction on colony migration is alleviated upon disruption of IdsD secretion (16). A Δ*ids* strain lacking IdsE and producing FLAG-IdsC displayed a small colony radius (Figure 3C), indicating successful exchange of IdsD (16). By contrast, a Δ*ids* strain lacking IdsE and producing FLAG-$IdsC^{\Delta DUF}$ displayed a large colony radius similar to strains lacking T6S activity (Figure 3C). Abolishing T6S activity in the strain expressing FLAG-$IdsC^{\Delta DUF}$ displayed no synergistic effects (Figure

3C). However, the decreased secretion could be due to a reduction in the subcellular concentration of IdsD, because IdsD levels are reduced in cells lacking IdsC. Given that the mKate-IdsD fusion appears to be present at roughly equivalent levels across the strains (Figure 2A), we repeated these assays in strains lacking IdsE and producing mKate-IdsD and either FLAG-IdsC or FLAG-IdsC$^{\Delta DUF}$. Similar results were obtained as with unlabeled IdsD (Figure SF6). As a complementary approach, we utilized an established *in vitro* secretion assay. The extracellular supernatants of liquid-grown Δ*ids* strains producing either FLAG-IdsC or FLAG-IdsC$^{\Delta DUF}$ were concentrated using trichloroacetic acid precipitations and examined by liquid chromatography tandem mass spectrometry. IdsD is detected in the supernatant of wild-type *P. mirabilis*, but is absent in supernatants of strains lacking T6S function (26, 43). We identified peptides for IdsD in the extracellular extract for the strain producing FLAG-IdsC (Figure 3D) but not in that of the strain producing FLAG-IdsC$^{\Delta DUF}$ (Figure 3D). Thus, IdsC is essential for IdsD secretion.

IdsC binding to and localization of IdsD is uncoupled from IdsD secretion

Comparison of the full-length IdsC sequence from the *P. mirabilis* strain background used in this study, BB2000, and a strain recognized as non-self, HI4320, showed a uniform length of 407 amino acids with only five single amino acid polymorphisms (99% pairwise identity) (Figure SF7). Comparing the BB2000 IdsC to the HI4320 IdsC, these amino acids are a serine to proline change at position 38 (S38P), a threonine to methionine change at position 121 (T121M), an arginine to glutamine change at position 186 (R186Q), alanine to valine at position 258 (A258V) and a methionine to leucine at position 309 (M309L). We hypothesized that these

IdsC residues might be important for the binding and secretion of IdsD, which in itself contains a strain-specific variable region essential for its binding to its self-recognition partner IdsE.

We focused on the S38P and R186Q polymorphisms. Lysates from T6S-functional BB2000-derived strains producing either FLAG-IdsC or a mutant variant, FLAG-IdsC$^{S38P/R186Q}$, were subjected to anti-FLAG co-immunoprecipitation assays. The load (L), non-binding (-), and binding (+) fractions were subjected to western blot analysis to test for interactions with IdsB (VgrG), IdsD, and IdsE. Both FLAG-IdsC and FLAG-IdsC$^{S38P/R186Q}$ pulled down IdsB and IdsD (Figure 4A). IdsE was largely absent from elutions with FLAG-IdsC; however, there was evidence of IdsE in elutions with the FLAG-IdsC$^{S38P/R186Q}$ mutant (Figure 4A). The trace amounts of IdsE pulled down by FLAG-IdsC$^{S38P/R186Q}$ are likely due to indirect interactions between IdsC and IdsE mediated by IdsD during *in vitro* reassortment. The FLAG-IdsC and FLAG-IdsC$^{S38P/R186Q}$ constructs were next separately moved into strain CCS05 expressing mKate-IdsD. Using epifluorescence microscopy, we observed that mKate-IdsD-associated fluorescence was localized into foci in both strains (Figure 4B). Therefore, FLAG-IdsC$^{S38P/R186Q}$ binds IdsD and supports IdsD cluster formation.

In light of these results, we predicted that FLAG-IdsC$^{S38P/R186Q}$ would support IdsD secretion. We subjected T6S-functional BB2000-derived strains lacking IdsE producing either FLAG-IdsC or FLAG-IdsC$^{S38P/R186Q}$ to the *in vivo* recognition assays as described above. Surprisingly, populations of cells producing FLAG-IdsC$^{S38P/R186Q}$ exhibited an increased colony radius with and without T6S activity (Figure 4C), indicating that IdsD was not exchanged between neighboring cells. We used trichloroacetic acid precipitations of the supernatants from liquid-grown cells T6S+ to confirm these results. We found that both IdsB and IdsD were detected in the extracellular extract for the strain producing FLAG-IdsC (Figure 4D). However,

255 while IdsB was readily detected, peptides for IdsD were lower for the strain producing FLAG-
256 IdsC$^{S38P/R186Q}$ (Figure 4D). These results indicated that IdsC binding of IdsD was uncoupled from
257 IdsD secretion. Further, T6S secretion of IdsB was not affected by the two amino acid changes,
258 but the specific secretion of IdsD was abrogated, strongly supporting that IdsC functions to both
259 bind and sequester IdsD into subcellular clusters and to separately mediate IdsD secretion via the
260 T6S machinery.

261 The results indicated that IdsC acts within the donor cell. If IdsC acts an immunity
262 protein, then one would predict that excess IdsC in the "correct" compartment would be
263 sufficient to bind and neutralize activities due to IdsD. However, it is unknown into which
264 cellular compartment IdsD is transported. Therefore, we tested expression of both periplasmic
265 and cytoplasmic IdsC in receiving cells. To test periplasmic expression of IdsC, we constructed
266 two distinct CCS05-derived strains carrying a modified pIds$_{BB}$ plasmid in which *idsE* is deleted
267 and FLAG-IdsC has been modified to include a signal sequence for targeting to the periplasm,
268 either that of PelB (53) or OmpA (54). Each strain was tested for self-recognition phenotypes
269 against strains BB2000 and Δ*ids*. If periplasmic FLAG-IdsC is sufficient to bind and neutralize
270 transferred IdsD, then these strains should recognize BB2000 as self and the colonies would
271 merge. However, we observed was that swarm colonies of strains producing FLAG-IdsC with
272 either the PelB or the OmpA signal sequence did not merge with BB2000 (Figure 5). To test
273 cytoplasmic expression of IdsC, we constructed an inducible plasmid to increase expression of
274 FLAG-IdsC in either strain BB2000 or BB2000::Δ*idsE*, which encodes a chromosomal deletion
275 of *idsE*. BB2000::Δ*idsE* shows decreased swarm expansion as compared to BB2000 (Figure 5).
276 If cytoplasmic IdsC is able to bind and neutralize transferred IdsD, then BB2000::*ΔidsE* should
277 exhibit wild-type swarm expansion as the concentration of inducer increases. However, the

278 BB2000::Δ*idsE* swarm colonies did not show restored swarm-expansion at any tested
279 concentration of inducer (Figure 5). These results support that IdsC does not bind IdsD received
280 from neighboring cells, and instead, works within the donor cell.
281
282 Discussion
283 Altogether, these results lead us to propose a model wherein IdsC, a DUF4123-containing
284 protein, binds and maintains IdsD protein levels in a producing cell, independently of secretion
285 (Figure 6). A chaperone-like function for DUF4123-containing proteins encoded next to T6S
286 effectors was recently proposed based on interactions partners and transport efficiencies (39, 40).
287 Our data solidifies this proposed role for DUF4123-containing proteins. We have also
288 meaningfully expanded this proposal by specifically defining a mechanistic model (Figure 5) in
289 which IdsC, a DUF4123-containing protein, binds and stabilizes the T6S substrate, IdsD,
290 independently of transport. We have shown that in addition to the essentiality of IdsC for IdsD
291 transport, IdsC functions in the subcellular localization of IdsD and maintenance of IdsD protein
292 levels.
293 The molecular mechanism by which IdsC delivers IdsD for secretion still remains to be
294 tackled and will likely need to be informed by tertiary structures, none of which are currently
295 available. We hypothesize that within a single cell, IdsD likely binds to IdsB (VgrG) and
296 associates with the T6S membrane-bound complex. We predict that IdsC might protect the
297 transmembrane domains of IdsD from spurious insertion into the donor cell's inner membrane
298 when IdsD is not docked in the T6S machinery. Such a mechanism has been proposed for other
299 T6S substrates (55). We further hypothesize that since IdsC binds IdsB, it might actually directly
300 hand IdsD over to IdsB and/or the T6S proteins when the IdsC-IdsD complex is localized at the

T6S machinery. In such a case, the amino acid changes we introduced in IdsC might alter interactions of IdsC-IdsD with proteins of the core T6S machinery. Alternatively, perhaps these amino acids affect IdsC-IdsD binding efficiency, impeding the hand-off to the T6S machinery.

Indeed, many organisms face the challenge of inhibiting T6S substrates from acting in the producing cell. The mechanism elucidated here would allow IdsC to prevent IdsD from interacting with its identity partner protein, IdsE, in the donor cell. We propose that both subcellular localization and transport through the T6S machinery function intrinsically to prevent substrate activity within the donor cell and that DUF4123-containing proteins are essential for directing this subcellular regulation. Of note, this proposed mechanism for effector regulation is distinct from previously described models in which binding of a cognate strain-specific protein is thought to prevent a T6S substrate from acting in the donor cell (29, 32, 41, 42). We surmise that a DUF4123-mediated sequestration might be generally applicable given the high conservation of IdsC between *P. mirabilis* strains.

This proposed mechanism for IdsC function is reminiscent of chaperone activities in other bacterial transport systems; and yet, several questions remain. Clusters of IdsD are present regardless of the transport machinery, raising the possibility that IdsC might gather IdsD into clusters when IdsD is not actively transported. These IdsD clusters could be for future delivery or alternatively, for sequestration of excess IdsD; such mechanisms require further study. The nucleation of these IdsC-IdsD complexes into clusters may be due to interactions between IdsD monomers or perhaps due to a yet unknown third protein factor. Interactions with the VgrG, PAAR-protein, or one or more of these factors, may help anchor IdsD to the membrane. DUF4123-domain proteins are commonly found upstream of T6S substrates even though the sequences for the predicted substrates are quite divergent (39). For the DUF4123-containing

proteins studied thus far, the DUF4123-domain proteins appear specific for the T6S substrate encoded immediately downstream (34, 39, 40). Naturally occurring amino acid variations within IdsC alleles did not prevent the binding and subcellular clustering of IdsD before transport, but did impact its secretion. These results highlight that regulation of T6S substrates before transport might be separate from their loading onto, or transport via, the T6S machinery. Further, DUF4123-containing proteins might be intermediaries between resting and actively transported substrates. Given that such mechanical aspects are yet unknown, further structural studies dissecting the role of individual amino acid residues within IdsC for binding and secretion of IdsD are required. More generally, further studies are required to determine whether a specific feature within the DUF4123 domain may be the critical marker for association with a specific T6S substrate and how specificity of substrate binding is obtained.

In conclusion, this research has also provided crucial insights into the communication of self-identity within a population. Prior research left us with the perplexing conclusion that IdsD only acts in recipient cells (15, 16, 24). Here we propose a simple model for the lack of IdsD activity within the donor cell: IdsC appears to couple IdsD sequestration with its localization. We posit that IdsD might exist in two conformations with distinct functions: in a complex including IdsC in the donor cell and in a self-identity complex with IdsE in the recipient cell (16, 24). Such a molecular mechanism (Figure 6) would restrict the communication of self-identity to occur between neighboring cells.

345 Materials and Methods

346 *Bacterial strains and media*

347 Strains are described in Table 1. For single isolated colonies, *E. coli* strains were
348 maintained on LB agar, and *P. mirabilis* strains were maintained on LSW- agar (56). *P. mirabilis*
349 was grown on CM55 Blood Agar Base agar (Oxoid, Basingstoke, England) for swarm assays.
350 For broth cultures, all strains were grown in LB broth under aerobic conditions at 16°C, 30°C, or
351 37°C. Antibiotics were used at the following concentrations: 100 microgram/milliliter (µg/mL)
352 carbenicillin, 15 µg/mL tetracycline, 35 µg/mL kanamycin, 50 µg/mL chloramphenicol, and 25
353 µg/mL streptomycin.

354

355 *Strain construction*

356 All chromosomal mutations in BB2000 and Δ*ids* were made as described in (16) using
357 pKNG101-derived suicide vectors (57). The $tssK_{null}$ strain introduced a $BB2000\_0814_{G1329T}$
358 mutation using plasmid pCS33a. The $tssK_{partial}$ strain introduced a $BB2000\_0814_{G1145A}$ mutation
359 using plasmid pCS33b. *BB2000_0814* (GenBank accession no. AGS59310.1) is a gene encoding
360 a TssK homolog (T6SS_VasE PFAM family PF05936). Mutations in the Δ*ids* background were
361 confirmed via whole genome sequencing by the Bauer Core Facility at Harvard University using
362 the protocol described in (16). Mutations into the BB2000 background were confirmed by
363 Polymerase Chain Reaction (PCR) amplification of *BB2000_0814* (primers: 5'-
364 CTCTCCGGCAATAATACGTAG-3' and 5'- CAGACCCACTACAGGCTTTAG-3') followed
365 by Sanger sequencing performed by GENEWIZ, Inc. (South Plainfield, NJ).

366

367 *Plasmid construction*

368 Detailed primers and plasmids are listed in Supplemental Table S1. Restriction digest and
369 subsequent ligation of gBlock gene fragments (Integrated DNA Technologies, Coralville, IA)
370 were used for cloning of both $pIds_{BB}$-derived (15) and pAD_{100}-derived (52) vectors. gBlock gene
371 fragments were first subcloned into TOPO pCR2.1 vector using the TOPO TA-Cloning Kit
372 (Thermo Fisher Scientific, Waltham, MA). All methods were performed according to
373 manufacturers' instructions. The FLAG epitope is DYKDDDDK and was introduced using
374 Quikchange reaction protocols (Agilent Technologies, Santa Clara, CA). The $pIds_{BB}$-derived
375 plasmids were constructed via restriction digest using listed restriction enzymes (New England
376 BioLabs, Ipswich, MA). Ligations were resolved in OneShot Omnimax2 T1R competent cells
377 (Thermo Fisher Scientific, Waltham, MA). Resultant plasmids were confirmed by Sanger
378 sequencing (Genewiz, Inc., South Plainfield, NJ), and correct resultant plasmids were then
379 transformed into *P. mirabilis* as described (15). All *P. mirabilis* constructs were tested for
380 functionality using a standard boundary formation assay (58). Ligations for plasmids derived
381 from pAD_{100} (52) were resolved in XL10-Gold Ultracompetent cells (Agilent Technologies,
382 Santa Clara, CA). Correct resultant plasmids were transformed into BL21(DE3) pLysS (Thermo
383 Fisher Scientific, Waltham, MA). A flexible linker (GSAGSAAGSGEF, (59)) is present between
384 the mKate2 sequence and IdsD. All vectors were confirmed by sequencing with site-specific
385 primers using the services of GENEWIZ, Inc. (South Plainfield, NJ).
386
387 *α-FLAG immunoprecipitation assays*
388 Assays were performed and analyzed as previously described (24). Modifications to those
389 protocols are as follows. *P. mirabilis* cells were harvested from swarm-permissive media after
390 incubation at 37°C for 16 - 20 hours. Control lysate (containing $pIds_{BB}$ with no FLAG-tagged

protein) was supplemented with 2 µg of purified FLAG-BAP protein (Sigma-Aldrich, St. Louis, MO). *E. coli* BL21 (DE3) pLysS cells (Thermo Fisher Scientific, Waltham, MA) were grown in 25 mL of LB supplemented with carbenicillin under shaking conditions at 30°C until optical density at 600 nm (OD_{600}) was between 0.6 and 1. Cultures were cooled on ice, induced with 1 mM IPTG, and incubated overnight shaking at 16°C. Cells were harvested by centrifugation and stored at -80°C. Lysates were mixed to a total volume of 1 mL of which 900 µL was applied to 40 µL pre-equilibrated α-FLAG M2 antibody resin (Sigma-Aldrich, St. Louis, MO; Biotools, Houston, TX). *P. mirabilis* and *E. coli* extracts were obtained separately as described above. Lysates were mixed to a total volume of 1 mL of which 900 µL was applied to 40 µL pre-equilibrated α-FLAG M2 antibody resin (Sigma-Aldrich, St. Louis, MO; Biotools, Houston, TX).

Antibody production

Antibodies specific to IdsB amino acids 713-723 (CRAKAMKKGTA), IdsD amino acids 4-18 (EVNEKYLTPQERKAR) (24), and IdsE amino acids 298-312 (EQILAKLDQEKEHHA) (24) were raised in rabbits using standard peptide protocols (Covance, Dedham, MA).

SDS-PAGE and western blots

Assays were performed and analyzed as previously described (24). Polyclonal primary antibody dilutions were rabbit α-IdsB (1:5000), rabbit α-IdsD (1:2000), rabbit α-IdsE (1:2000) and rabbit α-mKate (1:4000, OriGene, Rockville, MD). Monoclonal primary antibody dilutions were rabbit α-FLAG (1:4000, Sigma-Aldrich, St. Louis, MO) and mouse α-σ^{70} (1:1000, Thermo Fisher Scientific, Waltham, MA or BioLegend, San Diego, CA). Secondary antibodies were goat

α-rabbit or goat α-mouse antibodies conjugated to HRP (polyclonal, 1:5000, SeraCare Life Sciences, Milford, MA). The western blots are not quantitative.

Trichloroacetic acid precipitations (TCA) and liquid-chromatography tandem mass spectrometry analysis (LC-MS/MS)

All trichloroacetic acid precipitations were performed as previously described (26). Binding fractions from α-FLAG immunoprecipitations or supernatant fractions from TCA were separated by gel electrophoresis using 12% Tris-Tricine polyacrylamide gels and stained with Coomassie blue as previously described (16, 26). Supernatant fractions from TCA were cut into two bands at 75-150 kDa and 10-25 kDa. LC-MS/MS was performed by the Taplin Mass Spectrometry Facility (Harvard Medical School, Boston, MA). Technical advice provided by the Taplin Mass Spectrometry Facility led to a cutoff of three unique peptides to confirm protein hits. Bioinformatics analysis of Ids and T6S protein hits was done using Pfam 31.0 (60). Full data sets can be accessed at *<https://osf.io/ufphy/?view_only=d381570c43d14bc5acd38b071ed9a61e>*

Colony expansion

Colony expansion assays were conducted as previously described (16). Modifications to those protocols are as follows. Swarming-permissive plates supplemented with kanamycin were inoculated with 1 μL of overnight cultures normalized by OD_{600}. Plates were incubated at 37° for 17 hours and swarming radii recorded. For strains carrying anhydrotetraclycine-inducible plasmids, swarming-permissive plates were supplemented with anhydrotetraclycine and kanamycin and were kept under dark conditions to preserve inducer.

Microscopy

Strains were grown overnight shaking in LB supplemented with kanamycin at 37°. 1.0 mm-thick agar pads of swarming permissive media supplemented with kanamycin were inoculated with 2 µL of overnight cultures and incubated in a humidified chamber at 37° for 4 to 6 hours. Images were acquired either with a Leica DM5500B (Leica Microsystems, Buffalo Grove, IL) with a CoolSnap HQ^2 cooled CCD camera (Photometrics, Tucson, AZ) or an Olympus BX61 (Olympus Corporation, Waltham, MA) with a Hamamatsu C10600-10B CCD camera (Hamamtsu Phototonics K.K., Boston, MA). MetaMorph version 7.8.0.0 (Molecular Devices, Sunnyvale, CA) was used for image acquisition. All images were collected with the same exposure times unless otherwise stated: 10 millisecond (ms) for phase, 150 ms for RFP, and 50 ms for GFP. Figures were made in Fiji (61, 62) and Adobe Illustrator (Adobe Systems, San Jose, CA).

Author Contributions

M.Z.R, C.C.S, and K.A.G designed experiments; M.Z.R and C.C.S conducted experiments; M.Z.R, C.C.S and K.A.G wrote and edited manuscript.

Acknowledgements

We thank Lia Cardarelli and Achala Chittor for contributing experimental materials to this project, as well as members of the Gibbs, Losick, and Gaudet laboratories for thoughtful advice on the project and manuscript. This research was funded by a Howard Hughes Medical Institute

460 Gilliam Fellowship (M.Z.R.) and by Harvard University, the George W. Merck fund, and the
461 David and Lucile Packard Foundation.

References

1. **Aoki SK, Pamma R, Hernday AD, Bickham JE, Braaten BA, Low DA.** 2005. Contact-dependent inhibition of growth in *Escherichia coli*. Science **309:**1245-1248.
2. **Baud C, Guerin J, Petit E, Lesne E, Dupre E, Locht C, Jacob-Dubuisson F.** 2014. Translocation path of a substrate protein through its Omp85 transporter. Nat Commun **5:**5271.
3. **Aoki SK, Diner EJ, de Roodenbeke CT, Burgess BR, Poole SJ, Braaten BA, Jones AM, Webb JS, Hayes CS, Cotter PA, Low DA.** 2010. A widespread family of polymorphic contact-dependent toxin delivery systems in bacteria. Nature **468:**439-442.
4. **Morse RP, Nikolakakis KC, Willett JL, Gerrick E, Low DA, Hayes CS, Goulding CW.** 2012. Structural basis of toxicity and immunity in contact-dependent growth inhibition (CDI) systems. Proc Natl Acad Sci U S A **109:**21480-21485.
5. **Lin RJ, Capage M, Hill CW.** 1984. A repetitive DNA sequence, rhs, responsible for duplications within the *Escherichia coli* K-12 chromosome. J Mol Biol **177:**1-18.
6. **Hill CW, Sandt CH, Vlazny DA.** 1994. Rhs elements of *Escherichia coli*: a family of genetic composites each encoding a large mosaic protein. Mol Microbiol **12:**865-871.
7. **Poole SJ, Diner EJ, Aoki SK, Braaten BA, t'Kint de Roodenbeke C, Low DA, Hayes CS.** 2011. Identification of functional toxin/immunity genes linked to contact-dependent growth inhibition (CDI) and rearrangement hotspot (Rhs) systems. PLoS Genet **7:**e1002217.
8. **Koskiniemi S, Lamoureux JG, Nikolakakis KC, t'Kint de Roodenbeke C, Kaplan MD, Low DA, Hayes CS.** 2013. Rhs proteins from diverse bacteria mediate intercellular competition. Proc Natl Acad Sci U S A **110:**7032-7037.

9. **Engebrecht J, Nealson K, Silverman M.** 1983. Bacterial bioluminescence: isolation and genetic analysis of functions from *Vibrio fischeri*. Cell **32:**773-781.

10. **Engebrecht J, Silverman M.** 1984. Identification of genes and gene products necessary for bacterial bioluminescence. Proc Natl Acad Sci U S A **81:**4154-4158.

11. **Nealson KH, Hastings JW.** 1979. Bacterial bioluminescence: its control and ecological significance. Microbiol Rev **43:**496-518.

12. **Eberhard A, Burlingame AL, Eberhard C, Kenyon GL, Nealson KH, Oppenheimer NJ.** 1981. Structural identification of autoinducer of *Photobacterium fischeri* luciferase. Biochemistry **20:**2444-2449.

13. **Kaplan HB, Greenberg EP.** 1985. Diffusion of autoinducer is involved in regulation of the *Vibrio fischeri* luminescence system. J Bacteriol **163:**1210-1214.

14. **Stevens AM, Dolan KM, Greenberg EP.** 1994. Synergistic binding of the *Vibrio fischeri* LuxR transcriptional activator domain and RNA polymerase to the lux promoter region. Proc Natl Acad Sci U S A **91:**12619-12623.

15. **Gibbs KA, Urbanowski ML, Greenberg EP.** 2008. Genetic determinants of self identity and social recognition in bacteria. Science **321:**256-259.

16. **Saak CC, Gibbs KA.** 2016. The self-identity protein IdsD is communicated between cells in swarming *Proteus mirabilis* colonies. J Bacteriol **198:**3278-3286.

17. **Hirose S, Benabentos R, Ho HI, Kuspa A, Shaulsky G.** 2011. Self-recognition in social amoebae is mediated by allelic pairs of tiger genes. Science **333:**467-470.

18. **Benabentos R, Hirose S, Sucgang R, Curk T, Katoh M, Ostrowski EA, Strassmann JE, Queller DC, Zupan B, Shaulsky G, Kuspa A.** 2009. Polymorphic members of the lag gene family mediate kin discrimination in *Dictyostelium*. Curr Biol **19:**567-572.

19. **Hirose S, Santhanam B, Katoh-Kurosawa M, Shaulsky G, Kuspa A.** 2015. Allorecognition, via TgrB1 and TgrC1, mediates the transition from unicellularity to multicellularity in the social amoeba *Dictyostelium discoideum*. Development **142:**3561-3570.

20. **Ducret A, Fleuchot B, Bergam P, Mignot T.** 2013. Direct live imaging of cell-cell protein transfer by transient outer membrane fusion in *Myxococcus xanthus*. Elife **2:**e00868.

21. **Nudleman E, Wall D, Kaiser D.** 2005. Cell-to-cell transfer of bacterial outer membrane lipoproteins. Science **309:**125-127.

22. **Pathak DT, Wei X, Bucuvalas A, Haft DH, Gerloff DL, Wall D.** 2012. Cell contact-dependent outer membrane exchange in myxobacteria: genetic determinants and mechanism. PLoS Genet **8:**e1002626.

23. **Pathak DT, Wei X, Dey A, Wall D.** 2013. Molecular recognition by a polymorphic cell surface receptor governs cooperative behaviors in bacteria. PLoS Genet **9:**e1003891.

24. **Cardarelli L, Saak C, Gibbs KA.** 2015. Two Proteins Form a Heteromeric Bacterial Self-Recognition Complex in Which Variable Subdomains Determine Allele-Restricted Binding. MBio **6:**e00251.

25. **Gibbs KA, Wenren LM, Greenberg EP.** 2011. Identity gene expression in *Proteus mirabilis*. J Bacteriol **193:**3286-3292.

26. **Wenren LM, Sullivan NL, Cardarelli L, Septer AN, Gibbs KA.** 2013. Two independent pathways for self-recognition in *Proteus mirabilis* are linked by type VI-dependent export. MBio **4**.

27. **Basler M, Ho BT, Mekalanos JJ.** 2013. Tit-for-tat: type VI secretion system counterattack during bacterial cell-cell interactions. Cell **152:**884-894.

28. **Basler M, Mekalanos JJ.** 2012. Type 6 secretion dynamics within and between bacterial cells. Science **337:**815.

29. **Hood RD, Singh P, Hsu F, Guvener T, Carl MA, Trinidad RR, Silverman JM, Ohlson BB, Hicks KG, Plemel RL, Li M, Schwarz S, Wang WY, Merz AJ, Goodlett DR, Mougous JD.** 2010. A type VI secretion system of *Pseudomonas aeruginosa* targets a toxin to bacteria. Cell Host Microbe **7:**25-37.

30. **Mougous JD, Cuff ME, Raunser S, Shen A, Zhou M, Gifford CA, Goodman AL, Joachimiak G, Ordonez CL, Lory S, Walz T, Joachimiak A, Mekalanos JJ.** 2006. A virulence locus of *Pseudomonas aeruginosa* encodes a protein secretion apparatus. Science **312:**1526-1530.

31. **Pukatzki S, Ma AT, Sturtevant D, Krastins B, Sarracino D, Nelson WC, Heidelberg JF, Mekalanos JJ.** 2006. Identification of a conserved bacterial protein secretion system in *Vibrio cholerae* using the *Dictyostelium* host model system. Proc Natl Acad Sci U S A **103:**1528-1533.

32. **Russell AB, Hood RD, Bui NK, LeRoux M, Vollmer W, Mougous JD.** 2011. Type VI secretion delivers bacteriolytic effectors to target cells. Nature **475:**343-347.

33. **Cianfanelli FR, Alcoforado Diniz J, Guo M, De Cesare V, Trost M, Coulthurst SJ.** 2016. VgrG and PAAR Proteins Define Distinct Versions of a Functional Type VI Secretion System. PLoS Pathog **12:**e1005735.

34. **Bondage DD, Lin JS, Ma LS, Kuo CH, Lai EM.** 2016. VgrG C terminus confers the type VI effector transport specificity and is required for binding with PAAR and adaptor-effector complex. Proc Natl Acad Sci U S A **113:**E3931-3940.

35. **Bonemann G, Pietrosiuk A, Diemand A, Zentgraf H, Mogk A.** 2009. Remodelling of VipA/VipB tubules by ClpV-mediated threading is crucial for type VI protein secretion. EMBO J **28:**315-325.

36. **Hachani A, Lossi NS, Hamilton A, Jones C, Bleves S, Albesa-Jove D, Filloux A.** 2011. Type VI secretion system in *Pseudomonas aeruginosa*: secretion and multimerization of VgrG proteins. J Biol Chem **286:**12317-12327.

37. **Shneider MM, Buth SA, Ho BT, Basler M, Mekalanos JJ, Leiman PG.** 2013. PAAR-repeat proteins sharpen and diversify the type VI secretion system spike. Nature **500:**350-353.

38. **Whitney JC, Beck CM, Goo YA, Russell AB, Harding BN, De Leon JA, Cunningham DA, Tran BQ, Low DA, Goodlett DR, Hayes CS, Mougous JD.** 2014. Genetically distinct pathways guide effector export through the type VI secretion system. Mol Microbiol **92:**529-542.

39. **Liang X, Moore R, Wilton M, Wong MJ, Lam L, Dong TG.** 2015. Identification of divergent type VI secretion effectors using a conserved chaperone domain. Proc Natl Acad Sci U S A **112:**9106-9111.

40. **Unterweger D, Kostiuk B, Otjengerdes R, Wilton A, Diaz-Satizabal L, Pukatzki S.** 2015. Chimeric adaptor proteins translocate diverse type VI secretion system effectors in *Vibrio cholerae*. EMBO J **34:**2198-2210.

41. **Hachani A, Allsopp LP, Oduko Y, Filloux A.** 2014. The VgrG proteins are "a la carte" delivery systems for bacterial type VI effectors. J Biol Chem **289:**17872-17884.

42. **Whitney JC, Chou S, Russell AB, Biboy J, Gardiner TE, Ferrin MA, Brittnacher M, Vollmer W, Mougous JD.** 2013. Identification, structure, and function of a novel type VI secretion peptidoglycan glycoside hydrolase effector-immunity pair. J Biol Chem **288:**26616-26624.

43. **Saak CC, Zepeda-Rivera MA, Gibbs KA.** 2017. A single point mutation in a TssB/VipA homolog disrupts sheath formation in the type VI secretion system of *Proteus mirabilis*. PLoS One **12:**e0184797.

44. **Basler M, Pilhofer M, Henderson GP, Jensen GJ, Mekalanos JJ.** 2012. Type VI secretion requires a dynamic contractile phage tail-like structure. Nature **483:**182-186.

45. **Brunet YR, Henin J, Celia H, Cascales E.** 2014. Type VI secretion and bacteriophage tail tubes share a common assembly pathway. EMBO Rep **15:**315-321.

46. **Douzi B, Spinelli S, Blangy S, Roussel A, Durand E, Brunet YR, Cascales E, Cambillau C.** 2014. Crystal structure and self-interaction of the type VI secretion tail-tube protein from enteroaggregative *Escherichia coli*. PLoS One **9:**e86918.

47. **Silverman JM, Agnello DM, Zheng H, Andrews BT, Li M, Catalano CE, Gonen T, Mougous JD.** 2013. Haemolysin coregulated protein is an exported receptor and chaperone of type VI secretion substrates. Mol Cell **51:**584-593.

48. **Brunet YR, Espinosa L, Harchouni S, Mignot T, Cascales E.** 2013. Imaging type VI secretion-mediated bacterial killing. Cell Rep **3:**36-41.

49. **Zoued A, Durand E, Bebeacua C, Brunet YR, Douzi B, Cambillau C, Cascales E, Journet L.** 2013. TssK is a trimeric cytoplasmic protein interacting with components of

both phage-like and membrane anchoring complexes of the type VI secretion system. J Biol Chem **288:**27031-27041.

50. **Brunet YR, Zoued A, Boyer F, Douzi B, Cascales E.** 2015. The Type VI Secretion TssEFGK-VgrG Phage-Like Baseplate Is Recruited to the TssJLM Membrane Complex via Multiple Contacts and Serves As Assembly Platform for Tail Tube/Sheath Polymerization. PLoS Genet **11:**e1005545.

51. **Jeong H, Barbe V, Lee CH, Vallenet D, Yu DS, Choi SH, Couloux A, Lee SW, Yoon SH, Cattolico L, Hur CG, Park HS, Segurens B, Kim SC, Oh TK, Lenski RE, Studier FW, Daegelen P, Kim JF.** 2009. Genome sequences of *Escherichia coli* B strains REL606 and BL21(DE3). J Mol Biol **394:**644-652.

52. **Davidson AR, Sauer RT.** 1994. Folded proteins occur frequently in libraries of random amino acid sequences. Proc Natl Acad Sci U S A **91:**2146-2150.

53. **Lei SP, Lin HC, Wang SS, Callaway J, Wilcox G.** 1987. Characterization of the *Erwinia carotovora* pelB gene and its product pectate lyase. J Bacteriol **169:**4379-4383.

54. **Movva NR, Nakamura K, Inouye M.** 1980. Amino acid sequence of the signal peptide of ompA protein, a major outer membrane protein of *Escherichia coli*. J Biol Chem **255:**27-29.

55. **Whitney JC, Quentin D, Sawai S, LeRoux M, Harding BN, Ledvina HE, Tran BQ, Robinson H, Goo YA, Goodlett DR, Raunser S, Mougous JD.** 2015. An interbacterial NAD(P)(+) glycohydrolase toxin requires elongation factor Tu for delivery to target cells. Cell **163:**607-619.

56. **Belas R, Erskine D, Flaherty D.** 1991. Transposon mutagenesis in *Proteus mirabilis*. J Bacteriol **173:**6289-6293.

57. **Kaniga K, Delor I, Cornelis GR.** 1991. A wide-host-range suicide vector for improving reverse genetics in gram-negative bacteria: inactivation of the blaA gene of *Yersinia enterocolitica*. Gene **109:**137-141.

58. **Budding AE, Ingham CJ, Bitter W, Vandenbroucke-Grauls CM, Schneeberger PM.** 2009. The Dienes phenomenon: competition and territoriality in Swarming *Proteus mirabilis*. J Bacteriol **191:**3892-3900.

59. **Waldo GS, Standish BM, Berendzen J, Terwilliger TC.** 1999. Rapid protein-folding assay using green fluorescent protein. Nat Biotechnol **17:**691-695.

60. **Finn RD, Coggill P, Eberhardt RY, Eddy SR, Mistry J, Mitchell AL, Potter SC, Punta M, Qureshi M, Sangrador-Vegas A, Salazar GA, Tate J, Bateman A.** 2016. The Pfam protein families database: towards a more sustainable future. Nucleic Acids Res **44:**D279-285.

61. **Schindelin J, Arganda-Carreras I, Frise E, Kaynig V, Longair M, Pietzsch T, Preibisch S, Rueden C, Saalfeld S, Schmid B, Tinevez JY, White DJ, Hartenstein V, Eliceiri K, Tomancak P, Cardona A.** 2012. Fiji: an open-source platform for biological-image analysis. Nat Methods **9:**676-682.

62. **Schindelin J, Rueden CT, Hiner MC, Eliceiri KW.** 2015. The ImageJ ecosystem: An open platform for biomedical image analysis. Mol Reprod Dev **82:**518-529.

63. **Simon R, Priefer U, Puhler A.** 1983. A broad host range mobilization system for *in vivo* genetic engineering- transposon mutagenesis in gram-negative bacteria. Bio-Technol **1:**784-791.

642 Figure legends

643 **Figure 1. IdsD subcellular localization is dependent on IdsC but not the identity partner**
644 **protein, IdsE.** Epifluorescence microscopy was performed on the edges of swarming colonies
645 grown on swarm-permissive agar pads at 37°C. Frames are representative images. Left, Phase.
646 Middle, fluorescence in the RFP channel for mKate-IdsD, background subtracted. Right, false-
647 colored overlay in which for contrast mKate-IdsD fluorescence is in red and phase is in cyan. All
648 scale bars are 10 μm. Illustrations to the right depict models for IdsD localization at the
649 membrane based on predicted localizations. Three main components of the T6S (the baseplate,
650 the membrane-complex, and sheath) are shown. Black arrow represents tested IdsA (Hcp
651 homolog) secretion. N ≥ 3 per strain.
652 (A) A Δ*ids* strain producing FLAG-IdsC and mKate-IdsD *in trans*. Fluorescence associated
653 mKate-IdsD foci overlap at a 27% frequency with fluorescence associated with the T6S sheath
654 (Figure SF2).
655 (B) Strain CCS05, which is an Δ*ids*-derived strain in which T6S sheath formation is disrupted by
656 a chromosomal mutation in a TssB homolog (16), producing FLAG-IdsC and mKate-IdsD.
657 (C) Strain CCS05 producing FLAG-IdsC and mKate-IdsD and in which *idsE* is deleted as
658 previously described (16).
659 (D) Strain CCS05 producing FLAG-IdsC and mKate-IdsD and in which the DUF4123 domain of
660 IdsC is deleted.
661
662 **Figure 2. IdsD protein levels are reduced in the absence of IdsC.**
663 (A) Whole cell lysates were collected from strains with functional or disrupted T6S (16, 43)
664 producing mKate-IdsD and either FLAG-IdsC or FLAG-IdsC$^{\Delta DUF}$. Western blot analysis on

these samples was performed using polyclonal anti-IdsD, polyclonal anti-mKate, and monoclonal anti-sigma-70 (α-σ^{70}) antibodies. Black arrow indicates the approximately 150 kDa size of the mKate-IdsD fusion protein. Gray arrow indicates size of approximately 26 kDa mKate2 protein. The sizes of the protein ladder are noted on the left. IdsD is approximately 118 kDa. N = 3.

(B) Whole cell lysates were collected from Δ*ids*-derived strains carrying distinctly modified $pIds_{BB}$ vectors, as previously described (15). Each resultant Ids protein disruption is labeled above the sample. The control strain is Δ*ids* carrying unmodified $pIds_{BB}$. Western blot analysis was performed using polyclonal anti-IdsB, polyclonal anti-IdsD, and monoclonal anti-sigma-70 antibodies. The sizes of the protein ladder are noted on the left. The predicted size for IdsB is 82 kDa. N = 3.

Figure 3. IdsC binds IdsD and is essential for IdsD secretion.

(A) Schematic of IdsC (407 amino acids) drawn to scale with the predicted DUF4123 domain spanning from amino acids 128 to 255.

(B) IdsC-FLAG, $IdsC^{\Delta DUF}$-FLAG, and IdsD-His (24) were separately expressed in *E. coli* strain BL21(DE3) pLysS from the overexpression vector, pAD_{100} (52). Lysates were mixed as indicated in the diagram, and anti-FLAG co-immunoprecipitation assays were performed. Lysate from *E. coli* BL21(DE3) pLysS expressing IdsD-His_6 doped with purified FLAG-tagged *E. coli* bacterial alkaline phosphatase (FLAG-BAP) was used as a negative control. Soluble (L), non-binding (-) and binding (+) fractions were analyzed via western blot using polyclonal anti-IdsD, monoclonal anti-FLAG, and monoclonal anti-sigma-70 (α-σ^{70}) antibodies. Green boxes indicate

a band in the binding fraction; white boxes indicate no band in the binding fraction. The sizes of the protein ladder are noted on the left. N = 3.

(C) *In vivo* recognition assay for IdsD cell-to-cell transfer in which IdsD secretion causes a reduced swarm colony radius, while lack of transport results in an increased swarm colony radius (16). Strains producing FLAG-IdsC (DUF4123 +) or FLAG-IdsC$^{\Delta DUF}$ (DUF4123 -). T6S+ is a strain producing a fully functional T6S system. T6S- are derived from strain CCS05 (16). Average and standard deviation (s.d.) are shown. N = 10.

(D) Secreted Ids proteins from strains producing either FLAG-IdsC or FLAG-IdsC$^{\Delta DUF}$. The proteins from 75 – 250 kDa of TCA-extracted supernatants from liquid-grown cells were analyzed by LC-MS/MS as previously described (26). The non-secreted sigma-70 protein was used as a control for cell lysis. N = 1.

Figure 4. IdsC binding and subcellular localization of IdsD can be uncoupled from IdsD secretion.

(A) Strains were constructed in which FLAG-IdsC or FLAG-IdsC$^{S38P/R186Q}$ were produced *in trans* from modified pIds$_{BB}$ vectors. Lysates were subjected to anti-FLAG batch co-immunoprecipitations. Soluble (L), non-binding (-) and binding (+) fractions were analyzed via western blot using polyclonal anti-IdsB, polyclonal anti-IdsD, monoclonal anti-FLAG, and monoclonal anti-sigma-70 antibodies. Green boxes on right indicate a band in the binding fraction; a white box indicates no band in the binding fraction. The sizes of the protein ladder are noted on the left. N ≥ 3.

(B) Strain CCS05 (16, 43) producing FLAG-IdsC$^{S38P/R186Q}$ and mKate-IdsD. Left, Phase. Middle, fluorescence in the RFP channel for mKate-IdsD, background subtracted. Right, false-colored

overlay in which for contrast, mKate-IdsD fluorescence is in red and phase is in cyan. Scale bar is 10 μm.

(C) *In vivo* recognition assay for IdsD cell-to-cell transfer in which IdsD secretion results in reduced swarm colony radius, while abrogation of secretion results in an increased swarm colony radius (16). T6S+ are *P. mirabilis* strains producing a fully functional T6S system. T6S- are derived from strain CCS05 (16). Average and standard deviation (s.d.) are shown. N = 10.

(D) The proteins from 75 – 250 kDa of TCA-extracted supernatants from liquid-grown cells producing FLAG-IdsC or FLAG-IdsC$^{S38P/R186Q}$ from a modified pIds$_{BB}$ plasmid (15) were analyzed by LC-MS/MS as previously described (26). The non-secreted sigma-70 protein was used as a control for cell lysis.

Figure 5. IdsC does not neutralize IdsD transferred from neighboring cells. CCS05 expressing pIds$_{BB\text{-}\Delta IdsE}$ will boundary with BB2000 (3).

(A) To test whether periplasmic IdsC binds transferred IdsD, CCS05 strains carrying modified pIds$_{BB\text{-}\Delta IdsE}$ to express FLAG-IdsC with two signal sequences, PelB or OmpA, to target FLAG-IdsC to the periplasm, were tested for self-recognition phenotypes on kanamycin against BB2000 and Δ*ids* each carrying an empty plasmid that confers kanamycin resistance. BB2000 and Δ*ids* are expected to form a boundary (white arrows). If periplasmic FLAG-IdsC binds and neutralizes transferred IdsD, the expectation is that these strains will merge with BB2000. Test strains formed boundaries with BB2000 (grey arrows) and merged with Δ*ids* (yellow arrows). N = 3.

(B) *In vivo* recognition assay to determine whether cytoplasmic FLAG-IdsC would bind and neutralize transferred IdsD. BB2000 or BB2000::Δ*idsE* carrying an inducible plasmid (9) encoding FLAG-IdsC. Open circles indicate migration radii per replicate and bars indicate

733 average migration radius. If cytoplasmic FLAG-IdsC binds and neutralizes transferred IdsD the
734 expectation is that swarming radii of BB2000::Δ*idsE* would be restored to BB2000 levels upon
735 induction of FLAG-IdsC expression. N = 3.
736
737 **Figure 6**. **Model for IdsD regulation before delivery into a neighboring cell.** We propose that
738 IdsC is necessary for the presence and subcellular clustering of IdsD in donor cells and that IdsC
739 mediates IdsD transport at the T6S machinery partially through interactions with IdsB (VgrG).
740 We posit that the IdsC clustering of IdsD provides a simple mechanism to explain the prevention
741 of identity-defining IdsD-IdsE interactions in the donor cell.
742

743 **Table 1. Strains used.**

Strain	Detailed description	Source
Proteus mirabilis strains		
BB2000	Wild-type	(56)
Δ*ids*	Δ*ids::Tn-Cm(R)*	(15)
Δ*ids* c. $pIds_{BB}$	Δ*ids* carrying a plasmid expressing the *ids* operon from strain BB2000 under control of its native *ids* upstream region; this plasmid was first described as pids_{BB2000} in (15).	(15)
Δ*ids* c. pKG101	Δ*ids* carrying a plasmid expressing promoterless green fluorescent protein.	(25)
BB2000 c. pKG101	BB2000 carrying a plasmid expressing promoterless green fluorescent protein.	(25)
Δ*ids* c. $pIds_{BB\text{-}FLAG\text{-}IdsC\text{-}mKate2\text{-}IdsD}$	Δ*ids* carrying a modified $pIds_{BB}$ plasmid in which an N-terminal FLAG epitope tag is encoded in-frame with *idsC* and an N-terminal mKate2 fluorophore is encoded in frame with *idsD*.	This study
Δ*ids*::$BB2000\_0821_{wt}$-*sfgfp*	Δ*ids* with chromosomal *BB2000_0821* fused to *sfgfp* replacing the wildtype allele.	(43)
Δ*ids*::$BB2000\_0821_{wt}$-*sfgfp* c. $pIds_{BB\text{-}FLAG\text{-}IdsC\text{-}mKate2\text{-}IdsD}$	Δ*ids*::$BB2000\_0821_{wt}$-*sfgfp* carrying a modified $pIds_{BB}$ plasmid in which an N-terminal FLAG epitope tag is encoded in-frame with *idsC* and	This study

	an N-terminal mKate2-fluorophore is encoded in frame with *idsD*.	
CCS05	Δ*ids* with chromosomal *BB2000_0821* with a single T → G point mutation at base pair 95. This produces the protein $TssB_{L32R}$, resulting in a disrupted T6S sheath.	(16)
CCS05 c. $pIds_{BB\text{-}FLAG\text{-}IdsC\text{-}mKate2\text{-}IdsD}$	CCS05 carrying a modified $pIds_{BB}$ plasmid in which an N-terminal FLAG epitope tag is encoded in-frame with *idsC* and an N-terminal mKate2-fluorophore is encoded in frame with *idsD*.	This study
*BB2000_0808**	*BB2000_0808::Tn-Cm(R)*. First described as *tssN** in (26).	(26)
*BB2000_0808** c. $pIds_{BB\text{-}FLAG\text{-}IdsC\text{-}mKate2\text{-}IdsD}$	*BB2000_0808** carrying a modified $pIds_{BB}$ plasmid in which an N-terminal FLAG epitope tag is encoded in-frame with *idsC* and an N-terminal mKate2-fluorophore is encoded in frame with *idsD*.	This study
Δ*ids::BB2000_0814* $_{G1145A}$	Modified protein(s): BB2000 with chromosomal *BB2000_0814* with a G→A point mutation at base pair 1145. This results in the production of $TssK_{S382N}$ ($TssK_{partial}$)	This study

Δ*ids*::*BB2000_0814*$_{G1145A}$ c. pIds$_{BB\text{-}FLAG\text{-}IdsC\text{-}mKate2\text{-}IdsD}$	Δ*ids* with chromosomal *BB2000_0814* with a G→A point mutation at base pair 1145 linked to carrying a modified pIds$_{BB}$ plasmid in which an N-terminal FLAG epitope tag is encoded in-frame with *idsC* and an N-terminal mKate2-fluorophore is encoded in frame with *idsD*.	This study
Δ*ids*::*BB2000_0814*$_{G1329T}$	BB2000 with chromosomal *BB2000_0814* with a G→T point mutation at base pair 1329. This results in the production of TssK$_{W443C}$(TssK$_{null}$).	This study
Δ*ids*::*BB2000_0814*$_{G1329T}$ c. pIds$_{BB\text{-}FLAG\text{-}IdsC\text{-}mKate\text{-}IdsD}$	Δ*ids* with chromosomal *BB2000_0814* with a G→T point mutation at base pair 1329 carrying a modified pIds$_{BB}$ plasmid. Plasmid has an N-terminal FLAG epitope tag encoded in-frame with *idsC* and an N-terminal mKate2-fluorophore is encoded in frame with *idsD*.	This study
BB2000::*BB2000_0821*$_{wt}$-*sfgfp*, *BB2000_0814*$_{G1145A}$	*BB2000* with chromosomal *BB2000_0821* linked to super-folder *gfp* and *BB2000_0814* with a G → A point mutation at base 1145.	This study
BB2000:: *BB2000_0821*$_{wt}$-*sfgfp*, *BB2000_0814*$_{G1329T}$	*BB2000* with chromosomal *BB2000_0821* linked to super-folder *gfp* and *BB2000_0814* with a G → T point mutation at base 1329.	This study
BB2000::	*BB2000* with chromosomal *BB2000_0821*	This study

BB2000_0814$_{G1145A}$	*BB2000_0814* with a G → A point mutation at base 1145.	
BB2000:: *BB2000_0814*$_{G1329T}$	*BB2000* with chromosomal *BB2000_0814* with a G → T point mutation at base 1329.	This study
CCS05 c. pIds$_{BB\text{-}FLAG\text{-}IdsC\text{-}mKate2\text{-}IdsD\text{-}\Delta IdsE}$	CCS05 carrying a modified pIds$_{BB}$ plasmid with an N-terminal FLAG epitope tag encoded in-frame with *idsC*, an N-terminal mKate2-fluorophore encoded in frame with *idsD* and an in-frame deletion of *idsE*.	This study
CCS05 c. pIds$_{BB\text{-}FLAG\text{-}IdsC\Delta DUF\text{-}mKate2\text{-}IdsD}$	CCS05 carrying a modified pIds$_{BB}$ plasmid in which an N-terminal FLAG epitope tag is encoded in-frame with *idsC* with nucleotides 373-762 deleted and an N-terminal mKate2-fluorophore is encoded in frame with *idsD*.	This study
Δ*ids* c. pIds$_{BB\text{-}FLAG\text{-}IdsC\Delta DUF\text{-}mKate2\text{-}IdsD}$	Δ*ids* carrying a modified pIds$_{BB}$ plasmid in which an N-terminal FLAG epitope tag is encoded in-frame with *idsC* with nucleotides 373-762 deleted and an N-terminal mKate2-fluorophore is encoded in frame with *idsD*.	This study
Δ*ids* c. pIds$_{BB\text{-}\Delta IdsABC}$	Δ*ids* carrying a modified pIds$_{BB}$ plasmid with an in-frame deletion of *idsA* through *idsC*. The plasmid was first described as ABC- in (15).	(15)
Δ*ids* c. pIds$_{BB\text{-}\Delta IdsDEF}$	Δ*ids* carrying a modified pIds$_{BB}$ plasmid with	(15)

	an in-frame deletion of *idsD* through *idsF*. The plasmid was first described as DEF- in (15).	
Δ*ids* c. $pIds_{BB\text{-}IdsBmt}$	Δ*ids* carrying a modified $pIds_{BB}$ plasmid with a 711-bp disruption of IdsB. The plasmid was first described as B- in (15).	(15)
Δ*ids* c. $pIds_{BB\text{-}IdsCmt}$	Δ*ids* carrying a modified $pIds_{BB}$ plasmid with insertion of three stop codons resulting in disruption of IdsC. The plasmid was first described as C- in (15).	(15)
Δ*ids* c. $pIds_{BB\text{-}IdsFmt}$	Δ*ids* carrying a modified $pIds_{BB}$ plasmid with a 1.9 kbp insertion resulting in disruption of IdsF. The plasmid was first described as F- in (15).	(15)
Δ*ids* c. $pIds_{BB\text{-}FLAG\text{-}IdsC}$	Δ*ids* carrying a modified $pIds_{BB}$ plasmid in which an N-terminal FLAG epitope tag is encoded in-frame with *idsC*.	This study
Δ*ids* c. $pIds_{BB\text{-}FLAG\text{-}IdsC\Delta DUF}$	Δ*ids* carrying a modified $pIds_{BB}$ plasmid in which an N-terminal FLAG epitope tag is encoded in-frame with *idsC* with nucleotides 373-762 deleted.	This study
Δ*ids* c. $pIds_{BB\text{-}FLAG\text{-}IdsC\text{-}\Delta IdsE}$	Δ*ids* carrying a modified $pIds_{BB}$ plasmid in which an N-terminal FLAG epitope tag is encoded in-frame with *idsC* and an in-frame deletion of *idsE*.	This study

CCS05 c. pIds$_{BB\text{-}FLAG\text{-}IdsC\text{-}\Delta IdsE}$	CCS05 carrying a modified pIds$_{BB}$ plasmid in which an N-terminal FLAG epitope tag is encoded in-frame with *idsC* and an in-frame deletion of *idsE*.	This study
Δ*ids* c. pIds$_{BB\text{-}FLAG\text{-}IdsC\Delta DUF\text{-}\Delta IdsE}$	Δ*ids* carrying a modified pIds$_{BB}$ plasmid in which an N-terminal FLAG epitope tag is encoded in-frame with *idsC* with nucleotides 373-762 deleted and an in-frame deletion of *idsE*.	This study
CCS05 c. pIds$_{BB\text{-}FLAG\text{-}IdsC\Delta DUF\text{-}\Delta IdsE}$	CCS05 carrying a modified pIds$_{BB}$ plasmid in which an N-terminal FLAG epitope tag is encoded in-frame with *idsC* with nucleotides 373-762 deleted and an in-frame deletion of *idsE*.	This study
Δ*ids* c. pIds$_{BB\text{-}FLAG\text{-}IdsCS38P/R186Q}$	Δ*ids* carrying a modified pIds$_{BB}$ plasmid in which an N-terminal FLAG epitope tag is encoded in-frame with *idsC* containing a T→C mutation at nucleotide 112 and a G→A mutation at nucleotide 557.	This study
CCS05 c. pIds$_{BB\text{-}FLAG\text{-}IdsCS38P/R186Q\text{-}mKate2\text{-}IdsD}$	CCS05 carrying a modified pIds$_{BB}$ plasmid in which an N-terminal FLAG epitope tag is encoded in-frame with *idsC* containing a T→C mutation at nucleotide 112 and a G→A	This study

	mutation at nucleotide 557. N-terminal mKate2-fluorophore is encoded in frame with *idsD*.	
Δ*ids* c. $pIds_{BB\text{-}FLAG\text{-}IdsCS38P/R186Q\text{-}\Delta IdsE}$	Δ*ids* carrying a modified $pIds_{BB}$ plasmid in which an N-terminal FLAG epitope tag is encoded in-frame with *idsC* containing a T→C mutation at nucleotide 112 and a G→A mutation at nucleotide 557. In-frame deletion of *idsE*.	This study
CCS05 c. $pIds_{BB\text{-}FLAG\text{-}IdsCS38P/R186Q\text{-}\Delta IdsE}$	CCS05 carrying a modified $pIds_{BB}$ plasmid in which an N-terminal FLAG epitope tag is encoded in-frame with *idsC* containing a T→C mutation at nucleotide 112 and a G→A mutation at nucleotide 557. In-frame deletion of *idsE*.	This study
CCS05 c. $pIds_{BB\text{-}PelB\text{-}FLAG\text{-}IdsC\text{-}\Delta IdsE}$	CCS05 carrying a modified $pIds_{BB}$ plasmid in which a PelB signal sequence is encoded upstream of a N-terminal FLAG epitope tag encoded in-frame with *idsC*. In-frame deletion of *idsE*.	This study
CCS05 c. $pIds_{BB\text{-}OmpA\text{-}FLAG\text{-}IdsC\text{-}\Delta IdsE}$	CCS05 carrying a modified $pIds_{BB}$ plasmid in which an OmpA signal sequence is encoded upstream of a N-terminal FLAG epitope tag	This study

	encoded in-frame with *idsC*. In-frame deletion of *idsE*.	
BB2000::ΔidsE	BB2000 with a chromosomal *idsE* deletion.	This study
BB2000::ΔidsE c. pTet-$_{FLAG\text{-}IdsC}$	*BB2000::ΔidsE* carrying an anhydrotetracycline inducible plasmid encoding *idsC* with an upstream N-terminal FLAG-epitope tag.	This study
BB2000 c. pTet-$_{FLAG\text{-}IdsC}$	*BB2000* carrying an anhydrotetracycline inducible plasmid encoding *idsC* with an upstream N-terminal FLAG-epitope tag.	This study
Escherichia coli strains		
BL21(DE3) pLysS c. pAD100	BL21(DE3) pLysS carrying an IPTG-inducible, high copy plasmid, containing a non-expressed FLAG- and His_6- tagged fragment of Fok1.	(52)
BL21(DE3) c. pAD-D_{BB}-His_6	BL21(DE3) pLysS carrying a C-terminal His_6-tagged *idsD* from strain BB2000 subcloned into pAD100 in place of Fok1.	(24)
BL21(DE3) pLysS c. pAD-IdsC-FLAG	BL21(DE3) pLysS carrying a C-terminal FLAG-tagged *idsC* subcloned into pAD100 in place of Fok1.	This study
BL21(DE3) c. pAD-$IdsC^{\Delta DUF}$-	BL21(DE3) carrying a C-terminal FLAG-tagged *idsC* with nucleotides 382-765 deleted	This study

FLAG	subcloned into pAD100 in place of Fok1.	
S17λpir	Mating strain	(63)
XL10 Gold Ultracompetent Cells	Cloning strain for pAD100-derived plasmids.	Agilent Technologies, Santa Clara, CA.
One Shot Omnimax 2 T1R Competent Cells	Cloning strain for pIds-derived plasmids.	Thermo Fisher Scientific, Waltham, MA.
OneShot BL21(DE3) pLysS Competent Cells	Strain for protein overexpression from pAD100-derived plasmids.	Thermo Fisher Scientific, Waltham, MA.

744

745

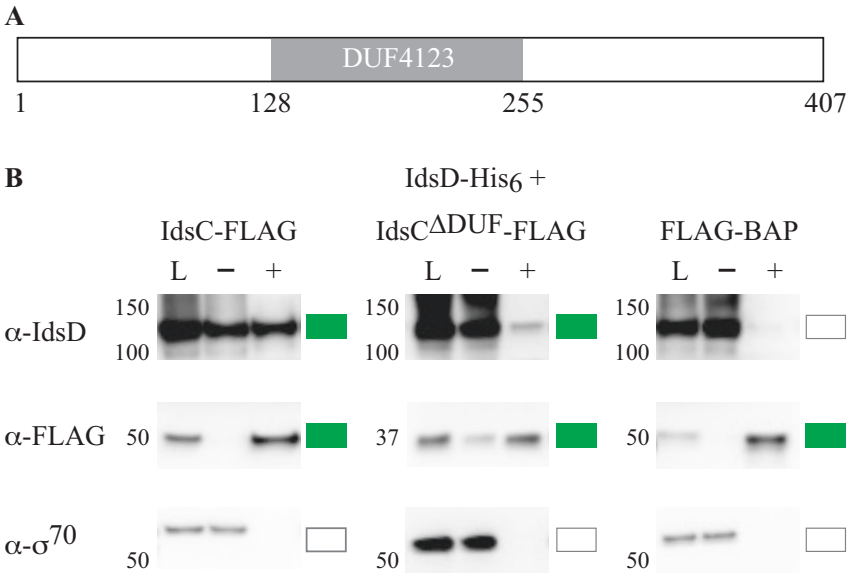

C

T6S	+	–	+	–
DUF4123	+	+	–	–
average (mm)	9.1	22.2	18.8	18.9
s.d.	1.10	4.21	3.68	2.92

D

	Protein	No. peptides (unique/total)	% Coverage
FLAG-IdsC	IdsB	4/4	8.9
	IdsD	3/3	3.1
	σ^{70}	0/0	0
FLAG-IdsC$^{\Delta DUF}$	IdsB	0/0	0
	IdsD	0/0	0
	σ^{70}	0/0	0

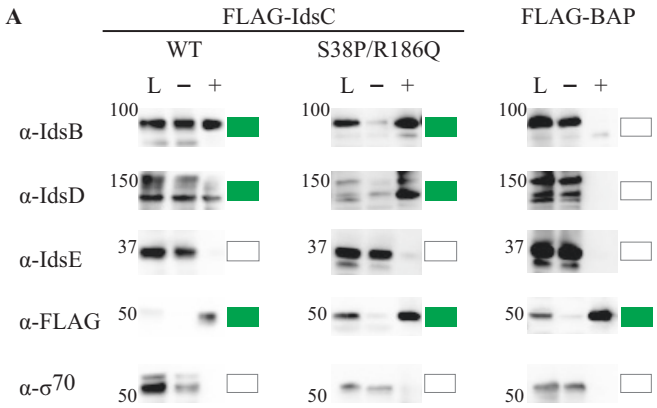

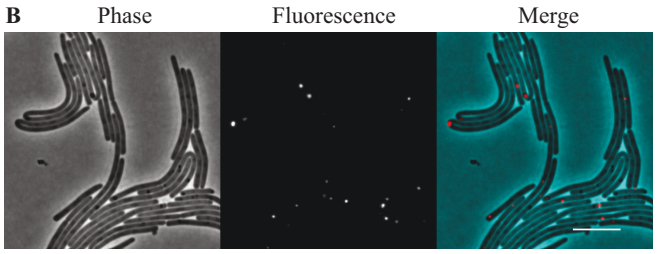

C

T6S	FLAG-IdsC +	FLAG-IdsC –	FLAG-IdsC$^{S38P/R186Q}$ +	FLAG-IdsC$^{S38P/R186Q}$ –
average (mm)	13.2	20.4	25.3	26.7
s.d.	0.92	1.71	0.95	1.49

D

	Protein	No. peptides (unique/total)	% Coverage
FLAG-IdsC	IdsB	10/12	3.10
	IdsD	6/6	2.37
	σ^{70}	2/2	2.24
FLAG-IdsC$^{S38P/R186Q}$	IdsB	7/8	3.07
	IdsD	2/2	2.56
	σ^{70}	0/0	0

PLOS ONE

RESEARCH ARTICLE

A single point mutation in a TssB/VipA homolog disrupts sheath formation in the type VI secretion system of *Proteus mirabilis*

Christina C. Saak, Martha A. Zepeda-Rivera, Karine A. Gibbs*

Department of Molecular and Cellular Biology, Harvard University, Cambridge, Massachusetts, United States of America

* kagibbs@mcb.harvard.edu

Citation: Saak CC, Zepeda-Rivera MA, Gibbs KA (2017) A single point mutation in a TssB/VipA homolog disrupts sheath formation in the type VI secretion system of *Proteus mirabilis*. PLoS ONE 12(9): e0184797. https://doi.org/10.1371/journal.pone.0184797

Editor: J. Seshu, University of Texas at San Antonio, UNITED STATES

Received: March 10, 2017

Accepted: August 31, 2017

Published: September 26, 2017

Data Availability Statement: All relevant data are within the paper and its Supporting Information files. Data files are also available from the Open Science Framework (DOI: 10.17605/OSF.IO/KDZYU).

Funding: This research was funded by a Howard Hughes Medical Institute Gilliam Fellowship for Advanced Study (MZR) and by the David and Lucile Packard Foundation, the George W. Merck Fund, and Harvard University. The funders had no role in study design, data collection and analysis,

Abstract

The type VI secretion (T6S) system is a molecular device for the delivery of proteins from one cell into another. T6S function depends on the contractile sheath comprised of TssB/VipA and TssC/VipB proteins. We previously reported on a mutant variant of TssB that disrupts T6S-dependent export of the self-identity protein, IdsD, in the bacterium *Proteus mirabilis*. Here we determined the mechanism underlying that initial observation. We show that T6S-dependent export of multiple self-recognition proteins is abrogated in this mutant strain. We have mapped the mutation, which is a single amino acid change, to a region predicted to be involved in the formation of the TssB-TssC sheath. We have demonstrated that this mutation does indeed inhibit sheath formation, thereby explaining the global disruption of T6S activity. We propose that this mutation could be utilized as an important tool for studying functions and behaviors associated with T6S systems.

Introduction

Type VI secretion (T6S) systems, widely found among Gram-negative bacteria, are cell-puncturing devices that deliver cargo proteins from one cell into another or into the environment [1–22]. T6S function, and ultimately cargo delivery, depends on a contractile sheath made up of TssB/VipA (Pfam family PF05591) and TssC/VipB (Pfam family PF05943) proteins [6, 23, 24]. TssB and TssC bind one another to form protomers, which in turn assemble into the contractile sheath [25–27]. Subcellular visualization of the T6S machinery has often relied on the fusion of TssB to fluorescent proteins such as superfolder Green Fluorescent Protein (sfGFP) and mCherry, thereby allowing the detection of sheath dynamics and interactions between TssB and TssC, as well as measuring the active firing of T6S machines within a population [4–6, 17, 18, 28–32]. While many model systems for T6S contain multiple loci encoding different T6S machines, *Proteus mirabilis* strain BB2000 is one of many less-studied organisms with a single T6S system and single alleles for TssB (BB2000_0821) and TssC (BB2000_0820) [33, 34]. We have previously reported that a point mutation in *BB2000_0821* results in the blocked export of proteins belonging to the Ids recognition system [35]. This mutation lies in an unstructured region of the TssB monomer that was previously unexamined. Here we show

decision to publish, or preparation of the manuscript.

Competing interests: The authors have declared that no competing interests exist.

that the identified point mutation disrupts global T6S export function. Based on published structures of the TssB-TssC sheath in other organisms, we mapped the point mutation to a region involved in sheath formation [25–27]. We specifically demonstrate that this point mutation inhibits sheath polymerization and that this is the likely mechanism for disrupted T6S export. Since this single point mutation disrupts global T6S function without disrupting the structure of the operon, and likely the core membrane components, we posit that the mutation provides a valuable tool for studying T6S-associated phenotypes in multiple organisms.

Materials and methods

Bacterial strains and media

Strains and plasmids used in this study are described in Table 1. *P. mirabilis* strains were maintained on LSW$^-$ agar [36]. CM55 blood agar base agar (Oxoid, Basingstoke, England) was used for swarm-permissive nutrient plates. Overnight cultures of all strains were grown in LB broth under aerobic conditions at 37˚C. Antibiotics used were: 35 microgram/milliliter (μg/ml)

Table 1. Strains used in this study.

Strain	Notes	Source
HI4320	Wild-type strain	[37, 38]
Δ*ids*::*tssB*$_{wt}$	This strain, derived from the *P. mirabilis* wild-type strain BB2000, produces TssB$_{wt}$ and none of the Ids proteins.	[39]
*icmF**::*tssB*$_{wt}$	This strain was previously reported as strain *tssN**. It contains a transposon insertion in gene *BB2000_0808*, which encodes the TssM/IcmF homolog in *P. mirabilis*.	[34]
Δ*ids*::*tssB*$_{mut}$	This strain was previously reported as strain CCS05. It produces the TssB$_{L32R}$ mutant variant and is deficient in T6S-mediated transport.	[35]
Δ*ids*::*tssB*$_{wt}$ carrying (c.) pLW101	This strain carries a derivative of the low-copy plasmid pIdsBB [39], which encodes the entire *ids* operon under control of its native promoter, and in which a FLAG epitope (N-DYKDDDDK-C) was inserted immediately before the *idsA* stop codon [34]. This strain was used for the LC-MS/MS studies.	[34]
Δ*ids*::*tssB*$_{mut}$ c. pLW101	This strain carries pLW101. This strain was used for the LC-MS/MS studies.	[35]
Δ*ids*:: *tssB*$_{wt}$-*sfgfp*	This strain produces TssB$_{wt}$ fused to sfGFP.	This study
Δ*ids*::*tssB*$_{mut}$-*sfgfp*	This strain produces TssB$_{L32R}$ fused to sfGFP.	This study
*icmF**::*tssB*$_{wt}$-*sfgfp*	This *icmF**::*tssB*$_{wt}$-derived strain produces TssB$_{wt}$ fused to sfGFP.	This study
Δ*ids*::*tssB*$_{wt}$ c. pIdsBB-ΔE	This strain was previously reported as strain CCS06. It produces BB2000-derived IdsD from a pIdsBB [39]-derived plasmid, but not IdsE. It also produces TssB$_{wt}$.	[35]
Δ*ids*::*tssB*$_{mut}$ c. pIdsBB-ΔE	This strain produces BB2000-derived IdsD from a pIdsBB [39]-derived plasmid, but not IdsE. It also produces TssB$_{L32R}$.	[35]
Δ*ids*::*tssB*$_{wt}$-*sfgfp* c. pIdsBB-ΔE	This strain produces BB2000-derived IdsD from a pIdsBB [39]-derived plasmid, but not IdsE. It also produces TssB$_{wt}$ fused to sfGFP.	This study
Δ*ids*::*tssB*$_{mut}$-*sfgfp* c. pIdsBB-ΔE	This strain produces BB2000-derived IdsD from a pIdsBB [39]-derived plasmid, but not IdsE. It also produces TssB$_{L32R}$ fused to sfGFP.	This study
S17λpir	*E. coli* mating strain for moving plasmids into *P. mirabilis*	[40]
SM10λpir	*E. coli* mating strain for moving suicide vector pKNG101 [41] into *P. mirabilis*	[42]

* contains a mini-Tn*5*-Cm insertion

https://doi.org/10.1371/journal.pone.0184797.t001

kanamycin, 50 μg/ml chloramphenicol, 15 μg/ml tetracycline, and 25 μg/ml streptomycin. Kanamycin was added for plasmid maintenance where appropriate.

Construction of strains Δ*ids*::*tssB*$_{wt}$-*sfgfp* and Δ*ids*::*tssB*$_{mut}$-*sfgfp*

BB2000-derived Δ*ids*::*tssB*$_{wt}$-*sfgfp* and Δ*ids*::*tssB*$_{mut}$-*sfgfp* were constructed using 5′-GATTA GCAGCAATATCGAGCTC-3′ as the forward and 5′- GCGCGCTCTAGACCTTAAGTTAAAC CAAATATAGCTG-3′ as the reverse primer to amplify *BB2000_0821*, encoding the *P. mirabilis* TssB homolog, and its upstream region from genomic DNA of the wild-type strain BB2000 [36] or of the BB2000-derived mutant strain Δ*ids*::*tssB*$_{mut}$ [35]. The polymerase chain reaction (PCR) product was digested with DpnI (New England Biolabs, Ipswich, MA). Overlap extension PCR [43] was used to combine the PCR product and a gBlock (Integrated DNA Technologies, Inc., Coralville, IA) containing the gene encoding sfGFP (gBlock sequence:

5′CGCGGGCCCGGTATTACCCCATAAATAGTGCTCATGGTCTTGTTTAACATTTTCTGAA
TAGTTAAACATTTTTACAGGGTTTTCTGTTGGAGAGTATGGCAAACGTAATAAGAAAC
GCGGTGCTGTTAACCCTAAATAACGGGAATCTTCTGCTTCACGCAGTGAGCGCCATTTAGT
GTGTGCAGGGCCTTCAAAAACAGATTTTAGATCTTTAATTGCCGGCAGTTCAGCGTAGCTAT
TAATACCAAAGAAATTAGGTGAAACAGATGATAGGAATGGCGCGTGAGCCATTGCACCAA
CAGTACTAACATACTGCATTAACTTCATATCTGGCGCAGTATTGTTAAAGGCGTAGTTAC
CAATAACTGTTGCAACAGGTTCACCACCAAATTGGCCGTATCCTGAAGAGTAGACGTGTTG
ATAGAAGCCTGATTGAACAATTTCTGGAGAAAATTCAAAATCTTCTAATAACTCTTCTT
TAGTTGCATGAAGAATATTGATCTTAATATTTTCTCTAAAATCAGTGCGATCAACGAGTA
ATTTTAAAGAACGCCATGAAGCTTCAATTTCTTGAAATTTAGGCGCGTGAAGAATTTCGTC
AACTTGAGTACTTAGTTTATTATCAAGTTCAACAAGCATTTTATCGATTAATAATCGATTG
ATCTGTTGGTCTTCAGATTCACTGGCGAAAATATTACTAATAAAAGCAGCAACACCTTG
TTTGGCAATATCGTATGCTTCTGTTTCTGGAGACATACGTGATTGAGCCATAATTTCATCA
AGTAAAGAGCCTGTAGATGCGGGGGCTTGTTGCTCTTGAGCTTCTGCATTTAGTGACATGA
AATAATCCTCTATAAACATTATTTGTAGAGCTCATCCATGCCATGTGTAATCCCAGCAGC
AGTTACAAACTCAAGAAGGACCATGTGGTCACGCTTTTCGTTGGGATCTTTCGAAAGGACAG
ATTGTGTCGACAGGTAATGGTTGTCTGGTAAAAGGACAGGGCCATCGCCAATTGGAGTAT
TTTGTTGATAATGGTCTGCTAGTTGAACGGAACCATCTTCAACGTTGTGGCGAATTTTG
AAGTTAGCTTTGATTCCATTCTTTTGTTTGTCTGCCGTGATGTATACATTGTGTGAGTTAA
AGTTGTACTCGAGTTTGTGTCCGAGAATGTTTCCATCTTCTTTAAAATCAATACCTTTT
AACTCGATACGATTAACAAGGGTATCACCTTCAAACTTGACTTCAGCACGCGTCTTGTA
GGTCCCGTCATCTTTGAAAGATATAGTGCGTTCCTGTACATAACCTTCGGGCATGGCACT
CTTGAAAAAGTCATGCCGTTTCATGTGATCCGGATAACGGGAAAAGCATTGAACACCATAG
GTCAGAGTAGTGACAAGTGTTGGCCATGGAACAGGTAGTTTTCCAGTAGTGCAAATAAATTTA
AGGGTGAGTTTTCCGTTTGTAGCATCACCTTCACCCTCTCCACGGACAGAAAATTTGTGCCC
ATTAACATCACCATCTAATTCAACAAGAATTGGGACAACTCCAGTGAAAAGTTCTTCTCCTT
TGCTTCCTCCTCCAGCAGCAGCTTTTTGATTAGCAGCAATATCGAGCTC-3′).

5′CGCGGGCCCGGTATTACCCCATAAATAGTGC-3′ and 5′- GCGCGCTCTAGACCTTAAG TTAAACCAAATATAGCTG-3′ were used as the forward and reverse primers, respectively. Restriction digestion with ApaI and XbaI (New England Biolabs, Ipswich, MA) was used to introduce the overlap extension PCR product into the suicide vector pKNG101 [41]. The resulting vectors pCS48a (*tssB*$_{mut}$-*sfgfp*) and pCS48b (*tssB*$_{wt}$-*sfgfp*) were introduced into the mating strain *E. coli* SM10λpir [42] and then mated into BB2000-derived Δ*ids* [39]. The resultant matings were subjected to antibiotic selection using tetracycline and streptomycin on LSW$^-$ agar. Candidate strains were subjected to sucrose counter-selection to select for clones that integrated the target DNA sequence into the chromosome in exchange for the wild-type

DNA sequence [44]. 5′ – GCCATCAACATCAAGTACTTTG–3′ and 5′ – CATGAGCAGTCC AAATTGATC–3′ were used as the forward and reverse primers, respectively, to amplify the exchanged chromosomal regions by colony PCR. PCR reactions were purified and the entire exchanged region was sequenced to confirm strains. Sequencing was performed by GENEWIZ, Inc. (South Plainfield, NJ).

Trichloroacetic acid precipitations, SDS-PAGE, and LC-MS/MS

Trichloroacetic acid precipitations were performed as previously described [34]. Gel fragments corresponding to molecular weights of approximately 10 to 20, 20 to 40, 40 to 60 and 60 to 250 kilodaltons (kDa) were excised and subjected to liquid chromatography-mass spectrometry/mass spectrometry (LC-MS/MS), which was performed by the Taplin Biological Mass Spectrometry Facility (Harvard Medical School, Boston, MA).

Colony expansion and co-swarm inhibition assays

Overnight cultures were normalized to an optical density at 600 nm (OD_{600}) of 0.1 and swarm-permissive nutrient plates were inoculated with one microliter (μl) of normalized culture. Plates were incubated at 37˚C for 16 hours, and radii of actively migrating swarms were measured. Additionally, widths of individual swarm rings within the swarm colonies were recorded.

For co-swarm inhibition assays, strains were processed as described and mixed at a ratio of 1:1 where indicated. Swarm-permissive nutrient plates supplemented with Coomassie Blue (20 μg/ml) and Congo Red (40 μg/ml) were inoculated with one μl of normalized culture/culture mixes. Plates were incubated at 37˚C until boundary formation was visible by eye.

Modeling of $TssB_{wt}$ and $TssB_{L32R}$

Swiss-Model [45–48] was used for all modeling, and the atomic model, PDB ID: 3j9g (from http://www.rcsb.org [25, 49, 50]) was used as a template. Resulting.pdb files were modified in PyMOL v1.8.4.1 [51].

Microscopy

One millimeter thick swarm-permissive agar pads were inoculated directly from overnight cultures. The agar pads were incubated at 37˚C in a modified humidity chamber. After 4.5–5.5 hours, the pads were imaged by phase contrast as well as epifluorescence microscopy using a Leica DM5500B (Leica Microsystems, Buffalo Grove, IL) and a CoolSnap HQ^2 cooled CCD camera (Photometrics, Tucson, AZ). MetaMorph version 7.8.0.0 (Molecular Devices, Sunnyvale, CA) was used for image acquisition.

Western blotting

To test for the production of the sfGFP-fused proteins, cells were isolated from swarm-permissive nutrient plates supplemented with chloramphenicol after 16–20 hours, resuspended in 5 ml LB broth, and normalized to an OD_{600} of 1. Cells were pelleted by centrifugation and the pellet was resuspended in sample buffer and boiled. Samples were separated by gel electrophoresis using 12% Tris-tricine polyacrylamide gels, transferred onto 0.45 micrometer nitrocellulose membranes, and probed with polyclonal rabbit anti-GFP (1:4000, ThermoFisher Scientific, Waltham, MA) or mouse anti-σ^{70} (1:1000, BioLegend, San Diego,CA, catalog number 663202) followed by goat anti-rabbit or goat anti-mouse conjugated to horseradish peroxidase. The polyclonal rabbit anti-GFP antibody was supplied at a concentration of 2 mg/ml

(Thermo Fisher Scientific, Waltham, MA, catalog number A-11122, immunogen: GFP from jellyfish *Aequorea Victoria*). The goat anti-mouse secondary antibody was used at a 1:5000 dilution (KPL, Inc., Gaithersburg, MD, catalog number 214–1806) as was the goat anti-rabbit secondary (KPL, Inc., Gaithersburg, MD, catalog number 074–1506). A Precision Plus Protein™ Dual Color Standards molecular size marker (Bio-Rad Laboratories, Inc., Hercules, CA) was included as a size control. Membranes were developed with the Immun-Star HRP Substrate Kit (Bio-Rad Laboratories, Hercules, CA) and visualized using a Chemidoc (Bio-Rad Laboratories, Hercules, CA). TIFF images were exported and figures were made in Adobe Illustrator (Adobe Systems, San Jose, CA).

Results

The *tssB* mutant strain does not export self-recognition proteins

Several self-recognition proteins in *P. mirabilis* strain BB2000 are exported by its T6S system; these include the Hcp (Pfam family PF05638) homologs IdsA and IdrA, the VgrG (Pfam family PF05954) homologs IdsB and IdrB, and the self-identity protein IdsD [34]. We previously reported that a strain expressing a point mutation (L32R) from gene *BB2000_0821*, which encodes the *P. mirabilis* TssB homolog, results in the lack of IdsA, IdsB, and IdsD export [35]. To determine whether global T6S export was disrupted or whether the defect was specific to proteins belonging to the Ids system, we examined the Idr-specific secretion profile of the mutant strain. We collected supernatants of liquid-grown cells producing either $TssB_{wt}$ or $TssB_{L32R}$. These supernatants were subjected to trichloroacetic acid precipitations followed by LC-MS/MS analysis. We identified peptides belonging to IdrA (Hcp), IdrB (VgrG) and the putative Idr effector IdrD in the supernatants of the wild type, but not of the mutant strain (Table 2).

To confirm these secretion profiles, we employed an *in vivo* assay for Idr self-recognition activity. The Idr proteins contribute to inter-strain competitions during swarm migration [34], which is a highly coordinated, flagella-based social motility in *P. mirabilis* [52–54]. Briefly, the assay consists of mixing two different strains of *P. mirabilis* at a 1:1 ratio and allowing for swarm migration; at the completion of swarm migration, one strain dominates over the other and thus occupies the outer edges of the swarm colony [34]. The dominating strain can be identified by swarm boundary formation assays in which two genetically identical strains merge to form a single larger swarm, while two genetically distinct strains remain separate and form a visible boundary (Fig 1A) [39, 55–57]. *P. mirabilis* strain BB2000 dominates over the genetically distinct strain HI4320, permitting BB2000 to occupy the outer edges of a mixed swarm colony, which thus merges with the swarm colony of BB2000 and forms a boundary with the swarm colony of HI4320 [34]. Absence of Idr proteins or of T6S in BB2000 allows for HI4320 to dominate the mixed swarm instead [34]. Loss of the Ids proteins in BB2000 has no effect [34]. We therefore performed these assays using BB2000-derived strains that lack the Ids proteins (*Δids*) and produce either $TssB_{wt}$ or the mutant $TssB_{L32R}$. As a control, we used the BB2000-derived strain, *icmF**, which contains a disruption in the gene encoding the T6S core membrane component TssM/IcmF (Pfam family PF12790); this mutant strain is defective for T6S function [33, 34]. As expected, *Δids* producing $TssB_{wt}$ dominated over strain HI4320, and conversely, strain HI4320 dominated over *icmF** (Fig 1B). *Δids* producing the mutant $TssB_{L32R}$ did not dominate over HI4320 (Fig 1B), indicating that Idr-dependent inter-strain competition was disrupted in this strain. As co-swarm inhibition of HI4320 by BB2000-derived strains is dependent on the export of Idr self-recognition proteins, we conclude that a strain producing $TssB_{L32R}$ is defective in the export of Idr proteins. Together, the secretion profile and swarm assays support that this mutation ($TssB_{L32R}$) causes a global loss in T6S export activity.

Table 2. Idr-specific LC-MS/MS results of supernatant fractions from strains producing $TssB_{wt}$ or $TssB_{L32R}$.

Strain	TssB variant produced	Protein	Predicted size (kDa)	Gel slice (approx. kDa range)	No. of unique peptides	No. of total peptides	Coverage (%)
Δ*ids*::*tssB*$_{wt}$ c. pLW101	$TssB_{wt}$	σ^{70}	71.11	60–250*	0	0	0
				40–60	0	0	0
				20–40	2	2	4.37
				10–20	0	0	0
		IdrA	18.99	60–250[1]	2	3	13.95
				40–60	0	0	0
				20–40[2]	8	29	55.81
				10–20*[3]	4	21	26.74
		IdrB	80.23	60–250*	4	4	7.26
				40–60	0	0	0
				20–40	2	2	4.52
				10–20	2	2	6.58
		IdrD	178.29	60–250*	2	2	1.33
				40–60	2	2	1.27
				20–40	7	10	3.16
				10–20	8	59	3.73
Δ*ids*::*tssB*$_{mut}$ c. pLW101	$TssB_{L32R}$	σ^{70}	71.11	60–250*	0	0	0
				40–60	0	0	0
				20–40	0	0	0
				10–20	0	0	0
		IdrA	18.99	60–250	0	0	0
				40–60	0	0	0
				20–40	0	0	0
				10–20*[1]	2	2	13.95
		IdrB	80.23	60–250*	0	0	0
				40–60	0	0	0
				20–40	0	0	0
				10–20	0	0	0
		IdrD	178.29	60–250*	0	0	0
				40–60	0	0	0
				20–40	0	0	0
				10–20	0	0	0

* Expected kDa range according to molecular weight

[1] Given the high degree of sequence similarity between the Hcp homologs IdsA and IdrA, all unique peptides could be assigned to IdsA or IdrA

[2] 3 unique (3 total) are IdrA, others could be assigned to IdsA or IdrA

[3] 2 unique (2 total) are IdrA, others could be assigned to IdsA or IdrA

https://doi.org/10.1371/journal.pone.0184797.t002

The L32R mutation in the TssB homolog prohibits sheath formation

To understand the disrupted T6S export, we modeled the *P. mirabilis* BB2000 T6S sheath structure on a published structure of the *Vibrio cholerae* T6S sheath [25] (Fig 2). We then mapped the L32R point mutation onto this *P. mirabilis* model structure (Fig 2). The point mutation causes a hydrophobic leucine at position 32 to be substituted with a positively charged arginine, which has a larger side chain and different electrochemical properties (Fig 2A). Amino acid 32 maps to an unstructured region between the first two beta sheets of TssB (Fig 2B and 2C) [25, 26]. The first beta sheet is involved in interactions between TssB-TssC

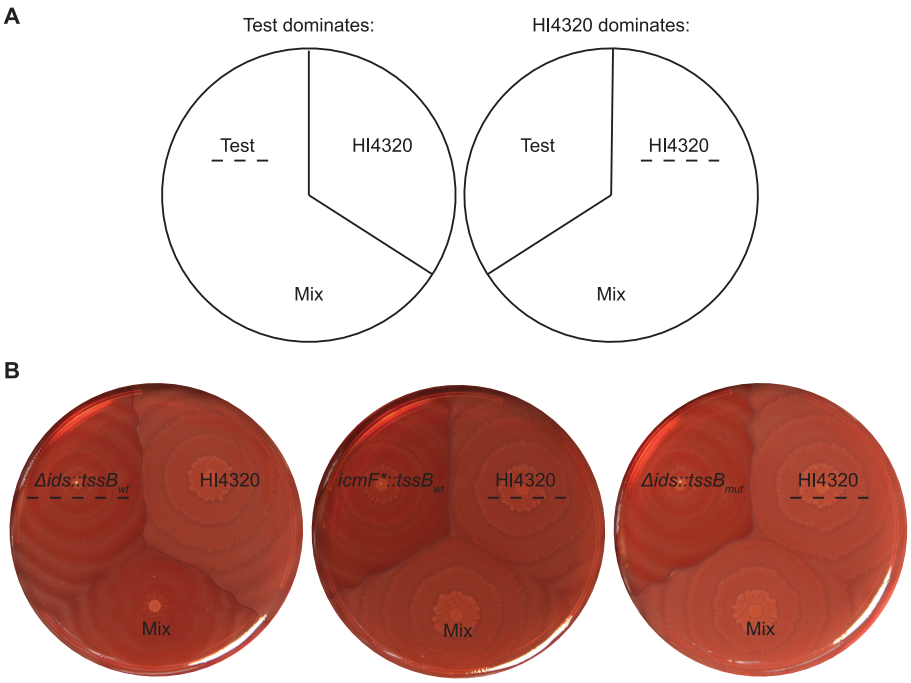

Fig 1. The L32R mutation disrupts Idr function. (A) Schematic of the Idr-dependent co-swarm assay. Strains are inoculated either as monocultures or as 1:1 mixed cultures onto swarm-permissive media as previously described [34]. The dominating strain in the mixed culture will occupy the outer swarm edges; boundary formation assays [39, 55–57] are then used to determine the identity of the dominating strain. The test strain dominated the mixed swarm if the mixed swarm colony forms a visible boundary with strain HI4320. Conversely, strain HI4320 dominated the mixed swarm if the mixed swarm does not form a boundary with strain HI4320. The dominating strain is indicated by a dashed line. (B) The Idr-dependent co-swarm assay using the indicated strains. BB2000-derived Δ*ids*::*tssB*$_{wt}$ produces TssB$_{wt}$; it lacks the entire *ids* operon [39]. BB2000-derived *icmF**::*tssB*$_{wt}$ produces TssB$_{wt}$; it contains a chromosomal transposon insertion in the gene encoding the core T6S membrane component, TssM/IcmF [34]. Δ*ids*::*tssB*$_{mut}$ [35] produces the mutant variant TssB$_{L32R}$.

https://doi.org/10.1371/journal.pone.0184797.g001

protomers that hold together the strands of the sheath helix, while the second beta sheet is involved in TssB-TssC interactions within individual protomers (Fig 2B and 2C) [25, 26]. Given the position within the T6S sheath, we hypothesized that the L32R mutation interferes with sheath formation.

We introduced the mutation into a Δ*ids* strain producing TssB fused to sfGFP to directly observe sheath formation *in vivo*. To validate the functionality of this tool in *P. mirabilis* strain BB2000, we examined the ability of the TssB-sfGFP variants to export self-recognition proteins using established assays. We subjected Δ*ids*::*tssB*$_{wt}$-*sfgfp* and Δ*ids*::*tssB*$_{mut}$-*sfgfp* to Idr-dependent inter-strain competitions with strain HI4320 as described above. Surprisingly, HI4320 dominated over both strains (Fig 3A), which suggested that T6S export is impaired in both strains. A more quantitative assay for T6S function is a swarm expansion assay using the Ids proteins; in this assay, a reduced swarm colony radius indicates that the self-identity determinant IdsD has been exported and that T6S is functional [35]. As previously reported [35], the

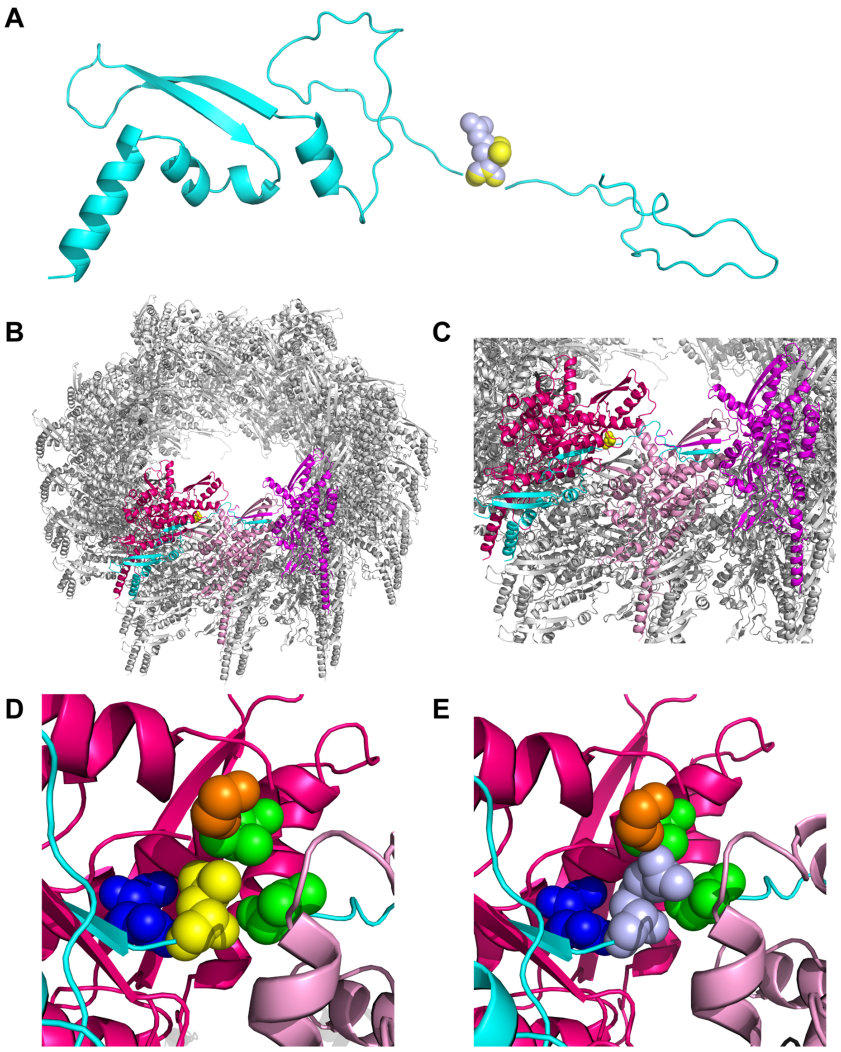

Fig 2. The L32R mutation on a model of the *P. mirabilis* BB2000 T6S sheath. (A) Cartoon representation of the *P. mirabilis* BB2000 TssB monomer (cyan) modeled after the *V. cholerae* TssB homolog [25]. The wild-type TssB variant has a leucine (yellow) at position 32. The mutant variant $TssB_{L32R}$ has an arginine (light blue) at position 32. (B, C) Cartoon representation of a portion of the wild-type *P. mirabilis* BB2000 T6S sheath containing $TssB_{wt}$ and the *P. mirabilis* BB2000 TssC homolog (BB2000_0820) at two magnifications. It was modeled after the *V. cholerae* contracted sheath [25]. In this model, one complete TssB-TssC protomer is highlighted, with TssB shown in cyan and TssC shown in pink. Two additional TssC monomers are highlighted in magenta and light pink. The wild-type TssB variant has a leucine (yellow) at position 32, which we have mapped to a

predicted unstructured region between two beta sheets. Both beta sheets are thought to be involved in making contacts to TssC monomers [25, 26]. (D, E) Magnified view of residue 32 and the neighboring residues (glycine in orange, valine in green, and arginine in dark blue). (D) Wild-type leucine in yellow. (E) Mutant arginine in light blue. Swiss-Model [45–48] was used for all modeling, and the atomic model 3j9g (from http://www.rcsb.org [25, 49, 50]) was used as a template. Resulting.pdb files were modified in PyMOL v1.8.4.1 [51].

https://doi.org/10.1371/journal.pone.0184797.g002

presence of wild-type TssB results in a reduced swarm colony radius, while disrupted T6S function due to the presence of $TssB_{L32R}$ leads to a larger swarm colony radius (Fig 3B). We examined the strain producing $TssB_{wt}$-sfGFP and found that its swarm colony radius was modestly increased in comparison to that of the strain producing untagged $TssB_{wt}$ (Fig 3B); therefore, fusion of sfGFP to $TssB_{wt}$ caused a modest reduction in T6S function. Interestingly, the reduced functionality of $TssB_{wt}$-sfGFP in comparison to $TssB_{wt}$ was sufficient to prevent a BB2000-derived strain to outcompete HI4320 in the *idr*-specific co-swarm assay (Fig 3A), further supporting earlier observations of distinct functions for Ids and Idr proteins [34]. As expected, the strain producing $TssB_{L32R}$-sfGFP exhibited an even larger swarm colony radius, similar to that of a strain producing untagged $TssB_{L32R}$ (Fig 3B). This observation demonstrates a lack of T6S export [35] and thus confirms that strains producing $TssB_{L32R}$ do no export the T6S substrate, IdsD.

We next employed the TssB-sfGFP tool to determine the ability of the mutant TssB variant to support T6S sheath formation, thereby testing the hypothesis that $TssB_{L32R}$ does not support sheath formation. Fluorescence associated with $TssB_{wt}$-sfGFP appears in multiple discrete (short or elongated) structures throughout cells on swarm-permissive agar (Fig 4A). This fluorescence pattern is consistent with previous reports for TssB-sfGFP [6, 59]. In cells producing the mutant fusion protein, diffuse fluorescence signal was present, and no elongated structures or puncta were observed (Fig 4A). Therefore, the discrete structures, thought to be sheaths, did not form. To further examine whether the discrete fluorescence was likely representative of assembled T6S sheaths, we produced $TssB_{wt}$-sfGFP in the *icmF** strain, which lacks the membrane-associated complex of the T6S machinery and which we thus predicted to lack sheaths. Again we observed that fluorescence was diffuse in these cells (Fig 4A), indicating the likely absence of sheath formation.

A possible explanation for the diffuse fluorescence pattern in a strain producing $TssB_{L32R}$-sfGFP could be that the mutant TssB is less stable than the wild-type variant, which could result in the cleavage of sfGFP from the fusion protein and ultimately a diffuse signal. We examined whole cell extracts that were collected from swarming colonies and then subjected these extracts to western blotting followed by incubation with anti-GFP antibodies. We found no striking differences among the strains producing wild-type or mutant TssB-sfGFP (Fig 4B). For both strains, we observed a dominant band corresponding to the size of the TssB-sfGFP fusion protein and a fainter band corresponding to the size of monomeric sfGFP (Fig 4B). This result suggests that while cleavage of the TssB-sfGFP fusion occurs, it does so for both the wild-type and mutant TssB-sfGFP variants. We conclude that cleavage of the sfGFP does not account for the differences in fluorescence patterns of these strains. Therefore, the L32R mutation in TssB is sufficient to prohibit sheath formation in *P. mirabilis*.

Discussion

Here we have described the critical contribution of a single residue in TssB for sheath formation and global T6S export activity. We have shown that a L32R mutation in the *P. mirabilis* TssB variant inhibits sheath assembly (Fig 4A) without altering relative amounts of this protein (Fig 4B). The mutated leucine residue in the *P. mirabilis* variant corresponds to amino acid 26

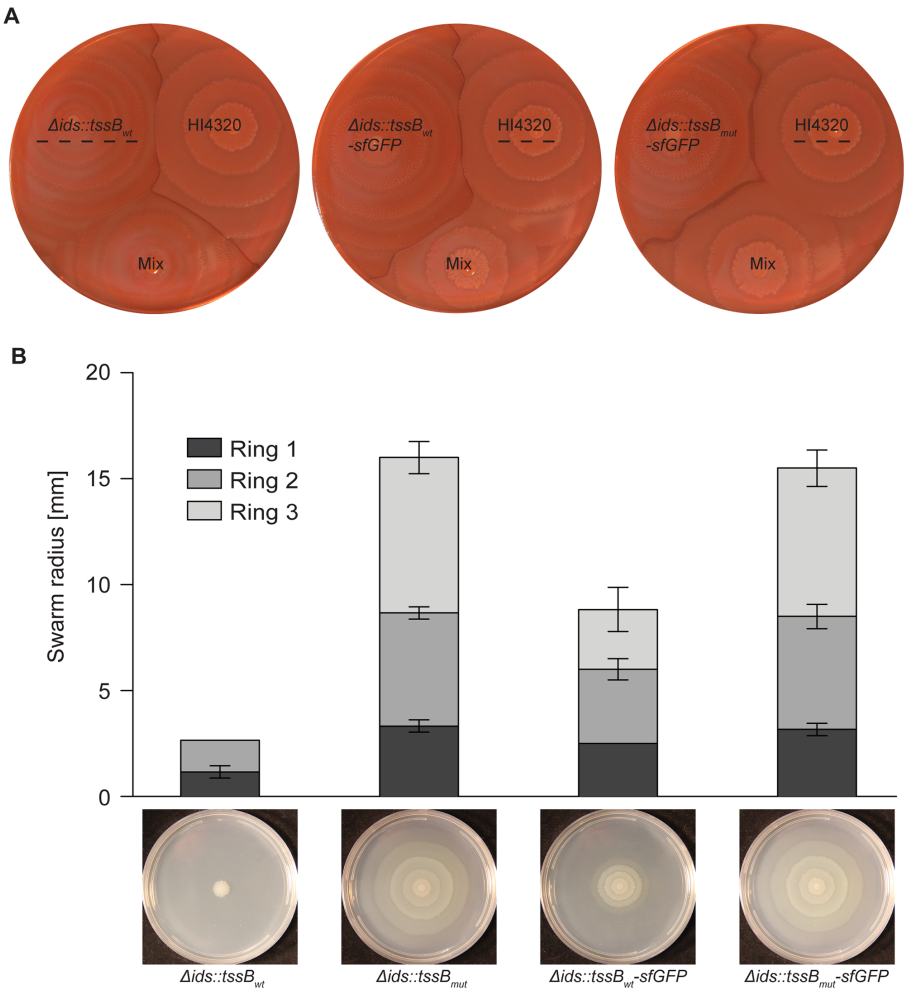

Fig 3. The $TssB_{wt}$-sfGFP fusion is partially functional in *P. mirabilis*. (A) Idr-dependent co-swarm assays were performed as described in Fig 1. Δ*ids*::*tssB*$_{wt}$ produces $TssB_{wt}$; Δ*ids*::*tssB*$_{wt}$-*sfgfp* produces wild-type TssB fused to sfGFP ($TssB_{wt}$-sfGFP); and Δ*ids*::*tssB*$_{mut}$-*sfgfp* produces the L32R mutant variant of TssB fused to sfGFP ($TssB_{L32R}$-sfGFP). The dominating strain is indicated with a dashed line on all plates. (B) Swarm assay in which a reduced swarm colony radius denotes that IdsD has been exported and transferred to an adjacent cell, where it remained unbound due to the lack of its binding partner IdsE [35, 58]. Wild-type T6S function results in a reduced swarm colony radius; disrupted T6S function results in larger swarm colony radii. Shown is the colony expansion after 16 hours on swarm-permissive agar surfaces of monoclonal Δ*ids*-derived swarms producing IdsD and lacking IdsE [35]. Strains contain the indicated *tssB* alleles. Widths of individual swarm rings within a swarm colony are marked by different shades. Representative images of swarm colonies after 24 hours are shown below the graph. N = 3, error bars show standard deviations of individual swarm ring widths.

https://doi.org/10.1371/journal.pone.0184797.g003

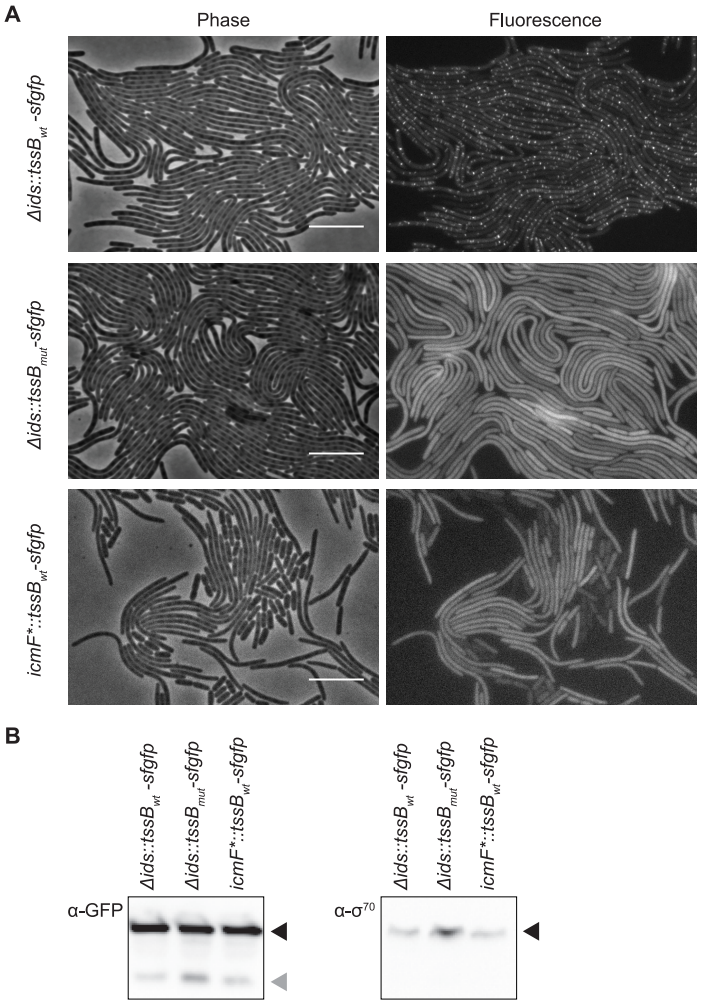

Fig 4. Sheath formation is inhibited by the L32R mutation. (A) Swarm agar pads were inoculated with indicated strains and incubated at 37˚C in a humidity chamber. After 4.5–5.5 hours, agar pads were imaged using phase contrast and epifluorescence microscopy to visualize cell bodies and TssB-sfGFP variants, respectively. BB2000-derived Δ*ids*::*tssB*$_{wt}$-*sfgfp* produces wild-type TssB fused to sfGFP (TssB$_{wt}$-sfGFP); it lacks the entire *ids* operon [39]. Δ*ids*::*tssB*$_{mut}$-*sfgfp* produces the L32R mutant variant of TssB fused to sfGFP (TssB$_{L32R}$-sfGFP). *icmF**::*tssB*$_{wt}$-*sfgfp* produces TssB$_{wt}$-sfGFP; it is derived from BB2000 and contains a chromosomal transposon insertion in the gene encoding the core T6S membrane component, TssM/IcmF [34]. Scale bars, 10 μm. (B) Whole cell extracts from swarming colonies of Δ*ids*::*tssB*$_{wt}$-*sfgfp*, Δ*ids*::*tssB*$_{mut}$-*sfgfp* and *icmF**::*tssB*$_{wt}$-*sfgfp* were collected after 16–20 hours on swarm-permissive plates. Samples were analyzed using western blot analysis and probed with an anti-GFP antibody to detect TssB-sfGFP and anti-

σ^{70} as a loading control. Bands corresponding to the sizes of TssB-sfGFP and σ^{70} are indicated with black arrowheads, while bands corresponding to the size of monomeric sfGFP are indicated with a grey arrowhead. A negative control sample of a swarm colony not producing any TssB-sfGFP fusion can be found in S1 Fig.

https://doi.org/10.1371/journal.pone.0184797.g004

in the Pfam model, T6SS_TssB (Pfam family PF05591) [24, 60–62]. Leucine 26 is highly conserved in available sequences for Enterobacterales and is also well conserved across the majority of Gammaproteobacteria; the conserved three amino acid sequence amongst Enterobacterales is E/Q-L-P [63–65]. Remarkably, the leucine residue maps to an unstructured region between the first two predicted beta sheets of the TssB protein (Fig 2). While the two beta sheets flanking this residue are predicted to be involved in interactions with separate TssC monomers in structural models of the sheath (Fig 2), the contribution of the unstructured region was less apparent [25, 26]. Upon closer evaluation, we posit that this leucine residue might contribute to a hydrophobic pocket (Fig 2D). A conversion to arginine then likely leads to both steric and electrostatic conflicts within this pocket (Fig 2E). The hydrophobic pocket and the examined leucine residue within it might be critical for interactions between TssB and TssC in individual protomers or alternatively, for interprotomer interactions of TssB and TssC that hold together the strands of the sheath helix. More examination is needed to elucidate these physical interactions. Nonetheless, the observation that the L32R mutation results in diffuse TssB-sfGFP signal within the cytoplasm (Fig 4A) supports the crucial role of this leucine for sheath assembly.

Visualization of sheath formation and its subcellular localization has proven valuable in multiple bacteria. TssB-sfGFP fusion proteins have been previously reported for *V. cholerae* [6] and *P. mirabilis* strain HI4320 [59]; the homologous TssB-sfGFP was designed equivalently in *P. mirabilis* strain BB2000 and introduced to the native locus on the chromosome replacing the wild-type allele. This sfGFP fusion protein showed reduced T6S function as compared to the wild-type variant (Fig 3). As similar defects were not reported previously [6, 59], we posit that possible differences in the protein sequences and tertiary structures between species and strains might be accentuated by the addition of sfGFP. Alternatively, these discrepancies in T6S on the species and strain level might reflect differences in the sensitivity of the respective assays chosen to detect T6S function (Fig 3). Regardless, the reduced T6S function in *P. mirabilis* strain BB2000 producing TssB-sfGFP appears to allow for greater visualization of elongated sheaths before disassembly (Fig 4). Elongated sheaths were stable over the course of the observation. Similar delayed dynamics might also be true for other microorganisms with nearly identical TssB sequences and a single T6S machinery such as *Providencia sp*. By contrast, TssB-sfGFP-containing sheaths rapidly transition between elongated structures and single foci during imaging in *V. cholerae* [4–6]. Stable, elongated TssB-sfGFP structures, such as those observed in *P. mirabilis* BB2000, could be utilized for subcellular co-localization assays using epifluorescence microscopy or for structural examination of the T6S machinery via cryo-electron microscopy.

In conclusion, the L to R mutation has the potential to be an impactful tool, especially in bacteria with a single T6S machinery. We have found that the L32R point mutation in the TssB homolog from *P. mirabilis* strain BB2000 allows for the disruption of the T6S sheath, which in turn causes global T6S malfunction. These results provide insight into the importance of the TssB N-terminal region for sheath assembly, which has not been fully investigated, and highlights a critical residue that was previously overlooked. These data also complement a previous detailed analysis of the TssB C-terminal region [28]. Last, the L to R mutation abrogates T6S function without disrupting the overall *tss* operon structure and without removing entire proteins from cells. As such, potential secondary effects that could convolute experimental

outcomes are minimized and questions regarding the subcellular localization of T6S-associated components and protein-protein interactions can be answered in a nearly native state. Here, we show that this previously under-appreciated residue is indeed crucial for sheath assembly and raise new questions of how unstructured regions within TssB contribute to TssB-TssC interactions.

Supporting information

S1 Fig. $TssB_{L32R}$ is as stable as a sfGFP-fusion protein as $TssB_{wt}$. To test for the production of the sfGFP-fused TssB proteins, cells were isolated from swarm-permissive nutrient plates supplemented with chloramphenicol after 22 hours and resuspended in 3 ml LB broth. 2 ml of each cell suspension were collected and cells were pelleted by centrifugation. The pellet was resuspended in sample buffer and boiled. Samples were separated by gel electrophoresis using 12% Tris-tricine polyacrylamide gels (amount loaded was normalized to OD_{600} of cell suspension before centrifugation), transferred onto 0.45 micrometer nitrocellulose membranes, and probed with a monoclonal mouse anti-GFP primary antibody. The mouse anti-GFP antibody was supplied at a concentration of 1 mg/ml and diluted 1:2500 (Thermo Fisher Scientific, Waltham, MA, catalog number: MA5-15256, clone GF28R, immunogen: GFP from jellyfish *Aequorea Victoria* N-terminal peptide-KLH conjugated). A negative control not expressing TssB-sfGFP was included to ensure antibody specificity. The blots were then incubated with a polyclonal, horseradish peroxidase-linked goat anti-mouse secondary antibody. The goat-anti-mouse secondary antibody was used at a 1:5000 dilution (KPL, Inc., Gaithersburg, MD, catalog number: 214–1806). A Precision Plus Protein™ Dual Color Standards molecular size marker (Bio-Rad Laboratories, Inc., Hercules, CA) was included as a size control. Membranes were developed with the Immun-Star HRP Substrate Kit (Bio-Rad Laboratories, Hercules, CA) and visualized using a Chemidoc (Bio-Rad Laboratories, Hercules, CA). TIFF images were exported and figures were made in Adobe Illustrator (Adobe Systems, San Jose, CA). Expected sizes for the TssB-sfGFP fusions and monomeric sfGFP are indicated; specific clones used in assays are indicated by arrows below.
(EPS)

Acknowledgments

We thank Dr. Thomas Bernhardt for the gift of the *sfgfp* sequence as well as Dr. Kenneth Skinner for helpful advice on the structural modeling. We also thank the members of Dr. Rachelle Gaudet's research group, as well as the Gibbs research group, for thoughtful discussions.

Author Contributions

Conceptualization: Christina C. Saak, Karine A. Gibbs.

Data curation: Christina C. Saak.

Formal analysis: Christina C. Saak, Martha A. Zepeda-Rivera, Karine A. Gibbs.

Funding acquisition: Martha A. Zepeda-Rivera, Karine A. Gibbs.

Investigation: Christina C. Saak, Martha A. Zepeda-Rivera.

Methodology: Christina C. Saak, Martha A. Zepeda-Rivera, Karine A. Gibbs.

Project administration: Christina C. Saak, Karine A. Gibbs.

Resources: Christina C. Saak, Martha A. Zepeda-Rivera, Karine A. Gibbs.

Supervision: Karine A. Gibbs.

Validation: Christina C. Saak, Martha A. Zepeda-Rivera.

Visualization: Christina C. Saak, Karine A. Gibbs.

Writing – original draft: Christina C. Saak.

Writing – review & editing: Christina C. Saak, Martha A. Zepeda-Rivera, Karine A. Gibbs.

References

1. Mougous JD, Cuff ME, Raunser S, Shen A, Zhou M, Gifford CA, et al. A virulence locus of *Pseudomonas aeruginosa* encodes a protein secretion apparatus. Science. 2006; 312(5779):1526–30. https://doi.org/10.1126/science.1128393 PMID: 16763151
2. Pukatzki S, Ma AT, Sturtevant D, Krastins B, Sarracino D, Nelson WC, et al. Identification of a conserved bacterial protein secretion system in *Vibrio cholerae* using the *Dictyostelium* host model system. Proc Natl Acad Sci U S A. 2006; 103(5):1528–33. https://doi.org/10.1073/pnas.0510322103 PMID: 16432199
3. Pukatzki S, Ma AT, Revel AT, Sturtevant D, Mekalanos JJ. Type VI secretion system translocates a phage tail spike-like protein into target cells where it cross-links actin. Proc Natl Acad Sci U S A. 2007; 104(39):15508–13. https://doi.org/10.1073/pnas.0706532104 PMID: 17873062
4. Basler M, Ho BT, Mekalanos JJ. Tit-for-tat: type VI secretion system counterattack during bacterial cell-cell interactions. Cell. 2013; 152(4):884–94. https://doi.org/10.1016/j.cell.2013.01.042 PMID: 23415234
5. Basler M, Mekalanos JJ. Type 6 secretion dynamics within and between bacterial cells. Science. 2012; 337(6096):815. https://doi.org/10.1126/science.1222901 PMID: 22767897
6. Basler M, Pilhofer M, Henderson GP, Jensen GJ, Mekalanos JJ. Type VI secretion requires a dynamic contractile phage tail-like structure. Nature. 2012; 483(7388):182–6. https://doi.org/10.1038/nature10846 PMID: 22367545
7. Shneider MM, Buth SA, Ho BT, Basler M, Mekalanos JJ, Leiman PG. PAAR-repeat proteins sharpen and diversify the type VI secretion system spike. Nature. 2013; 500(7462):350–3. https://doi.org/10.1038/nature12453 PMID: 23925114
8. Hood RD, Singh P, Hsu F, Guvener T, Carl MA, Trinidad RR, et al. A type VI secretion system of *Pseudomonas aeruginosa* targets a toxin to bacteria. Cell Host Microbe. 2010; 7(1):25–37. https://doi.org/10.1016/j.chom.2009.12.007 PMID: 20114026
9. Russell AB, Hood RD, Bui NK, LeRoux M, Vollmer W, Mougous JD. Type VI secretion delivers bacteriolytic effectors to target cells. Nature. 2011; 475(7356):343–7. https://doi.org/10.1038/nature10244 PMID: 21776080
10. Russell AB, LeRoux M, Hathazi K, Agnello DM, Ishikawa T, Wiggins PA, et al. Diverse type VI secretion phospholipases are functionally plastic antibacterial effectors. Nature. 2013; 496(7446):508–12. https://doi.org/10.1038/nature12074 PMID: 23552891
11. Whitney JC, Chou S, Russell AB, Biboy J, Gardiner TE, Ferrin MA, et al. Identification, structure, and function of a novel type VI secretion peptidoglycan glycoside hydrolase effector-immunity pair. J Biol Chem. 2013; 288(37):26616–24. https://doi.org/10.1074/jbc.M113.488320 PMID: 23878199
12. MacIntyre DL, Miyata ST, Kitaoka M, Pukatzki S. The *Vibrio cholerae* type VI secretion system displays antimicrobial properties. Proc Natl Acad Sci U S A. 2010; 107(45):19520–4. https://doi.org/10.1073/pnas.1012931107 PMID: 20974937
13. Miyata ST, Kitaoka M, Brooks TM, McAuley SB, Pukatzki S. *Vibrio cholerae* requires the type VI secretion system virulence factor VasX to kill *Dictyostelium discoideum*. Infect Immun. 2011; 79(7):2941–9. https://doi.org/10.1128/IAI.01266-10 PMID: 21555399
14. Brooks TM, Unterweger D, Bachmann V, Kostiuk B, Pukatzki S. Lytic activity of the *Vibrio cholerae* type VI secretion toxin VgrG-3 is inhibited by the antitoxin TsaB. J Biol Chem. 2013; 288(11):7618–25. https://doi.org/10.1074/jbc.M112.436725 PMID: 23341465
15. Unterweger D, Miyata ST, Bachmann V, Brooks TM, Mullins T, Kostiuk B, et al. The *Vibrio cholerae* type VI secretion system employs diverse effector modules for intraspecific competition. Nat Commun. 2014; 5:3549. https://doi.org/10.1038/ncomms4549 PMID: 24686479
16. Durand E, Derrez E, Audoly G, Spinelli S, Ortiz-Lombardia M, Raoult D, et al. Crystal structure of the VgrG1 actin cross-linking domain of the *Vibrio cholerae* type VI secretion system. J Biol Chem. 2012; 287(45):38190–9. https://doi.org/10.1074/jbc.M112.390153 PMID: 22898822

17. Brunet YR, Espinosa L, Harchouni S, Mignot T, Cascales E. Imaging type VI secretion-mediated bacterial killing. Cell Rep. 2013; 3(1):36–41. https://doi.org/10.1016/j.celrep.2012.11.027 PMID: 23291094

18. Durand E, Nguyen VS, Zoued A, Logger L, Pehau-Arnaudet G, Aschtgen MS, et al. Biogenesis and structure of a type VI secretion membrane core complex. Nature. 2015; 523(7562):555–60. https://doi.org/10.1038/nature14667 PMID: 26200339

19. Hachani A, Lossi NS, Hamilton A, Jones C, Bleves S, Albesa-Jove D, et al. Type VI secretion system in *Pseudomonas aeruginosa*: secretion and multimerization of VgrG proteins. J Biol Chem. 2011; 286 (14):12317–27. https://doi.org/10.1074/jbc.M110.193045 PMID: 21325275

20. Hachani A, Allsopp LP, Oduko Y, Filloux A. The VgrG proteins are "a la carte" delivery systems for bacterial type VI effectors. J Biol Chem. 2014; 289(25):17872–84. https://doi.org/10.1074/jbc.M114.563429 PMID: 24794869

21. Ma LS, Hachani A, Lin JS, Filloux A, Lai EM. *Agrobacterium tumefaciens* deploys a superfamily of type VI secretion DNase effectors as weapons for interbacterial competition in planta. Cell Host Microbe. 2014; 16(1):94–104. https://doi.org/10.1016/j.chom.2014.06.002 PMID: 24981331

22. Wang T, Si M, Song Y, Zhu W, Gao F, Wang Y, et al. Type VI secretion system transports Zn2+ to combat multiple stresses and host immunity. PLoS Pathog. 2015; 11(7):e1005020. https://doi.org/10.1371/journal.ppat.1005020 PMID: 26134274

23. Bonemann G, Pietrosiuk A, Diemand A, Zentgraf H, Mogk A. Remodelling of VipA/VipB tubules by ClpV-mediated threading is crucial for type VI protein secretion. Embo J. 2009; 28(4):315–25. https://doi.org/10.1038/emboj.2008.269 PMID: 19131969

24. Kapitein N, Bonemann G, Pietrosiuk A, Seyffer F, Hausser I, Locker JK, et al. ClpV recycles VipA/VipB tubules and prevents non-productive tubule formation to ensure efficient type VI protein secretion. Molecular microbiology. 2013; 87(5):1013–28. https://doi.org/10.1111/mmi.12147 PMID: 23289512

25. Kudryashev M, Wang RY, Brackmann M, Scherer S, Maier T, Baker D, et al. Structure of the type VI secretion system contractile sheath. Cell. 2015; 160(5):952–62. https://doi.org/10.1016/j.cell.2015.01.037 PMID: 25723169

26. Kube S, Kapitein N, Zimniak T, Herzog F, Mogk A, Wendler P. Structure of the VipA/B type VI secretion complex suggests a contraction-state-specific recycling mechanism. Cell Rep. 2014; 8(1):20–30. https://doi.org/10.1016/j.celrep.2014.05.034 PMID: 24953649

27. Clemens DL, Ge P, Lee BY, Horwitz MA, Zhou ZH. Atomic structure of T6SS reveals interlaced array essential to function. Cell. 2015; 160(5):940–51. https://doi.org/10.1016/j.cell.2015.02.005 PMID: 25723168

28. Zhang XY, Brunet YR, Logger L, Douzi B, Cambillau C, Journet L, et al. Dissection of the TssB-TssC interface during type VI secretion sheath complex formation. PLoS One. 2013; 8(11):e81074. https://doi.org/10.1371/journal.pone.0081074 PMID: 24282569

29. Zoued A, Durand E, Bebeacua C, Brunet YR, Douzi B, Cambillau C, et al. TssK is a trimeric cytoplasmic protein interacting with components of both phage-like and membrane anchoring complexes of the type VI secretion system. J Biol Chem. 2013; 288(38):27031–41. https://doi.org/10.1074/jbc.M113.499772 PMID: 23921384

30. Brunet YR, Henin J, Celia H, Cascales E. Type VI secretion and bacteriophage tail tubes share a common assembly pathway. EMBO Rep. 2014; 15(3):315–21. https://doi.org/10.1002/embr.201337936 PMID: 24488256

31. Brunet YR, Khodr A, Logger L, Aussel L, Mignot T, Rimsky S, et al. H-NS Silencing of the Salmonella Pathogenicity Island 6-Encoded Type VI Secretion System Limits Salmonella enterica Serovar Typhimurium Interbacterial Killing. Infect Immun. 2015; 83(7):2738–50. https://doi.org/10.1128/IAI.00198-15 PMID: 25916986

32. Gerc AJ, Diepold A, Trunk K, Porter M, Rickman C, Armitage JP, et al. Visualization of the Serratia Type VI Secretion System Reveals Unprovoked Attacks and Dynamic Assembly. Cell Rep. 2015; 12 (12):2131–42. https://doi.org/10.1016/j.celrep.2015.08.053 PMID: 26387948

33. Sullivan NL, Septer AN, Fields AT, Wenren LM, Gibbs KA. The complete genome sequence of *Proteus mirabilis* strain BB2000 reveals differences from the *P. mirabilis* reference Strain. Genome Announc. 2013; 1(5).

34. Wenren LM, Sullivan NL, Cardarelli L, Septer AN, Gibbs KA. Two independent pathways for self-recognition in *Proteus mirabilis* are linked by type VI-dependent export. mBio. 2013; 4(4).

35. Saak CC, Gibbs KA. The self-identity protein IdsD is communicated between cells in swarming *Proteus mirabilis* colonies. J Bacteriol. 2016; 198(24):3278–86. https://doi.org/10.1128/JB.00402-16 PMID: 27672195

36. Belas R, Erskine D, Flaherty D. Transposon mutagenesis in *Proteus mirabilis*. J Bacteriol. 1991; 173 (19):6289–93. PMID: 1655704

37. Pearson MM, Sebaihia M, Churcher C, Quail MA, Seshasayee AS, Luscombe NM, et al. Complete genome sequence of uropathogenic *Proteus mirabilis*, a master of both adherence and motility. J Bacteriol. 2008; 190(11):4027–37. https://doi.org/10.1128/JB.01981-07 PMID: 18375554

38. Warren JW, Tenney JH, Hoopes JM, Muncie HL, Anthony WC. A prospective microbiologic study of bacteriuria in patients with chronic indwelling urethral catheters. J Infect Dis. 1982; 146(6):719–23. PMID: 6815281

39. Gibbs KA, Urbanowski ML, Greenberg EP. Genetic determinants of self identity and social recognition in bacteria. Science. 2008; 321(5886):256–9. https://doi.org/10.1126/science.1160033 PMID: 18621670

40. Simon R, Priefer U, Pühler A. A broad host range mobilization system for *in vivo* genetic engineering: transposon mutagenesis in gram negative bacteria. Nat Biotechnology. 1983; 1:784–91.

41. Kaniga K, Delor I, Cornelis GR. A wide-host-range suicide vector for improving reverse genetics in gram-negative bacteria: inactivation of the *blaA* gene of *Yersinia enterocolitica*. Gene. 1991; 109 (1):137–41. PMID: 1756974

42. de Lorenzo V, Herrero M, Jakubzik U, Timmis KN. Mini-Tn5 transposon derivatives for insertion mutagenesis, promoter probing, and chromosomal insertion of cloned DNA in gram-negative eubacteria. J Bacteriol. 1990; 172(11):6568–72. PMID: 2172217

43. Vallejo AN, Pogulis RJ, Pease LR. PCR Mutagenesis by Overlap Extension and Gene SOE. CSH Protoc. 2008; 2008:pdb prot4861.

44. Sturgill GM, Siddiqui S, Ding X, Pecora ND, Rather PN. Isolation of lacZ fusions to *Proteus mirabilis* genes regulated by intercellular signaling: potential role for the sugar phosphotransferase (Pts) system in regulation. FEMS microbiology letters. 2002; 217(1):43–50. PMID: 12445644

45. Biasini M, Bienert S, Waterhouse A, Arnold K, Studer G, Schmidt T, et al. SWISS-MODEL: modelling protein tertiary and quaternary structure using evolutionary information. Nucleic Acids Res. 2014; 42 (Web Server issue):W252–8. https://doi.org/10.1093/nar/gku340 PMID: 24782522

46. Arnold K, Bordoli L, Kopp J, Schwede T. The SWISS-MODEL workspace: a web-based environment for protein structure homology modelling. Bioinformatics. 2006; 22(2):195–201. https://doi.org/10.1093/bioinformatics/bti770 PMID: 16301204

47. Bordoli L, Kiefer F, Arnold K, Benkert P, Battey J, Schwede T. Protein structure homology modeling using SWISS-MODEL workspace. Nat Protoc. 2009; 4(1):1–13. https://doi.org/10.1038/nprot.2008.197 PMID: 19131951

48. Guex N, Peitsch MC, Schwede T. Automated comparative protein structure modeling with SWISS-MODEL and Swiss-PdbViewer: a historical perspective. Electrophoresis. 2009; 30 Suppl 1:S162–73.

49. Berman H, Henrick K, Nakamura H. Announcing the worldwide Protein Data Bank. Nat Struct Biol. 2003; 10(12):980. https://doi.org/10.1038/nsb1203-980 PMID: 14634627

50. Berman HM, Westbrook J, Feng Z, Gilliland G, Bhat TN, Weissig H, et al. The Protein Data Bank. Nucleic Acids Res. 2000; 28(1):235–42. PMID: 10592235

51. Schrodinger L. The PyMOL Molecular Graphics System, Version 1.8. 2015.

52. Hoeniger JFM. Development of flagella by *Proteus mirabilis*. J gen Microbiol. 1964; 40:29–42.

53. Jones BV, Young R, Mahenthiralingam E, Stickler DJ. Ultrastructure of *Proteus mirabilis* swarmer cell rafts and role of swarming in catheter-associated urinary tract infection. Infect Immun. 2004; 72 (7):3941–50. https://doi.org/10.1128/IAI.72.7.3941-3950.2004 PMID: 15213138

54. Rauprich O, Matsushita M, Weijer CJ, Siegert F, Esipov SE, Shapiro JA. Periodic phenomena in *Proteus mirabilis* swarm colony development. J Bacteriol. 1996; 178(22):6525–38. PMID: 8932309

55. Budding AE, Ingham CJ, Bitter W, Vandenbroucke-Grauls CM, Schneeberger PM. The Dienes phenomenon: competition and territoriality in swarming *Proteus mirabilis*. J Bacteriol. 2009; 191(12):3892–900. https://doi.org/10.1128/JB.00975-08 PMID: 19251852

56. Senior BW. The Dienes phenomenon: identification of the determinants of compatibility. J Gen Microbiol. 1977; 102(2):235–44. https://doi.org/10.1099/00221287-102-2-235 PMID: 925679

57. Dienes L. Further observations on the reproduction of bacilli from large bodies in *Proteus* cultures. Proc Soc Exp Biol Med. 1947; 66(1):97–8. PMID: 20270685

58. Cardarelli L, Saak C, Gibbs KA. Two proteins form a heteromeric bacterial self-recognition complex in which variable subdomains determine allele-restricted binding. mBio. 2015; 6(3):e00251. https://doi.org/10.1128/mBio.00251-15 PMID: 26060269

59. Alteri CJ, Himpsl SD, Pickens SR, Lindner JR, Zora JS, Miller JE, et al. Multicellular bacteria deploy the type VI secretion system to preemptively strike neighboring cells. PLoS Pathog. 2013; 9(9):e1003608. https://doi.org/10.1371/journal.ppat.1003608 PMID: 24039579

60. Finn RD, Bateman A, Clements J, Coggill P, Eberhardt RY, Eddy SR, et al. Pfam: the protein families database. Nucleic Acids Res. 2014; 42(Database issue):D222–30. https://doi.org/10.1093/nar/gkt1223 PMID: 24288371

61. Wu QR. [Study on BCG vaccination and incidence of children's tuberculous meningitis in Liaoning province]. Zhonghua Jie He He Hu Xi Za Zhi. 1991; 14(3):173–5, 92. PMID: 1913969

62. Bingle LE, Bailey CM, Pallen MJ. Type VI secretion: a beginner's guide. Curr Opin Microbiol. 2008; 11 (1):3–8. https://doi.org/10.1016/j.mib.2008.01.006 PMID: 18289922

63. McWilliam H, Li W, Uludag M, Squizzato S, Park YM, Buso N, et al. Analysis Tool Web Services from the EMBL-EBI. Nucleic Acids Res. 2013; 41(Web Server issue):W597–600. https://doi.org/10.1093/nar/gkt376 PMID: 23671338

64. Li W, Cowley A, Uludag M, Gur T, McWilliam H, Squizzato S, et al. The EMBL-EBI bioinformatics web and programmatic tools framework. Nucleic Acids Res. 2015; 43(W1):W580–4. https://doi.org/10.1093/nar/gkv279 PMID: 25845596

65. Sievers F, Wilm A, Dineen D, Gibson TJ, Karplus K, Li W, et al. Fast, scalable generation of high-quality protein multiple sequence alignments using Clustal Omega. Mol Syst Biol. 2011; 7:539. https://doi.org/10.1038/msb.2011.75 PMID: 21988835